Characterization of TopoisomeraseIIβ-associated Base excision repair and Senescence in Cultured cerebellar granule neurons

DOCTOR OF PHILOSOPHY

By
K. Preeti Gupta

January 2013
Enrollment No. 07LBPH02

Department of Biochemistry
School of Life Sciences
University of Hyderabad
Prof. C. R. Rao Road
Hyderabad-46, A.P., INDIA

Characterization of TopoisomeraseIIβ-associated Base excision repair and Senescence in Cultured cerebellar granule neurons

THESIS SUBMITTED FOR THE AWARD OF DEGREE
'DOCTOR OF PHILOSOPHY' IN BIOCHEMISTRY

By
K. Preeti Gupta

To
University of Hyderabad

Department of Biochemistry
School of Life Sciences
University of Hyderabad
Prof. C. R. Rao Road
Hyderabad-46, A.P., INDIA

January 2013

Enrollment No. 07LBPH02

University of Hyderabad
(Central University established in 1974 by Act of Parliament)
School of Life Sciences
Department of Biochemistry
Prof. C. R. Rao Road, Hyderabad-500 046, INDIA

DECLARATION

I hereby declare that the work presented in this thesis entitled "Characterization of TopoisomeraseIIβ-associated Base excision repair and Senescence in cultured cerebellar granule neurons" is entirely original work and was carried out by me in the Department of Biochemistry, University of Hyderabad, Hyderabad, under the supervision of Prof. Anand. K. Kondapi. I further declare that to the best of my knowledge this work has not formed the basis for the award of any degree or diploma of any university or institution.

Date:

K. Preeti Gupta

07LBPH02

University of Hyderabad
(Central University established in 1974 by Act of Parliament)
School of Life Sciences
Department of Biochemistry
Prof. C. R. Rao Road, Hyderabad-500 046, INDIA

CERTIFICATE

This is to certify that this thesis entitled "Characterization of TopoisomeraseIIβ-associated Base excision repair and Senescence in cultured cerebellar granule neurons" is a record of bonafide work done by Mrs. K. Preeti Gupta, a research scholar for Ph.D. programme in the Department of Biochemistry, University of Hyderabad under my guidance and supervision.

The thesis has not been submitted previously in part or full to this or any other University or Institution for the award of any degree or diploma.

(Signature of Supervisor)

(Head of the Department)

(Dean of the School)

ACKNOWLEDGEMENTS

It gives me immense pleasure to thank all the people associated with me, while pursuing the Ph.D.

With deep sense of gratitude and respect, I thank my supervisor, Prof. Anand. K. Kondapi, for his guidance in shaping this piece of work & also for the encouragement, confidence and patience shown especially in the first two years during which I hardly had any data. His words have given me strength. He gave me the freedom to design my experiments and allowed me to work in my own way. Thank you Sir.

I thank the former and present Dean, SLS, Prof. M. Ramanadham and Prof. Aparna Dutta Gupta & former and present Heads of the Department of Biochemistry Prof. M. Ramanadham, Prof. K. V.A. Ramaiah and Prof. O. H. Setty for the general and department facilities. I thank the former and present Heads of Department of Biotechnology, Animal Sciences and Plant Sciences.

I thank DC members, Prof. K. V.A. Ramaiah and Dr. Mrinal. K. Bhattacharya for their valuable inputs.

I sincerely thank Prof. Rao K. S for his valuable inputs to my work and manuscript; Prof ADG for initiating the FACS and Genomics workshops (CREBB); Prof. N. Giritharan and the entire staff of NCLAS, NIN for their prompt response; Prof C. R. Rao (Dept. of Computer Sciences) for his help in statistical analysis; Mr. P. M. Rao (Retd. Chief Editor, IBM) for proof reading my manuscripts.

I thank the entire faculty of SLS for the help and guidance during this research tenure. I specially would like to thank the faculties- Prof. P. S. Sastry, Prof. B. Senthilkumaran, Prof. Aparna Datta Gupta, Prof. P. B. Kirti, Prof. Prakash Babu, Prof. Niyaz Ahmed, Dr. Sharmishta B., Dr. Krishna Veni Mishra, Dr. Arunkumar K. and Dr. Y. Suresh and their lab students for allowing me to use their lab facilities.

I thank all my teachers at St. Joseph's Public School (Hyd.), St. Ann's Degree College (Hyd.), Kasturba Medical College, KMC (Manipal) for instilling the ideas of research and ethics. Heartfelt thanks to Dr. Sneha Gogte (St. Ann's). A special mention of my seniors- Dr. Rajkumar, Dr. Umakanta Swain, Dr. Kannapiran and Dr. Roy for their help and guidance.

I wish to thank Ms. Nalini for her amicable assistance in confocal microscopy; Mr. Chandra Shekhar & Mr. Sadanand for radioactivity facility maintenance; Mr. Srinivas Murthy for help in paper work; Mr. Lallanji for technical assistance; Ms. Leena Bashim, Ms. Mounika, for the assistance in Genomics and Proteomics facilities.

I sincerely thank ICMR for the fellowship. I thank the funding bodies, ICMR, CSIR, DBT, and DST for funding my work through periodic grants. The infrastructure developed under various programs including UGC-UPE, X plan, CREBB and DST-FIST is duly acknowledged. I

thank my Dad and CSIR for sponsoring my trip to attend Gordon Research Conference (poster presentation), LA, USA.

I thank all my seniors and lab mates- Drs. Raj, Kannapiran, Sai Krishna, Uday, Bhaskar and Upendra, Balakrishna, Kishore, Sarada, Anil, Srinivas, Satish, Farhan, HariKiran, Kurumurty, Sonali, Lakshmi, Jagadish, Prashant and Drs. Ramakrishna, Radhakrishna, Chaitanya, Prabhakar and Sridevi for the cheerful atmosphere in the lab; Srinivas Reddy for help in FACS data acquisition. I must thank the lab attenders- Srinivas (paper work), Bhanu Chander (errands to the city to procure lab stuff) & Chandra Mohan (for taking care of animal room).

Special thanks to Farhan, Kishore, Sarada, Pankaz, Manisha, Swetha, Nallam Kishore, Suhail, Benjamin, Venkat, Pratibha, Raj, Murgananth, SriVidya, Dr. Suraj, Pushyami and Jyotsna, who made my work feasible at difficult times. I thank Balakrishna for his ideas & criticism and Dr. Sridevi for the moral support and for all the help received in standardising & carrying out molecular work.

I thank my parents Mr. & Mrs. Vijaya Gupta, Sandhya, for believing in me and allowing me to pursue Ph.D.; my mother, for all the love, support & shaping my thoughts & my father for all the independence and for giving me everything that I ever wished for.

My sisters Aarti and Swati, for their love and gestures shown during these all these tough years of study- right from my M.Sc. days- for taking upon themselves my share of responsibilities. My brother-in-law, Mr. Harsha, my little Ved & Nidhi for the fun packed weekends.

Words fall short as I thank my in-laws, especially my mother-in-law, Mrs. Sushila Bhatia for her immense support & patience and my father-in-law, Mr. R.C. Bhatia for all the care & encouragement as I slowly learnt to carry out the twin responsibilities of lab & home.

I sincerely thank my grandfather, Mr. P. M. Rao, without whose love, encouragement & belief all through and especially, during the years' gap after M.Sc., this day wouldn't have seen the dawn. This was his dream for me and I hope I have lived up to his expectations.

I sincerely thank my husband, Mr. Rakesh, whose seemless care, patience, love, emotional support and confidence helped me tide over the difficult phases of Ph.D.

Last but not the least; I thank the good Lord for guiding me all through and for his generous blessings.

Preeti

CONTENTS

INTRODUCTION 1

Ageing 2

DNA damage and repair theory 3

Topoisomerases 4

Topoisomerase II β and DNA repair 9

Topoisomerase II β and Brain ageing 10

Neurons 10

Cell culture as a model for ageing 12

Cerebellar granule neurons (CGNs) as a model for ageing 13

DNA damage 14

Reactive oxygen species and DNA damage in neurons 16

DNA repair 17

Nucleotide excision repair (NER) 19

Mismatch repair (MMR) 20

Base excision repair (BER) 21

Rationale 30

MATERIALS AND METHODS 32

ROLE OF TOPOIIβ IN BASE EXCISION REPAIR IN *IN VITRO* CULTURED CGNS 53

Introduction 54

Results 58

Discussion 85

Conclusion 88

CHARACTERIZING SENESCENCE-ASSOCIATED STRESS RESPONSES AND REPAIR IN *IN VITRO* CULTURED CGNS 89

Introduction 90

Results 93

Discussion 114

Conclusion 118

ANALYSIS OF GENE EXPRESSION ELEVATION DURING AGEING OF CGNS IN CULTURE 119

Introduction 120

Results 124

Discussion 133

Conclusion 137

CONCLUSIONS 138

PUBLICATIONS FROM THESIS 142

REFERENCES 143

FIGURES

Figure 1: Cerebellar granule neurons in culture....68

Figure 2: siRNA mediated TopoIIβ downregulation....69

Figure 3: Reverse transcription PCR (RT-PCR)....71

Figure 4: TopoIIβ downregulation affects repair of ENU mediated SSBs in CGNs....72

Figure 5: TopoIIβ knockdown neurons are deficient in G-U BER activity....74

Figure 6: UDG activity is not enhanced in TopoIIβ deficient condition during ENU treatment....76

Figure 7: AP endonuclease activity slightly increased by TopoIIβ downregulation....79

Figure 8: LIG activity is affected in the ECGNT^{-} cells during recovery from ENU mediated strand breaks....81

Figure 9: TopoIIβ activity *per se* not required for LIG activity....84

Figure 10: MTT assay and Real-Time PCR....101

Figure 11: Senescence associated-β-galactosidase assay....102

Figure 12: Cellular ROS and GSH in ageing CGNs....103

Figure 13: Assessment of DNA damage with age in *in vitro* cultured CGNs....104

Figure 14: Characterizing mitochondrial membrane potential in ageing CGNs by flowcytometry....105

Figure 15: Validation of differential gene expression by qPCR....107

Figure 16: Validation of differential gene expression by qPCR....108

Figure 17: Effect of *in vitro* ageing on G-U BER and ligase activity in CGNs....109

Figure 18: Decline in UDG activity in ageing CGN extracts....111

Figure 19: AP endonuclease activity in ageing CGNs....112

Figure 20: Gap repair assay in *in vitro* ageing CGNs....113

Figure 21: Heat map of differentially expressed genes in ageing CGNs..... 128

Figure 22: Heat map of differentially expressed genes..... 129

Figure 23: Classification of differentially expressed genes based on function..... 130

Figure 24: Validation of differential gene expression by qPCR..... 131

Figure 25: Semi quantitative PCR analysis..... 132

ABBREVIATIONS

AD	: Alzheimer's disease
AP	: Apurinic/Apyrimidinic
APE 1	: AP endonuclease 1
A-T	: Ataxia Telengiectasia
ATP	: Adenosine triphosphate
BER	: Base excision repair
BSA	: Bovine Serum Albumin
bp	: Base pairs
CGNs	: Cerebellar granule neurons
$CGNT^{-}$	: Cerebellar granule neurons downregulated for TopoIIβ
CNS	: Central Nervous System
CR	: Calorie Restriction
CS	: Cockayne's Syndrome
cDNA	: Complementary DNA
CO_2	: Carbon dioxide
DAPI	: 4',6-diamidino-2-phenylindole
dATP	: 2'-deoxyadenosine 5'- triphosphate
dCTP	: 2'-deoxycytidine 5'- triphosphate
dGTP	: 2'-deoxyguanosine 5'- triphosphate
dTTP	: 2'-deoxythymidine 5'- triphosphate
DNA	: Deoxyribonucleic acid
dNTPs	: Deoxynucleotidetriphosphates
dsDNA	: Double-stranded DNA
dRPase	: 5'- 2-deoxyribose-5-phosphate lyase
DSBs	: Double strand breaks
DTT	: Dithiothreitol
$ECGNT^{-}$	: Extracts of TopoIIβ knockdown cells
ENU	: N- ethyl N-nitroso urea
EDTA	: Ethylene diamine tetra acetic acid
FBS	: Fetal Bovine Serum
FACS	: Fluorescence-activated cell sorting
GFAP	: Glial cell fibrilary acidic protein
HRP	: Horse radish peroxidase
IgG	: Immunoglobulin G
IR	: Ionizing radiation
kDa	: Kilodaltons
LIG	: Ligase
mg	: Milligram
mM	: Millimolar

mRNA	: Messenger RNA
MTT	: 3-(4,5-dimethylthiozol-2-yl)-2,5 diphenyltetrazolium bromide
NAD	: Nicotinamide adenine dinucleotide
NER	: Nucleotide excision repair
NHEJ	: Non homologous end joining
NSE	: Neuron specific enolase
PAGE	: Polyacrylamide gel electrophoresis
PARP-1	: Poly ADP- ribose polymerase 1
PD	: Parkinon's disease
PDL	: Poly-D-lysine
PMSF	: Phenylmethyl sulfonyl flouride
POLβ	: DNA polymerase β
POPOP	: 2, 2'–p-Phenylene–bis [5-phenyloxazole]
PPO	: 2, 5-diphenyl–1, 3–oxazole
PBS	: Phosphate buffer saline
siRNA	: Small interfering RNA
SSBs	: Single strand breaks
TBS	: Tris buffered saline
TCA	: Trichloroacetic acid
TCR	: Transcription coupled repair
TopoIIβ	: Topoisomerase IIβ
UDG	: Uracil-DNA glycosylase
µg	: Microgram
µL	: Microlitre
µM	: Micromolar

INTRODUCTION

Ageing

Ageing is a phenomenon that occurs in every living organism and can be defined as diminishing of normal physiological functions, being progressive, deleterious and an irreversible process, leading ultimately to death. During ageing, reactive intermediates are known to cause damage to bio-molecules i.e. DNA, proteins and lipids, thus leading to functional variation in cells (Bokov et al., 2004). These changes occur little by little and progress inevitably over time. However, the rate of the progression of such damage can be very different from person to person. Diseases of old age (diseases which increase in frequency with age, such as arthritis, osteoporosis, heart disease, cancer, Alzheimer's Disease, etc.) are often distinguished from ageing *per se*. Ageing depends on several processes that may interact simultaneously and may operate at many levels of functional organization (Franceschi et al., 2000). Research in ageing is beginning to find out the reasons for these changes and the genetic and environmental factors that control them. There is evidence supporting at least 5 common characteristics of ageing in mammals (Troen, 2003).

1. Increased mortality with age after maturation.
2. Changes in biochemical composition in tissues with age.
3. Progressive decrease in physiological capacity with age.
4. Reduced ability to respond adaptively to environmental stimuli with age.
5. Increased susceptibility and vulnerability to disease.

Many theories of ageing have been proposed in this century, and very often the proposer attempts to explain the whole complex process of ageing in terms of a

single theory. These attempts are probably doomed to failure, since it has become obvious that ageing is multicausal or multifactorial. Modern technology and research techniques have allowed the researchers to test many of these theories of ageing. One theory, which enjoys considerable logic and rationale, is the DNA damage and repair theory.

DNA damage and repair theory

Alexander, (1967) was the first to suggest that DNA damage *per se*, apart from its role in inducing mutations, may be a primary cause of ageing. This theory postulates that the DNA damage, which is bound to occur in the body of an organism, is repaired efficiently up to a certain age of an organism, but thereafter is compromised in a predetermined manner. Thus, from some point of lifespan, DNA repair capacity decreases, therefore DNA damage accumulates. This accumulation of DNA damage leads to the breakdown of all the vital processes in the cell finally leading to death. In mammals, long-lived neurons, differentiated muscle cells and other differentiated cell types that do not divide or divide slowly, accumulate DNA damage with age. These cells are likely candidates to govern the rate of mammalian ageing. In brain, the level of DNA repair is low, endogenous damages accumulate with age, mRNA synthesis declines and protein synthesis is reduced. Furthermore, cell loss occurs, tissue function declines and functional impairments directly related to the central processes of ageing occur. Thus, for the brain, there appears to be a direct relationship between the accumulation of DNA damage and the important feature of ageing. The DNA-damage and repair theory occupies a central role in explaining the mechanisms

of the ageing phenomenon at a basic and fundamental level. This concept has the necessary depth to compliment many other theories of ageing either partly or fully. Moreover, the work presented in this thesis pertains to the DNA-repair capacity of brain cells during ageing. In view of this, an attempt has been made below to briefly review the existing knowledge about DNA damage and DNA-repair in ageing cells with a special emphasis on cerebellar granule neurons (CGNs).

Living cells face the tremendous task of maintaining an intact genome during the lifespan. DNA damage induces chromosomal reorganization leading to activation of transcription process for expression of repair genes (Ju et al., 2006), formation of multimeric repair complexes (Fan and Wilson, 2005), stabilization of damaged regions (Pfeiffer and Vielmetter, 1988), rearrangement and re-sealing of broken ends of the DNA through correction, processing, synthesis and ligation. During this process, torsional stress will be embedded in the upstream and downstream of the damaged site. The maintenance of torsional integrity is promoted by a class of enzymes known as topoisomerases.

Topoisomerases

Virtually every facet of nucleic acid physiology is influenced by the topological state of DNA (Wang, 1985). Topoisomerase catalyzes three types of reactions - relaxation of supercoiled DNA, inter-conversions between single stranded DNA rings and linking of single stranded rings of complimentary sequences. Clearly, the cell's ability to regulate the topological state of DNA is imperative for its

viability. Two classes of ubiquitous enzymes, Type I and Type II Topoisomerases, modulate DNA topology.

a) Topoisomerase I can relieve torsional constraints in DNA by passing a single strand of DNA through a transient nick made in the complementary strand (Wang, 1985). It plays important role in DNA replication (Goto and Wang, 1985) and transcription (Garg et al., 1987; Gilmour et al., 1986).

b) Topoisomerase II can relieve both torsional and interlocking constraints in double stranded nucleic acids by passing an intact helix through a transient double stranded break made in a second helix (Osheroff, 1989; Wang, 1985). Topoisomerase II is essential to the eukaryotic cell. It is required for chromosome segregation (Holm et al., 1985; Uemura and Yanagida, 1984), maintenance of chromosome structure (Earnshaw et al., 1985) and plays role in DNA replication and recombination (Wang, 1985). DNA Gyrase is a prokaryotic Topoisomerase II and its catalytic activity is same as that of eukaryotic enzyme.

Human Topoisomerase II

Topoisomerase II (TopoII) is uniformly distributed along the chromosomes (Heck et al., 1988; Hsiang et al., 1988) and is uniquely required for segregation of completely replicated daughter molecules during mitosis (Snapka et al., 1988) and meosis (Holm et al., 1985; Uemura and Tanagida, 1986).

In mammals TopoII is found in two isoforms, 170 kDa, α and 180 kDa, β (Woessner et al., 1991). Both the isoforms show structural similarity but are genetically, immunologically and biochemically distinct. They show distinct cellular localization and cell cycle expression profiles. TopoIIα activity is shown

to be highest during the G2/ M phase of the cell cycle (Heck et al., 1988). Whereas, TopoIIβ isoform shows constant expression throughout the cell cycle (Woessner et al., 1991). TopoIIα is distributed in the nucleoplasm (Woessner et al., 1991) in contrast to TopoIIβ, which is localized in the nucleolus during interphase and in the cytoplasm during mitosis (Negri et al., 1992). Both the isoforms show different patterns of tissue distribution. TopoIIα is shown to be higher in testes, spleen, bone marrow and liver. The genes coding for the TopoIIα and β proteins map to chromosomes 17q21-22 and 3p24 respectively.

Structure of Topoisomerase II β (Berger et al., 1996)

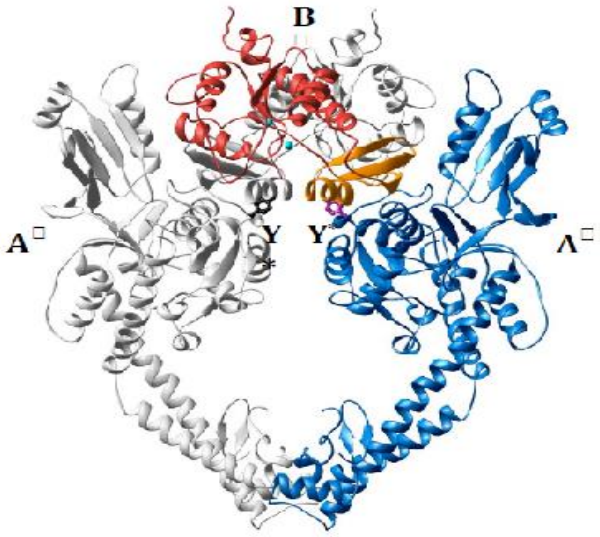

Structure of Topoisomerase II Ageing

The crystal structure of TopoII was worked out by Berger et al., (1996). The study shows that TopoII in its active form is a heart shaped homodimer with a large central hole. The monomer is a flat crescent shaped fragment, which can be divided into three discrete domains. The first is the binding domain in the N-terminal region (B' region). It has a consensus sequence for ATP binding and has

the capacity to hydrolyze ATP. This domain dimerizes with the other monomer upon binding to ATP and imposes a conformational change all over the enzyme, required for catalytic activity. The second is the DNA binding domain or the DNA breakage/reunion domain, present in the A' region. The active site tyrosine's, which associate with the broken ends of DNA during the catalytic cycle, are present in this domain. The third is the primary dimer interface in the C-terminal region, which forms the dimer interface of the enzyme by associating with the other monomer. Apart from forming the dimer interface, this region is also implicated in regulation of enzyme activity and nuclear localization.

Catalytic Activity of Topoisomerase II (Berger et al., 1996)

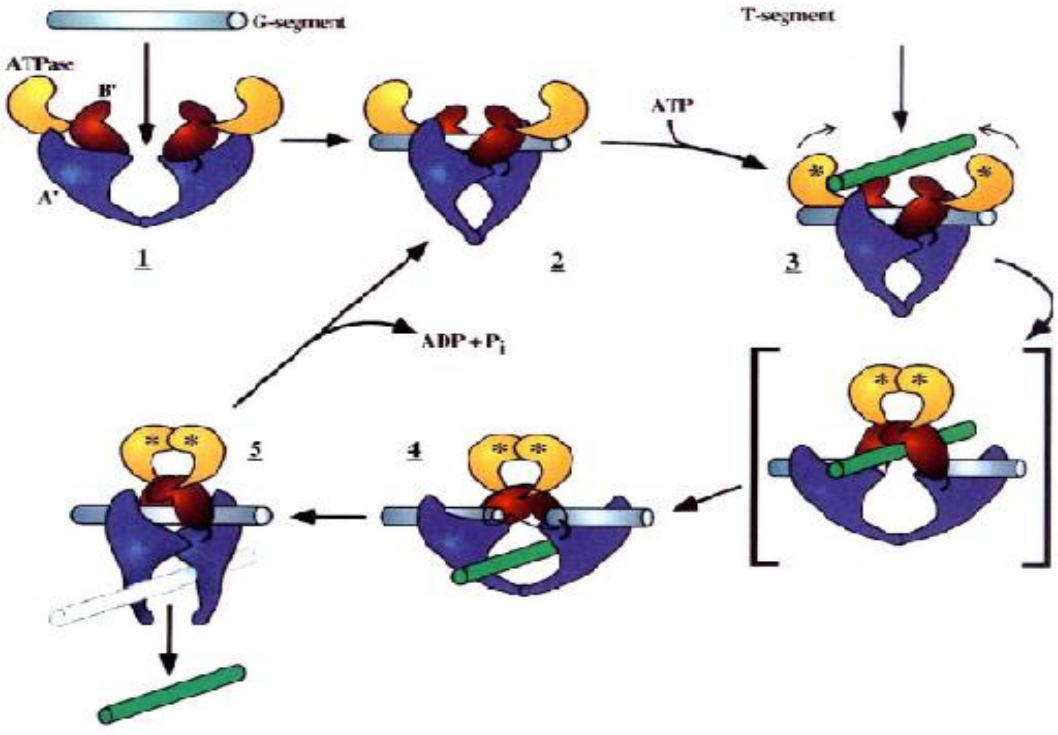

Catalytic Activity of Topoisomerase II

In its catalytic cycle (Berger et al., 1996), the topoisomerase II dimer first binds to a duplex DNA segment termed as the 'G' (gated) segment and undergoes a conformational change. It then binds to ATP through its ATP binding domain and also binds to a second DNA segment called the 'T' (transported) segment. This binding causes a series of conformational changes in the enzyme, which causes the A' regions to be pulled apart from each other, leading to cleavage of the G-segment in both the strands, four base pairs apart. The active site tyrosine in the DNA binding domains then forms covalent bonds.

The molecular model for the catalytic reaction of Topoisomerase II

The ATPase domain, B' and A' subfragments are coloured yellow, red and blue respectively. The G-segment DNA (containing the DNA gate) is grey, and the transported T-segment is green with the nicked DNA strands through a trans-esterification reaction between the phenolic hydroxyl groups of the tyrosine and the 5'-phosphoryl ends of the nicked DNA. Concomitantly, the ATP domains dimerize and the T-segment is transported through the gate formed by the nicked DNA into the central hole. Following this transport, the G-segment is rejoined by a second trans-esterification reaction and the T-segment is transported out of the enzyme through the opening formed in the dimer interface. The monomers immediately dimerize at the interface and the ATP is hydrolyzed and released. This regenerates the starting state and the enzyme is ready to begin a fresh catalytic cycle. The DNA cleavage/relegation reactions do

not require energy from a high-energy co-factor (like ATP) because the phosphate bond energy is conserved in the two successive trans-esterification reactions (Roca, 1995). The ATP binding and hydrolysis is only involved in introducing conformational changes in the enzyme for carrying out its catalytic functions and not for DNA nicking and resealing.

Functions of Topoisomerase II

TopoII enzyme has an ability to promote topological interconversions of DNA. It plays an important role in various cellular processes such as chromosome segregation, chromosome condensation, replication, transcription, maintaining the genomic integrity and recombination (Ju et al., 2006; Osheroff et al., 1991; Wang, 1996).

Topoisomerase II β and DNA repair

The catalytic activity of TopoII is known to be stimulated by abasic, oxidized and monoalkylated DNA (Sabourin and Osheroff, 2000). Since these studies covered only plasmids containing abasic sites, it is difficult to extrapolate the significance of these findings to highly structured cellular DNA. TopoIIβ has been reported to participate in the repair of melphalan induced DNA crosslinks in myelogenous leukemia, wherein TopoIIβ levels are determinant of the magnitude of DNA crosslinks and cell survival, following treatment with melphalan (Emmons et al., 2006).

Topoisomerase II β and Brain ageing

A significant activity of Topoisomerase IIβ (TopoIIβ) in nuclei isolated from postmitotic neuronal cells was reported before (Tsutsui et al., 2001). TopoIIβ is also shown to be expressed in other nonproliferating and fully differentiated tissues (Capranico et al., 1992). Of the two isoforms, beta isoform is predominant in the brain (Tsutsui et al., 2001). The level of TopoIIβ in the brain decreases during ageing (Kondapi et al., 2004) and TopoIIβ deficient SK-N-SH, neuroblastoma cells and granule neurons show sensitivity to peroxide mediated DNA damage in a non-homologous end-joining pathway (Mandraju et al., 2008; Mandraju et al., 2011), thus implicating the role of TopoIIβ in DNA repair pathways.

Neurons

Neurons are nerve cells that transmit nerve signals to and from the brain at up to 200 mph. Neuron consists of a cell body (or soma) with branching dendrites (signal receivers) and a projection called an axon, which conducts the nerve signal. At the other end of the axon, the axon terminals transmit the electro-chemical signal across a synapse (the gap between the axon terminal and the receiving cell). German scientist by the name Heinrich Wilhelm Gottfried von Waldeyer-Hartz coined the term "neuron" in 1891 (he also coined the term "chromosome"). The axon is a long extension of a nerve cell that takes information away from the cell body. Bundles of axons are known as nerves or, within the CNS (central nervous system), as nerve tracts or pathways. Dendrites

bring information to the cell body. Myelin coats and insulates the axon (except for periodic breaks called nodes of Ranvier), increasing transmission speed along the axon. Myelin is synthesized by Schwann's cells and consists of 70-80% lipids (fat) and 20-30% protein. The cell body (soma) contains the neuron's nucleus (with DNA and typical nuclear organelles). Dendrites branch from the cell body and receive messages. A typical neuron has about 1,000 to 10,000 synapses (that is, it communicates with 1,000- 10,000 other neurons, muscle cells, glands, etc.).

Different types of neurons

There are different types of neurons. They all carry electro-chemical nerve signals, but differ in structure (the number of processes, or axons, emanating from the cell body) and are found in different parts of the body.

- **Sensory neurons or Bipolar neurons** carry messages from the body's sense receptors (eyes, ears, etc.) to the CNS. These neurons have two processes. Sensory neurons account for 0.9% of total neurons. Examples are retinal cells and olfactory epithelium cells.
- **Motoneurons or Multipolar neurons** carry signals from the CNS to muscles and glands. These neurons have many processes originating from the cell body. Motoneurons account for 9% of all neurons. (Examples are spinal motor neurons, pyramidal neurons and Purkinje cells.)
- **Interneurons or Pseudopolar** cells form all the neural wiring within the CNS. These have two axons (instead of an axon and a dendrite). One axon communicates with the spinal cord and the other communicates with either

the skin or muscle. These neurons have two processes. Examples are dorsal root ganglia cells.

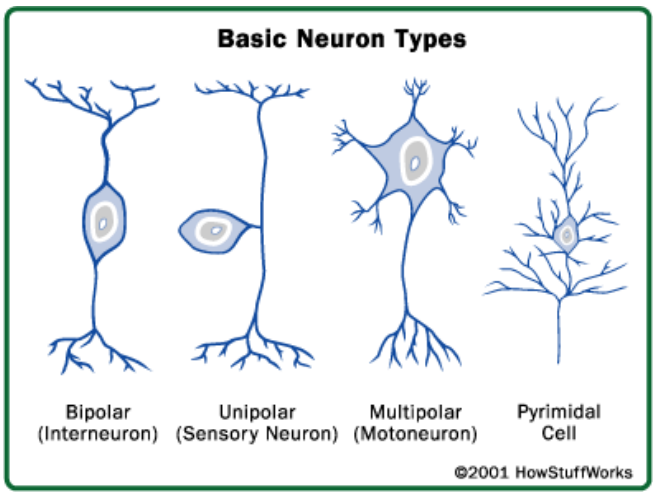

Cell culture as a model for ageing

Animal models used in ageing research are chosen primarily because of their short life span. The use of short-lived animals for ageing research assumes that there is relevance to the much longer human life span and that fundamental ageing processes are conserved between species. Cell culture approaches make it easier and possible to study tissue-specific and cell-specific ageing rather than using animal models which are complex.

The ageing experiments using cell cultures can be dated back to twentieth century. Carrel (1912) performed a series of experiments, where he dissociated cells from chicks, placed them in culture, and showed by subculturing that the cells were seemingly capable of proliferating indefinitely. The conclusion was that organismal mortality (and ageing) was a consequence of multicellularity. The logic behind this equivalence, however, was faulty.

Cell cultures are widely used as models to study the molecular mechanisms of ageing. Numerous studies performed on cultured human fibroblasts (Wistrom and Villeponteau, 1990), T lymphocytes (Pawelec et al., 1997) and several other types of mammalian cells (Augustin-Voss et al., 1993; Peterson, 1995) demonstrated that normal dividing cells have a finite proliferation capacity *in vitro*. This phenomenon is interpreted as ageing at the cellular level and is known as ''replicative senescence'' (Hayflick, 1985b). Replicative senescence is limited to cells that have the ability to divide *in vivo*, and hence does not apply to postmitotic cells such as mature neurons or muscle. There are other factors that lead cells to senescence, such as oxidative stress, double DNA breaks, expression of certain oncogenes (e.g. activated RAS or RAF), modifications in chromatin structure or changes in energy metabolism (Campisi, 2001). However, the question remains, whether investigation of replicative senescence will shed insight into the senescence of postmitotic differentiated cells (Cristofalo, 1996; Rubin, 1997). Several investigators suggested that the ''stationary phase'' cell cultures (Rubin, 1997) might be a more advisable model to study mechanisms of ageing of postmitotic differentiated cells.

Cerebellar granule neurons (CGNs) as a model for ageing

Ageing of neuronal cells *in vitro* was not described until the end of the twentieth century (Lesuisse and Martin, 2002; Toescu and Verkhratsky, 2000a). Providing the optimal conditions over long period of time was the biggest obstacle. Hippocampal and cortical neurons have been described as being able to survive up to 60 days in culture (Lesuisse and Martin, 2002).

CGNs constitute the largest homogenous neuronal population of mammalian brain. CGNs of the cerebellum are vital for co-ordination and control. Associated disorders and symptoms of cerebellum include tremors, nystagmus (involuntary movement of the eye) and ataxia (lack of co- ordination). Previously, long-term cultures of CGNs were shown to survive *in vitro* for a maximum of 17 days (Ishitani et al., 1996), while, CGNs could be maintained for 23 DIV (days *in vitro*) in studies on the Ca^{2+} homeostasis related to ageing (Toescu and Verkhratsky, 2000b). CGNs were chosen for this study because primary cultures of postnatal rat cerebellum make an excellent model system for molecular and cell biological studies of neuronal development and function. CGNs have been used to study cellular and molecular correlates of mechanisms of survival/ apoptosis and neurodegeneration/ neuroprotection (Contestabile, 2002). Many fundamental insights into the phenomena of apoptosis, migration and differentiation in neurons in the mammalian central nervous system have come from investigating granule neurons *in vitro*. These cells may prove invaluable in uncovering the connecting links between senescence and repair pathways.

DNA damage

Genomic integrity is very essential for the survival of any organism and damage to it may be dangerous to the survival of the organism since genetic information of all organisms and many viruses is stored in the form of stable DNA moleculs. Any deleterious mutation in the coding region of an important enzyme or protein of an open reading frame of a gene results in the abnormal expression of the

gene. DNA is subject to both endogenous and exogenous events. Many of the DNA modifications have been shown to be mutagenic *in vitro* and *in vivo* (Loeb, 1989). The endogenous DNA damaging agents are free radicals, reactive oxygen species (ROS) and alkylation of DNA. Free radicals are generated during several metabolic processes in the cell and also ionizing radiation and they react with many cellular components especially DNA. Free radicals produce a variety of oxidative DNA damage including single strand breaks (SSB) and double strand breaks (DSB) AP sites and cross links (Rao, 2007). ROS can be cause of spontaneous DNA damage and alkylation of DNA by S-adenosyl-L-methionine the normal intracellular methyl group donor (Barrows and Magee, 1982; Rydberg and Lindahl, 1982). This leads to the formation of N7 methyl guanine, N3b methyl adenine, N3 methyl thymine and small amounts of O6-methyl guanine. The methylation of adenine and guanine bases cause destabilization of the N-glycosylic bond, resulting in an increased spontaneous cleavage and the formation of AP sites (Lindahl and Nyberg, 1972).

The major source of exogenous DNA damage is UV, X-ray, gamma rays and mutagens and carcinogens present in human diet such as polycyclic aromatic hydrocarbons (PAH), aflotoxin B1 and nitrosamine (Ames, 1983). UV forms cyclobutane pyrimidine dimers (Setlow, 1982). UV irradiation also induces DNA-protein cross links and single strand breaks (Lai et al., 1987; Peak et al., 1985). Ionizing radiation causes single and double strand breaks and cross-links (Hutchinson, 1985; Scholes, 1983). PAH, aflotoxin B1 and nitrosamines react with DNA, inducing several types of damages including single and double strand breaks and bulky adducts.

Approximate frequencies of occurrence of endogenous DNA damage in mammalian cells

Damage	Events per cell per day	Reference
Depurination	10,000	(Lindahl and Nyberg, 1972)
Depyrimidination	600	(Lindahl and Karlstrom, 1973)
Deamination	100-300	(Lindahl and Nyberg, 1974)
Single-strand breaks (Including all types of base damage viz. oxidative damage, adduct formation with reducing sugars, methylation, cross-links)	10,000	(Saul 1985)
Double-strand break	9	(Bernstein and Bernstein 1991)
Interstand cross link	8	(Bernstein and Bernstein 1991)
DNA-protein cross link	unknown	(Bernstein and Bernstein 1991)

Reactive oxygen species and DNA damage in neurons

Reactive oxygen species (ROS) are continuously formed as a consequence of normal metabolism and in response to environmental factors such as UV light, ionizing radiation, heat and pollution (Ames et al., 1986 and Halliwell et al., 1999). ROS encompass a variety of chemical species including superoxide anions (O2•), hydroxyl radicals (•OH) and hydrogen peroxide (H_2O_2) (Halliwell et al., 1999) Metabolic stress inevitably rises the levels of ROS in tissue. If the amount of ROS overwhelms the capacity of cells to counteract these harmful species, oxidative stress occurs and can induce various types of cell damage such as

modifications of proteins, lipids and DNA leading to mitochondrial and ultimately cellular dysfunction (Beckman and Ames, 1998; Young and Woodside, 2001). Neurons seem to be particularly vulnerable to oxidative stress due to the substantial amount of oxygen consumption by the brain, the low glutathione content and a high proportion of polyunsaturated fatty acids in neurons (Christen, 2000; Rutten et al., 2002). Furthermore, neuron is a postmitotic cell, which implies that, in case they are irreversibly damaged or lost, they cannot be replaced. Accumulation of DNA damage in neurons has long been suggested to be one of the major forms of damage involved in brain ageing and neurodegeneration (Bohr et al., 1998; Hamilton et al., 2001). More than 100 different types of DNA lesions have been reported, including base modifications (for instance, 8-oxo- 7, 8-dihydro-2`-deoxyguanosine [8-oxo-dG], thymidine glycol, and 8-hydroxycytosine), single- and double-strand breaks, and interstrand cross-links (Cooke et al., 2003; Vijg and Uitterlinden, 1987). Among these, DNA single strand breaks (SSBs) are the most common ones and are the most common lesions induced by ROS and exogenous genotoxins such as ionizing radiation and alkylating agents (Caldecott, 2004).

DNA repair

As a major defense against the environmental damage to cells, DNA-repair is present in all the organisms studied to date, including bacteria, yeast, fish, amphibians, rodents and humans. The DNA repair process would minimize cell killing, mutations, persistent DNA damage and errors in replication. Although the number of gene products that are involved in DNA repair is large in many

organisms (more than 100 genes), nature makes use of a rather limited number of protein domains for DNA repair processes (Aravind and Koonin, 1999; Wood et al., 2005).

There are three major DNA repair pathways to counteract the different types of DNA damage.

1) A simple reversal of damage

2) Recombinational repair including the end joining

3) Excision repair including mismatch repair

1) A simple reversal of damage

Direct reversal of DNA damage is a simple and important way of dealing with certain DNA lesions. Examples for this mechanism are the removal of alkyl groups by the ubiquitous enzyme alkyltransferase, reversal of the UV-induced pyrimidine dimer by the enzyme photolyase, or direct ligation of DNA single strand breaks (Friedberg et al. 1995, (Eisen and Hanawalt, 1999). Reversal of damage can take place by a single protein, e.g. O6–methyl guanine methyltransferase, which removes methyl groups from O6 –methyl guanine thus avoiding a mismatch formation since O6 –methyl guanine can pair with both C and T (Mitra and Kaina, 1993). In these modes of repair there is no cleavage of DNA, but chemical alterations are simply reversed *in situ*.

2) Recombinational type of repair

Both DNA DSBs and interstrand cross-links are unusual lesions, since they alter both strands of the DNA molecule (Thompson and Schild, 1999). If left unrepaired, DSBs lead to broken chromosomes and cell death, and if repaired incorrectly, they can lead to chromosome rearrangements and cancer (Chu,

1997). Recombination can occur either by the homologous recombination repair (HRR) or non-homologous end joining (NHEJ), the latter mode being less accurate.

3) Excision repair including mismatch repair

Excision repair is the most prominent and perhaps most universal in maintaining the genomic integrity. Essentially, the strategy of this pathway consists of 4 steps.

1) Recognition of the damage site

2) Excision of the damaged portion

3) Resynthesis of the removed sequence by DNA polymerases

4) Ligation of the newly synthesized strand by ligases.

The excision repair consists of 3 major pathways: nucleotide excision repair (NER), base excision repair (BER) and mismatch repair (MMR).

Nucleotide excision repair (NER)

NER is a highly sophisticated and versatile DNA damage removal pathway. NER removes predominantly bulky DNA adducts and damage that distorts the DNA structure considerably. NER is able to handle a multitude of DNA lesions, the most relevant of which may be the damage inflicted on DNA by the UV component of sunlight (de Laat et al., 1999). Substrates for NER are damage due to exposure to UV irradiation, adduct by with a variety of compounds like cisplatin, psolaren and carcinogens like acetlyaminoflourine etc. NER differs from BER in that the excision patch is quite long in NER when compared to the shorter patch in BER.

In the case of UV induced damage, incision occurs precisely at 6 bases 3' to the damage and 22 bases 5' to the damage, thus releasing a 29 nucleotide fragment (Tanaka and Wood, 1994). It is for this reason that NER is considered as 'long patch repair'.

Mismatch repair (MMR)

MMR plays a significant postreplicative role in safeguarding the integrity of the genome virtually in all organisms from bacteria to mammals. This repair pathway corrects base–base and insertion/deletion (I/D) mismatches that have escaped the proofreading function of replicative polymerases. The human and the bacterial DNA MMR systems are very similar not only in structure, but also in function.

MMR confers to the genome a 100–1000 fold protection against mutations arising during DNA replication (Loeb, 1994). The MMR machinery scans and repairs newly replicated DNA by excising the mutated strand in either direction to the mismatch. In its absence, cells assume a mutator phenotype in which the rate of spontaneous mutation is greatly elevated. The discovery that defects in MMR segregate with certain cancer predisposition syndromes highlights its essential role in mutation avoidance. Mutations in one of the human DNA MMR genes, hMSH2, account for approximately half of all cases of genetically linked hereditary nonpolyposis colorectal cancer (Fishel et al., 1993; Hemminki et al., 1994) and inactivation of the mouse MSH2 gene results in a lymphoproliferative disorder and a predisposition to malignancy (de Wind et al., 1995).

Base excision repair (BER)

The BER pathway consists essentially of 4 steps and can be divided into two sub pathways; one termed 'short patch or single nucleotide replacement pathway' and the other 'long patch pathway' involving the insertion of upto 13 nucleotides. Step one of short patch pathway consists of the recognition and cleavage of an altered base (DB) from the deoxyribose phosphate moiety by an appropriate DNA-glycosylase. This enzyme also allows the AP endonuclease (Ape1) to reach the site. Multiple DNA glycosylases with varying substrate specificity are continuously scanning the DNA. For example, eight human nuclear glycosylases have been cloned to date (Scharer and Jiricny, 2001). Some DNA-glycosylases recognize and remove 8-oxo-dG opposite C (Radicella et al., 1997; Rosenquist et al., 1997), oxidative forms of bases like thymine glycol, cytosine glycol, dihydrouracil (Hilbert et al., 1997) and alkylated adenine like 3-methyl adenine, ethenoadenine and hypoxanthine (Chakravarti et al., 1991; Samson et al., 1991). In the second step, the DNA chain at the 5'-side of the abasic site is cleaved by a major endonuclease Ape1 specific for abasic damage. Ape1 is the major AP endonuclease in humans, also known as HAP1, APEX, and REF1 (Demple et al., 1991; Robson et al., 1992; Seki et al., 1992). The enzyme flips out the baseless deoxyribose and cleaves it on the 5' side. Also, like in the case of the 1st step, this enzyme, still bound to DNA, attracts and interacts with DNA Polymerase β (Pol β), which is involved in the next step in the repair pathway. The glycosylase dissociates from DNA at this point. In the third step, Pol β fills up the one-nucleotide gap and also releases the 5'-2-deoxyribose-5 phosphate (dRP). At the same time, DNA ligase III - XRCC1 (X-ray repair cross-complementing, gene I)

complex arrives at the site. In the fourth step, DNA ligase III seals the nick and Pol β dissociates from the site. Subsequently the XRCC1 and ligase III complex comes off from the site, leaving behind repaired DNA. Human XRCC1 not only complexes with DNA ligase III but also interacts with other core enzymes involved in BER and is therefore thought to play a crucial role in protein exchanges in the pathway. Eukaryotes, in contrast to prokaryotes, contain more than one DNA ligase, and these enzymes have distinct roles in DNA metabolism. Five DNA ligase activities, I-V, have been purified from mammalian cell extracts. Ligase III is more specifically involved in DNA repair and recombination. The predominant route for BER is the 'short patch or single nucleotide pathway'.

In case of long patch repair, Pol β is replaced by Pols δ or ε, which conducts strand displacement synthesis (Fortini et al., 1998). This long patch repair requires the activator proliferating nuclear antigen (PCNA) and a 'flap' structure specific endonuclease-1 (FEN1) activity to cut the flap like structure produced by strand displacement synthesis (Klungland and Lindahl, 1997; Wu et al., 1996). Nealon et al., (1996) suggested that while Pol β is the major BER polymerase in human cells, other polymerases also contribute to a significant extent.

Schematic representation of base excision repair (BER) (Rao, 2007)

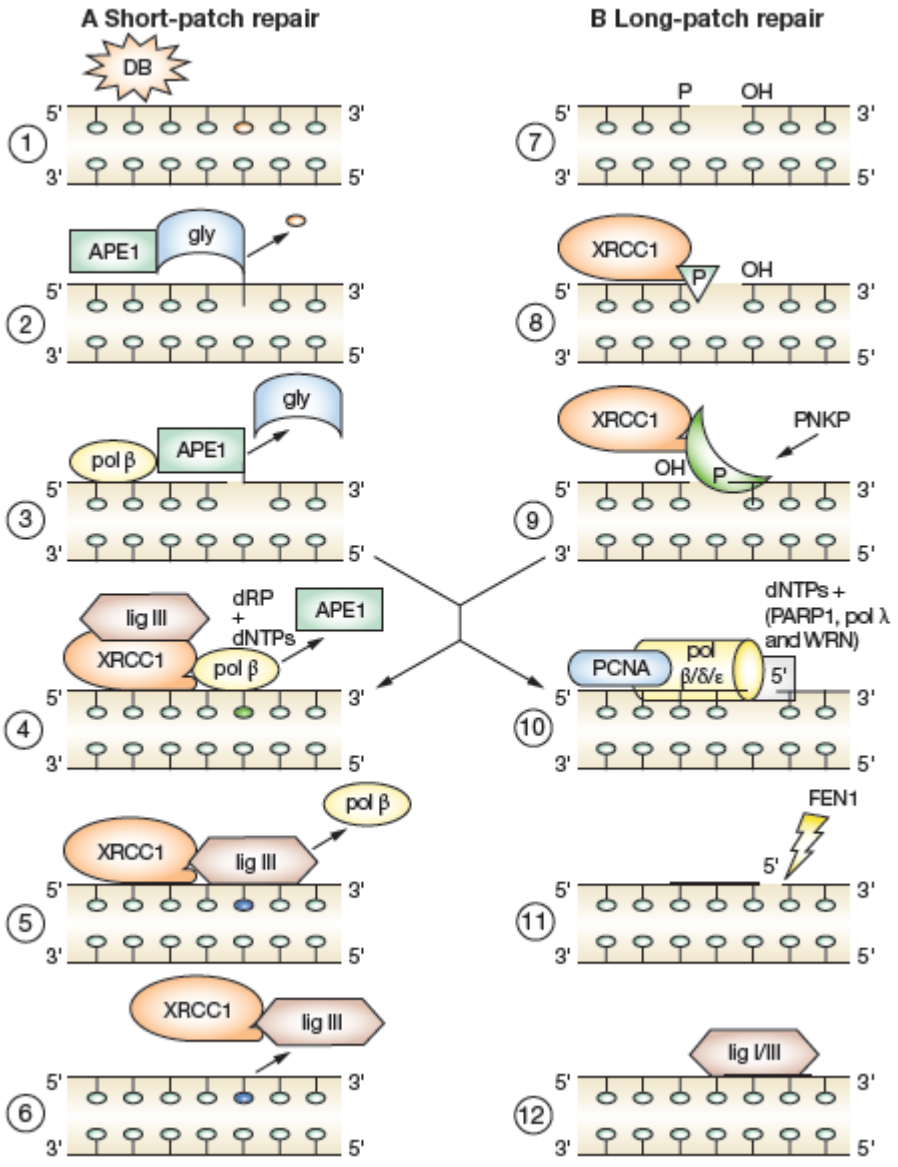

Crossing over of the pathways can occur at points 2 and 7. Abbreviations: DB, damaged base; GLY-DNA, glycosylase; Pol β/ δ/ ε, DNA polymerase β/ δ/ ε respectively; LIG I/III, DNA-ligase I/III; PARP1, poly (ADP-ribose) polymerase 1;dNTPs, deoxynucleoside triphosphates.

DNA repair and human neurological disorders of ageing

DNA repair disorders refer to a group of conditions that are characterized by a failure of distinct cellular DNA repair mechanisms to function properly. The consequences of these failures are far reaching and extend to abnormalities

related to normal growth and development, ageing (normal and premature), programmed cell death and cancer inherited conditions. Some of these inherited disorders are closely associated with defective DNA-repair. A few have been briefly explained below.

Xeroderma pigmentosum (XP)

XP is a DNA repair disorder related to the NER pathway. It is an autosomal recessive disorder characterized by cutaneous photosensitivity, pigmentary changes and a propensity for the early development of malignancies in sun exposed mucocutaneous areas, including the eye (Kraemer et al., 1987). Photosensitivity and the high cancer incidence observed in XP patients are due to mutations in genes that are unique to global genomic repair and have no role in transcription-coupled repair; for example XPC and DDB1 (XPE), and replication polymerase η (Day, 1975; Epstein et al., 1970; Eveno et al., 1995; Kraemer et al., 1994; Rao, 2007). Most cases are symptomatic in childhood, except for an adult variant form. The predominant symptoms include sun sensitivity and photophobia. Also seen are neurological abnormalities in about 20% of the patients (Kraemer et al., 1987; Vermeulen et al., 1994). Mutations in seven different genes have been reported in patients with XP. These include genes involved in complementation groups (XPA, ERCC3 [XPB], XPC, ERCC2 [XPD], DDB1, ERCC4 and ERCC5) that have a role in NER (Subba Rao 2007).

Cockayne syndrome (CS)

CS was first reported in 1936 by Edward Alfred Cockayne, a British physician. CS is an early-onset, progressive neurological disorder characterized by dwarfism, microcephaly, mental retardation, sensitivity to sunlight, retinal degeneration, partial deafness and facio-skeletal and/orgait abnormalities with no increased cancer incidence (Soffer et al., 1979). In terms of its neuropathology, the CS brain shows increased fibrosis, neuronal dystrophy and an accumulation of senile plaques and/or neurofibrillary tangles along with progressive demyelination or dysmyelination (Bohr et al. 2005). This syndrome is not associated with cancer or loss of personality. The two proteins found to be mutated in this syndrome, ERCC8 and ERCC6, have been shown to be required for transcription-coupled repair (Subba Rao 2007).

Ataxia telangiectasia (AT) and Nijmegen breakage syndrome (NBS)

AT is characterized primarily by cerebellar degeneration, immunodeficiency, genome instability, clinical radiosensitivity and cancer predisposition. NBS shares all these features except cerebellar deterioration. The cellular phenotypes of AT and NBS are almost indistinguishable, however, include chromosomal instability, radiosensitivity, and defects in cell cycle checkpoints normally induced by ionizing radiation (Shiloh, 1997).

The protein product of the gene responsible for AT, designated ATM, is a member of a family of kinases characterized by a carboxy-terminal

phosphatidylinositol 3-kinase-like domain. The NBS1 protein is specifically mutated in patients with NBS and forms a complex with the DNA repair proteins, Rad50 and Mre11 (Zhao et al., 2000). Each of these proteins function in differing aspects of DSB resolution and/or DNA-damage-checkpoint responses. It is hypothesized that the neurological dysfunction of the associated disorders arise from (i) a defect in the processing of DSBs presumably by the NHEJ pathway and/or (ii) an inappropriate DNA-damage response, quite possibly during neural development (Kulkarni and Wilson, 2008).

Alzheimer's disease (AD)

AD is a degenerative disorder of the CNS in humans. The disorder is thought to be caused by misfolding of β-amyloid and Tau proteins, which aggregate and deposit as plaques and neurofibrillary tangles (NFTs) in AD brain (Smith et al., 2000). AD is characterized by progressive neuronal degeneration, which is regarded as a feature of accelerated ageing. In AD, neurons in cerebral cortex, basal forebrain and locus ceruleus are progressively lost. There are evidences which suggest that 8-hydroxyguanine, 8-hydroxyadenine and 5, 6- diamino-5-formamidopyrimidine accumulate abnormally in both nuclear and mtDNA isolated from vulnerable brain regions in amnestic mild cognitive impairment. The earliest clinical manifestation of AD and a decrease in 8-oxoguanosine glycosylase activity was observed in the nuclear fraction of AD hippocampal and parahippocampal gyri (HPG), superior and middle temporal gyri (SMTG), and inferior parietal lobule (IPL) (Lovell and Markesbery, 2007; Lovell et al., 2000; Markesbery and Lovell, 2006).

It is noteworthy that the two DNA repair pathways that are most likely to be adversely affected in AD are BER and end NHEJ, due to limited DNA base damage processing by DNA glycosylases, reduced DNA synthesis capacity by DNA Pol β and reduced NHEJ activity as well as protein levels of DNA PK catalytic subunits (Fishel et al., 2007; Weissman et al., 2007).

Parkinson's disease (PD)

PD, which is characterized by muscle rigidity, tremors, and in extreme cases, a loss of physical movement (akinesia), is caused by degeneration of dopaminergic cells in the brain's susbtantia nigra, the region that controls voluntary movement, produces the neurotransmitter dopamine, and regulates mood (Kulkarni and Wilson, 2008). Increased levels of oxidative stress as well as expression of the mitochondrial BER enzyme 8-oxoguanosine DNA glycosylase (Ogg1) have been reported to occur in the substantia nigra region of the brain in patients with PD (Fukae et al., 2005). Robbins et al., (1983) found that cell lines from six patients with PD were significantly more sensitive to X-rays than the normal cell lines. Sensitivity to UV irradiation was normal in these patients. These results suggest that such a DNA repair defect could cause rapid, abnormal accumulation of spontaneously occurring DNA damage in PD and AD neurons *in vivo*, which results in premature death.

Spinocerebellar ataxia with axonal neuropathy-1 (SCAN1) and Triple- A syndrome

In SCAN1, there is a progressive degeneration of postmitotic neurons. (El-Khamisy et al., 2005) have recently demonstrated that this neurodegenerative

disease results from a mutation in the gene encoding tyrosyl DNA phosphodiesterase 1 (TDP1). TDP1 in human cells is required for the repair of chromosomal SSBs arising from abortive topoisomerase I activity or oxidative stress. TDP1 is a part of the multi protein SSB repair complex and directly interacts with DNA ligase IIIα, and this complex is inactive in SCAN1 cells. These findings suggest that, the TDP1-dependent SSB repair pathway is defective in differentiated neurons of SCAN1 patients. Normally, SSBs or gaps are repaired in neurons through BER, in which both DNA ligase IIIα and XRCC1 participate, along with polynucleotide kinase (Rao 2003b). It therefore seems that the TDP1-dependent SSB repair is a slightly different mode of repair, and could be of considerable importance in brain cells where it deals with SSBs resulting from a variety of causes. Triple-A (achalasia–addisonian–alacrima) syndrome, which is due to a repair defect of DNA SSBs was found to be caused by a mutation in a gene called AAAS (located on chromosome 12q13), which codes for a protein named ALADIN.

Hutchinson-Gilford progeria syndrome (HGP)

HGP is an extremely rare genetic disease that accelerates the ageing process to about seven times the normal rate. Because of this accelerated ageing, a child of ten years will have similar respiratory, cardiovascular, and arthritic conditions that a 70-year-old would have. Currently, there is no cure for this disease, and because of its rare nature, no definitive cause can be pinpointed. Some physical features of progeria children include dwarfism, wrinkled/aged-looking skin, baldness, and a pinched nose. Mental growth is equivalent to other children of

the same age. Most children with progeria live no longer than their early teenage years. Cultured HGP fibroblasts have been reported to have decreased ability to repair single strand breaks following gamma irradiation (Epstein et al., 1974; Little et al., 1975).

More than 150 human genetic disease syndromes involve abnormalities in normal ageing and repair. Syndromes like AT, PD, XP and CS display elevated DNA damage and premature ageing. Although we know of no single mutation that lengthens the maximum life span, it is evident that the number of mutations shorten life. The work presented in this thesis was conceptualized to essentially characterize the ageing and TopoIIβ involvement in the BER in an *in vitro* cell culture model, CGNs, to find clues that would slow down ageing process. Use of an *in vitro* culture model like CGNs helps to perform more number of studies in a short span of time thus enabling cell type-specific study. There has been abundant amount of work done in order to understand the ageing phenomena and age-associated degenerative diseases. Nevertheless, the causes of ageing and age associated diseases (such as Parkinson's or Alzheimer's) are still unanswered. Understanding the mechanism of molecular events that control neuronal degeneration, cell death is critical for design and development of new strategies that help prevention and treatment of neurodegenerative diseases and ageing process. Brain ageing and neurodegenerative diseases share a common predisposing factor, which poses several basic questions. First, how can a neuron survive for years and remain functionally competent? Second, do neurons possess unique mechanisms for the repair of DNA and protein damage and protection against toxic free radicals? And finally, how and when do these quality

control and repair systems break down? Studying neurodegenerative diseases or creating and studying ageing model systems should help towards this goal.

The present study constitutes the continued effort of this laboratory to assess the validity of the hypothesis that accumulation of DNA-damage and decreased DNA-repair capacity is at least one of the major naturally chosen genetic switches for initiating the phenomenon of ageing and its associated disabilities. The emphasis of this work is on brain cells.

Rationale

- Correlation of decrease in repair capacity of ageing brain with concomitant decrease in TopoIIβ levels and deficient peroxide induced DSB repair in TopoIIβ knock-down neuronal cell lines as well as in primary granule neurons, implicates an association of TopoIIβ in sustaining the double stranded break repair capacity through NHEJ pathway.

- It is understandable that TopoIIβ, due to its DSB inducing and rejoining activity, may be associated with DSB repair activity for the maintenance of torsional integrity. But then, what might be its role in Base Excision Repair, a repair pathway that is more predominant in brain specifically in neurons at a high frequency? The present study investigates the role of TopoIIβ in ENU mediated BER activity. Results presented in Chapter 3 indeed point out that TopoIIβ is critical component for BER activity in granule neurons.
- To model damage and repair events occurring during ageing, we analyzed the factors involved in DNA damage and repair processing during natural ageing of granule neurons in culture. The studies presented in Chapter 4

corroborates with the "Oxidative damage of DNA and repair theory" of ageing.

- It would be interesting to identify the key molecular markers upregulated during ageing in line with the downregulation of TopoIIβ to understand the molecular events of senescence and to identify the hallmark of senescence. An attempt was made to identify a few genes in Chapter 5 of this thesis.

Thus, the objectives were framed as below:

Objectives

1) Role of TopoIIβ in Base excision repair in CGNs

2) Modeling Senescence-associated stress responses and repair in *in vitro* cultured CGNs

3) Analysis of gene expression elevation during ageing of CGNs in culture

CHAPTER 2

MATERIALS AND METHODS

2.1. Chemicals

The following antibodies were used in the present study at the indicated dilutions: Anti-TopoIIβ monoclonal at 1: 500 (BD Biosciences, NJ, USA); Anti-β actin monoclonal at 1: 1000 (Sigma chemical Co., MO, USA); goat anti-mouse HRP IgG at 1: 5000 (Upstate, MA, USA). Reagents used were: poly-D-lysine, ENU, Bradford reagent, creatine phosphate, creatine phospho kinase, NAD, ATP, Sephadex G 50, acrylamide, bis-acrylamide, DAPI, Camptothecin (Sigma chemical Co., MO, USA); Earle's balanced salt solution (EBSS), minimal essential medium (MEM), penicillin streptomycin, fetal bovine serum (FBS), Trypsin, Glutamax (GIBCO, NY, USA); dNTPs (Fermentas, MD, USA); pure enzymes T_4 DNA ligase (Invitrogen, NY, USA); APE1 (Trevigen, MD, USA); UDG and T_4 polynucleotide kinase (Bangalore Genei, India); recombinant human DNA polymerase β was kindly gifted by Dr. Rajendra Prasad and Dr. Samuel Wilson, (Laboratory of Structural Biology, National Institute of Environmental Health Sciences, Research Triangle Park, NC, USA); [γ-^{32}P]ATP and [α-^{32}P]dCTP were purchased from BRIT (Mumbai, India); Super signal west pico chemiluminescent substrate (Pierce, IL, USA). All the other chemicals and reagents were of biochemical grade.

2.2. Animals

Wistar rats were maintained in accordance with the animal ethics committee approval, University of Hyderabad. The rats were maintained in a pathogen-free environment with a 12 h light and darkness cycle. Food and water were provided *ad libitum*.

2.3. Cell culture and treatment

Primary CGNs were prepared from the cerebella of postnatal 6- to 8-day-old Wistar pups by cervical dislocation and the tissue was stored in ice-cold EBSS. The tissue was minced in 0.1% trypsin as previously described (Wilkin, 1995). The CGN cultures were prepared by triturating and diluting the cell pellet with the plating medium (MEM supplemented with 10% FBS, 33 mM glucose, 24.5 mM KCl, 1x Glutamax, 5 mg/mL and 5000 U/mL of penicillin streptomycin). Cells were plated at 2.5 × 10^6 cells/ 60 mm dish and were grown at 37 °C in 5 % humidified CO_2 atmosphere. After 24 h of plating, the entire medium was changed and 10 μM of cytosine arabinoside, a mitotic inhibitor was added to inhibit the growth of astrocytes and glial cells. Neuronal cell cultures were fed weekly once by replacing with fresh culture medium. Day of neuronal isolation was considered as day 1 and CGNs were aged for 5 weeks (5W). Cells were pelleted week-wise (at an interval of 7 days) starting from day 3. The cells were maintained for 7 days after which they were treated with 1 and 2 mM, ENU for 12 h. The treated cells were also recultured for 48 h in fresh medium for recovery and induction of repair activity. At the end of 12 h and 48 h of recovery, the cells were pelleted and extracts prepared as described in Section 2.10.

2.4. CGNs as long-term culture

CGNs were cultured for 5 weeks. The culture was split into 5 dishes to carry out experiments. Day of neuronal isolation was considered as day 1 and CGNs were aged for 5 weeks (5W). Cells were pelleted week-wise at an interval of 7 days,

starting from day 3. 1W to 5W corresponds to 1st week to 5th week. At one week intervals, the assays described below were performed.

2.5. Cell viability assay

Neuronal cell viability in *in vitro* culture conditions was quantified by measuring reduction of MTT to purple insoluble dye and formazan by the mitochondrial dehydrogenases in live cells (Mosmann, 1983). Briefly, CGNs were seeded in PDL coated 96 well plates in triplicate at a density of 0.1 x 10^6 cells per well in 200 µL of complete media. At one week's interval the cells were subjected to this assay. 20 µL of MTT (stock- 5 mg/mL) was added to each of the wells and incubated for 4 h at 37 °C in 5% humidified CO_2 atmosphere. The plates were then centrifuged at 1,500 rpm for 20 min at room temperature and the medium was carefully aspirated. DMSO was added to dissolve the formazan crystals and absorbance was then measured at 570 nm using a V-550 spectrophotometer (Jasco, CA, USA) with DMSO as blank. Neuronal cell viability was determined and expressed as a percentage of the control (1W old cells were taken as control).

2.6. Senescence-associated β-galactosidase (SA-β-gal) assay

Senescent cells in culture express β galactosidase that converts X-Gal substrate into intracellular blue precipitate at pH 6, causing the cell to stain blue (Dimri et al., 1995). So, SA-β-gal was used as a marker for senescence. CGNs at the time of isolation were seeded onto PDL coated cover slips. Post fixation with 2% formaldehyde/ 0.2% glutaraldehyde for 3-5 min at room temperature, cells were washed thrice with PBS and incubated in freshly prepared 5-bromo-4-chloro-3-

indolyl-β-D-galacto-pyranoside (X-gal) staining solution, (40 mM sodium phosphate, pH-6, 40 mM citric acid, 2 mM $MgCl_2$, 150 mM NaCl, 5 mM potassium ferricyanide, 5 mM potassium ferrocyanide, and 1 mg/mL X-gal) in the dark for 10 h at 37 °C (Dimri, 1995 et al). The cells were then washed in 1x PBS, mounted and bright field images were captured using an Olympus digital camera attached to an Olympus BX51 epifluorescence microscope. The positive percentages were determined by counting stained and unstained cells under a microscope at 20x magnification in 4 random fields. A minimum of 200 cells were counted and results were presented as the mean ± SD.

2.7. Immunofluorescence

Adherent CGN cultures grown on poly-D-lysine coated cover slips were washed with phosphate buffered saline (PBS). The cultures were fixed and permeabilised in 4% paraformaldehyde prepared in PBS with 0.05% Tween-20 for 5 min at room temperature. The cells were gently washed thrice with 1x PBS and blocked with 10% FBS in PBS for 1h at room temperature. The fixed cultures were incubated overnight with primary antibody at 4 °C. Next day, they were washed thrice with 1x PBS each time for 5 min. To this, secondary antibody was added with a nuclear dye, DAPI (1µg/mL) and incubated for 1 h at room temperature. This was followed by three washes and the cover slips were mounted onto glass slides with 50% glycerol. Finally, the slides were viewed under confocal microscope and images captured.

2.8. siRNA synthesis

TopoIIβ downregulation was brought about using siRNA that was synthesized as described later. Double stranded siRNA oligos were synthesized *in vitro* (Donze and Picard, 2002). In brief, desalted DNA oligonucleotides **(Table 1)** were procured from (Sigma chemical Co., MO, USA). The oligonucleotide-directed production of small RNA transcripts with T7 RNA polymerase has been described (Milligan and Uhlenbeck, 1989). For each transcription reaction, 1 nM of each oligonucleotide was annealed in 50 µL of TE buffer (10 mM Tris-HCl, pH 8.0, and 1 mM EDTA) by heating at 95 °C; after 2 min, the heating block was switched off and allowed to cool slowly to obtain double-strand DNA. Transcription was performed in 50 µL of transcription mix: 1x T7 transcription buffer (40 mM Tris-HCl, pH 7.9, 6 mM $MgCl_2$, 10 mM DTT, 10 mM NaCl and 2 mM spermidine), 1 mM dNTPs, 0.1 U yeast pyrophosphatase (Sigma chemical Co., MO, USA), 40 U RnaseOUT (Ambion, NY, USA) and 100 U T7 RNA polymerase (Invitrogen, NY, USA) containing 200 pmol of the double-strand DNA as template. After incubation at 37 °C for 2 h, 1 U RNase-free DNase (Ambion, NY, USA) was added at 37 °C for 15 min. Sense and antisense 21-nt RNAs generated in separate reactions were annealed by mixing both crude transcription reactions, heating at 95 °C for 5 min followed by 1 h at 37 °C to obtain 'T7 RNA polymerase synthesized small interfering double-strand RNA' (T7 siRNA). The mixture (100 µL) was then adjusted with 0.2 M sodium acetate, pH 5.2, and precipitated with 2.5 volumes of ethanol. After centrifugation, the pellet was washed once with 70% ethanol, dried and resuspended in 50 µL of water.

Table 1: Oligonucleotide sequences for *in vitro* transcription of TopoIIβ siRNA

Name	siRNA sense template sequence	siRNA antisense template sequence
TopoIIβ siRNA	5'-AAA GCT TAA CAA TCA AGC CCG CTA TAG TGA GTC GTA TTA -3'	5'- AAC GGG CTT GAT TGT TAA GCT CTA TAG TGA GTC GTA TTA -3'
TopoIIβ scrambled siRNA	5'- ACA CTC GAT CAA TCC AAG GAA CTA TAG TGA GTC GTA TTA -3'	5'- CAC TGG ATT GAT CGA GAT GTT CTA TAG TGA GTC GTA TTA -3'
T7 promoter	5'- TAA TAC GAC TCA CTA TAG -3'	

2.9. siRNA transfection

CGNs (1x 10^6 million) were transfected using Lipofectamine 2000 (Invitrogen, NY, USA) with 0.5 μm of non-silencing and silencing TopoIIβ siRNA. Western blot analysis was carried out with time lapse of 36 h after treatment with siRNA.

2.10. Western blotting

Protein extracts were prepared as described (Gupta et al., 2012). Briefly, 5 × 10^6 cells were harvested by scraping in ice-cold PBS and pelleted by centrifugation at 1500 × g for 5 min. The cell pellet was suspended in 100 μL of extraction buffer (20 mM Tris-HCl, pH 7.5, 0.1 mM β-mercaptoethanol, 1 mM $MgCl_2$, 0.1 mM EDTA, 5% glycerol, 0.1% Triton X-100, 0.5 mM KCl, 0.5 mM PMSF and 1 μg/mL pepstatin and leupeptin). The homogenate was kept at 4 °C for 1 h, followed by sonication for 15–20s and centrifuged at 100,000 × g for an hour in an ultracentrifuge. The supernatant containing the cytosolic and nuclear proteins was used for all the activity assays.

The protein concentration in cell lysates was measured using the Bradford reagent (Bradford, 1976). Forty micrograms of protein was separated by 7.5% sodium dodecyl sulfate polyacrylamide gel electrophoresis (SDS-PAGE) followed by transferring the gel to nitrocellulose membrane (Towbin et al., 1979). The membrane was blocked with 5% non-fat dry milk in TBS containing 0.05% Tween-20 for 1 h and then incubated overnight at 4 °C with corresponding protein specific antibody. After washing and incubating for 1 h at 22 °C with a secondary antibody conjugated with horseradish peroxidase, the membranes were washed and immunoreactive bands were visualized by chemiluminescence. To evaluate relative levels of protein, the integrated optical density of signal was determined by densitometry of scanned images using the ImageJ 1.43u software, NIH, USA.

2.11. Comet assay

DNA damage was evaluated using comet assay. Alkaline comet assay (ACA) detects single-strand breaks (SSBs), double-strand breaks (DSBs) and alkali labile sites (Singh et al., 1988)at a pH>13. Neutral comet assay (NCA) is carried out at neutral pH and scores only for double strand breaks (Ostling and Johanson, 1984). Approximately 10^5 cells were washed and suspended in 500 µL of ice-cold 1x PBS and 1.5 mL of 1% agarose was added to each sample. The agarose-cell suspension was gently layered on a frosted-glass microscopic slide that was pre-coated with 0.75% agarose and was allowed to solidify for 5 min on ice and was immediately transferred to ice-cold lysis buffer (2.5 M NaCl, 100 mM EDTA, 10 mM Tris (pH 10.0) and 1% Triton X-100) and incubated overnight at 4 °C. For ACA, after lysis, slides were equilibrated for 1 h in electrophoresis buffer

(300 mM NaOH and 1 mM EDTA, pH 13). After electrophoresis (1 h, 1V/cm), slides were neutralized with 0.4 M Tris, pH 7.5, for 30 min. For NCA, the lysis procedure is the same as described before. The slides were washed with 1x Tris-borate EDTA (TBE) buffer solution, pH 8.3 for 10 min and subjected to electrophoresis (20 min, 1V/cm). The slides were removed and washed in deionized water for 5 min. The neutralized slides placed in 100% ethanol for 5 min and then air-dried. The DNA was then stained with 20 µg/mL of ethidium bromide (Sigma Chemical Co., MO, USA) for 20 min and slides washed twice, each time for 5 min in 1x TBE.

To ensure random sampling, 50 images/ slide were captured using confocal microscope (Lieca, IL, USA). Comet parameters like tail length and tail moment were scored using CometScore™ Freeware v1.5 (TriTek Corporation, Sumerduck, VA, US). Tail moment is a measure of both the amount of DNA and distribution of DNA in the tail (Olive and Banath, 2006).

2.12. Oligonucleotides

For end labeling, equimolar concentrations of oligos **(Table 2)** and [γ-^{32}P]ATP (specific activity- 3000 Ci/mmol) were added to the reaction mixture containing T_4 polynucleotide kinase (2.5 U/pmol of substrate) and T_4 PNK buffer (70 mM Tris-HCl, pH 7.6, 10 mM $MgCl_2$ and 5 mM DTT). The reaction was carried out at 37 °C for 40 min and terminated by adding 5 µL of 0.5 M EDTA. For annealing, equimolar concentrations of oligos as indicated in **Table 2** were hybridized in a reaction mixture containing 50 mM NaCl and 5 mM $MgCl_2$ at 70 °C and allowed to cool gradually to room temperature. The annealed product was purified through

a Sephadex G50 column (Sigma chemical Co., MO, USA) and stored at -20 °C for use.

Table 2: Oligonucleotide sequences for *in vitro* activity assays

Assay	Sequence
G-U BER 	Oligo 1: 5'-GCC ATT G**U**G CTA CCG ATC GCG- 3' (21 mer) Oligo 2: 3'-CGG TAA C**G**C GAT GGC TAG CGC- 5' (21 mer)
UDG 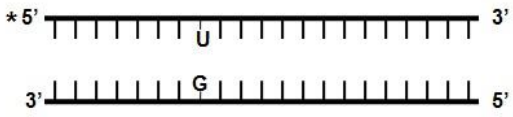	Oligo 1: *5'-GCC ATT G**U**G CTA CCG ATC GCG- 3' (21 mer) Oligo 2: 3'-CGG TAA C**G**C GAT GGC TAG CGC- 5' (21 mer)
AP 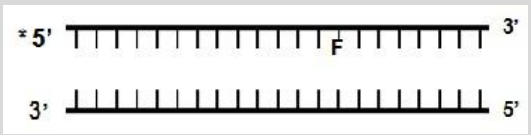	Oligo 3: *5'-CGC GAT CGG TAG C**F**C AAT GGC-3' (21mer) Oligo 4: 3'-GCG CTA GCC ATC GCG TTA CCG-5' (21 mer)
GAP 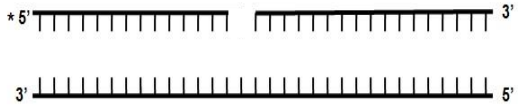	Oligo 5: *5'-CGA GCC ATG GCC GC-3' (14 mer) Oligo 6: 5'-AGA TTT TTT GCG GTG CC-3' (17 mer) Oligo 7: 5'-GGC ACC GCA AAA AAT CTG GCG GCC ATG GCT CG-3' (32 mer)
LIGASE 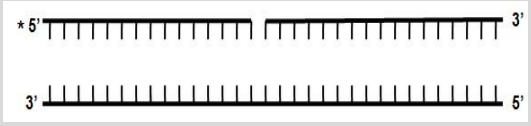	Oligo 8: *5 '-CGA GCC ATG GCC GCC-3' (15 mer) Oligo 6: 5'-AGA TTT TTT GCG GTG CC-3' (17 mer) Oligo 7: 5'-GGC ACC GCA AAA AAT CTG GCG GCC ATG GCT CG-3' (32 mer)

[γ-^{32}P]ATP end labeling has been indicated by *

Schematic representation of *in vitro* G-U BER assay

Preparation of substrate DNA for enzyme activity assays

End Labeling

- Equimolar concentrations of oligos + [γ- ^{32}P]ATP
- T4 PNK (2.5U/ pmol of subs.) + 10x T4 PNK buffer
- 40 min at 37 °C
- Terminate by adding 5 µL, 0.5 M EDTA

Annealing

- Equimolar concentrations of oligos +
- 50 mM NaCl + 5 mM $MgCl_2$
- 5 min at 70 °C
- Allow to cool gradually to RT

Purification

- Manually packed Sephadex G50 column

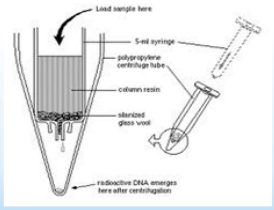

In vitro G-U BER assay

3 pmol of G-U oligo duplex

8th position

5'-gccattgUgctaccgatcgcg- 3' (21 mer)

3'-cggtaacGcgatggctagcgc- 5' (21 mer)

Protein extract (15 µg) + 1x Comp. BER buffer

Incubate for 20 min at 37 °C

Terminate reaction- 5 µL, 0.5 M EDTA

PCI extraction

Ethanol precipitation

Wash with 70% alcohol

Dry the tube overnight

Denature with bromophenol blue dye

20% Poly acrylamide urea denaturing gel (PAGE), 2300 V~3 h

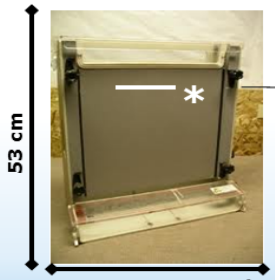

2.12.1. *In vitro* G-U base excision repair assay (G-U BER)

In vitro G-U BER assay was performed as described previously (Beard et al., 2006). U containing DNA oligo duplex was prepared by annealing oligo 1 to oligo 2 **(Table 2).** The BER activity of the neuronal extracts was assayed using the above mentioned substrate. The reaction mixture in a final volume of 50 µL contained 3 pmol of substrate, 4 mM ATP, 5 mM creatine phosphate, 100 µg/mL CPK, 0.5 mM NAD, 10 mM $MgCl_2$, 10 µCi [α-^{32}P]dCTP and BER buffer containing 50 mM HEPES, pH 7.5, 20 mM KCl, 2 mM DTT, 1 mM EDTA, pH 8. The reaction was initiated by adding 15 µg of neuronal extract and was incubated at 37 °C for 20 min. Incorporation of [α-^{32}P]dCTP by CGN extracts was used as a measure of G-U BER. The reaction was stopped by the addition of 5 µL 0.5 M EDTA. The reaction mixture was purified by extraction with phenol: chloroform: isoamyl alcohol (25:24:1). The repaired oligo duplex was recovered after 2 h by ethanol precipitation at -80 °C in the presence of glycogen at 1 µg/µL of original reaction mixture volume. The supernatant was discarded and tubes containing oligos were allowed to dry overnight, 6 µL of 6x loading dye (0.002% bromophenol blue and xylene cyanol in formamide) was added to each of the tubes and oligo duplexes were denatured at 90 °C for 5 min and snap-cooled. The reaction products along with markers were separated by electrophoresis in a 20% polyacrylamide sequencing gel electrophoresis (PAGE) with 7 M urea in 90 mM Tris-borate EDTA buffer, pH 8.3 at 2300 V for 3 h. The repaired products (21 mer) were analysed by phosphorimager followed by densitometric scan.

2.12.2. Uracil DNA- glycosylase assay

The assay was carried out as described (Swain and Subba Rao, 2011). Uracil (U) containing DNA oligoduplex was prepared by annealing a previously 5'-[γ-^{32}P]ATP labeled oligo 1 to unlabeled oligo 2 **(Table 2).** UDG activity of the neuronal extracts was assayed using the above mentioned substrate. The reaction mixture in a final volume of 20 µL containing 200 fmol of oligo duplex, 10 µg of neuronal cell extract and 1x UDG buffer (50 mM Tris-HCl, pH 7.4, 1 mM EDTA, 1 mM DTT, 25 µg/mL bovine serum albumin) was incubated at 37 °C for 20 min. The reaction was terminated by adding 3x alkali loading dye (300 mM NaOH and 97% formamide).

The reaction products along with markers were separated by electrophoresis in a 20% polyacrylamide sequencing gel electrophoresis (PAGE) with 7 M urea in 90 mM 1x TBE buffer, pH 8.3 at 2300 V for 3 h. The repaired products (21 mer) were analysed by phosphorimager followed by densitometric scan using ImageJ 1.43u software, NIH, USA. The percentage of product formed was determined using the formula [product/ (product + substrate)* 100].

2.12.3. AP endonuclease assay

The assay was performed as described (Swain and Subba Rao, 2011). Oligo duplex substrate for AP endonuclease assay was prepared by annealing a previously 5'-[γ-^{32}P]ATP labeled F containing oligo 3 to unlabeled oligo 4 **(Table 2)**, F being tetrahydrofuran, a synthetic analog of AP site. AP endonuclease activity of the neuronal extracts was assayed using the above mentioned substrate. The reaction mixture in a final volume of 20 µL containing 200 fmol of

oligo duplex,1x APE1 buffer (10 mM HEPES-KOH, pH 7.4, 100 mM KCl, 10 mM $MgCl_2$) and 0.5 µg of neuronal extract was incubated at 37 °C for 10 min. The reaction was terminated using 5 µL of 0.5 M EDTA. The reaction products were analyzed by 20% PAGE with 7 M urea and phosphorimaging as described in Section 2.12.1. The percentage of product formed was determined using the formula [product/ (product + substrate)* 100].

2.12.4. Gap *repair assay*

Gap repair assay was performed as described (Krishna et al., 2005). One gap containing DNA oligo duplex substrate was prepared by annealing a 5'-[γ-^{32}P]ATP labeled oligo 5 (14 mer) and an ATP labeled oligo 6 (17 mer) to unlabeled oligo 7(32 mer) as shown in **Table 2.**

The reaction mixture in a final volume of 30 µL contained 400 fmol of the gapped oligo duplex, 20 mM HEPES pH 7.5, 1 mM $MgCl_2$, 0.1 mM DTT, 0.1 mg/mL bovine serum albumin, 2% glycerol, 20 µM of all the four dNTPS and 1mM ATP. The reaction was initiated by adding 15 µg of neuronal extract followed by incubation at 37 °C for 20 min. Filling up of one gap in the oligo duplex substrate by polymerase of CGN extract would yield 15 mer and further ligation by ligase of the CGN extract would result in 32 mer. The reaction was stopped by adding 5 µL of 0.5 M EDTA. The reaction mixture was purified by extraction with phenol: chloroform: isoamyl alcohol (25:24:1). The repaired oligo duplex was recovered by ethanol precipitation at -80°C for 2 h in the presence of glycogen at 1 µg/µL of original reaction mixture volume. Supernatant was discarded and tubes containing oligos were allowed to dry overnight and 6 µL of 6x loading dye

(0.002% bromophenol blue and xylene cyanol in formamide) was added to each of the tubes and oligo duplexes were denatured at 90 °C for 5 min and snap-cooled. The reaction products were analyzed using 20% PAGE with 7 M urea and phosphoimaging as described in Section 2.12.1. The percentage of gap repaired product (15 mer) formed was determined using the formula [product/ (product+ substrate)* 100].

2.12.5 Ligase assay

We designed a nicked substratum for LIG assay (Gupta et al., 2012). An oligo duplex having a nick in one of the strands was prepared by annealing a previously 5'-[γ-^{32}P]ATP labeled oligo 8 and an ATP labeled oligo 6 to unlabeled oligo 7 as shown in **Table 2**. Repair *via* DNA ligation by protein equivalent of 10 µg of the neuronal extract was assayed using 400 fmol of nicked substrate in the BER reaction buffer. The reaction mixture was incubated for 15 min at 37 °C and the reaction was terminated by heating the mixture at 70 °C for 10 min. The repaired oligo duplex was recovered after 2 h by ethanol precipitation at -80 °C in the presence of glycogen at 1 µg/µL of original reaction mixture volume. The supernatant was discarded and tubes containing oligos were allowed to dry overnight. 6 µL of loading dye (0.002% bromophenol blue and xylene cyanol in formamide) was added to each of the tubes and oligo duplexes were denatured at 90 °C for 5 min and snap-cooled. The reaction products were analyzed 20% PAGE with 7 M and autoradiography as described in Section 2.12.1. The end product, 32 mer was densitometrically quantified using ImageJ 1.43u software, NIH, USA.

2.13. Immunoprecipitation

Young (2-4 day) rat brain tissue extract was prepared in extraction buffer mentioned in Section 2.10. Approximately 1 mg protein was precleared with mice pre immune IgG and 100 µL of protein A agarose. The precleared protein was incubated overnight at 4 °C with 0.5 µg of TopoIIβ antibody. 100 µL of protein A agarose slurry was added and rocked for another 30 min *at* room temperature. Protein A agarose mix was washed with IP buffer of increasing concentrations of 150, 300, 500 and 750 mM NaCl, twice at each concentration by centrifuging at 1500 × g for 3 min. Supernatant or wash through was collected. Protein A agarose beads along with immunoprecipitated TopoIIβ was taken for the reaction.

Microarray data was divided into 3 sets- Set 1- First week was taken as control and compared with week 2, 3 and 4; Set 2- Second week was taken as control and compared with week 3 and 4; Set 3- Third week was taken as control and compared with week 4.

2.14. Detection of intracellular ROS accumulation

Intracellular ROS accumulation was monitored using 7µM CMH_2DCFDA (5-(and-6)-chloromethyl-2′, 7′-dichlorodihydrofluorescein diacetate, acetyl ester) for 20 min. The cells were then rinsed twice with HEPES buffer and scanned on a Tekan multilabel reader- INFINITE 200 PRO (Tecan, Mannedorf, Switzerland) at excitation and emission wavelengths of 485 and 535 nm, respectively. The final

values were corrected for intracellular protein in each well and expressed in terms of fluorescence/ µg protein (Kaur et al., 2008).

2.15. Determination of free thiol levels

The content of intracellular free thiols was determined by using the fluorescent indicator, MCB (Mono chloro-bimane) at 40 µM concentration. After 20 min of MCB incubation, the cells were washed twice with cold HEPES buffer. The resulting fluorescence was detected on a Tekan multilabel reader- INFINITE 200 PRO (Tecan, Mannedorf, Switzerland) at an excitation wavelength of 360 nm and an emission wavelength of 465 nm. The final values of fluorescence were corrected for intracellular protein in each well and expressed in terms of fluorescence/ µg protein (Kaur et al., 2008).

2.16. Measuring mitochondrial membrane potential

Mitochondrial membrane potential represents an important physiological parameter as it reflects the cell capacity to generate ATP and is therefore a key indicator of cell health. Cationic dye Rhodamine 123 (R123, Sigma Chemicals Co., MO, USA) was used to analyse trends in $\Delta\Psi m$ in ageing CGNs. Cultured CGNs were seeded at a density of 1 x 10^6 cells/ well into a 12 well plate and cultured for 5 weeks as described in Section 2.3. For FACS analysis, CGNs were transferred to a HEPES- based medium containing (mM): 140 NaCl, 5 KCl, 1.5 $CaCl_2$, 1 $MgCl_2$, 20 glucose, 10 HEPES, pH adjusted to 7.4 and loaded with R123 (10 µM) for 30 min at 37 °C in 5% humidified CO_2 incubator (Xiong et al., 2004). Cells were washed twice with HEPES buffer and finally resuspended in sheath fluid prior to analysis. Cells were periodically pelleted from culture and tested

for ΔΨm. R123 accumulates in the mitochondria in live cells (Toescu and Verkhratsky, 2000a). As the cell ages, the mitochondrial membrane gets depolarised (Xiong et al., 2004) causing fluorescence due to R123 to decrease. This is the cause for decreased signal output during FACS or imaging studies.

Changes in the ΔΨm occurring during ageing were detected by flowcytometry (Cy Flow space, Partek). Data was collected using the data acquisition program, Flo Max software 2008 (version 2.57) and fluorescence was measured using an FL-1 detector. Five thousand cells were analysed per sample.

2.17. Microarray Analysis

CGNs were cultured for four weeks. The samples were collected at an interval of seven days starting from day 3. First week (day 3) was regarded as control with which second, third and fourth week samples were compared. The samples were collected in duplicate and processed for microarray analysis at Genotypic Technology Pvt Ltd, Bangalore, India, using Whole Rat Genome Microarray Kit, 4x44K array manufactured by Agilent 60-mer SurePrint technology (Cat no-G4131F). Briefly, total RNA was isolated from control and aged cells by using TRIZOL (Invitrogen, NY, USA) as per manufacturer's protocol. Using RNeasy mini-kit columns (Qiagen, Hilden, Germany) RNA samples were further purified. Total RNA integrity was assessed using RNA 6000 Nano Lab Chip on the 2100 Bioanalyzer (Agilent, Palo Alto, CA) following the manufacturer's protocol. Total RNA purity was assessed by the NanoDrop® ND-1000 UV–Vis Spectrophotometer (Nanodrop Technologies, Rockland, USA). All the samples

were analysed in duplicate. The samples were labeled, hybridized and scanned for fluorescent signals.

Data was analysed using GeneSpring GX version 11.5 and Microsoft Excel. Fold change used for upregulation was >0.8 and downregulation <0.8 in each of the replicates and >1 in the Geomean fold of the replicated samples. P- value < 0.05 was considered statistically significant. Microarray data was divided into 3 sets- Set 1- First week was taken as control and compared with week 2, 3 and 4; Set 2- Second week was taken as control and compared with week 3 and 4; Set 3- Third week was taken as control and compared with week 4. Differentially regulated genes were clustered using gene tree to identify significant gene expression patterns. Genes were classified based on functional category and pathways using GeneSpring GX Software and Biointerpreter.

2.18. Real-Time PCR Analysis

The microarray cDNA analysis was validated by quantitative real time PCR (qPCR). Ten µL of cDNA synthesis was carried out using 1 µg of total RNA, random hexamers and Super Script™ First-Strand Synthesis System (Invitrogen, NY, USA) using gene specific primers as in **Table 3** (Eurofins Genomics, Bangalore, India) and Power SYBR green PCR Master Mix (Applied Biosystem, CA, USA). Absence of genomic DNA in total RNA was ensured by DNaseI treatment (Fermentas, GmbH, Germany). 18s rRNA was used as an internal control. To ensure no contamination of PCR reagents with the cDNA, no template controls (NTC) were set up. PCR analysis was performed with ABI Prism H7500 fast thermal cycler (Applied Biosystem, CA, USA). Each sample was run in

triplicate in a final volume of 10 µL containing 0.2 µL of 1st strand cDNA template, 20 pmol of each primer, and 5 µL of Power SYBR Green PCR master mix. Fluorescence resulting from DNA amplification was analyzed. Relative fold change was assayed using $2^{-\Delta\Delta C_T}$ method (Livak and Schmittgen, 2001).

Table 3: Primer list for Real time PCR

S. No	Gene	Forward primer (5' →3')	Reverse primer (5' →3')	Amplicon size
1	UNG	CGC ACA CCA AGC CAA TTC CCA TAA	AGG TTC TGA TTC AGC CAC GAC ACA	81
2	SMUG	TTT CCA GAG CCT GTG GGT GTC ATC TA	TTG GCA GTA GCG AGT CAC GTA GTT	84
3	APEX	GTT CTT CCT CAC CAA TGC CAT AAG AG	AGG CTT GGA TTG GGT AAA GGA AGA AGC	215
4	POL B	CAC AGC TCA ATG GCA CCT AAC	AGT GAC CAG ACG CTG TGA TG	220
5	POL M	AGA GGT GAC ACA TGT GGT GAT GGA	TCC TGC TGC CAT GCT CTC TGT AAA	142
6	POL L	AGG GTT CCT CAC AGA TGA CTT GGT	AAA CTC ACT GTA GGG CAC CAC GAT	136
7	LIG 1	AGA CAG CAG AGG CCA GAA AGA TGT	TCT GGG AGA CTT TCC AAG CCA TGT	130
8	LIG 3	TAC TGG AGG CAG CAA TGG TGA GAA	TTC TTG GCA CTG GCA GAG GAC TTA	102
9	TOP2B	GAC AGA GGA AGG TAG TAG AGC CTG	CGT TTT CTT CGG TTT CTT GCT GGC	168
10	A2M	TCA CTC ATC CTG TTG TCC GCA ATG CCC TCT	ACC AGC AAG GGC AAA TGC ATA GGC CAA CA	128
11	GNA14	ACC AAA GCA AGA TGT CAA AGC TGC CAG GGA	TCC TTG ACA GCA GCA AAC ACG AAG CGG AT	147
12	GRIA1	ATG CCA ACC AGT TTG AGG GCA ATG ACC GCT	TTC TCC CAC CAT GCC ATT CCA AGC CTT TGT	167
13	MASP	TGC CGA GTG GAA TGC AGT GGC AAT CTC TT	AGG GCA CCT CGG GAT GGT CTT CAA TGT CAA	184
14	NPY	TGC TCG TGT GTT TGG GCA TTC TGG CTG A	ATC AGT GTC TCA GGG CTG GAT CTC TTG CCA	169
15	SLIT2	AGA ACG GCA CCA GCT TCC ATG GCT GTA T	TGG GCA CAC ACT TTC TTG TGG CAT GGT TCA	133
16	GLB	TCA AGG ATG GGC AGC CAT TCC GCT ACA T	TGG ATT GCA TCC AGC CCA GCC ATC TTC AT	118
17	18S	GCT ACC ACA TCC AAG GAA GGC AGC	CGG CTG CTG GCA CCA GAC TTG	200

2.19. Statistical analysis

The experiments were performed in triplicate and repeated independently thrice. Data was averaged and presented as mean ± SD. Statistical analysis was done using GraphPad Prism 5 (demo version, GraphPad Software, SanDiego, CA, USA), One Way ANOVA with *Tukey post hoc* test. P-value <0.05 was considered statistically significant. The test was used to compare control with TopoIIβ downregulated condition at a particular treatment level and with 2- 5W aged cells.

CHAPTER 3

ROLE OF TOPOIIβ IN BASE EXCISION REPAIR IN *IN VITRO* CULTURED CGNS

Introduction

DNA repair, being a fundamental evolutionary process for maintaining the genomic integrity, assumes vital importance in postmitotic, yet highly active tissues like the brain (Kass and Jasin, 2010; Wilson and McNeill, 2007), and is very important to restore cellular and biological functioning. DNA is under constant attack by DNA damaging agents which may be either endogenous like peroxide or environmental like nitrosoamines. The repair processes are activated by stimulating the production of various proteins participating in the reorganization of chromosome, leading to the repair of damaged DNA through various events namely activation of expression of repair genes (Ju et al., 2006), formation of multimeric repair complexes (Fan and Wilson, 2005), stabilization of damaged regions (Pfeiffer and Vielmetter, 1988), rearrangement and re-sealing of broken ends of the DNA through correction, processing, synthesis and ligation. During this process, torsional stress will be embedded in the upstream and downstream of the damaged site. The maintenance of torsional integrity is promoted by a class of enzymes known as topoisomerases. These topoisomerases play vital roles in a number of fundamental nuclear processes, including DNA replication, transcription, recombination as well as chromosome organization and segregation (Osheroff et al., 1991; Wang et al., 1991).

Topoisomerase II is present in two isoforms: 170 kDa alpha (Topoisomerase IIα) and 180 kDa beta (Topoisomerase IIβ) (Drake et al., 1987; Tsai-Pflugfelder et al., 1988). A significant activity of Topoisomerase IIβ (TopoIIβ) in nuclei isolated from postmitotic neuronal cells was reported earlier (Tsutsui et al., 2001).

TopoIIβ is also shown to be expressed in other nonproliferating and fully differentiated tissues (Capranico et al., 1992). Of the two isoforms, beta isoform is predominant in the brain (Tsutsui et al., 2001). The level of TopoIIβ in the brain decreases during ageing (Kondapi et al., 2004) and TopoIIβ deficient SK-N-SH, neuroblastoma cells and granule neurons show sensitivity to peroxide mediated DNA damage in a non-homologous end-joining pathway (Mandraju et al., 2011; Mandraju et al., 2008), thus implicating the role of TopoIIβ in DNA repair pathways. Further, the catalytic activity of TopoII is known to be stimulated by abasic, oxidized and monoalkylated DNA (Sabourin and Osheroff, 2000). Since these studies covered only plasmids containing abasic sites, it is difficult to extrapolate the significance of these findings to highly structured cellular DNA. TopoIIβ has been reported to participate in the repair of melphalan induced DNA crosslinks in myelogenous leukemia, wherein TopoIIβ levels are determinant of the magnitude of DNA crosslinks and cell survival, following treatment with melphalan (Emmons et al., 2006).

N- ethyl N- nitrosourea (ENU) is a point mutagen and carcinogen (Warren et al., 1990). It is an SN1 monofunctional alkylating agent and transfers its ethyl group to oxygen and nitrogen radicals in DNA, which results in mispairing and base-pair substitutions (Beranek, 1990; Justice et al., 1999). The popular forms of DNA adducts include N7-ethyl guanine (N7-G), O6- ethyl guanine (O6-G), O2-ethyl thymine (O2-T), N3-ethyl adenine (N3-A), O2- ethyl cytosine (O2-C) and O4-ethyl thymine (O4-T) (Beranek et al., 1983; Heflich et al., 1982). Such a base modification is identified by the repair machinery or is subjected to replication. However, upon replication, a distinct increase in the frequency of transitions

GC→AT and AT→GC and AT→TA transversions is seen (O'Neill, 1982; Rinchik et al., 2002; Tchekneva et al., 2007). ENU treated cells upon replication show 50 % mutated cells where as if base excision repair (BER) or nucleotide excision repair (NER) were to occur, then either 100 % or 0 % of the population would be mutated (O'Neill, 1982). NER players recognize the DNA adducts caused due to the nitrosourea compounds, probably by the distortion of the base-pairing stability (Tosal et al., 2001). An O6 or O4 alkyl residue is repaired by alkyl DNA alkyl transferase (AGT) (O'Neill, 2000). N7eG adducts are not harmful yet their downstream processing like deprotonation, depurination, decomposition and C8G adduct formation can lead to DNA strand breaks (Gates et al., 2004). N7eG is recognized and exclusively repaired by N-methyl purine DNA-glycosylase (MPG) (Hang et al., 1997; Lee et al., 2009), an initiator glycosylase of the BER pathway (Lau et al., 1998). This generates an abasic site and initiates the BER pathway (Srivastava et al., 1998).

The present study is a special focus on the BER pathway initiated during ENU mediated DNA damage and the role of TopoIIβ in promoting BER activity. BER pathway is known to repair single-base lesions like alkylated and oxidized base forms in DNA. Excision of a methylated base or of uracil (U) calls for a replacement of only the modified nucleotide and is termed single-nucleotide BER or short-patch BER. A monofunctional glycosylase (e.g., N-methylpurine- or UDG) initiates the reaction, followed by strand cleavage at 5' to the apurinic/ apyrimidinic (AP) site by Apurinic endonuclease 1 (APE1) which generates a 5'-deoxyribose phosphate (dRP) moiety. This is followed by DNA synthesis and removal of dRP by polymerase β (POLβ) and finally ligation of the nick by a DNA

ligase (Horton et al., 2002; Rao, 2007; Wilson and Bohr, 2007; Wilson and McNeill, 2007). The long-patch BER may remove the dRP residue along with several downtream nucleotides by flap-endonuclease I (FEN1) that along with DNA ligase I interacts with proliferating cellular nuclear antigen (PCNA) to complete repair synthesis (Fortini et al., 2003). The most rate limiting factors of BER in ageing neurons are POLβ and ligase (Krishna et al., 2005).

The principal objective of our study is to characterize the function of TopoII isoforms in DNA damage and repair in primary neurons, without the interference of the replicative functions. This is because the exact role of the TopoIIβ in irreversibly differentiated cells like neurons is not yet understood. In the present investigation, using N-ethyl N-nitroso urea (ENU) mediated DNA damage as a model; we studied the damaged base repair efficiency of CGNs in the presence as well as in the absence of TopoIIβ via the BER pathway. Investigations were carried out by downregulating TopoIIβ using siRNA mediated knockdown in CGNs. We also assayed the activities of the various enzymes in the BER pathway. Similarly, parallel studies were carried out *in vitro* ageing CGNs (Bhanu et al., 2010). The study has essentially shown that BER capacity of CGNs is impaired during ageing as well as in the TopoIIβ downregulated condition leading to the conclusion that TopoIIβ is essential for normal BER activity in CGNs, especially the cellular LIG activity, and therefore may play a role in the decreased BER capacity of ageing CGNs.

Experimental strategy

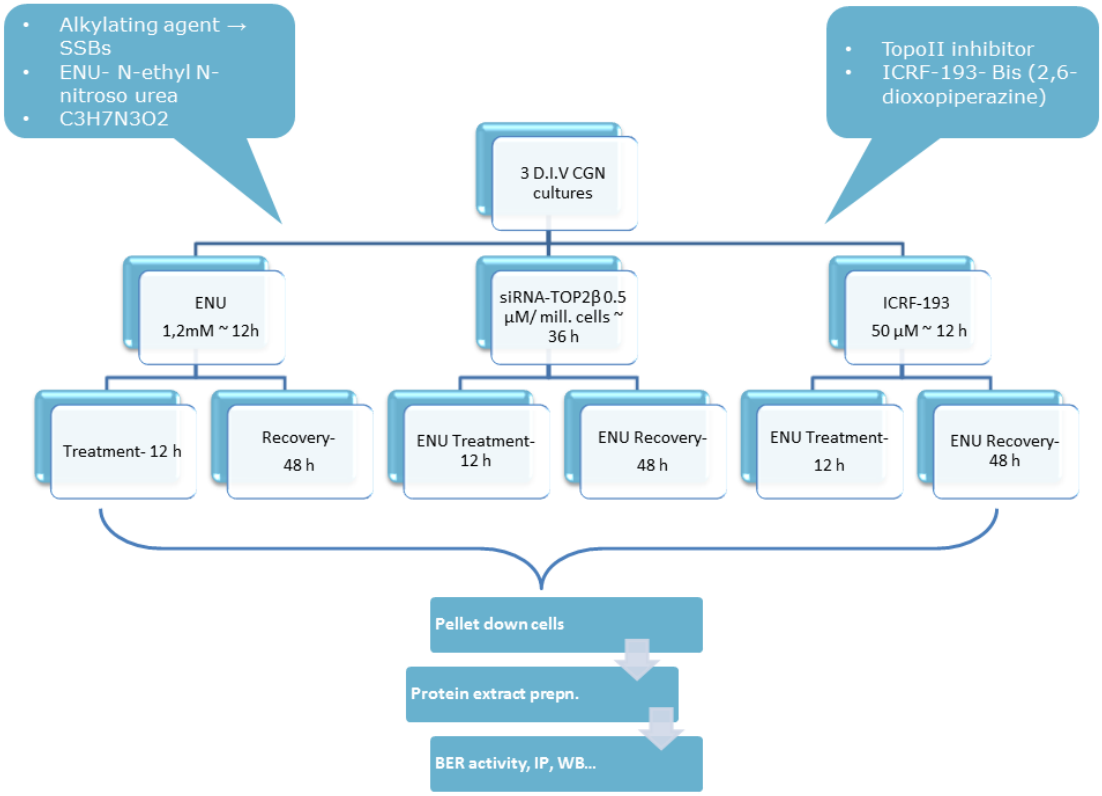

Results

3.1. Isolation of pure CGN cultures

Granule neurons were isolated from 7 day old Wistar rat pups and cultured in EMEM with glucose, KCl, Glutamax and 10% FBS as described in Section 2.3. Neuronal specific enolase (NSE) is a marker for neurons and glial fibrillar acidic protein (GFAP) is a marker for astrocytes and glial cells. In order to ascertain the degree of homogeneity of the neuronal culture, CGNs were immunostained with anti-NSE and anti-GFAP polyclonal antibodies and detected with FITC conjugated secondary antibodies. Stained cells were captured under Leica confocal

microscope **(Figure 1A)**. Cultured CGNs were isolated to 90% homogeneity from rat cerebellum. A similar finding was seen when the extracts of SK-N-SH, CGNs and astrocytes were resolved on SDS-PAGE and later probed with anti-NSE and GFAP antibodies and detected with chemiluminescent reagent **(Figure 1B)**.

3.2. siRNA mediated TopoIIβ downregulation

In the present investigation, using N-ethyl N-nitroso urea (ENU) mediated DNA damage as a model; we studied the damaged base repair efficiency of CGNs in the presence as well as in the absence of TopoIIβ *via* the BER pathway. Investigations were carried out by downregulating TopoIIβ using siRNA mediated knockdown in CGNs as described in Section 2.8. The transfection efficiency of Lipofectamine 2000 was evaluated by transfecting CGNs with pEGFP-N2 plasmid for 6 h and the cells were then scored for GFP fluorescence under Leica confocal microscope. Transfection efficiency was found to be greater than 95% as seen in **Figure 2A**. **Figure 2B** illustrates lowered expression levels of TopoIIβ by ICC studies. CGNs were transfected with TopoIIβ siRNA (40ng/ million cells) and TopoIIβ scrambled siRNA (negative control). Cells were harvested after 36 h. Total RNA extracts prepared and immunocytochemistry performed. CGNs were immunostained with a DNA dye, DAPI (Blue), anti-TopoIIβ and detected with FITC conjugated secondary antibody (green). Seen are immunofluorescence, fluorescence-transmission merged images of CGNs corresponding to healthy control, TopoIIβ scrambled siRNA and TopoIIβ siRNA treatment.

3.3. Reverse transcription PCR (RT-PCR)

Figure 3A depicts semi quantitative gene expression of TopoIIβ in control cells and CGNT^{-} cells. To estimate the extent of downregulation, CGNs were treated with TopoIIβ-siRNA and TopoIIβ- scrambled siRNA. Lanes 1 to 5 correspond to expression levels in healthy control CGNs (C), CGNs treated for TopoIIβ scrambled siRNA (S) and ECGNT^{-}cells (TopoIIβ-siRNA), no template control (NTC) and 50 base pair DNA ladder (L). GAPDH used as loading control. The bands were densitometrically quantified using ImageJ 1.43u software, NIH, USA. TopoIIβ level was found to be significantly low in ECGNT^{-} using One Way ANOVA (*** $P < 0.001$). TopoIIβ isoform was downregulated by 60% in CGNT^{-} cells.

3.4 TopoIIβ downregulated neurons (CGNT^{-}) showed increased DNA damage

The induction of DNA damage by ENU was investigated using alkaline comet assay which provides a measure of SSBs, DSBs and alkali labile sites. Cultured CGNs were treated with ENU at 1, 2 mM concentrations for 12 h (1T and 2T), subjected to fresh media change and allowed to recover for 48 h (1R and 2R) from DNA damage. After 12 h of treatment and 48 h of recovery, cells were pelleted and processed for alkaline comet assay. **Figure 4A** shows comets upon treatment in control batch and CGNT^{-} batch. There was a concentration dependent production of DNA damage in control batch. However, the CGNT^{-} cells were more prone to DNA damage upon ENU treatment. **Figure 4B** shows comets due to DNA damage after 12 h and recovery after 48 h upon treatment with 50 μM ICRF-193. Average of 50 cells was chosen for every experiment (n=3). DNA

damage was measured in terms of tail moment. ICRF-193 treatment resulted in significant DNA damage. Tail moment was found to be statistically higher in CGNT^{-} batch, when compared with the control batch among similar treatments

The results showed that downregulation of TopoIIβ in comparison to healthy CGNs (Figure 4A) induced higher strand breaks during both treatment and recovery and were inefficient to repair during recovery. This suggests that CGNT^{-} have decreased BER capacity, thus becoming more sensitive to DNA damage by ENU. This was further confirmed by increased DNA damage in CGNs when cultured in the presence of 50 μM ICRF-193 (treatment), which was restored during recovery due to the reversibility of the ICRF-193 mediated action after 48 h of drug removal (Figure 4B). TopoIIβ downregulation affects repair of ENU mediated SSBs in CGNs.

*3.5. TopoIIβ downregulated neurons (*CGNT^{-}*) showed decreased BER capacity*

Since CGNT^{-} showed higher DNA damage upon treatment with ENU, we have analyzed the BER activity of the cell-free extracts prepared from ENU treated, recovered and TopoIIβ downregulated granule neurons (ECGNT^{-}). **Figure 5A** depicts a representative autoradiogram showing G-U BER activity in CGNs upon ENU treatment and TopoIIβ downregulation. CGNs and CGNT^{-} were incubated in the presence of indicated concentrations of ENU for 12 h (treatment) followed by 48 h of recovery by washing the cells in a fresh medium and then recultured in complete medium. Cell-free extracts were prepared and checked for G-U BER activity using U containing synthetic radio labeled oligonucleotides. Lane 1 is G-U BER activity in control untreated cells (C); lanes 2 and 3 show activity of protein

extracts in terms of 21 mer G-U BER product formation from CGNs treated for 1 and 2 mM ENU for 12 h (IT and 2T); lanes 4 and 5 show the same for treatment followed by 48 h of recovery (1R and 2R), respectively; lane 6 shows activity from untreated ECGNT^{-} (C); lanes 7 and 8 show the same in ECGNT^{-}, 12 h ENU treatment (1T and 2T) and lanes 9 and 10 for treatment followed by 48 h recovery (1R and 2R). Lane 11 depicts 21 mer; lane 12 is pure enzyme control (P); lane 13 depicts blank (B), i.e. 3 pmol of G-U BER substrate. **Figure 5B** depicts the effect of ICRF-193 on G-U BER activity. TopoIIβ inhibitor ICRF-193 was used to demonstrate the direct participation of TopoIIβ catalytic activity in the repair of G-U mismatch. 0.5, 10, 100 μM ICRF-193 (corresponding to lanes 2, 3 and 4) was directly added to *in vitro* G-U BER reaction. Lanes 5, 6 and 7 correspond to blank (B), pure enzyme control (P) and 21 mer (21). The amount of 21 mer G-U BER product formed was densitometrically measured using ImageJ as described in Section 2.12.1. The difference in the activities of control and CGNT^{-} extracts among similar treatments was found to be highly significant

The results showed that G-U BER activity was almost absent during treatment, while it was partially restored during recovery (Figure 5A). TopoIIβ inhibitor, ICRF-193 was used to demonstrate the direct participation of catalytic activity of TopoIIβ in the repair of G-U mismatch. But the TopoII catalytic inhibitor was found ineffective against the G-U BER activity, when added *in vitro* to the reaction at concentrations of 0.5, 10, 100 μM (Figure 5B) suggesting TopoIIβ catalytic activity *per se* may not be involved in promoting BER activity. Hence, TopoIIβ knockdown neurons were deficient in G-U BER activity.

3.6. Effect of lowered levels of TopoIIβ on the activities of enzymes in BER pathway

BER pathway involves base hydrolysis of the mismatched base, U by UDG followed by depurination by APE1. The base substitution is promoted by POLβ followed by sealing of the repaired ends by LIG. The activities of UDG, APE and LIG were analyzed in CGNT^{-} during treatment and recovery from ENU-mediated DNA damage. The substrate is 200 fmol of 5'-[γ-^{32}P]ATP end labeled 21 mer double stranded U containing oligonucleotide for UDG activity. It involves base hydrolysis of U, resulting in a 7 mer product. **Figure 6A** is a representative autoradiogram showing UDG activity upon ENU treatment and TopoIIβ downregulation. Lane 1 illustrates UDG activity in control untreated cells (C); lanes 2 and 3 show activity of protein extracts in terms of 7 mer product formation from CGNs treated with 1 and 2 mM ENU for 12 h (IT and 2T); lanes 4 and 5 show the same for treatment followed by 48 h of recovery (1R and 2R) respectively; lane 6 shows activity from untreated ECGNT^{-} (C); lanes 7 and 8 show the same in ECGNT^{-}, 12 h treatment (1T and 2T) and lanes 9 and 10 for treatment followed by 48 h recovery (1R and 2R). Lane 11, activity by 0.5 U of pure enzyme, UDG (P); lane 12, activity in blank (B), i.e. 200 fmol of substrate; lane 13 depicts 21 mer (21). Treatments given as indicated in the figure. **Figure 6B** shows representative autoradiogram showing UDG activity in CGN extracts treated with TopoIIβ scrambled siRNA to rule out any direct effect of siRNA on UDG activity. The experimental procedure and product quantification were done as described in Section 2.12.3. Percentage of glycosylated product was measured in arbitrary units and densitometric analysis carried out using ImageJ. The

difference in the UDG activities of control and CGNT^{-} extracts among similar treatments was found to be highly significant. **Figure 6D** shows the effect of ICRF-193 on UDG activity, in culture and *in vitro.* Lane 1 shows UDG activity in healthy CGNs; lanes 2 and 3, UDG activity upon direct addition of 0.5 and 10 μM ICRF-193; lanes 4 and 5, activity upon 12 h treatment and 48 h recovery from 50 μM ICRF-193; lanes 6 and 7, activity upon treatment with ICRF-193 (12 h) followed by 1 mM ENU (12 h) and recovery (48 h) as indicated. Lanes 8, 9 and 10, activity by 0.5 U pure enzyme, UDG (P), blank (B) and 21 mer (21). The difference in the UDG activities of extracts of control and ICRF-193 treated CGNs was found to be highly significant. UDG activity is not enhanced in TopoIIβ deficient condition during ENU treatment. While the addition of ICRF-193 *in vitro,* at 0.5 and 10 μM concentration had no effect on UDG activity. ICRF-193 mediated downregulation of TopoIIβ at 50 μM reduced UDG activity during treatment.

Figure 7A is a representative autoradiogram showing AP endonuclease (APE) activity. The substrate is 200 fmol of 5'-[γ-^{32}P]ATP end labeled 21 mer double stranded oligonucleotide containing F, tetrahydrofuran (AP site analog). The APE activity involves the cleavage of phosphodiester backbone on the 3' side of F. Lane 1 illustrates activity in control untreated cells (C); lanes 2 and 3 show activity of protein extracts in terms of 14 mer AP product formation from CGNs treated for 1 and 2 mM ENU for 12 h (IT and 2T); lanes 4 and 5 show the same for treatment followed by 48 h of recovery (1R and 2R) respectively; lane 6 shows activity from untreated ECGNT^{-} (C); lanes 7 and 8 show the same in ECGNT^{-}, 12 h treatment (1T and 2T) and lanes 9 and 10 for treatment followed

by 48 h recovery (1R and 2R). Lane 11, activity by 1 U of pure enzyme, human APE1 (P); lane 12, activity in blank (B), i.e. 200 fmol of substrate; lane 13 depicts 21 mer (21). **Figure 7B** shows APE activity in CGN extracts treated with TopoIIβ scrambled siRNA to rule out any direct effect of siRNA on APE activity. Percentage of 13 mer product was measured in terms of arbitrary units. Experimental procedure and densitometric quantification were carried out as described in Section 2.12.3. Change in AP endonuclease activity amongst control and $CGNT^{-}$ was found to be insignificant.

Figure 8A is a representative autoradiogram depicting LIG activity. Cells were treated as described in Section 2.3. Lane 1 corresponds to LIG activity in control untreated cells (C); lanes 2 and 3 show LIG activity of protein extracts in terms of ligated product formation from 1 and 2 mM ENU treated CGNs for 12 h (1T and 2T); lanes 4 and 5 show the same for treatment followed by 48 h of recovery (1R and 2R);lane 6 shows activity from untreated $ECGNT^{-}$ (C); lanes 7 and 8 show the same in $ECGNT^{-}$ subjected to 12 h ENU treatment (1T and 2T); lanes 9 and 10 for treatment followed by 48 h recovery (1R and 2R); lane 11 corresponds to LIG activity by 10 U of pure enzyme, T_4 DNA ligase (P); lane 12 corresponds to blank (B), i.e. 400 fmol of substrate DNA; lanes 13 and 14 to 32 mer and 15 mer marker, respectively and lane 15 to LIG activity due to scrambled TopoIIβ siRNA (S). **Figure 8B** illustrates the effect of TopoIIβ inhibitor, ICRF-193 on LIG activity. Experimental procedure as described in Section 2.12.5. Lanes 1, 2 and 3 correspond to activity in control (C), 0.5 and 10 μm ICRF-193 additions to *in vitro* LIG reaction. Lanes 4 to 7 correspond to 15 mer (15), pure enzyme (P), blank (B) and 32 mer (32), respectively. The amount of 32 mer ligated product formed was

densitometrically measured using ImageJ. **Figure 8E** illustrates the effect of ICRF-193 treatment on LIG activity in cultured CGNs. Lanes 1 to 4 correspond to LIG activity in pure enzyme (P), blank (B), 32 mer (32) and 15 mer (15), respectively. Lane 5 shows LIG activity in control (C); lanes 6 and 7 correspond to activity in ICRF-193 treated and recovered culture; lanes 8 and 9 correspond to activity in ICRF-193 (12 h) and ENU (12 h) treated and recovered cultures at indicated concentrations. The amount of 32 mer ligated product formed was densitometrically measured using ImageJ.

LIG activity was significantly affected in extracts prepared from both ENU-treated and recovered CGNT^{-}. Also, ICRF-193 did not alter LIG activity. Furthermore, 50 μM ICRF-193 treatment resulted in decreased LIG activity in ENU-treated ECGNT^{-}. Hence, we conclude that LIG activity is affected in the ECGNT^{-} cells during recovery from ENU mediated strand breaks.

3.7 TopoIIβ activity per se not required for LIG activity

Figure 9A is a representative autoradiogram depicts TopoIIβ is not directly involved in the ligation step. Lanes 1 to 4 correspond to LIG activity in control, ECGNT^{-}, ECGNT^{-}+ TopoIIβ immunoprecipitated (IP), wash through after TopoIIβ pull down. Lanes 5 to 8 correspond to pure enzyme control (P), blank (B), 32 mer (32) and 15 mer (15). Figure 9 depicts significant decrease in ligated product formation in the absence of TopoIIβ as well as in TopoIIβ supplemented condition, indicating that TopoIIβ is not directly involved in the ligation step.

To elucidate direct participation of TopoIIβ in BER pathway, ICRF-193 was directly added to the reaction. We found no significant change in the activities of

the extracts in terms of product formation in all the three assays- G-U BER, UDG, and LIG (Figure. 5B, 6D and 8B). These results together point out that TopoIIβ catalytic activity does not participate in the BER activity. The observed significant decrease of G-U BER activity as well as the activities of UDG and LIG in TopoIIβ downregulated neurons unequivocally establishes that TopoIIβ plays a crucial role and its knock down would significantly affect the BER activity, especially in regulating UDG and LIG activities.

Figure 1

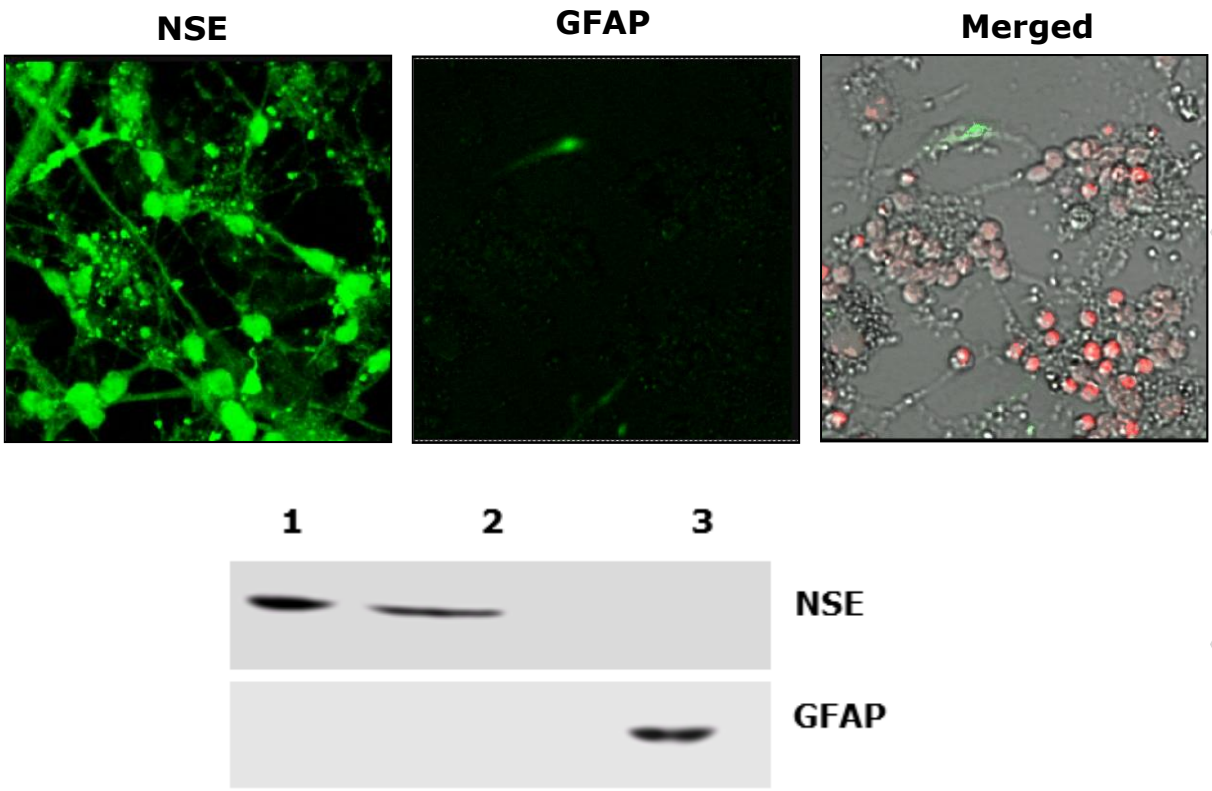

Figure 1: Cerebellar granule neurons in culture

Granule neurons were isolated from 7 day old Wistar rat pups and cultured in EMEM with glucose, KCl, Glutamax and 10% FBS. **Panel A**– Cells were immunostained with neuronal specific enolase (NSE) and glial fibrillar acidic protein (GFAP) polyclonal antibodies and detected with FITC conjugated secondary antibodies. Stained cells were captured under confocal microscope (Leica). **Panel B** shows a western blot of the SK-N-SH, CGNs and Astrocytes corresponding to lanes 1, 2 and 3. 40 µg protein was resolved on SDS-PAGE and transferred to NC membrane. Later probed with antibodies and detected with chemiluminescent reagent.

Figure 2

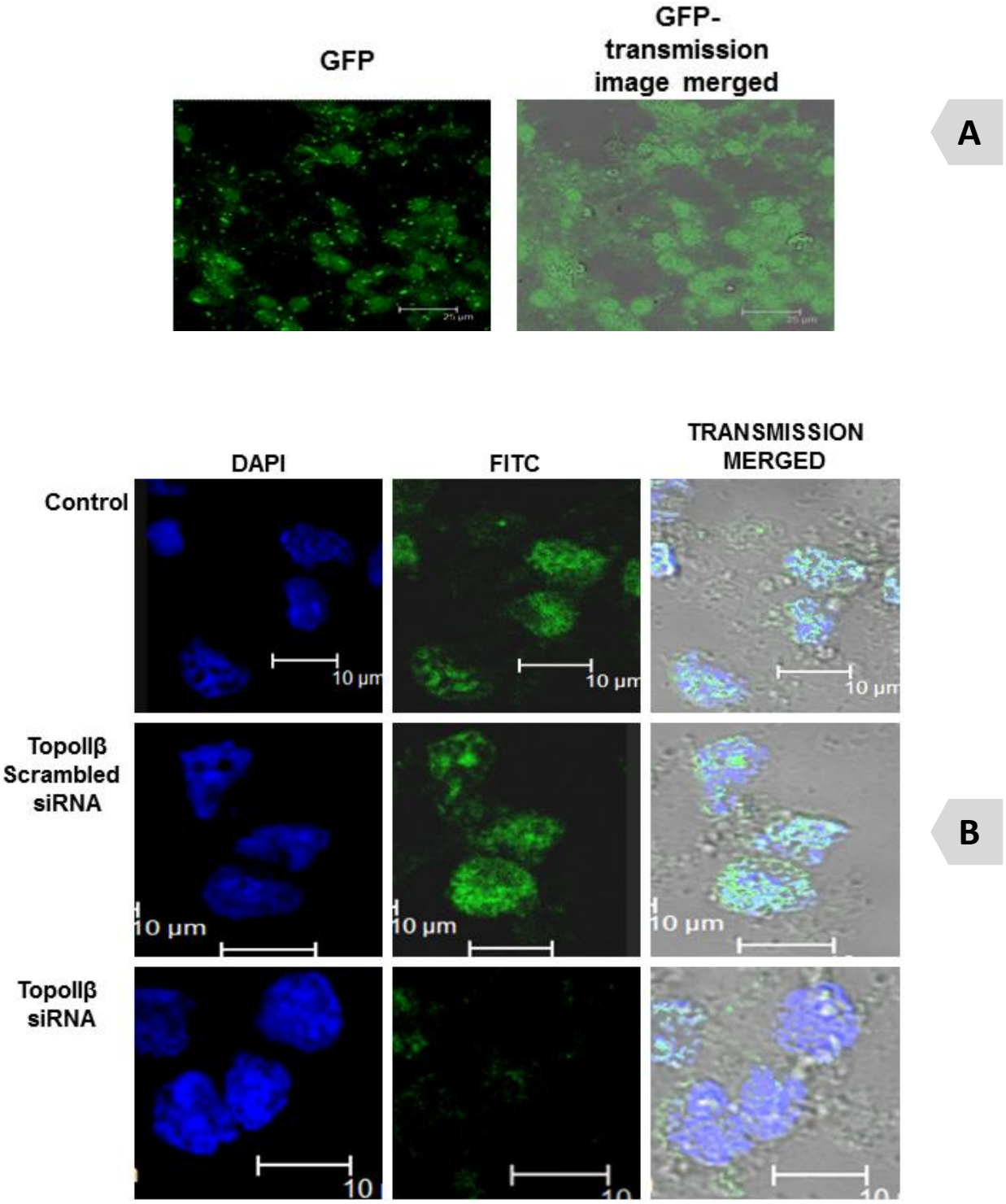

Figure 2: siRNA mediated TopoIIβ downregulation

Panel A depicts transfection efficiency of Lipofectamine 2000. CGNs were transfected with pEGFP-N2 plasmid using Lipofectamine 2000 for 6 h to

determine its transfection efficiency and the cells were viewed under Leica confocal microscope. At random 100 cells were scored for GFP fluorescence. GFP fluorescence in CGNs reflects the successful transfection of pEGFP-N2 plasmid. Transfection efficiency was greater than 95%. (Scale bar = 25 μm) (n = 3) . **Panel B** illustrates lowered expression levels of TopoIIβ by ICC studies. CGNs were transfected with TopoIIβsiRNA (40ng/ million cells) and TopoIIβ scrambled siRNA (negative control) using Lipofectamine 2000. Cells were harvested after 36 h. Protein extracts and total RNA extracts prepared and immunocytochemistry performed. CGNs were immunostained with a DNA dye, DAPI (Blue), anti-TopoIIβ and detected with FITC conjugated secondary antibody (green). Seen are immunofluorescence, fluorescence-transmission merged images of CGNs corresponding to healthy control, TopoIIβ scrambled siRNA and TopoIIβ siRNA treatment. (Scale bar = 10 μm).

Figure 3

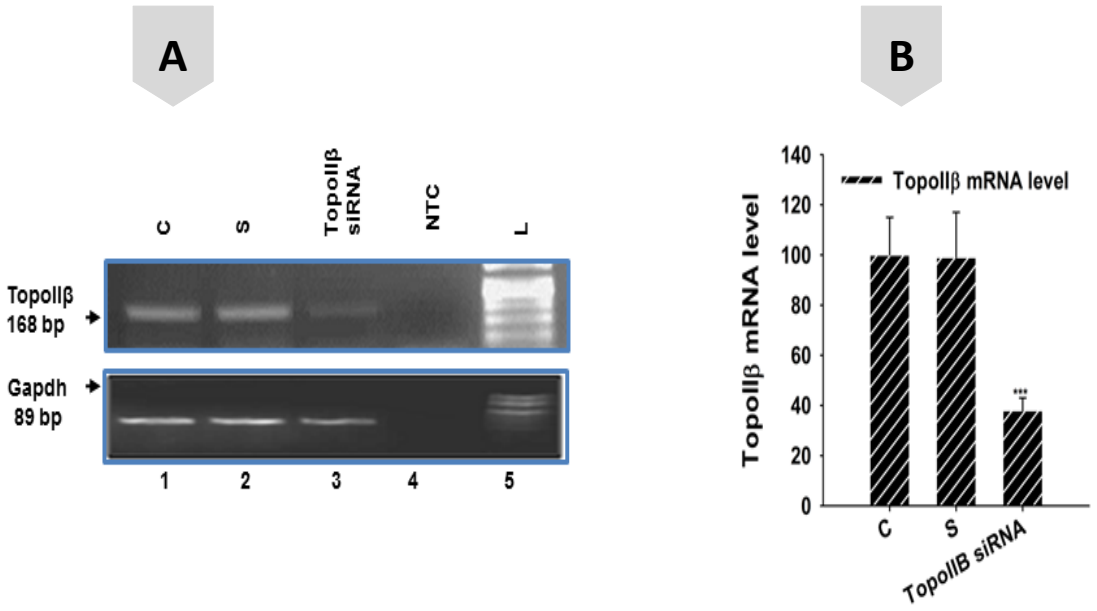

Figure 3: Reverse transcription PCR (RT-PCR)

Panel A shows a RT-PCR for TopoIIβ. Lanes 1 to 5 correspond to expression levels in healthy control CGNs (C), CGNs treated for TopoIIβ scrambled siRNA (S) and ECGNT¯cells (TopoIIβ-siRNA), no template control (NTC) and 50 base pair DNA ladder (L). GAPDH used as loading control. The bands were densitometrically quantified using ImageJ 1.43u software, NIH, USA. Experiment was done in triplicate and Mean ± SD is shown in bar graph **(Panel B)**. TopoIIβ level was found to be significantly decreased in ECGNT¯ using One Way ANOVA (*** $P < 0.001$).

Figure 4

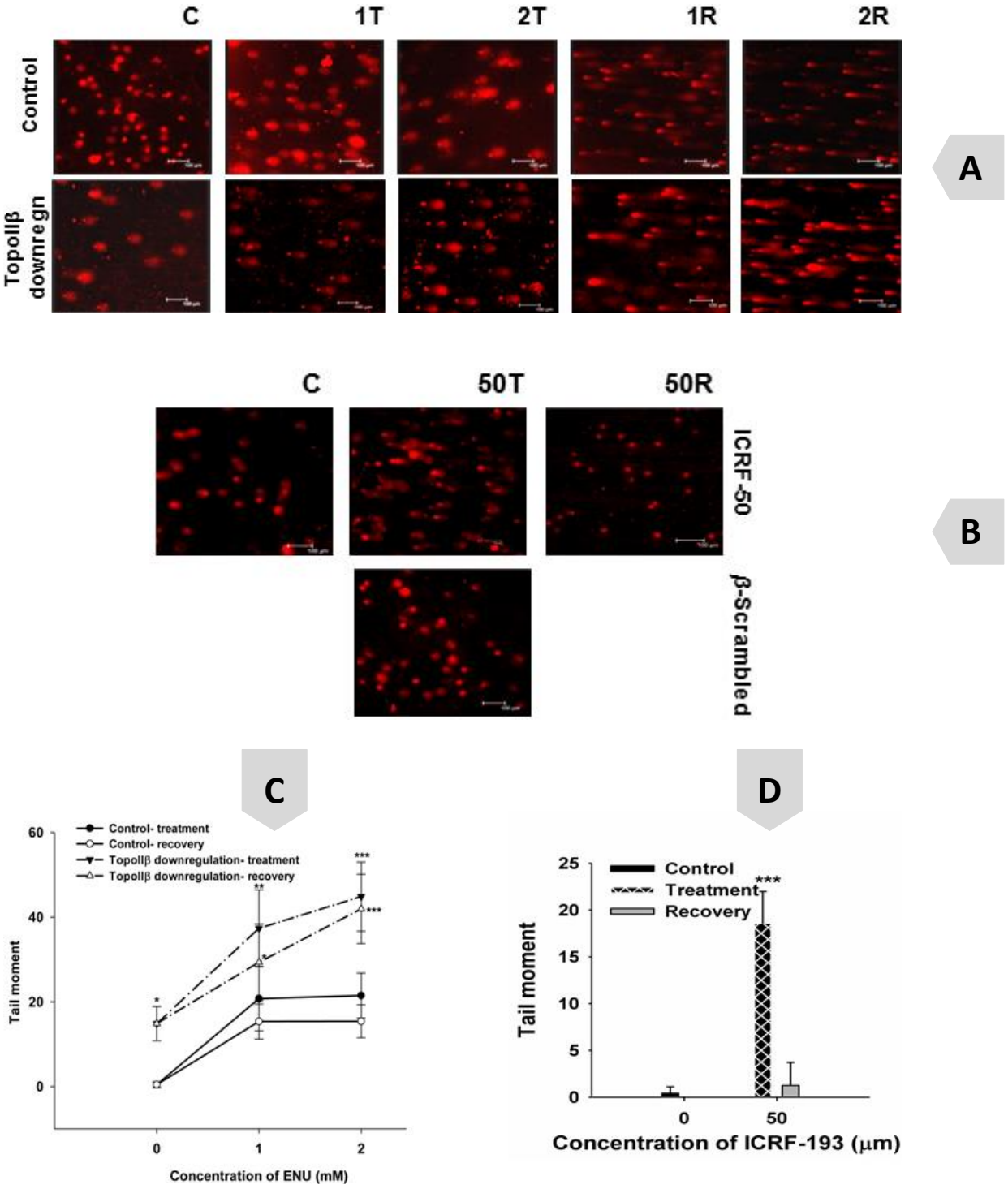

Figure 4: TopoIIβ downregulation affects repair of ENU mediated SSBs in CGNs

The induction of DNA damage by ENU was investigated using alkaline comet assay which provides a measure of SSBs, DSBs and alkali labile sites. Cultured CGNs were treated with ENU at 1, 2 mM concentrations for 12 h (1T and 2T), subjected to fresh media change and allowed to recover for 48 h (1R and 2R) from DNA damage. After 12 h of treatment and 48 h of recovery, cells were pelleted and processed for alkaline comet assay. **Panel A** shows comets on treatment in control batch, CGNT^{-} batch and TopoIIβ scrambled siRNA treated batch. **Panel B** shows comets due to DNA damage after 12 h and recovery after 48 h upon treatment with 50 μM ICRF-193. Corresponding bar charts depict Mean ± SD (**Panels C and D**). Average of 50 cells was chosen for every experiment (n=3). DNA damage was measured in terms of tail moment. There was a concentration dependent production of DNA damage in control batch. ICRF-193 showed DNA damage activity. DNA damage was quantified using Comet-IV software (Perceptive Instruments, Suffolk UK). Scale bar = 100μm. Tail moment was found to be statistically higher in CGNT^{-} batch, compared with the control batch among similar treatments using One Way ANOVA (*Holm-Sidak* method) (* $P < 0.05$, ** $P < 0.01$, *** $P < 0.001$).

Figure 5

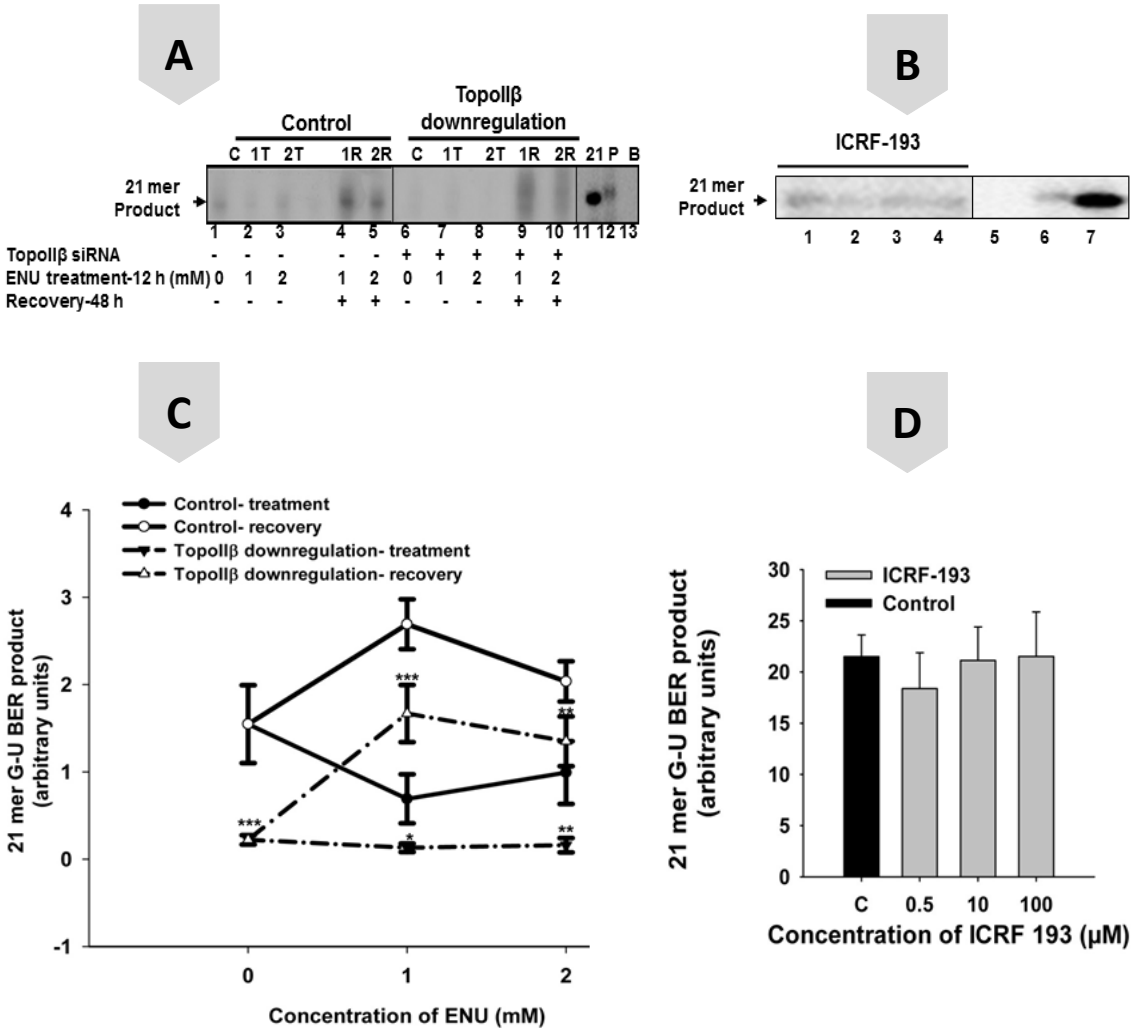

Figure 5: TopoIIβ knockdown neurons are deficient in G-U BER activity

Panel A depicts a representative autoradiogram showing G-U BER activity in CGNs upon ENU treatment and TopoIIβ downregulation. CGNs and CGNT^{-} were incubated in the presence of indicated concentrations of ENU for 12 h (treatment) followed by 48 h of recovery by washing the cells in a fresh medium and then recultured in complete medium. Cell-free extracts prepared and checked for G-U BER activity. Lane 1 is G-U BER activity in control untreated cells

(C); lanes 2 and 3 show activity of protein extracts in terms of 21 mer G-U BER product formation from CGNs treated for 1 and 2 mM ENU for 12 h (1T and 2T); lanes 4 and 5 show the same for treatment followed by 48 h of recovery (1R and 2R), respectively; lane 6 shows activity from untreated ECGNT^{-} (C); lanes 7 and 8 show the same in ECGNT^{-}, 12 h ENU treatment (1T and 2T) and lanes 9 and 10 for treatment followed by 48 h recovery (1R and 2R). Lane 11 depicts 21 mer; lane 12 is pure enzyme control (P); lane 13 depicts blank (B), i.e. 3 pmol of G-U BER substrate. **Panel B** depicts the effect of ICRF-193 on G-U BER activity. TopoIIβ inhibitor ICRF-193 was used to demonstrate the direct participation of TopoIIβ catalytic activity in the repair of G-U mismatch. 0.5, 10, 100 μM ICRF-193 (corresponding to lanes 2, 3 and 4) was directly added to *in vitro* G-U BER reaction. Lanes 5, 6 and 7 correspond to blank (B), pure enzyme control (P) and 21 mer (21). The amount of 21 mer G-U BER product formed was densitometrically measured using ImageJ 1.43u software, NIH, USA and the values represented as bar graphs. The difference in the activities of control and CGNT^{-} extracts among similar treatments was found to be highly significant using One Way ANOVA (*Holm-Sidak* method), (* $P < 0.05$, ** $P < 0.01$, *** $P < 0.001$). Bar charts depict Mean ± SD **(Panels C and D).**

Figure 6

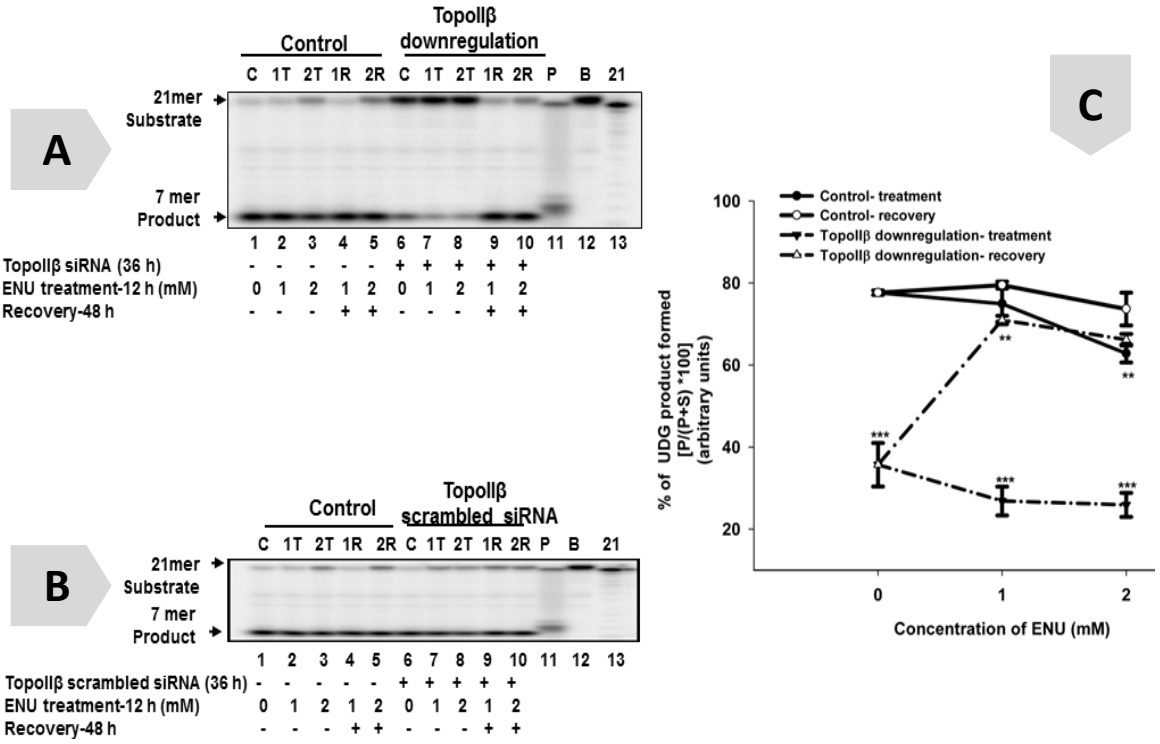

Figure 6: UDG activity is not enhanced in TopoIIβ deficient condition during ENU treatment

The substrate is 200 fmol of 5'-[γ-^{32}P]ATP end labeled 21 mer double stranded U containing oligonucleotide. UDG activity involves base hydrolysis of U, resulting in a 7 mer product. **Panel A** is a representative autoradiogram showing UDG activity upon ENU treatment and TopoIIβ downregulation. Lane 1 illustrates UDG activity in control untreated cells (C); lanes 2 and 3 show activity of protein extracts in terms of 7 mer product formation from CGNs treated with 1 and 2 mM ENU for 12 h (IT and 2T); lanes 4 and 5 show the same for treatment followed by 48 h of recovery (1R and 2R) respectively; lane 6 shows activity from untreated ECGNT^{-} (C); lanes 7 and 8 show the same in ECGNT^{-}, 12 h treatment (1T and 2T) and lanes 9 and 10 for treatment followed by 48 h recovery (1R and 2R). Lane

11, activity by 0.5 U of pure enzyme, UDG (P); lane 12, activity in blank (B), i.e. 200 fmol of substrate; lane 13 depicts 21 mer (21). Treatments given as indicated in the figure. **Panel B** shows representative autoradiogram showing UDG activity in CGN extracts treated with TopoIIβ scrambled siRNA to rule out any direct effect of siRNA on UDG activity. The experimental procedure and product quantification were done as described in Section 2.12.2 Percentage of glycosylated product was measured in arbitrary units. Densitometric analysis carried out using ImageJ 1.43u software, NIH, USA. Mean ± SD values represented in bar graphs **(Panel C)**. The difference in the UDG activities of control and $CGNT^{-}$ extracts among similar treatments was found to be highly significant using One Way ANOVA (*Holm-Sidak* method) (** $P < 0.01$, *** $P < 0.001$).

Figure 6

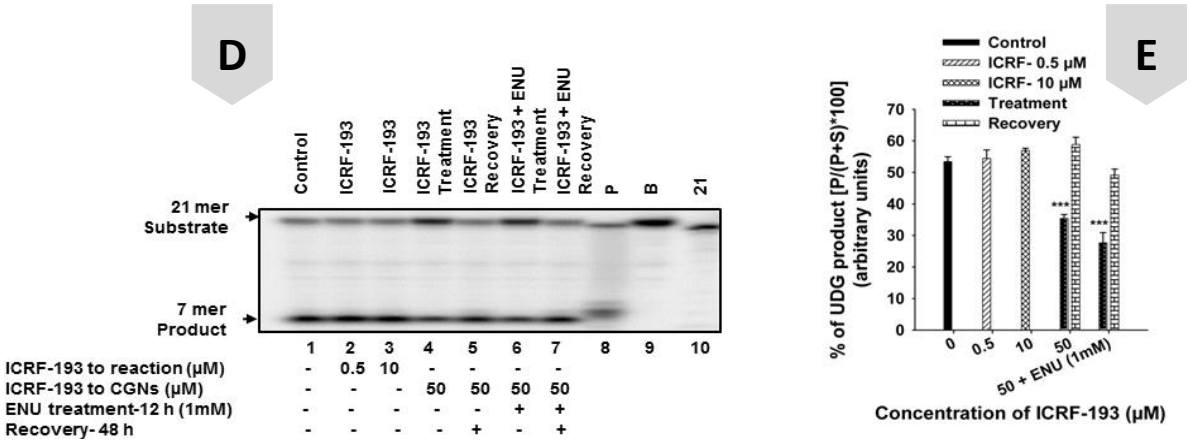

Panel D shows the effect of ICRF-193 on UDG activity, in culture and *in vitro.* Lane 1 shows UDG activity in healthy CGNs; lanes 2 and 3, UDG activity upon direct addition of 0.5 and 10 μM ICRF-193; lanes 4 and 5, activity upon 12 h treatment and 48 h recovery from 50 μM ICRF-193; lanes 6 and 7, activity upon treatment with ICRF-193 (12 h) followed by 1 mM ENU (12 h) and recovery (48 h) as indicated in the Figure. 4C. Lanes 8, 9 and 10, activity by 0.5 U pure enzyme, UDG (P), blank (B) and 21 mer (21). Percentage of glycosylated product was measured in arbitrary units. Densitometric analysis carried out using ImageJ 1.43u software, NIH, USA. Mean ± SD values represented in bar graphs (**Panel E**). The difference in the UDG activities of extracts of control and ICRF-193 treated CGNs was found to be highly significant using One Way ANOVA (*Holm-Sidak* method) (** $P < 0.01$, *** $P < 0.001$).

Figure 7

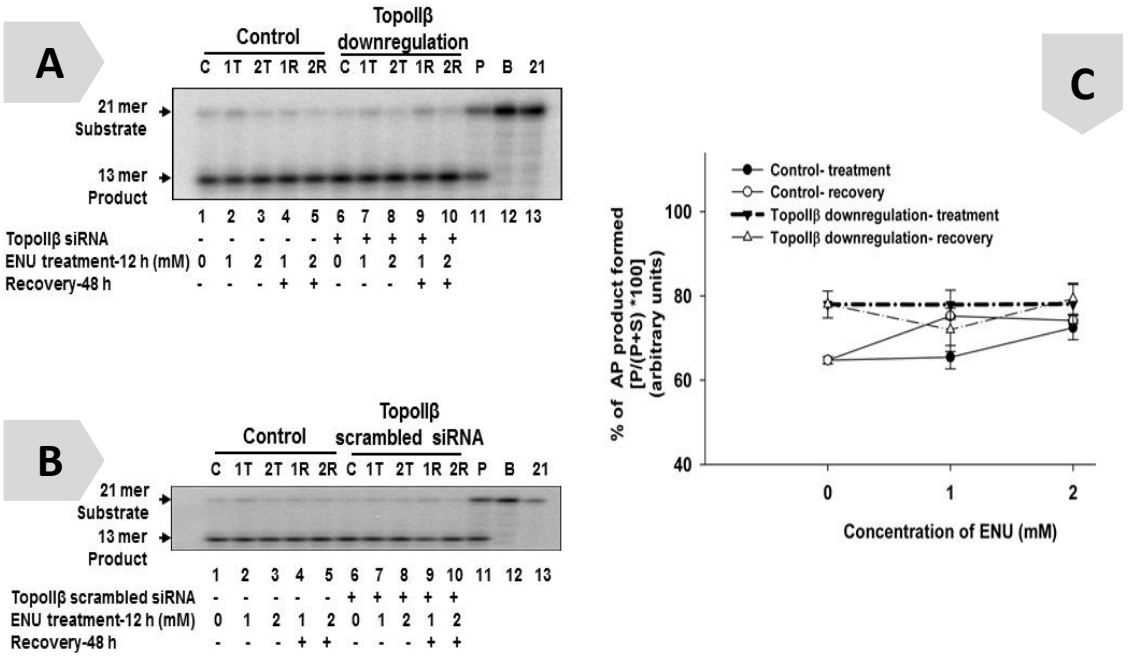

Figure 7: AP endonuclease activity slightly increased by TopoIIβ downregulation

Panel A is a representative autoradiogram showing AP endonuclease (APE) activity. The substrate is 200 fmol of 5'-[γ-^{32}P]ATP end labeled 21 mer double stranded oligonucleotide containing F, tetrahydrofuran (AP site analog). The APE activity involves the cleavage of phosphodiester backbone on the 3' side of F. Lane 1 illustrates activity in control untreated cells (C); lanes 2 and 3 show activity of protein extracts in terms of 14 mer AP product formation from CGNs treated for 1 and 2 mM ENU for 12 h (1T and 2T); lanes 4 and 5 show the same for treatment followed by 48 h of recovery (1R and 2R) respectively; lane 6 shows activity from untreated ECGNT^{-} (C); lanes 7 and 8 show the same in ECGNT^{-}, 12 h treatment (1T and 2T) and lanes 9 and 10 for treatment followed by 48 h recovery (1R and 2R). Lane 11, activity by 1 U of pure enzyme, human

APE1 (P); lane 12, activity in blank (B), i.e. 200 fmol of substrate; lane 13 depicts 21 mer (21). **Panel B** shows APE activity in CGN extracts treated with TopoIIβ scrambled siRNA to rule out any direct effect of siRNA on APE activity. Percentage of 13 mer product was measured in terms of arbitrary units. Experimental procedure and densitometric quantification were carried out as described in Section 2.12.3. Bar graph depicts Mean ± SD **(Panel C).**

Figure 8

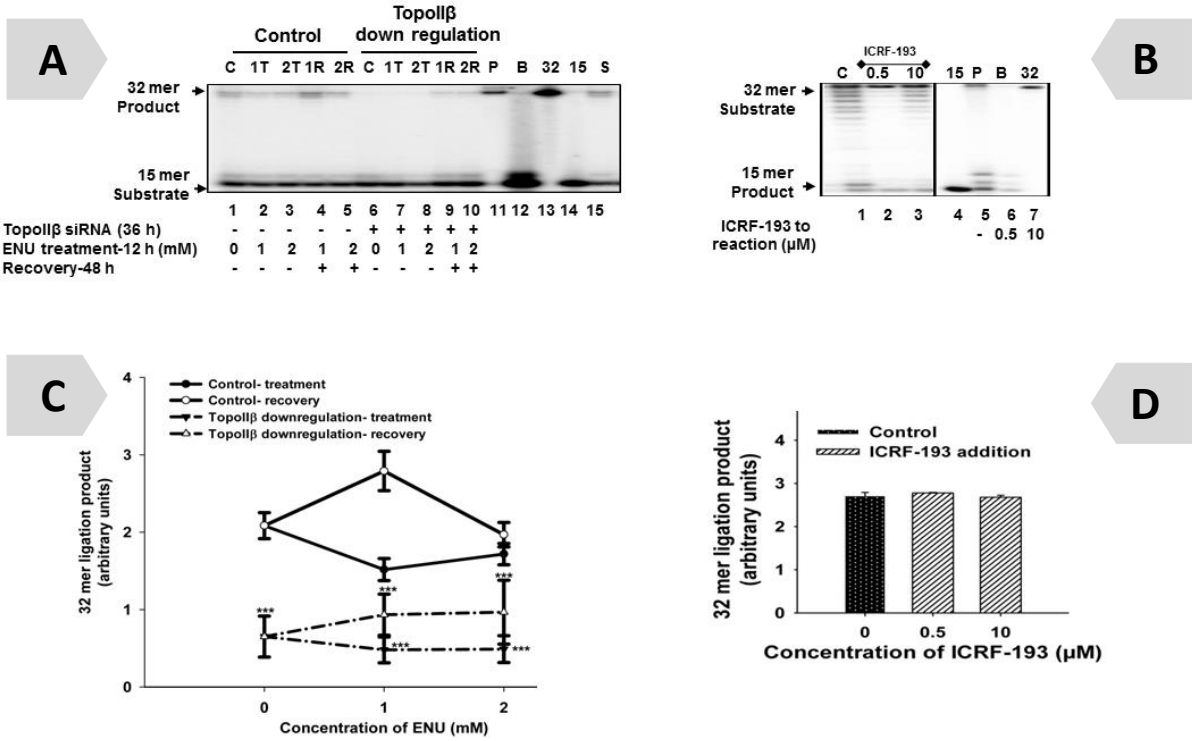

Figure 8: LIG activity is affected in the ECGNT⁻ cells during recovery from ENU mediated strand breaks

Panel A is a representative autoradiogram depicting LIG activity. CGNs and CGNT⁻ were incubated in the presence of indicated concentrations of ENU for 12 h (treatment) followed by 48 h of recovery by washing the cells in fresh medium and then recultured in complete medium. Lane 1 corresponds to LIG activity in control untreated cells (C); lanes 2 and 3 show LIG activity of protein extracts in terms of ligated product formation from 1 and 2 mM ENU treated CGNs for 12 h (1T and 2T); lanes 4 and 5 show the same for treatment followed by 48 h of recovery (1R and 2R);lane 6 shows activity from untreated ECGNT⁻ (C); lanes 7 and 8 show the same in ECGNT⁻ subjected to 12 h ENU treatment (1T and 2T); lanes 9 and 10 for treatment followed by 48 h recovery (1R and 2R); lane 11

corresponds to LIG activity by 10 U of pure enzyme, T_4 DNA ligase (P); lane 12 corresponds to blank (B), i.e. 400 fmol of substrate DNA; lanes 13 and 14 to 32 mer and 15 mer marker, respectively and lane 15 to LIG activity due to scrambled TopoIIβ siRNA (S). The activity in control CGN extract was found to be significantly higher than ECGNT$^-$, compared between similar treatments.

Panel B illustrates the effect of TopoIIβ inhibitor, ICRF-193 on LIG activity. Experimental procedure as described in Section 2.12.4. Lanes 1, 2 and 3 correspond to activity in control (C), 0.5 and 10 μm ICRF-193 additions to *in vitro* LIG reaction. Lanes 4 to 7 correspond to 15 mer (15), pure enzyme (P), blank (B) and 32 mer (32), respectively. The amount of 32 mer ligated product formed was densitometrically measured using ImageJ 1.43u software, NIH, USA. Mean ± SD values represented as bar graph **(Panels C and D).** The difference in the activities of control and CGNT$^-$ treated CGNs was found to be highly significant using One Way ANOVA (*Holm-Sidak* method) (** $P < 0.01$, *** $P < 0.001$).

Figure 8

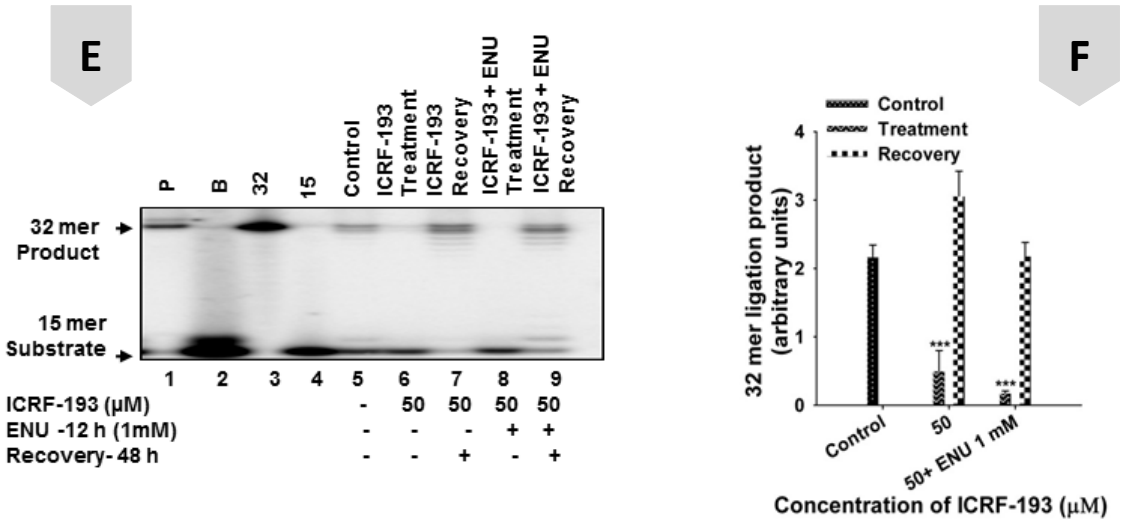

Panel E illustrates the effect of ICRF-193 treatment on LIG activity in cultured CGNs. Lanes 1 to 4 correspond to LIG activity in pure enzyme (P), blank (B), 32 mer (32) and 15 mer (15), respectively. Lane 5 shows LIG activity in control (C); lanes 6 and 7 correspond to activity in ICRF-193 treated and recovered culture; lanes 8 and 9 correspond to activity in ICRF-193 (12 h) and ENU (12 h) treated and recovered cultures at indicated concentrations. The amount of 32 mer ligated product formed was densitometrically measured using ImageJ 1.43u software, NIH, USA. Mean ± SD values represented as bar graph **(Panel F)**. The difference in the activities of control and ICRF-193 treated CGNs was found to be highly significant using One Way ANOVA (*Holm-Sidak* method) (** $P < 0.01$, *** $P < 0.001$).

Figure 9

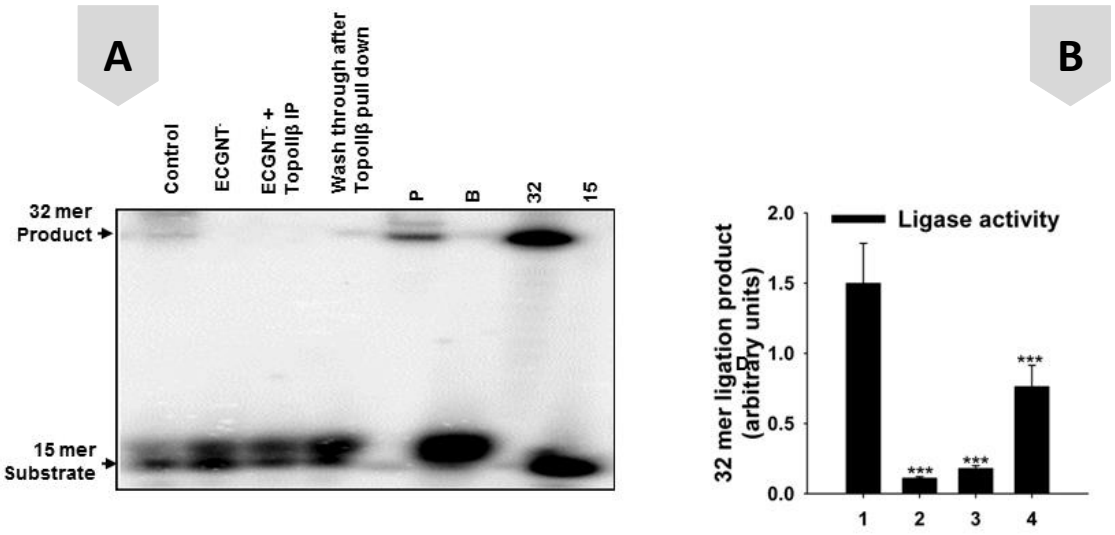

Figure 9: TopoIIβ activity *per se* not required for LIG activity

Panel A a representative autoradiogram depicts TopoIIβ is not directly involved in the ligation step. Lanes 1 to 4 correspond to LIG activity in control, ECGNT^{-}, ECGNT^{-}+ TopoIIβ immunoprecipitated (IP), wash through after TopoIIβ pull down. Lanes 5 to 8 correspond to pure enzyme control (P), blank (B), 32 mer (32) and 15 mer (15). Using One Way ANOVA (*Holm-Sidak* method), statistically significant lowered LIG activity was seen in ECGNT^{-}, ECGNT^{-}+ TopoIIβ immunoprecipitated condition (*** $P < 0.001$). Mean ± SD values depicted in bar graphs **(Panel B).**

Discussion

Abasic sites are the most commonly formed DNA lesions in the cell and are produced by numerous endogenous and environmental insults. Most abasic sites in cells exist as processed BER intermediates that contain DNA strand breaks proximal to the damaged residue (Krokan et al., 1983). Abasic sites, usually developed at the initial stage of BER, when present in a TopoII DNA cleavage site, they create suicidal substrates, namely BER intermediates containing 5'- or 3'-nicked abasic sites or dRP flaps that are not re-ligated readily by the enzyme and can generate permanent DNA cleavage (Wilstermann and Osheroff, 2001). Thus, they act as TopoII poisons and dramatically stimulate enzyme-mediated DNA cleavage leading to DSBs (Wilstermann and Osheroff, 2001). This is evident from the higher sensitivity of CGNs to ICRF-193 (Figure. 4B). Of the lesions examined to date, AP sites seem to be the most active (Bigioni et al., 1996; Kingma et al., 1995; Kingma et al., 1997; Kingma and Osheroff, 1997; Powell et al., 2005; Sabourin and Osheroff, 2000). When AP sites are located within TopoII cleavage sites, they significantly stimulate TopoII mediated DNA cleavage (Kingma et al., 1995; Sabourin and Osheroff, 2000). These results show that AP sites are potentially lethal. Methoxyamine-bound apurinic/ apyrimidinic (MX-AP) site in TopoII cleavage sites in DNA act as dual lethal targets, not only for functionally disrupting the BER pathway but also for potentially poisoning TopoII. MX-AP sites are refractory to the catalytic activity of AP endonuclease, indicating their ability to block BER. MX-AP sites are indeed cleaved by purified TopoII, thus suggesting that these sites stimulate TopoII mediated DNA cleavages (Yan et al.,

2007). The presence of TopoII cleavage sites in the vicinity of AP sites and methoxyamine related toxicity provides a possible overlap of the TopoII binding and cleavage sites in the vicinity of BER processing region thus implicating TopoIIβ activity in the regulation of BER intermediates in the pathway. The repair of AP sites is the primary defense system, which proceeds more rapidly compared to the repair of a single base such as a U or an 8-oxoguanine base (Boiteux and Guillet, 2004). If the BER pathway is interrupted, nonrepaired AP sites exhibit toxicity (Loeb, 1985). This suggests the importance of understanding the role of intact BER mechanism in recovering cells in relation to protection from the incidence of modifications of the base as well as AP sites. This will be more prominent in primary neurons, whose recovery is essential for restoration of neuronal functions. Although most of the above studies of TopoII activities against AP DNA were invoking TopoIIα and like enzymes, it is not clear if similar activities also take place in case of TopoIIβ, which is the only TopoII isoform expressed in primary neurons. Neurons are prone to high frequency of DNA damage due to increased reactive oxygen species and various other reasons. The present study is an effort to understand the DNA repair function of TopoIIβ in primary neurons.

The results of the present study using the siRNA mediated knock down of TopoIIβ clearly point out that BER activity, especially UDG and LIG requires the presence of TopoIIβ in neurons for protection against the possible encounter of insults from alkylating agents. The diminishing activity of TopoIIβ with age both in ageing rat brain (Kondapi et al., 2004) and in CGNs (Bhanu et al., 2010) points to the importance of restoration of TopoIIβ in ageing brain, specifically neurons

for protection from physiological insults. The significant decrease of G-U BER and LIG activities observed in ageing CGNs with concomitant decrease in the level of TopoIIβ (Bhanu et al., 2010) clearly implicates the role of TopoIIβ in the maintenance of BER capacity of neurons against their degeneration during ageing. The present study indicates the regulatory role of TopoIIβ rather than the catalytic role in the maintenance of BER activity.

TopoIIβ, unlike TopoIIα is present in all cell types and specifically present in terminally differentiated cells like neurons. The presence of TopoIIβ in these neurons implicate its role in various neuronal activities like neuronal development, maintenance and gene regulation, Some of the reports of probable interaction of TopoIIβ in repair initiation complexes (Ju et al., 2006) and non-homologous end joining (NHEJ) proteins (Mandraju et al., 2011) supports the possible interaction of TopoIIβ to various repair initiation complexes in promoting the repair process. The molecular activities provided could be through direct interaction of TopoIIβ with repair protein(s), stabilizing the repair complex or/and the presence of TopoIIβ in the repair complex may confer torsional integrity to the DNA during the repair and associated unwinding and re-winding of the DNA without torsional strain.

ICRF-193, bis (2,6-dioxopiperazine) is a strong catalytic inhibitor of Topoisomerase II at lower concentrations (Tanabe et al., 1991) and downregulates TopoIIβ protein expression at higher concentrations (Xiao et al., 2003). Hence, we used both conditions to check the association of TopoIIβ catalytic activity and the protein itself in BER pathway. ICRF-193 traps TopoII into circular clamps on chromatin which impedes the movement of elongating

RNA polymerases (Xiao et al., 2003). The suppression of the transcriptional induction of amphiphysin and synaptophysin, nerve terminal stabilizing proteins in CGNs upon ICRF treatment, suggests that TopoII may be involved in the transcriptional regulation (Tsutsui et al., 2001). TopoIIβ *per se* is not involved in BER activity but an active form of TopoIIβ is required for regulating the same. It is possible that TopoIIβ may be interacting with various cellular machineries in restoration of BER activity. This could also be *via* interacting with various partners involved in transcription (Ju et al., 2006).

The present study thus implicates an indirect but significant role of TopoIIβ in modulating or regulating the BER capacity, thus becoming an important and basic constituent factor for promoting the repair of DNA breaks through BER pathway. Further studies are required to elucidate the obvious regulatory functions of TopoIIβ in neurons.

Conclusion

TopoIIβ is essential for promoting the repair of ENU-mediated strand breaks *via* BER pathway. Our overall results suggest a role at least an indirect one of TopoIIβ in the repair of ENU induced BER pathway including the activities of UDG and LIG.

CHAPTER 4

CHARACTERIZING SENESCENCE-ASSOCIATED STRESS RESPONSES AND REPAIR IN *IN VITRO* CULTURED CGNS

Introduction

Cellular senescence is an irreversible arrest of cell proliferation (Hayflick, 1985a) and is activated by oxidative stress, DNA damage, oncogene activation, telomere shortening, etc. It is popularly believed to be a tumor suppressing mechanism (Lanigan et al., 2011; Lin et al., 2010) and causes age-related loss of tissue function (Lawless et al., 2010).

Key features of neuronal senescence include cell enlargement, an increase in senescence associated-β-gal activity (SA-β-Gal) (Dimri et al., 1995) and changes in calcium homeostasis (Bhanu et al., 2010) which contribute to the main cause of neuronal ageing (Khachaturian, 1994). Senescent cells secrete matrix degrading protein and cytokines which allows easy detection by immune cells. Growth factors secreted by these cells stimulate the proliferation of the surrounding cells. However, the ability of innate immune system to remove the senescent cells also gradually decreases with age (Fulop et al., 2011). Implications include cancer, ageing or neurodegenerative disorders (Fulop et al., 2011; Hung et al., 2010). These cells are also characteristic of protein secretion (Acosta et al., 2008; Coppe et al., 2008) and chromatin remodeling (Liu et al., 2012).

Senescent tissue is characterized by damaged mitochondria (Cortopassi and Wong, 1999; Lenaz, 1998). Aged mitochondria display a significant reduction of electron transport complexes and alteration in mitochondrial membrane potential (Hagen et al., 1997; Kwong and Sohal, 2000) . These changes are seen as a consequence of accumulated oxidative stress and damage in mitochondrial

DNA (Lenaz, 1998). ATP is needed to carry out most of the metabolic processes in the cell. Mitochondrion being the power house of the cell is required to have a functional electron transport chain which in turn needs two components to be intact: electrical pH gradient and a mitochondrial membrane potential ($\Delta\Psi m$). Hence, mitochondrial membrane potential measurements are thought to be indicative of mitochondrial impairment (Rana et al., 2011).

Brain ageing is characterized by progressive decline in DNA repair, metabolism and cell signaling pathways (LeBel and Bondy, 1992) which affects calcium homeostasis (Mattson, 1992). Ageing brain also shows increased free radical production and so accumulation of mitochondrial (mt) and nuclear (n) DNA damage (Johnson et al., 1999). Neurodegenerative diseases like Alzheimer's and Parkinson's show an increased incidence with age (Hung et al., 2010). The cause behind the occurrence of these diseases is largely unknown and hence understanding the hallmarks of senescence at cellular level is a much needed study to help find newer strategies towards the treatment of such diseases.

Genomic DNA is continuously exposed to DNA damaging agents (Maynard et al., 2009) both endogenous like ROS and exogenous agents which may result in DNA lesions. Genomic stability in neuronal cells is at great risk upon exposure to ROS (Rao, 2002). Moreover, neurons are metabolically highly active and supported by a low antioxidant defense mechanism. Hence, cells have evolved a distinct repair pathway, the Base Excision Repair (BER) which repair oxidative lesions, SSBs and abasic sites (Wilson and McNeill, 2007).

We chose cerebellar granule neuron (CGN) an *in vitro* culture model to study

neuronal senescence. Neurons form a very interesting cell model in culture to study ageing. Being terminally differentiated, the life of a neuron directly reflects on the age or is synchronous with the life of the organism. CGNs constitute the largest homogenous neuronal population in the mammalian brain.

Although much is known about replicative senescence, the knowledge of senescence mechanisms in neurons remains largely a void. This present work was planned to add to the existing knowledge, especially in terms of the DNA damage and repair properties of an ageing neuron. Through this paper we hope to draw a parallel between *in vitro* and *in vivo* ageing.

Experimental strategy

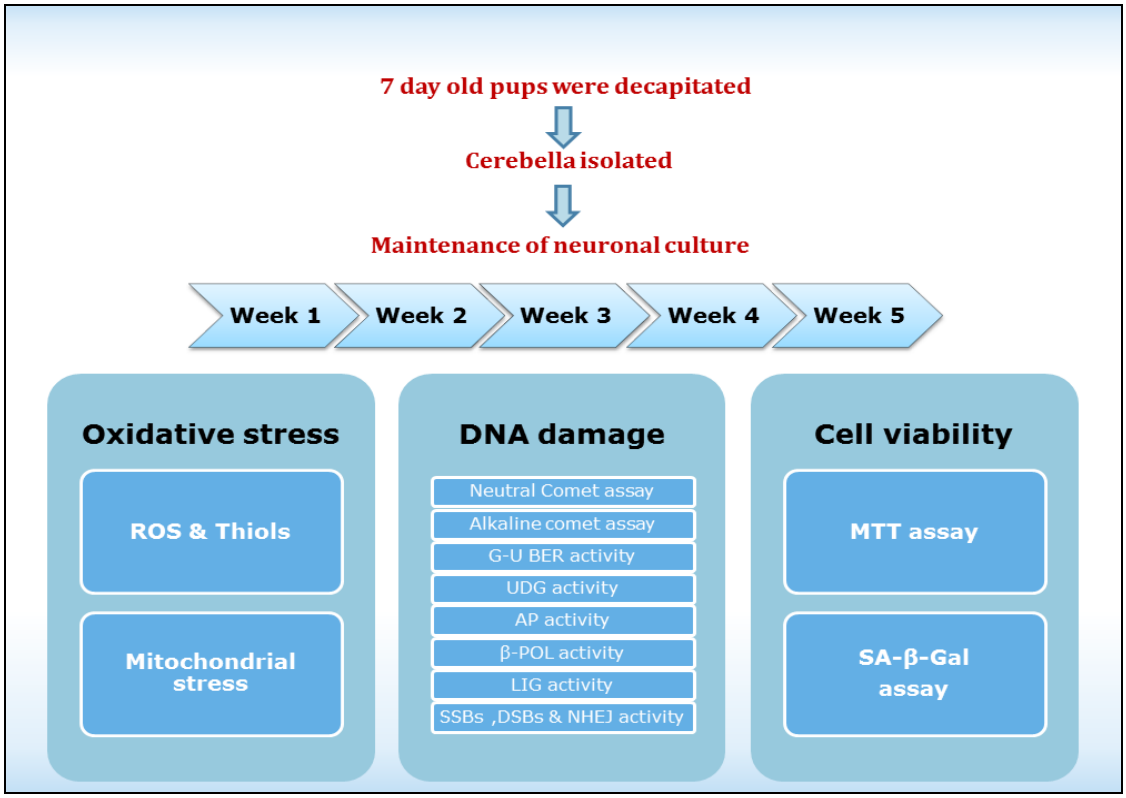

Results

4.1. Cell viability of CGNs and Real-Time PCR

CGNs showed viability until the 6th week (Bhanu et al., 2010). Hence in this paper, we address 1W, 3W and 5W as young, adult and old cultures respectively. The CGNs were aged in *in vitro* culture conditions as described under Section 2.3. No additional treatments were given. Asin the experimental plan, various assays were carried out to characterize senescence. **Figure 10A** shows cell viability assay for ENU. CGNs were incubated in presence of increasing concentrations of ENU as indicated for 24h, 12h and 6h and the cytotoxicity was determined by MTT assay. The cell viability was determined with respect to control untreated cells. At all concentrations cell viability was found to be greater than 80%. **Figure 10B** shows cytotoxicity detected by reduction of MTT in ageing CGNs. Results are expressed as mean ± SD (3 replicates in two independent experiments). Cell viability in first week was considered as 100 %. Values are presented as a percentage of activity in control cells. Cell viability markedly decreased by 40% in second week and was then stable in the consecutive weeks. **Figure 10C** shows fold change expression by quantitative Real-Time PCR for Topoisomerase II β. TOP2β reveals significant decrease in relative expression through the weeks as per statistical analysis, One Way ANOVA (*Tukey post hoc* test) (*P< 0.05, **P< 0.01, ***P< 0.001), 1W healthy CGNs were taken for control.

4.2 Senescence associated-β-galactosidase assay

SA-β-Gal is a known marker for senescence (Dimri et al., 1995). Hence, activity and transcript level of this marker was chosen as a standard for this work. **Figure 11A** shows senescence associated β galactosidase bright field microscopic images in ageing CGNs. **Figure 11B** shows that the percentage of SA-β-Gal-positive cells increased progressively with age, from 0% in the first week to 99% in 5th week. This increase in SA-β-gal may be due to stress accumulation under the prolonged culture period. Such a significant enhancement in the SA-β gal in cultured CGNs shows *in vitro* ageing similar to physiological ageing.

4.3. Age affects neuronal GSH and ROS levels

Results are expressed as mean ± standard deviation of replicates (n = 6) in two independent experiments in **Figure 12**. Values were corrected for protein content in each well and determined as a percentage of fluorescence with respect to control cells. **Figure 12A-** Free thiols showed a significant decline in ageing CGNs from 2W to 5W using One-way ANOVA (*Tukey post hoc* test) (*P< 0.05, **P< 0.01, ***P< 0.001). The percentage of GSH/μg protein was found to be 100, 76.3, 58.7, 40.5 and 36.7, 1W to 5W, respectively. **Figure 12B-** 3W onwards ROS levels significantly increased. **Figure 12C-** Gene expression profiling (microarray data) reflected lowered super oxide dismutase (SOD2), catalase (Cat), nitric oxide synthase (NOS1) and increased glutathione peroxidase (GPX1). **Figure 12D-** is an overview of altered gene expression in ageing CGNs wherein 1W healthy CGNs were taken for control.

4.4. Assessment of DNA damage with age in in vitro cultured CGNs

The integrity of genomic DNA under the effect of natural ageing in *in vitro* CGNs was accessed by comet assay in neutral and alkaline conditions (**Figure 13**). Comets of young CGNs (1W) appeared round and bright suggesting DNA damage to be minimal. However, with progress in age i.e. from 2W to 5W, a significant migration of DNA from nucleus was seen forming a 'comet' tail. Even a naked eye observation of the alkaline comets revealed an increase in tail length which can be directly correlated with an increase in SSBs, DSBs and alkali labile sites. This observation also applied to neutral comets that largely detect DSB. **Figure 13A** shows comets of ageing CGNs (1^{st} to 5^{th} week) in neutral condition and alkaline condition. **Figure 13B** shows corresponding bar charts depicting Mean ± SD. DNA damage was measured in terms of tail moment. There was a concentration dependent production of DNA damage in control batch. DNA damage was quantified using CometScore™ Freeware v1.5 (TriTek Corporation, Sumerduck, VA, US) in arbitrary units. Scale bar = 100 μm. Tail moment was found to be statistically higher as age progressed in comparison with the control (1W) batch using One Way ANOVA (*Tukey post hoc* test) (** $P < 0.01$, *** $P < 0.001$).

4.5 Characterizing mitochondrial membrane potential (ΔΨm) in ageing CGNs by flowcytometry

CGNs were stained with R123 and ΔΨm was quantified by flowcytometric analysis. **Figure 14** (**A- G)** corresponds to R123 profiles of CGNs subjected to ageing (1W to 5W) and CPT treatment. Counts vs. FL1 histograms of 1W to 5W and 10 μM CPT treated CGNs were generated using Flo Max software 2008

(Partek). Cells showing fluorescence intensity lower than 10^1 arbitrary units were gated. Percentage of cells in the gated population has been indicated in the histogram. The percentage of cells falling within this gate is indicative of low ΔΨm. **Figure 14H** corresponds to an overlay histogram (counts vs. FL1) of 1W to 5W old and 10 μM CPT treated CGNs. Cell count was plotted along Y-axis and intensity of fluorescence along X-axis. ΔΨm was shown by shift in the cell population towards the lower median values of FL1 scale. Peak shift to left indicates reduction in R123 fluorescence which is indicative of decrease in mitochondrial membrane potential with age.

Senescent cells were present in all weeks. Senescent cells were fewer in numbers in young 1W and 2W young CGN cultures (Figure 14A and B) and increased in 3W to 5W adult and old CGN cultures. CGNs of 1W and 2W- 89.05 and 88.84 %, respectively maintained healthy ΔΨm as measured by R123 (Figure 14A and B). Adult and old CGN cultures (3W to 5W) show large populations with significantly reduced fluorescence. 25.61, 53 and 59.3 % of CGN cultures were below the normal range as indicated in Figure 14 C-F. 1W old CGNs were taken as healthy control. Treatment of CGNs with 10 μM campothecin (CPT) for 18 h induces apoptosis (Bhanu et al., 2010). Such a cell culture was used as control for lowered ΔΨm. The one and two week-old CGNs seemed healthy with no significant change in the ΔΨm. As time progressed and as cells approached death, they began to show a dramatic increased depolarization of the mitochondrial membrane, which corroborates with neuronal cell viability. Peak shift to left correlates with the decrease in fluorescence, which in turn is a proof

of fall in ΔΨm as explained in Section 2.16. Overall, the ageing CGNs exhibited an alteration in the mitochondrial membrane potential during *in vitro* ageing,

4.6. Validation of differential gene expression by qPCR

Senescence-associated changes in the gene expression and repair activities of BER enzymes were analyzed in CGN cultures. **Figure 15A** shows fold change expression by Microarray analysis and **Figure 15B** shows validation by quantitative Real-Time PCR for BER genes - UNG, SMUG, APE 1 and TOP2β reveals significant decrease in relative expression of all genes mentioned except UNG. UNG shows a significant increase in relative gene expression through the weeks as per statistical analysis. **Figure 16A** depicts fold change expression by Microarray analysis and **Figure 16 (B,C)** is validation by qPCR for BER genes – POLβ, POLλ, POLμ, LIG1 and LIG3 reveals significant decrease in relative expression of all genes given except POLλ and POLμ. The latter two genes show a significant increase in relative gene expression through the weeks as per statistical analysis where in, 1W healthy CGNs were taken as control.

4.7. Effect of in vitro ageing on G-U BER and ligase activity in CGNs

Cultured CGNs were pelleted at the end of every week for 5 weeks and cell extracts prepared. **Figure 17A** depicts a representative autoradiogram showing G-U BER activity in ageing CGN extracts. The substrate for G-U BER assay is a 3 pmol of 21 mer double stranded uracil (U) containing oligonucleotide. The BER activity of the extracts involves base hydrolysis of U, cleaving the phosphodiester backbone followed by the polymerase gap filling and ligation. Lane 1 is a 21 mer;

lane 2 shows activity in blank (B), i.e. only 3 pmol of substrate; lanes 3 to 7 depict G-U BER activity in CGN extracts aged 1 (1W) to 5 weeks (5W), respectively. Seen is a gradual decline in the activity of the ageing extracts in terms of 21 mer product formed in arbitrary units. **Figure 17B** illustrates the effect of *in vitro* ageing on ligase (LIG) activity in CGNs. Substrate is a 400 fmol of 5'-[γ-^{32}P]ATP end labeled 32 mer double stranded oligonucleotide containing a nick. The LIG activity of the extracts involves sealing the nick in the phosphodiester backbone that results in a 32 mer product formation. Lanes 1 to 4 correspond to LIG activity by 10 U of pure enzyme, T_4 DNA ligase (P), 15 mer (15), 32 mer (32), blank (B), i.e. 400 fmol of substrate DNA; lanes 5 to 9 depict LIG activity in CGN extracts aged 1 (1W) to 5 weeks (5W), respectively. Representative autoradiogram shows gradual decline in the activity of the ageing extracts in terms of 32 mer product formed in arbitrary units. Activity in 1W old CGN extract was taken as control with which the activity in 2W to 5W CGN extracts was compared using One Way ANOVA (*Holm-Sidak* method). The difference in the activities was found to be statistically significant (*** $P < 0.001$). Bar charts depict Mean ± SD (**Figure 17 C and D**). Analysis of G-U BER activity in ageing CGNs showed that the G-U BER activity decreases significantly from the second week, with very low activity from fourth week of ageing CGNs. The LIG activity in extracts of ageing neurons showed a significant decrease from second week reaching very low levels by the fifth week in culture.

4.8. Age dependent decline of BER enzyme activities (UDG, POL and LIG)

Cultured CGNs were pelleted at an interval of seven days for 5 weeks and cell extracts prepared. 200 fmol of 5′-[γ-^{32}P]ATP labeled 21 mer oligo duplex containing U in its 8th position was incubated with CGN extract under conditions given in Section 2.12.2. **Figure 18A** is a sequencing gel image depicts UDG activity as visualized by the appearance of 7 mer repaired radioactive spot. Panel A: Lanes 4-8 correspond to UDG activity in 1st to 5th week extracts. Lane 1, activity in blank (B), i.e. 200 fmol of substrate; lane 2, activity by 0.5 U of pure enzyme, UDG (P) and lane 3 depicts 21 mer (21). The 7 mer product was quantified using *ImageJ* 1.43u software, NIH, USA and data was expressed in arbitrary units. Values are expressed in mean ± SD for data obtained from 3 independent experiments and same is represented in bar graphs (**Figure 18B**). The decrease in UDG activity from 1W to 5W was found to be significant using One Way ANOVA (*Tukey post hoc* test) (** $P < 0.01$, *** $P < 0.001$). The decrease in UDG activity from 1W to 5W was found to be significant. **Figure 19A** is a representative autoradiogram shows AP endonuclease (APE) activity in ageing CGNs – week wise. The substrate is 200 fmol of 5'-[γ-^{32}P]ATP end labeled 21 mer double stranded oligonucleotide containing F, tetrahydrofuran (AP site analog). The APE activity involves the cleavage of phosphodiester backbone on the 3' side of F resulting in a 13 mer product. Lane 1 illustrates APE activity in control CGNs (1W); lanes 2 to 5 correspond to 2W to 5W respectively. Lane 6, activity by 1 U of pure enzyme, human APE1 (P); lane 7, activity in blank (B), i.e. 200 fmol of substrate; lane 8 depicts 21 mer (21). Percentage of 13 mer product was measured in terms of arbitrary units. Experimental procedure and densitometric

quantification was carried out as described under Section 2.12.1. No change was observed in terms of 13 mer APE product formation. **Figure 20A** depicts a representative autoradiogram showing gap repair activity in ageing CGN extracts. The substrate for gap repair assay is a 400 fmol 5′-[γ-^{32}P]ATP labeled 32 mer oligo duplex containing one gap. The gap repair activity of the extracts involves polymerase gap filling and ligation. Lanes 1 to 5 depict to gap repair activity in 1W to 5W CGN cultures respectively; lanes 6 to 8 correspond to activity in blank (B), 32 mer marker and pure enzyme (P) i.e. 0.5 U of β polymerase respectively. Seen is a gradual decline in the activity of the ageing extracts in terms of 15 mer product formed (in arbitrary units). The difference in the activities of 4W, 5W in comparison to 1W was found to be statistically significant. A significant decrease in the gap repaired product was seen with decline in age (Figure. 20A). The fold change expression (microarray data) of the BER markers was validated by real time PCR. SMUG, APEX1, TOP2β, POLβ, LIG1, LIG3 significantly fell with age which corroborates well with enzyme activities. However, UDG and POL μ showed elevated expression levels with age (**Figures 15 and 16**).

Figure 10

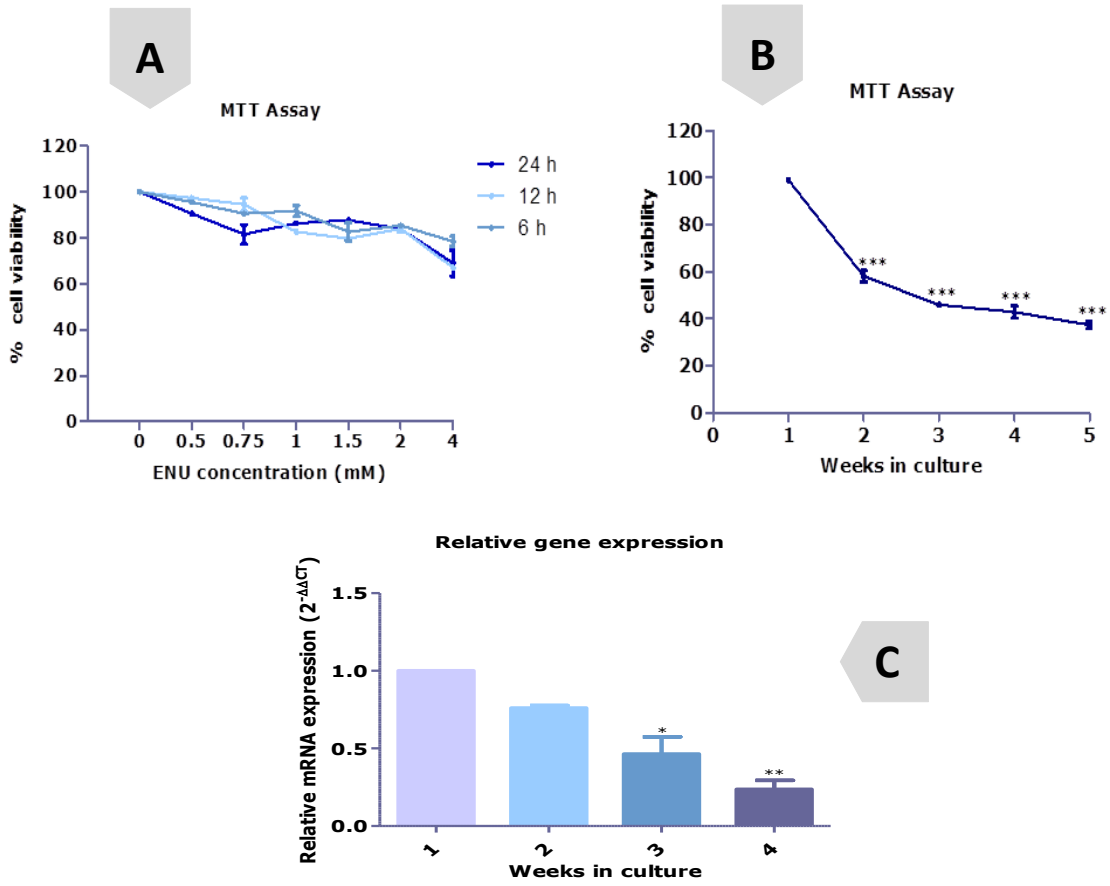

Figure 10: MTT assay and Real-Time PCR

Panel A shows cell viability assay for ENU- CGNs were incubated in presence of increasing concentrations of ENU as indicated for 24h, 12h and 6h and the cytotoxicity was determined by MTT assay. The cell viability was determined with respect to control untreated cells. At all concentrations cell viability was found to be greater than 80%. **Panel B** shows cytotoxicity detected by reduction of MTT in ageing CGNs. Results are expressed as mean ± SD (3 replicates in two independent experiments). Cell viability in first week was considered as 100 %. Values are presented as a percentage of activity in control cells. Cell viability markedly decreased by 40% in second week and was then stable in the consecutive weeks. **Panel C** shows fold change expression by quantitative Real-Time PCR for TopoIIβ. TOP2β reveals significant decrease in relative expression through the weeks as per statistical analysis, One Way ANOVA (*Tukey post hoc* test) (*P< 0.05, **P< 0.01, ***P< 0.001). 1W healthy CGNs were taken for control.

Figure 11

A

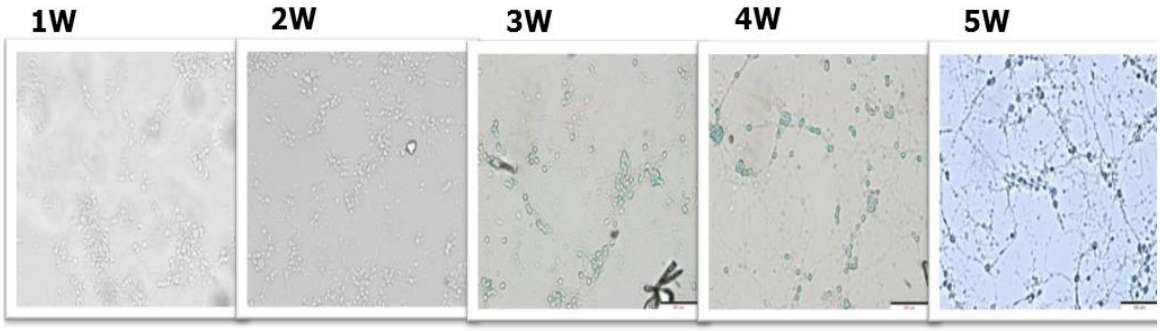

B

Days in culture	% of SA- β gal stained cells
7	0
14	2
21	75
28	98
35	99

Figure 11: Senescence associated-β-galactosidase assay

Panel A shows senescence associated β galactosidase bright field microscopic images in ageing CGNs.

Panel B- The percentage of SA-β-Gal-positive cells increased progressively with age, from 0% in the first week to 99% in 5th week. This increase in SA-β-gal may be due to stress accumulation under the prolonged culture period. Such a significant enhancement in the SA-β gal in cultured CGNs shows *in vitro* ageing similar to physiological ageing.

Figure 12

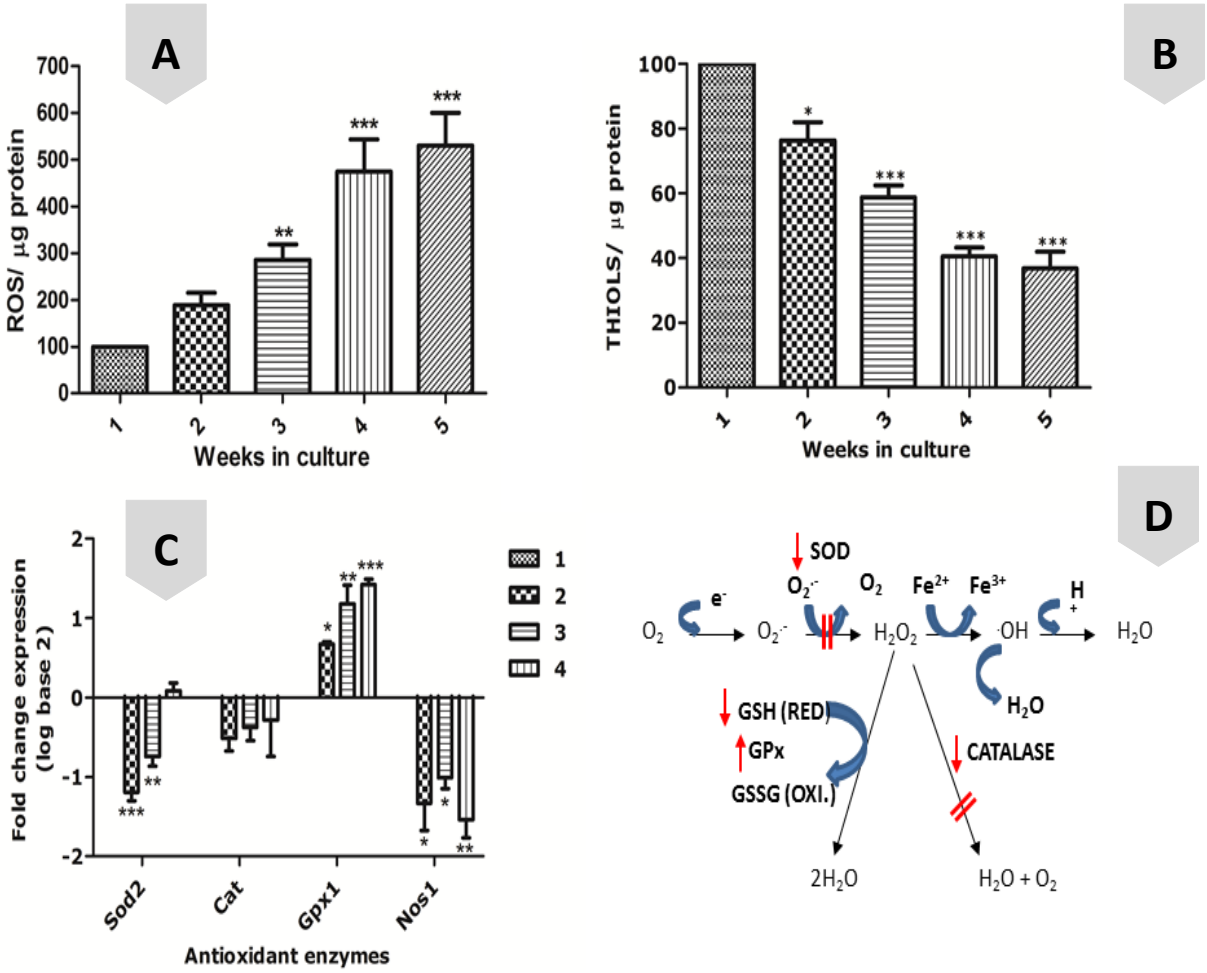

Figure 12: Cellular ROS and GSH in ageing CGNs

Results are expressed as mean ± standard deviation of replicates (n = 6) in two independent experiments. Values were corrected for protein content in each well and determined as a percentage of fluorescence with respect to control cells. **(Panel A)** Free thiols showed a significant decline in ageing CGNs from 2W to 5W using One-way ANOVA (*Tukey post hoc* test) (*P< 0.05, **P< 0.01, ***P< 0.001). **(Panel B)** 3W onwards ROS levels significantly increased. **(Panel C)** Microarray data analysis (week wise) showed significant decline in the fold change expression of SOD2, CAT, NOS1 and elevated levels of GPX1. (Panel D) Seen is an overview of altered gene expression in ageing CGNs. 1W healthy CGNs were taken for control.

Figure 13

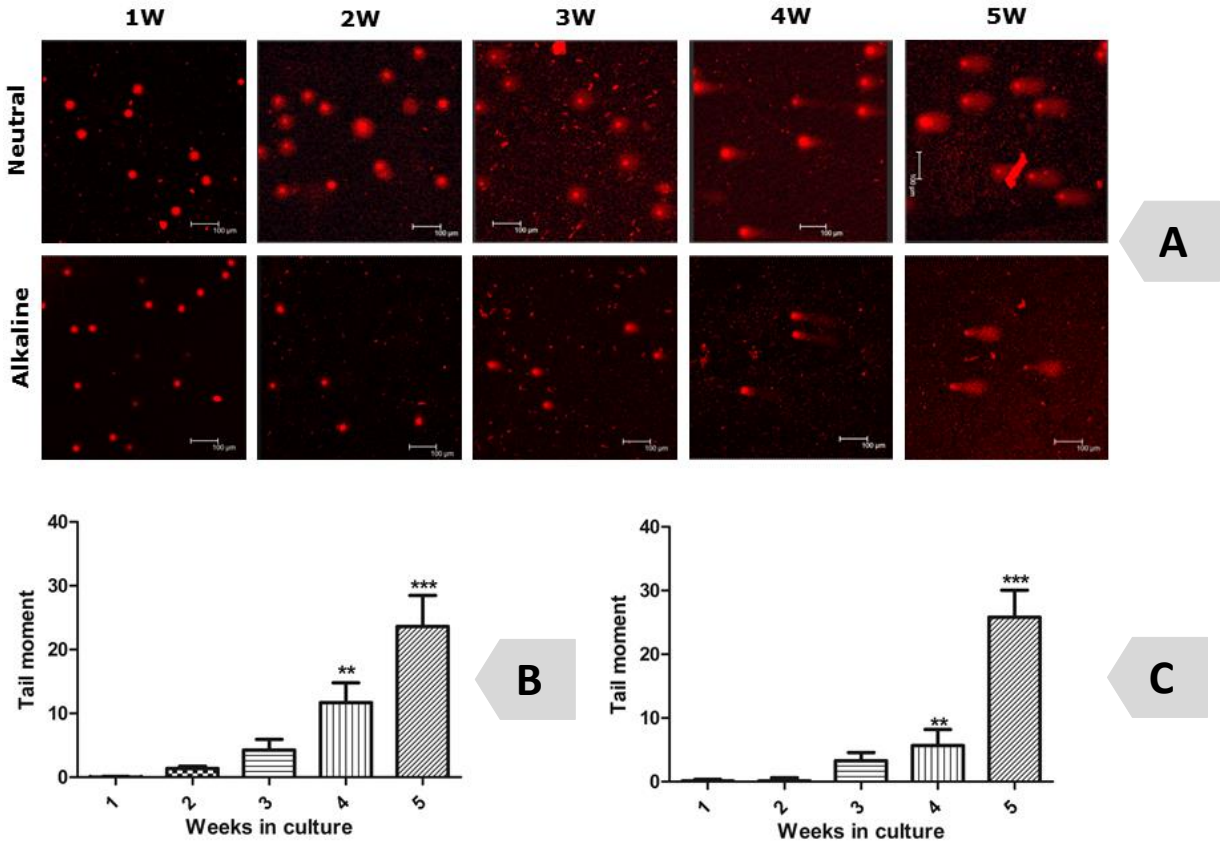

Figure 13: Assessment of DNA damage with age in *in vitro* cultured CGNs

Extent of native DNA damage in *in vitro* cultured CGNs was evaluated by comet assay. Panel A shows comets of ageing CGNs (1st to 5th week) in neutral condition and alkaline condition. Panel B shows corresponding bar charts depicting Mean ± SD. Average of 50 cells was chosen for every experiment (n=3). DNA damage was measured in terms of tail moment. There was a concentration dependent production of DNA damage in control batch. DNA damage was quantified using CometScore™ Freeware v1.5 (TriTek Corporation, Sumerduck, VA, US) in arbitrary units. Scale bar = 100 µm. Tail moment was found to be statistically higher as age progressed in comparison with the control (1W) batch using One Way ANOVA (*Tukey post hoc* test) (** $P < 0.01$, *** $P < 0.001$).

Figure 14

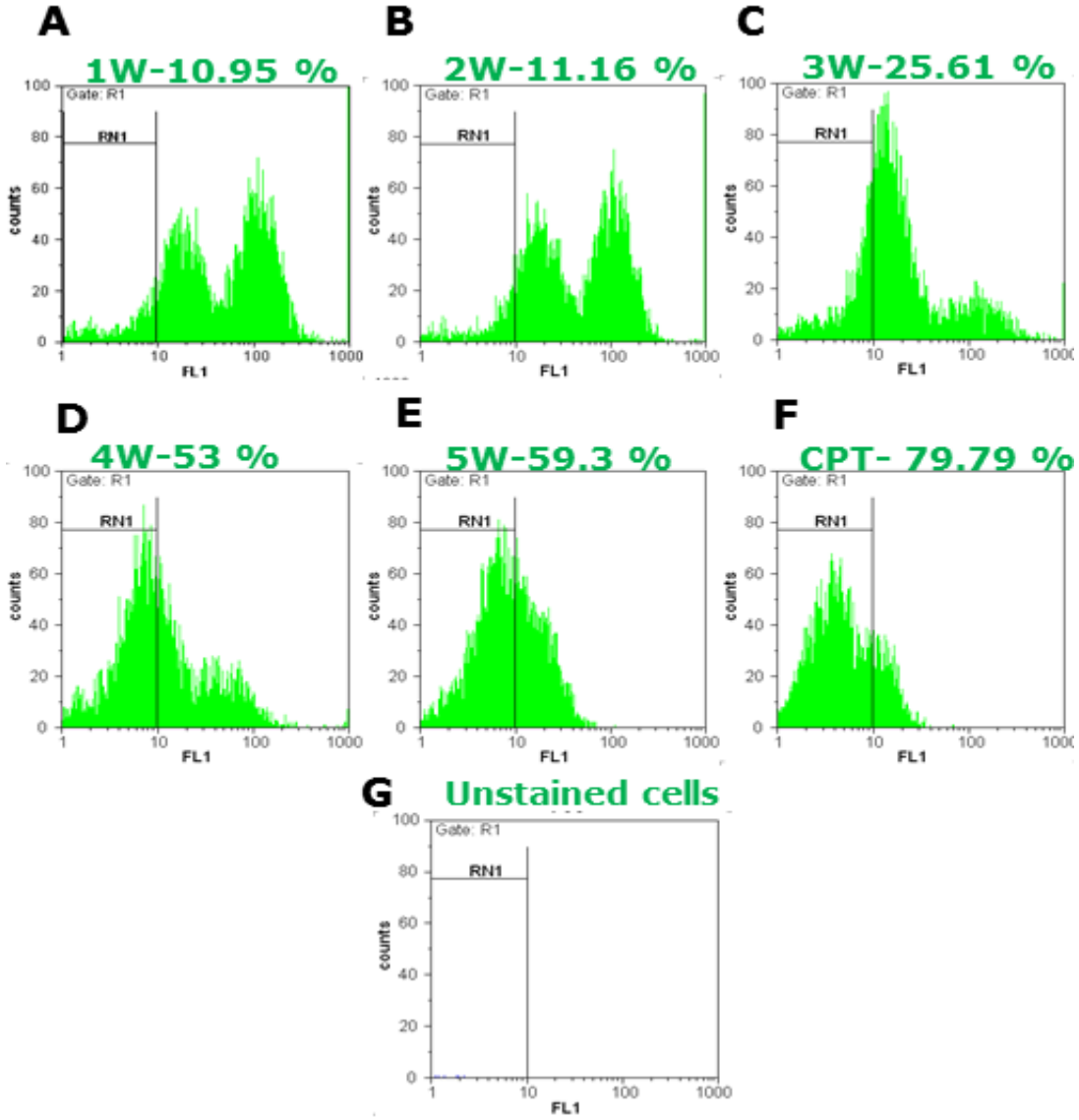

Figure 14: Characterizing mitochondrial membrane potential in ageing CGNs by flowcytometry

Panels A- F corresponds to R123 profiles of CGNs subjected to ageing (1W to 5W) and CPT treatment. Counts vs. FL1 histograms of 1W to 5W and 10 µM CPT treated CGNs were generated using Flo Max software 2008 (Partek). Cells showing fluorescence intensity lower than 10^1 arbitrary units were gated. Percentage of cells in the gated population has been indicated in the histogram. The percentage of cells falling within this gate is indicative of low mitochondrial membrane potential.

Figure 14

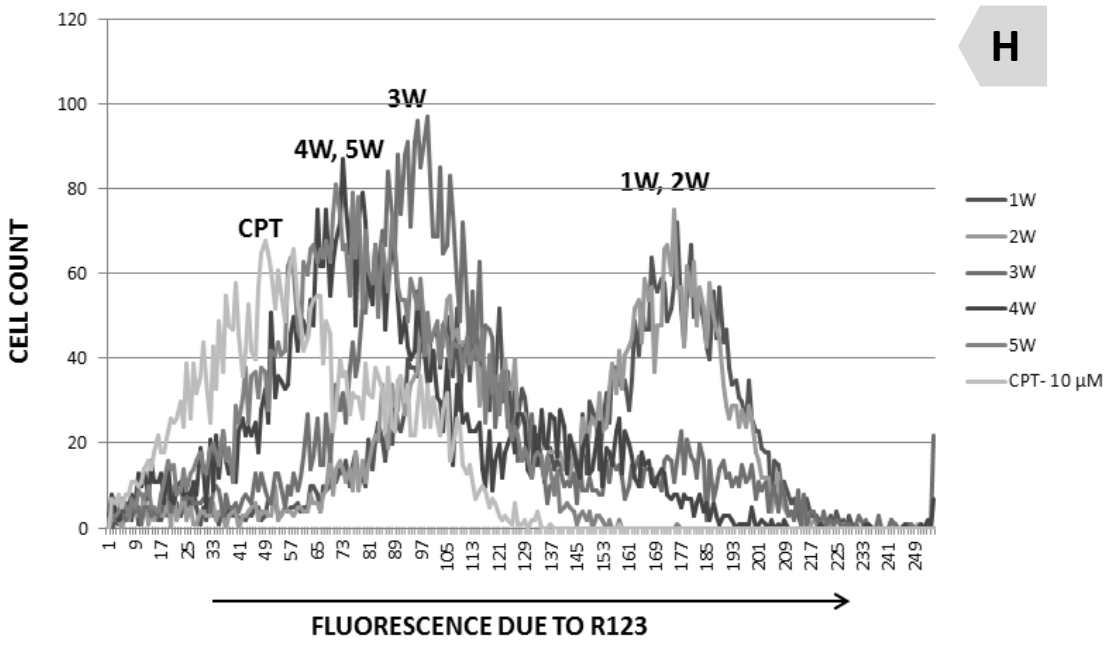

CGNs show alteration in the mitochondrial membrane potential during *in vitro* ageing

CGNs were stained with R123 and mitochondrial membrane potential was quantified by flowcytometric analysis. **Panel H** corresponds to an overlay histogram (counts vs. FL1) of 1W to 5W old and 10 µM CPT treated CGNs. Cell count was plotted along Y-axis and intensity of fluorescence along X-axis. Membrane depolarization was shown by shift in the cell population towards the lower median values of FL1 scale. Peak shift to left indicates reduction in R123 fluorescence which is indicative of decrease in mitochondrial membrane potential with age.

Figure 15

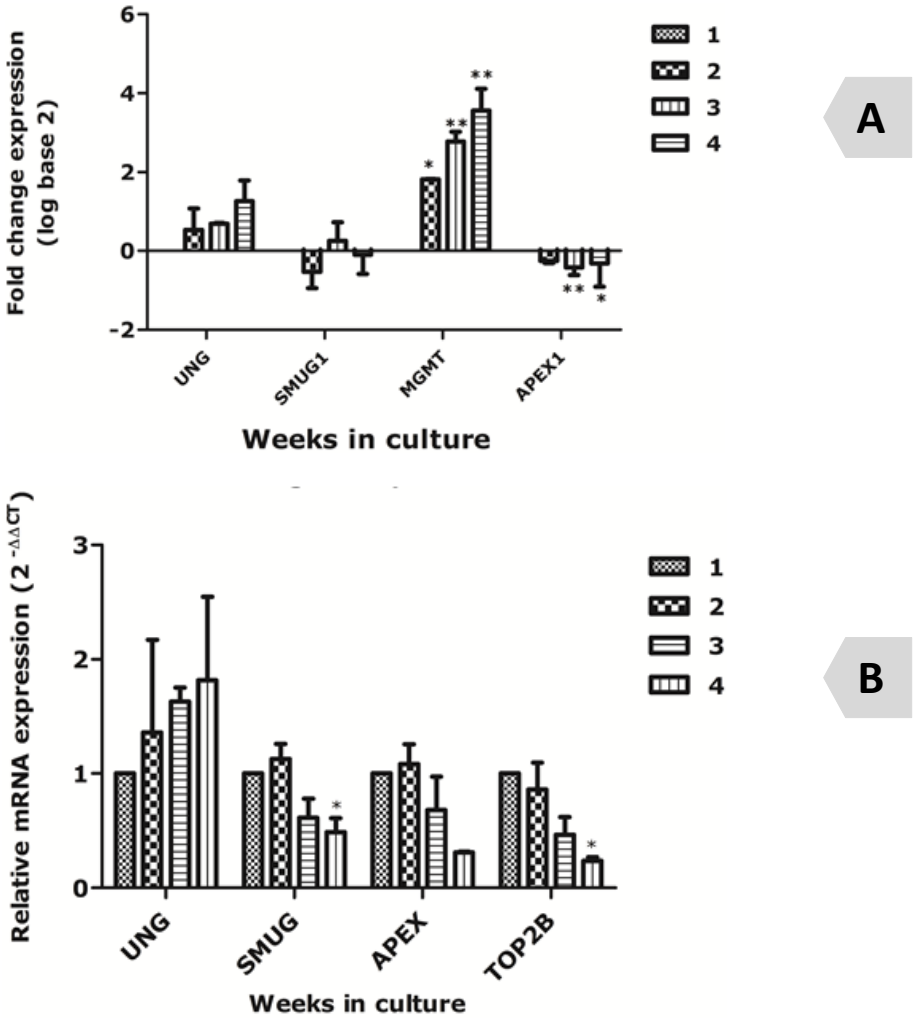

Figure 15: Validation of differential gene expression by qPCR

(A) Fold change expression by Microarray analysis **(B)** Validation by quantitative Real-Time PCR for BER genes - UNG, SMUG, APE 1 and TOP2β reveals significant decrease in relative expression of all genes mentioned except UNG. UNG shows a significant increase in relative gene expression through the weeks as per statistical analysis, One Way ANOVA (*Tukey post hoc* test) (*P< 0.05, **P< 0.01, ***P< 0.001). 1W healthy CGNs were taken for control.

Figure 16

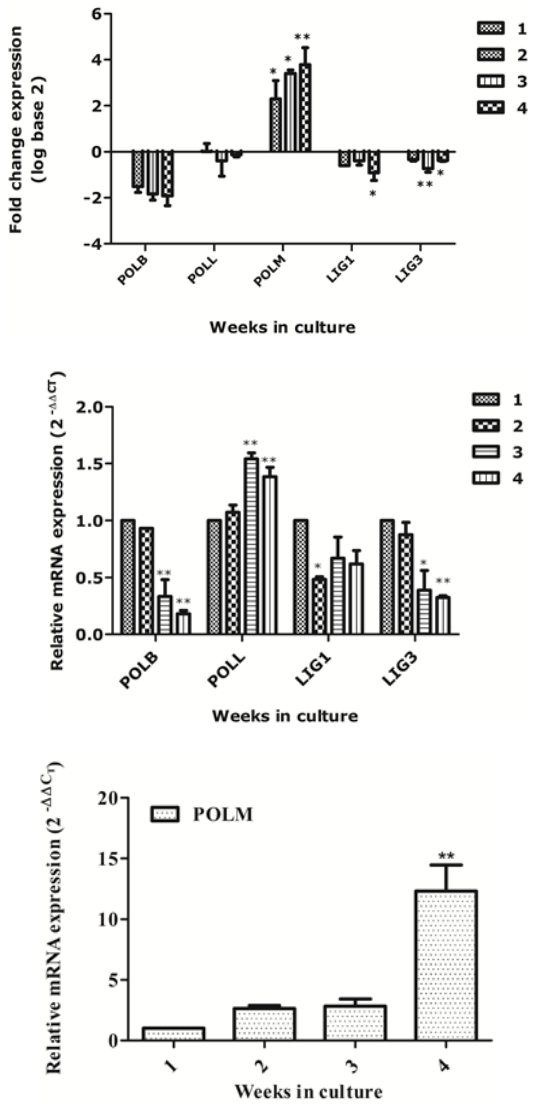

Figure 16: Validation of differential gene expression by qPCR

(A) Fold change expression by Microarray analysis **(B,C)** Validation by qPCR for BER genes – POLβ, POLλ, POLμ, LIG1 and LIG3 reveals significant decrease in relative expression of all genes given except POLλ and POLμ. The latter two genes show a significant increase in relative gene expression through the weeks as per statistical analysis, One Way ANOVA (*Tukey post hoc* test) (*P< 0.05, **P< 0.01, ***P< 0.001), 1W healthy CGNs were taken as control.

Figure 17

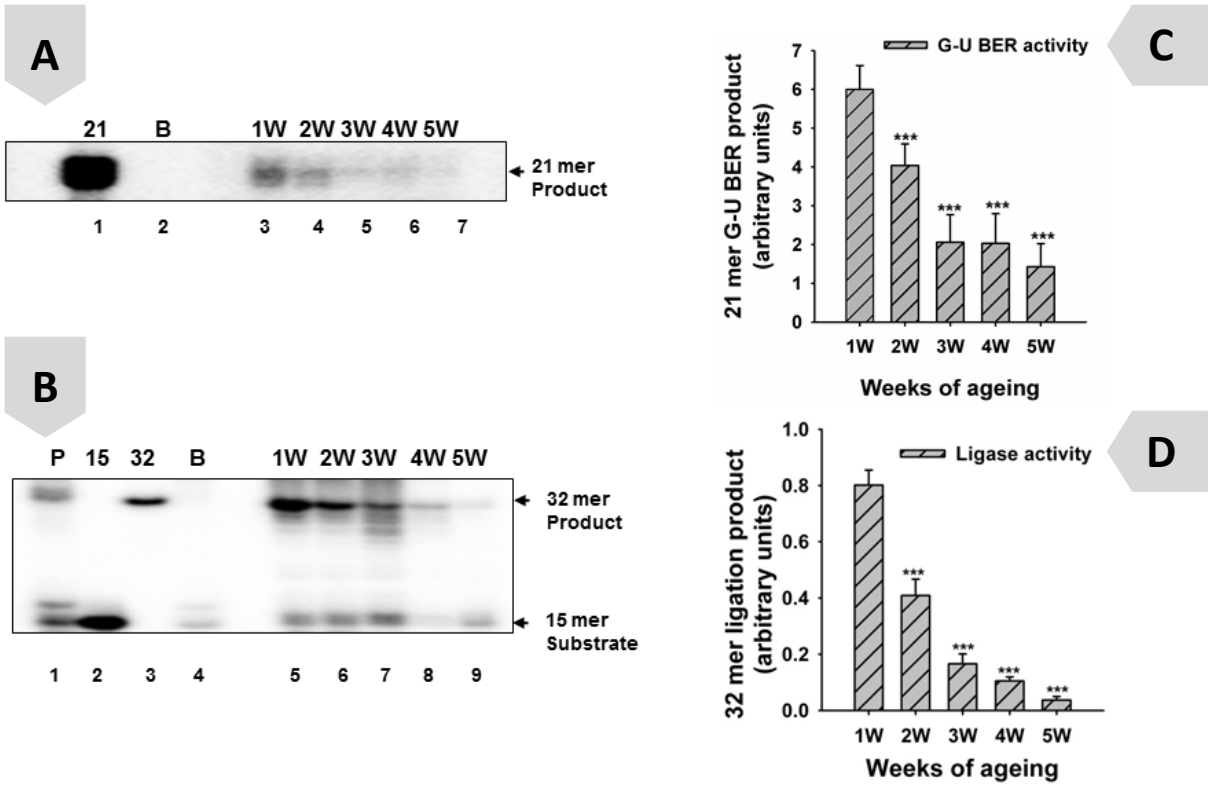

Figure 17: Effect of *in vitro* ageing on G-U BER and ligase activity in CGNs

Cultured CGNs were pelleted at the end of every week for 5 weeks and cell extracts prepared. **Panel A** depicts a representative autoradiogram showing G-U BER activity in ageing CGN extracts. The substrate for G-U BER assay is a 3 pmol of 21 mer double stranded uracil (U) containing oligonucleotide. The BER activity of the extracts involves base hydrolysis of U, cleaving the phosphodiester backbone followed by the polymerase gap filling and ligation. Lane 1 is a 21 mer; lane 2 shows activity in blank (B), i.e. only 3 pmol of substrate; lanes 3 to 7 depict G-U BER activity in CGN extracts aged 1 (1W) to 5 weeks (5W), respectively. Seen is a gradual decline in the activity of the ageing extracts in terms of 21 mer product formed in arbitrary units. Activity in 1W old CGN extract was taken as control with which the activity in 2W to 5W CGN extracts was compared using One Way ANOVA (*Holm-Sidak* method). The difference in the activities was found

to be statistically significant (*** P < 0.001). **Panel B** illustrates the effect of *in vitro* ageing on ligase (LIG) activity in CGNs. Substrate is a 400 fmol of 5'-[γ-32P]ATP end labeled 32 mer double stranded oligonucleotide containing a nick. The LIG activity of the extracts involves sealing the nick in the phosphodiester backbone that results in a 32 mer product formation. Lanes 1 to 4 correspond to LIG activity by 10 U of pure enzyme, T_4 DNA ligase (P), 15 mer (15), 32 mer (32), blank (B), i.e. 400 fmol of substrate DNA; lanes 5 to 9 depict LIG activity in CGN extracts aged 1 (1W) to 5 weeks (5W), respectively. Representative autoradiogram shows gradual decline in the activity of the ageing extracts in terms of 32 mer product formed in arbitrary units. Activity in 1W old CGN extract was taken as control. Using One Way ANOVA (*Holm-Sidak* method), the difference in the activities was found to be statistically significant (*** P < 0.001). Bar charts depict Mean ± SD (**Panel C and D**).

Figure 18

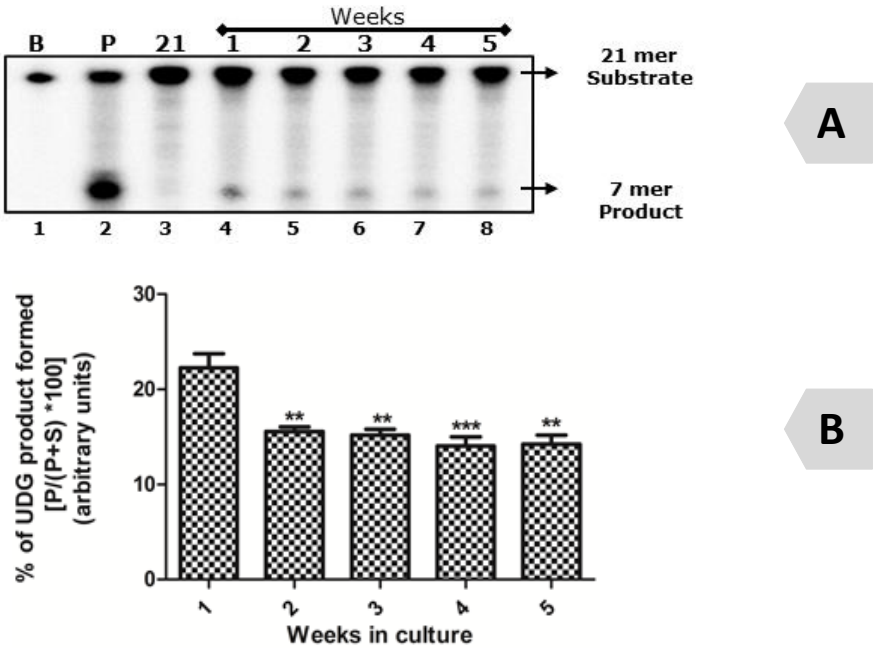

Figure 18: Decline in UDG activity in ageing CGN extracts

Cultured CGNs were pelleted at an interval of seven days for 5 weeks and cell extracts prepared. 200 fmol of 5′-[γ-^{32} P]ATP labeled 21 mer oligo duplex containing U in its 8th position was incubated with CGN extract under conditions given in Section 2.12.2. Sequencing gel image depicts UDG activity as visualized by the appearance of 7 mer repaired radioactive spot. **Panel A**: Lanes 4-8 correspond to UDG activity in 1st to 5th week extracts. Lane 1, activity in blank (B), i.e. 200 fmol of substrate; lane 2, activity by 0.5 U of pure enzyme, UDG (P) and lane 3 depicts 21 mer (21). The 7 mer product was quantified using *ImageJ* 1.43u software, NIH, USA and data was expressed in arbitrary units. Values are expressed in mean ± SD for data obtained from 3 independent experiments and same is represented in bar graphs **(Panel B)**. The decrease in UDG activity from 1W to 5W was found to be significant using One Way ANOVA (*Tukey post hoc* test) (** $P < 0.01$, *** $P < 0.001$).

Figure 19

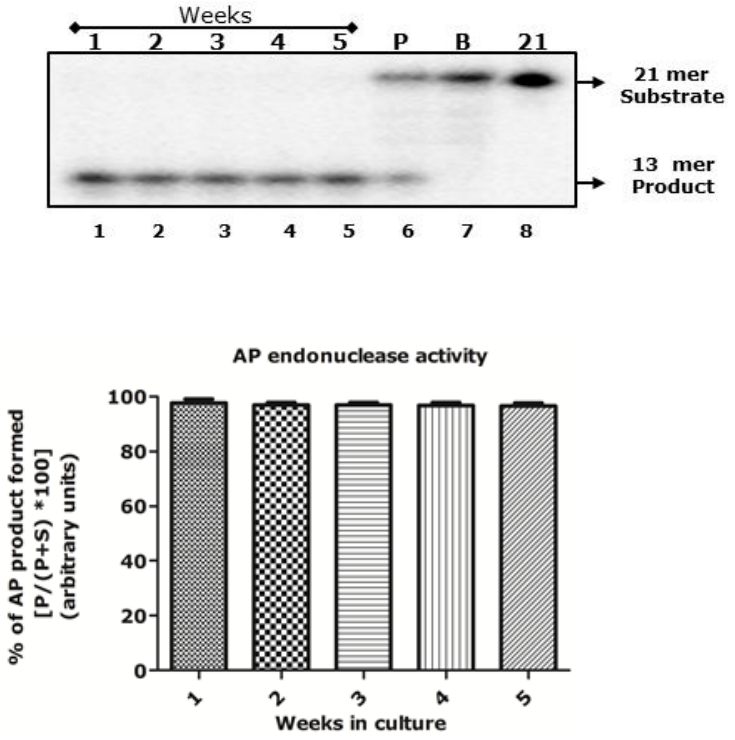

Figure 19: AP endonuclease activity in ageing CGNs

Panel A is a representative autoradiogram shows AP endonuclease (APE) activity in ageing CGNs – week wise. The substrate is 200 fmol of 5'-[γ-^{32}P]ATP end labeled 21 mer double stranded oligonucleotide containing F, tetrahydrofuran (AP site analog). The APE activity involves the cleavage of phosphodiester backbone on the 3' side of F resulting in a 13 mer product. Lane 1 illustrates APE activity in control CGNs (1W); lanes 2 to 5 correspond to 2W to 5W respectively. Lane 6, activity by 1 U of pure enzyme, human APE1 (P); lane 7, activity in blank (B), i.e. 200 fmol of substrate; lane 8 depicts 21 mer (21). Percentage of 13 mer product was measured in terms of arbitrary units. Experimental procedure and densitometric quantification was carried out as described under Section 2.12.3. Values are expressed in mean ± SD for data obtained from 3 independent experiments and same is represented in bar graphs **(Panel B)**. Difference in APE activity was found to be insignificant from 1W to 5W using One Way ANOVA (*Tukey post hoc* test).

Figure 20

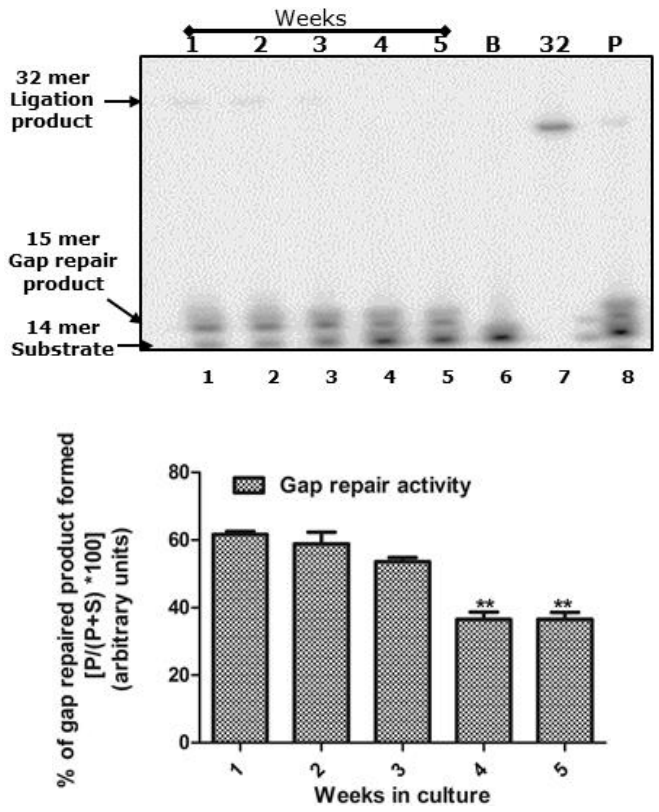

Figure 20: Gap repair assay in *in vitro* ageing CGNs

Panel A depicts a representative autoradiogram showing gap repair activity in ageing CGN extracts. The substrate for gap repair assay is a 400 fmol 5′-[γ-^{32}P]ATP labeled 32 mer oligo duplex containing one gap. The gap repair activity of the extracts involves polymerase gap filling and ligation. Lanes 1 to 5 depict to gap repair activity in 1W to 5W CGN cultures respectively; lanes 6 to 8 correspond to activity in blank (B), 32 mer marker and pure enzyme (P) i.e. 0.5 U of β polymerase respectively. Seen is a gradual decline in the activity of the ageing extracts in terms of 15 mer product formed (in arbitrary units). Activity in 1W old CGN extract was taken as control with which the activity in 2W to 5W CGN extracts was compared using One Way ANOVA (*Tukey post hoc* test). The difference in the activities of 4W, 5W in comparison to 1W was found to be statistically significant (** $P < 0.01$). Bar charts depict Mean ± SD **(Panel B)**.

Discussion

A composite study of degree of ROS, mitochondrial stress, DNA damage and repair in cellular environment is important dynamics for understanding senescence.

Exogenic and endogenic ROS generated during oxygen metabolism in the cells and induce activation of a variety of essential components including lipids, ribonucleic acids and proteins which may eventually lead to cellular wearing and death (Harman, 1972). When applied to the nervous system this may explain the loss of cognitive, sensory and motor functions characteristic of senescence (Lin and Beal, 2006). Moreover, oxidation of ion channels by ROS seems to be the root cause for neuronal ageing (Matalon et al., 2003). In addition, ROS can modulate the channel function by influencing cellular pathways that regulate gene trafficking, transcription, turnover and proteosomal degradation (Matalon et al., 2003).

Age associated decline in GSH has been reported in brain tissue (Liu, 2002). Our findings indeed are in line with the earlier findings. In the presence of ROS or H_2O_2, GSH is oxidized to GSSG. The latter being toxic is either transported outside the cell or is utilized to regenerate GSH by NADPH dependent Glutathione reductase (Lu, 1999). The mechanism underlying the age related decline in GSH levels is not so well understood. Either increased GSH consumption, lowered GSH production or altered activities of enzymes involved in the GSH metabolism could be a probable factor behind lowered GSH levels (Maher, 2005). Combination of increased ROS and depleted GSH enhances oxidative stress in

brain (Schulz et al., 2000). Oxidative stress and lowered GSH have been reported in patients with PD and AD in discrete brain areas (Dringen and Hirrlinger, 2003). Thus, ROS induced damage in DNA and associated DNA repair was carried out. Results of these studies showed DNA damage accumulation occurred very rapidly with age, i.e. till adult stage (3W) and reached maximum by the penultimate old stage (5W) (Figure 13). A similar observation was reported in brain tissue of ageing rats (Swain and Subba Rao, 2011). A similar trend was seen when ageing CGNs were subjected to ENU treatment (0.5 μM, 12 h). The capacity of ENU treated CGNs to recover from DNA damage decreased drastically with advance of age (Bhanu et al., 2010).

In our study, as CGNs aged, ΔΨm decreased progressively with age. Our results corroborate well with the earlier findings of (Xiong et al., 2004) who showed by imaging studies, a gradual and a time-dependent depolarization of mitochondria in CGNs *in vitro* after the addition of FCCP, a mitochondrial protonophore. Old neurons (22 DIV) showed a much longer ΔΨm recovery period when compared to young cultures (10 DIV). Aged mitochondria display a significant reduction in the activity of various electron transport chain complexes (Kwong and Sohal, 2000). These changes were more pronounced in tissues such as brain, heart and skeletal muscle, which comprise of postmitotic cells, than in liver and kidney. A variety of ageing cell types from several mammalian species are characterized by lowered mitochondrial membrane potential. As detailed by (Hagen et al., 1997) loading of hepatocytes with rhodamine 123 showed a 50% reduction of signal in the major population of mitochondria from old rats. Aged mitochondria of

human and animal species exhibited lowered ΔΨm (Mather and Rottenberg, 2002; Nicholls, 2004).

The physiological significance and mechanisms underlying the decreased ΔΨm are not well understood in neuronal cellular senescence. Decreased mitochondrial membrane potential has several reasons, like impaired calcium transporters, K transporters apoptosis mediated by BAD- BAX. Evidence suggests that defects in mitochondria function occur with ageing (Di Lisa and Bernardi, 2005; Jahangir et al., 2001) . Earlier studies (Bhanu et al., 2010) have shown no significant increase in caspase 3 activity implicating that the mode of neuronal death is not apoptosis-mediated.

Enhanced rate of intracellular free calcium $[Ca^{2+}]_i$ was seen in aged *in vitro* CGN cultures of Wistar rats (Bhanu et al., 2010) as well as in aged cerebellar granule neuronal brain slices *in vitro* (Bhanu et al., 2010; Xiong et al., 2004). Cytosolic $[Ca^{2+}]$i is associated with mitochondrial depolarization response (Xiong et al., 2004). Possible reason of survival of CGNs in spite of low membrane potential of mitochondria could be due to significant ATP generating capacity of older neurons (Xiong et al., 2004) and also CGNs generate a significant amount of ATP through cytoplasmic glycolysis (Nicholls and Budd, 2000).

Enhanced DNA damage in ageing CGNs corroborates with the activities of the repair enzymes, UDG and POL (Figures 18 and 20) which have also decreased significantly from 3W. Accumulated DNA damage and decreased DNA repair efficiency in a postmitotic neuron can cause the cell to become senescent leading

to the phenomenon of ageing (Gorbunova et al., 2007) and neurodegenerative disorders (Schumacher et al., 2008; Weissman et al., 2007).

(Gupta et al., 2012) showed an overall decline in GU-BER activity and ligase activity in ageing cultured CGNs. Subsequently, a significant decline in the Gap repair activity implies deficiency in repair efficiency during neuronal insults. Similar decline in BER activity was reported in ageing rat brain tissue extracts(Swain and Rao, 2012), along with a decrease in the protein levels of APEX, Lig I, Lig III and Pol β in ageing cortical neurons. (Cabelof et al., 2002; Intano et al., 2003; Xu et al., 2008) showed reduced BER and POLβ in the brains of old mice. The number of OGG1 and UDG sensitive sites also increased with age in DNA with simultaneous decrease in OGG1, UDG and APE1 activities (Swain et al., 2011). (Mazzarello et al., 1990) has suggested that misincorporation of uracil into DNA to be a possible contributor to neuronal ageing and abiotrophy. Also during neuronal development there is rapid decrease in UDG which could impair the removal of uracil present in DNA in adult neurons. However, misincorporation of dUMP into DNA might be confined to a low frequency by the action of dUTPase present at all developmental stages (Focher et al., 1990).

TopoIIβ in brain has shown highest activity in cerebellar region and that too only neuronal cell fraction. TopoIIβ protein levels and activity significantly decline during brain ageing (Kondapi et al., 2004). It is known to play a role in the DSB repair in SK-N-SH, a human neuroblastoma cell line (Mandraju et al., 2008) and in CGNs (Mandraju et al., 2011). In addition, TopoIIβ levels declined significantly with advancing age in CGNs (Bhanu et al., 2010). The TopoIIβ enzyme might play a regulatory role in modulating the BER capacity (Gupta et al., 2012). Thus,

TopoIIβ may be associated with the regulation of DNA repair enzymes leading to genome instability.

This might also be a reason for significant decline in BER with advancing age. Hence, TopoIIβ may have some unknown function in cerebellum and the low levels of TopoIIβ activity in ageing cerebellum may contribute to the genomic instability in cerebellar region of ageing brain.

Conclusion

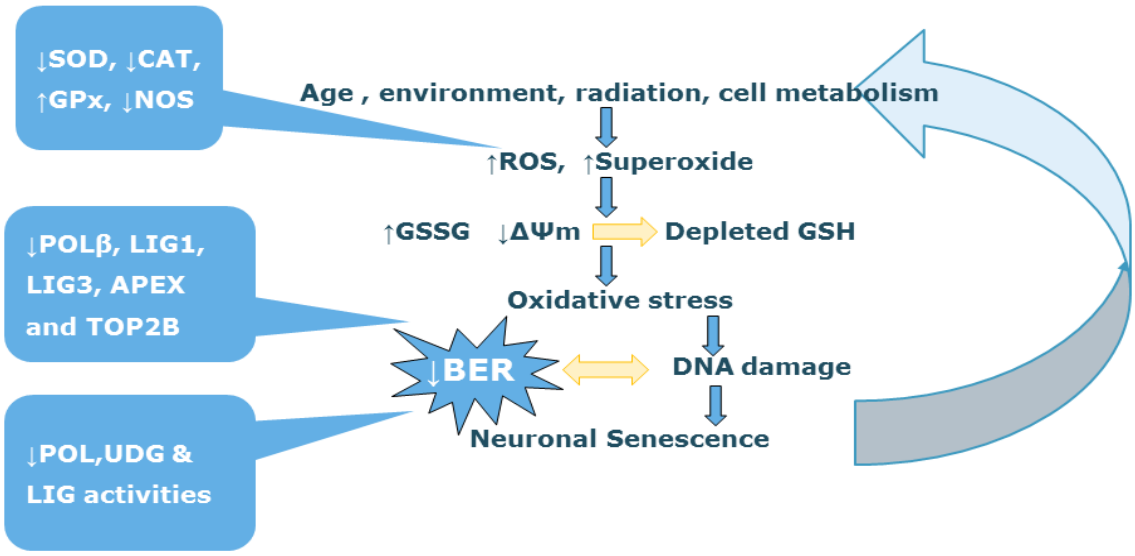

Senescence was characterized in in vitro cultured cerebellar granule neurons. Ageing CGNs demonstrated significant increase in ROS, lowered free thiols and lowered mitochondrial membrane potential. In senescent CGNs, the rate of DNA damage overrides the DNA repair capacity due to significant downregulated activities of BER enzymes including- Uracil DNA glycosylase, Polymerase and Ligase. The close similarity of in vivo ageing with in vitro ageing suggests that, cultured CGNs makes an ideal model for the study of premature neurodegeneration.

CHAPTER 5

ANALYSIS OF GENE EXPRESSION ELEVATION DURING AGEING OF CGNS IN CULTURE

Introduction

Over four decades ago, senescence was first described by Hayflick and colleagues as limited ability of the cells to proliferate in culture (Hayflick, 1965). Cellular senescence was proposed to be an anti-cancer or a tumor suppressing mechanism as it stops incipient cancer cells from proliferating (Braig and Schmitt, 2006) and hence, was considered beneficial. Senescence was proposed to recapitulate ageing of cells *in vivo* (Campisi and d'Adda di Fagagna, 2007).

Severe DNA damage especially DSBs provide constitutive signals to p53 to maintain senescence (Herbig et al., 2004; Rodier et al., 2007). It may either be a dysfunctional telomere initiated DNA damage response (Herbig et al., 2004) or histone deacetylase inhibition (HDAi) promoting euchromatin formation (Munro et al., 2004) or oncogene induced like overexpression of oncogenic RAS (Lin et al., 1998; Serrano et al., 1997; Zhu et al., 1998) or a sustained signaling by anti-proliferative cytokines like interferon β which in turn increases intracellular ROS. Any of these reasons could ultimately result in senescence.

Senescence may manifest as growth arrest and resistance to cell death mechanisms like apoptosis, etc. The cells display inability to progress through cell cycle in spite of being metabolically active (Di Leonardo et al., 1994; Herbig et al., 2004). This may be a G2-M arrest like in mouse fibroblasts with G1 DNA (Wada et al., 2004). One of the major problems posed by senescence is resistance to apoptosis which varies from cell to cell. Senescent human fibroblasts resist apoptosis caused by growth factor deprivation and oxidative stress but is susceptible to FAS death receptor mediated apoptosis (Chen et al., 2000; Tepper

et al., 2000). However, the factor that determines the fate of the cell is not very clear. The senescent cells are also characteristic of altered expression of cell cycle inhibitors and activators like p21 and p16, members of tumor suppressor genes governed by transcription regulators like p53 and pRB (Campisi and d'Adda di Fagagna, 2007). In addition, senescent cells may overexpress genes that encode secretory proteins which in turn alter tissue microenvironment (Chang et al., 2002; Yoon et al., 2004; Zhang et al., 2003). For example an *in vivo* study in baboons (Herbig et al., 2006) revealed that senescent cells account to more than 15% of cells in aged animals.

Physiologically, senescence may manifest in diseased conditions too like atherosclerosis, obesity and cancer. Atherosclerosis is a chronic inflammatory disease of the vascular smooth muscle vessels derived from human atherosclerotic plaques. These cells showed an impaired growth *in vitro* and underwent senescence earlier than cells from normal vessels (Chung et al., 2009; Minamino and Komuro, 2007). Evidence for obesity and its connection with accumulated senescent preadipocytes and endothelial cells, increased secretion of inflammatory cytokines and chemokines was reported (Tchkonia et al., 2010). Excessive calorie intake led to accumulation of oxidative stress in adipocyte tissue of mice with type 2 diabetes like disease and promoted senescence like changes. Cells undergoing reprogramming during senescence displayed not only permanent growth arrest but also changed morphology and function (Campisi and d'Adda di Fagagna, 2007). A striking increase in the secretion of pro-inflammatory cytokines by senescent cells exerts harmful effects on the local environment. This was termed as senescence associated secretory phenotype

(SASP) (Davalos et al., 2010). In all, it appears that senescent cells create an environment that supports the development of age related diseases which may manifest in reduced organ function (Franceschi et al., 2000). Hence senescent cells may act as a tumor suppressing mechanism (since these cells cannot divide) and support cancer development (via the senescence associated secretome)(Sikora et al., 2011).

In vivo senescent cells are found in humans, baboons, mouse skin, human, animal skeletal muscle, fat tissue and liver (Jeyapalan and Sedivy, 2008). The identification of senescent cells *in vivo* is of vital importance owing to the deleterious effects of senescent cells. The hallmark of cellular senescence is primarily altered cellular morphology (enlarged- flat-multivacuolated-multinucleolated), elevated SA-β-Gal activity, accumulation of DNA damage foci, SAHFs, chromosomal instability and induction of inflammatory secretome. A detailed list of markers for senescence has been given in **Table 4.** However, a plethora of these markers are not senescence specific and cannot be verified *in vivo* (γH2AX & SAHF). Further, there is a requirement of validated markers specific to neuronal senescence.

Lack of quantitative tests for reliable candidate markers for identification of senescent cells is a major drawback in cell population studies (Lawless et al., 2010). Therefore, this work was conceptualized to identify novel biomarkers for neuronal ageing and neurodegenerative diseases. Using microarray approach, real time PCR and clustering, a few genes have been identified as markers of potential interest.

Table 4: Markers for senescence

S. No	Marker	Reference	Expression seen in-
1	**BrDU (5-bromo-2'-deoxyuridine) incorporation, PCNA, Ki67**		Replicative senescence
2	**↑ TIFS (Telomere dysfunction induced foci)**	(Herbig et al., 2006)	p53 mediated senescence
3	**↑ SAHF (Senescence associated Heterochromatin foci)**	(Funayama and Ishikawa, 2007)	Replicative senescence P16 mediated senescence
4	**↑ SA-β-Gal**	(Dimri et al., 1995; Wang et al., 2009)	Cannot be detected by histochemical staining May be induced by stress in culture
5	**γH2AX (Phosphorylated histone H2AX)**	(Wang et al., 2009) (Nakamura et al., 2008)	DSB marker
6	**A2M (Activated telangiectasia mutated kinase)**	(Di Micco et al., 2008)	Senescent fibroblasts + ATM pathway
7	**Heterochromatin loss**	(Villeponteau, 1997)	
8	**p16 (cyclin-dependent kinase inhibitors)**	(Beausejour et al., 2003)	Not expressed in all the cells Seen in tumor cells only that have lost pRb function
9	**Intracellular Ca2+**	(Thibault et al., 2001)	Neurons
10	**TopoIIβ**	(Bhanu et al., 2010)	CGNs
11	**DEC1 (differentiated embryo-chondrocyte expressed-1), p15**	(Collado and Serrano, 2006)	Promising But expressed in oncogene induced senescence.
12	**P16INK4A (cyclin-dependent kinase inhibitors)**	(Ressler et al., 2006) (Yang et al., 2008)	Replicative & Oncogene induced senescence

Experimental Plan

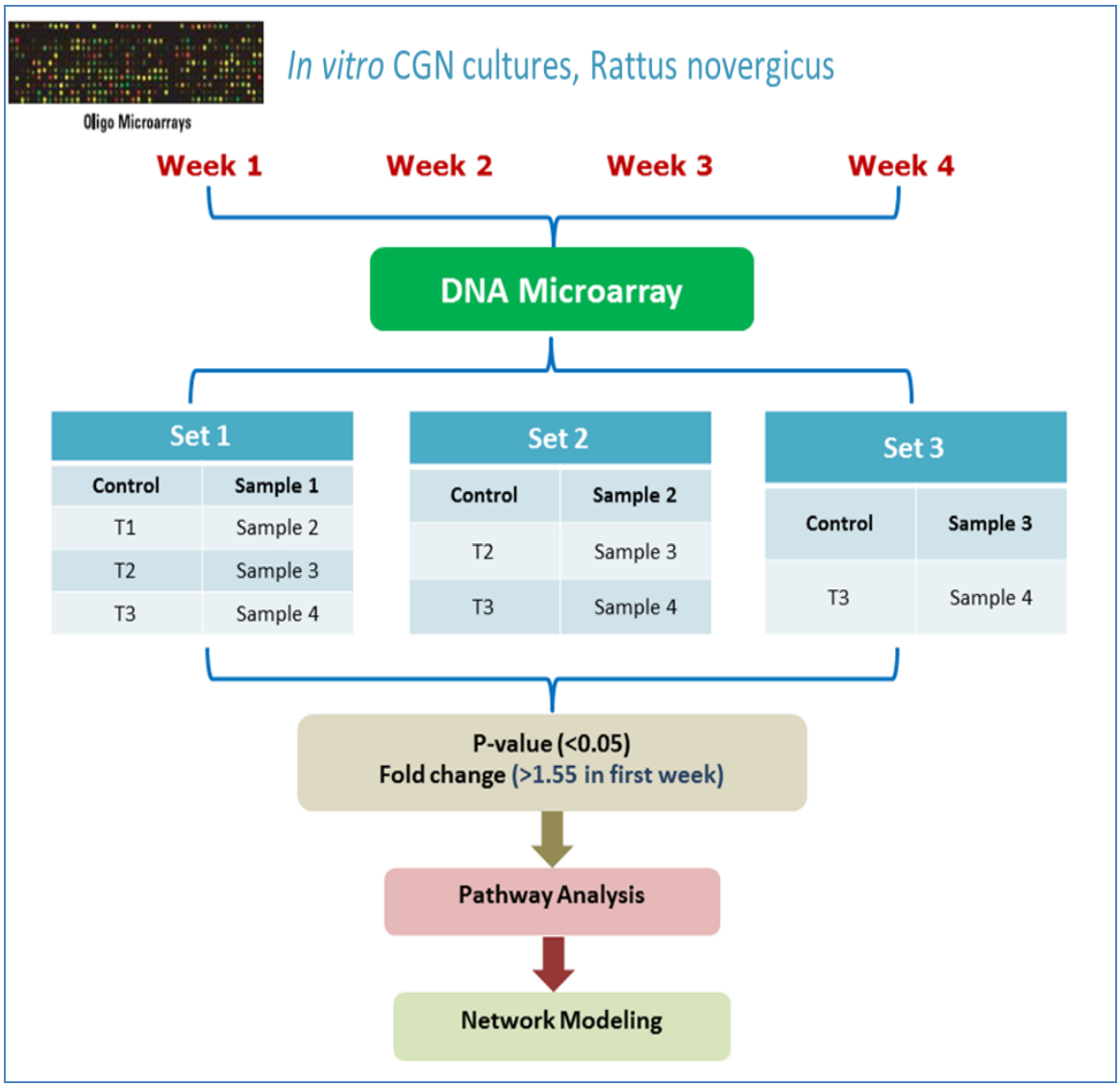

Results

CGNs were chosen for this study as, primary cultures of postnatal rat cerebellum make an excellent model system for molecular and cell biological studies of neuronal development and function. Many fundamental insights into the phenomena of apoptosis, migration and differentiation in neurons in the

mammalian central nervous system have come from investigating granule neurons *in vitro*. These cells may prove invaluable in uncovering the senescence pathways. Keeping this in view, the ageing CGNs were processed for microarray analysis and the data was subjected to clustering and differential expression.

Differential gene expression allows researchers to look at a specific gene's behavior over a set of samples. However, it allows us to look at only one gene at a time. So, there exists a need to look at a more complex network of genetic changes. For example, genetic changes could directly result in a shift to cancer, or a genetic change may be more indirectly linked. Clustering allows us to look at genetic changes that can be grouped together. It throws out a notion that all genetic changes are independent events. With the appropriate statistics, we can then discover upregulated pathways, processes, cellular components, identify new members and validate differential expression in these groups (Filkov V. Chapter 27). So, we attempted to see if there were any alterations in the pathways.

In the recent past, knowledge of differential gene expression has helped to understand the molecular mechanisms that drive AD pathogenesis, HIV infection and several others (Liang et al., 2008; Mantelingu et al., 2007). A heat map of transcript levels was created for the complete rat genome to display those statistically significant (P-value < 0.05 with multiple testing corrections applied) (**Figure 21**). Fold change used for upregulation and downregulation was 0.8 in each of the replicates and was >1 in the Geomean fold of the replicated samples. Normalized expression signals were represented on a log scale wherein colder colors correspond to lower levels of expression and warmer colors correspond

to higher levels of expression. Heat maps were generated with Gene cluster v2.0 by Genotypic technologies. **Figure 21 (A – C)** show comparisons of other weeks with 1W, 2W and 3W as in set 1, set 2 and set 3 respectively. As this data was very exhaustive, with the help of literature, about 25 vital pathways known to play a role in senescence were identified. Using Biointerpreter software, the genes falling under these pathways were screened and a heat map was generated as in **Figure 22**. Again **Figure 22 (A – C)**show comparisons of other weeks with 1W, 2W and 3W as in set 1, set 2 and set 3 respectively. This data was classified on the basis of gene function. **Figure 23** depicts gene ontology of microarray differentials representing number of genes downregulated and upregulated in ageing CGNs from 1W to 4W.

Fold change of >1.55 in the second week and P-value < 0.05 amongst the duplicates were employed as two parameters to identify novel markers. This search resulted in identifying genes – A2M, GNA14, GRIA1, MASP1, NPY and SLIT2. The gene expression patterns were further validated by real time PCR. **Figure 24** shows expression of genes of interest in *in vitro* aged rat brain CGNs. Quantitative analysis of gene expression in 2, 3 and 4W was compared to 1W using $2^{-\Delta\Delta C_T}$ method (Livak and Schmittgen, 2001). Comparative C_T method was employed to evaluate the gene transcript pattern in ageing cultures. q-RT PCR analysis reveals significant increase in relative expression of all genes through the weeks as per statistical analysis, One Way ANOVA (*Tukey post hoc* test) (*P< 0.05, **P< 0.01, ***P< 0.001) where 1W healthy CGNs were taken as control. Values are represented as mean ± SD and n = 6.

Figure 25 A and B show semi-quantitative gene expression of A2M, GNA14, GRIA1, MASP1, NPY, SLIT2 and GLB1. All the genes showed significant increased expression in 2W, 3W and 4W over 1W. Lanes 1-4 correspond to 1W to 4W transcript levels, lane 5 is no template control (NTC) and lane 6 is 50 bp low range ladder. Semi quantitative analysis was done to ensure single product amplification.

Figure 21

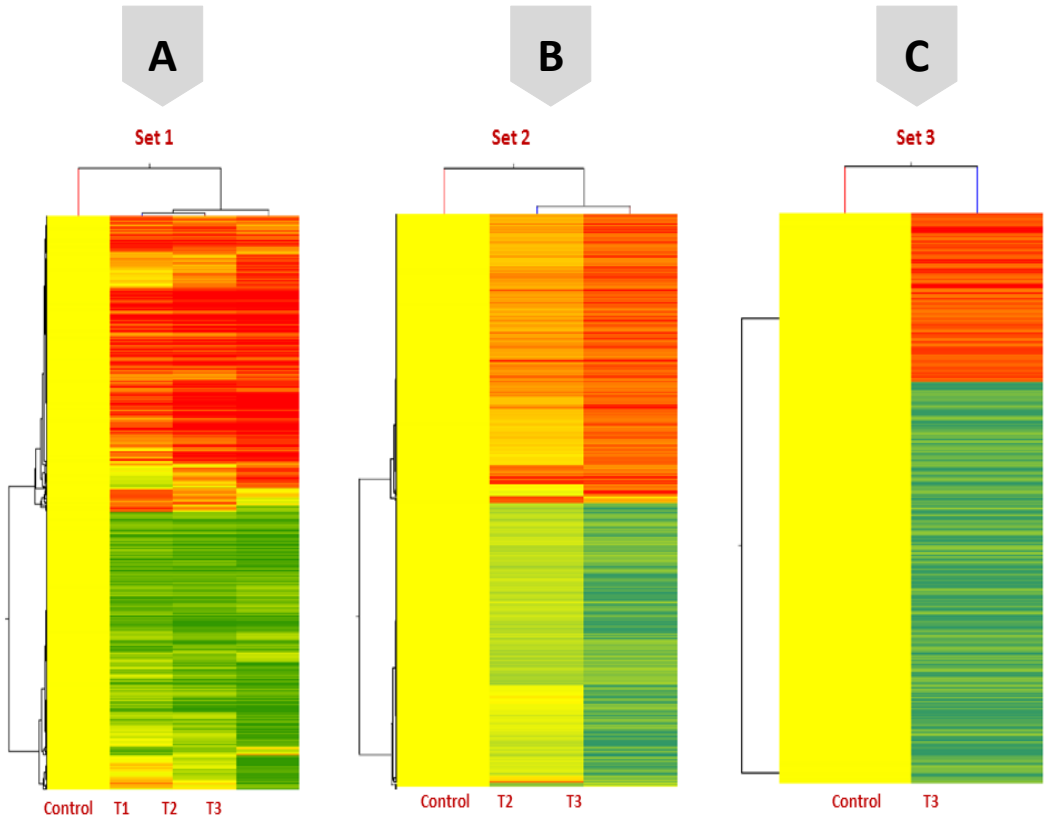

Samples hybridized	Up	Down
T1	2773	2547
T2	4300	3609
T3	5165	4500

Samples hybridized	Up	Down
T2	1021	415
T3	2840	2331

Samples hybridized	Up	Down
T3	522	1253

Figure 21: Heat map of differentially expressed genes in ageing CGNs

A heat map was created for the entire genome to display those statistically significant (P-value < 0.05 with multiple testing corrections applied). Fold change used for upregulation and downregulation was 0.8 in each of the replicates and >1 in the Geomean fold of the replicated samples. Normalized expression signals are represented on a log scale for which colder colors correspond to lower levels of expression and warmer colors correspond to higher levels of expression. Heat maps were generated with Gene cluster v2.0. **Panels A, B and C** show comparisons of other weeks with 1W, 2W and 3W as in set 1, set 2 and set 3 respectively.

Figure 22

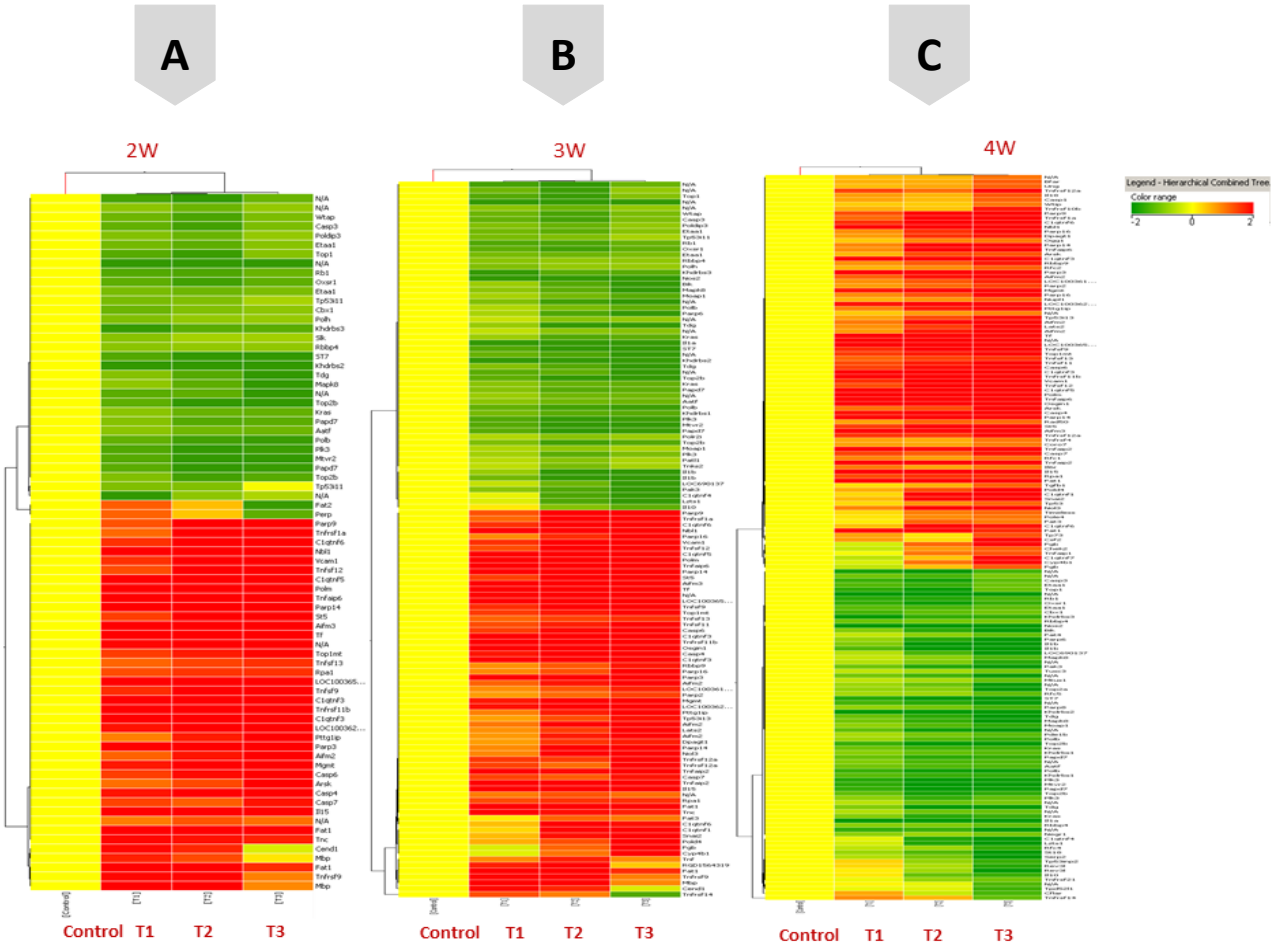

Figure 22: Heat map of differentially expressed genes

A heat map was created to display those statistically significant genes (P-value < 0.05 with multiple testing corrections applied) belonging to 25 vital pathways in ageing CGN cultures. Normalized expression signals are represented on a log scale for which colder colors correspond to lower levels of expression and warmer colors correspond to higher levels of expression. Heat maps were generated with Gene cluster v2.0. **Panels A, B and C** show comparisons of other weeks with 1W, 2W and 3W as in set 1, set 2 and set 3 respectively.

Figure 23

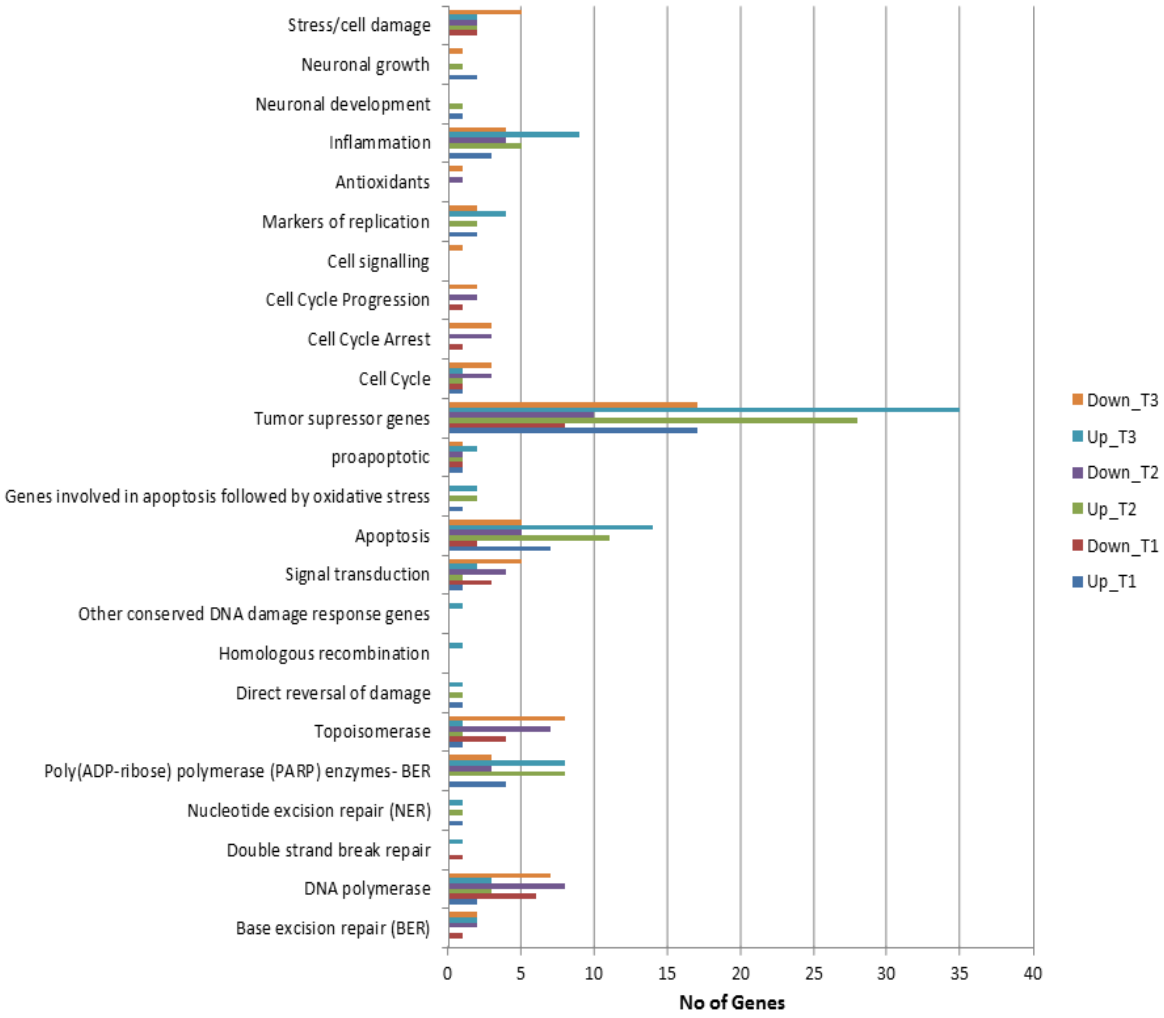

Figure 23: Classification of differentially expressed genes based on function

Gene Ontology of microarray differentials representing number of genes downregulated and upregulated in ageing CGNs from 1W to 4W is shown in the bar chart. Fold change value of 0.8 and P-value < 0.05 was considered to be statistically significant.

Figure 24

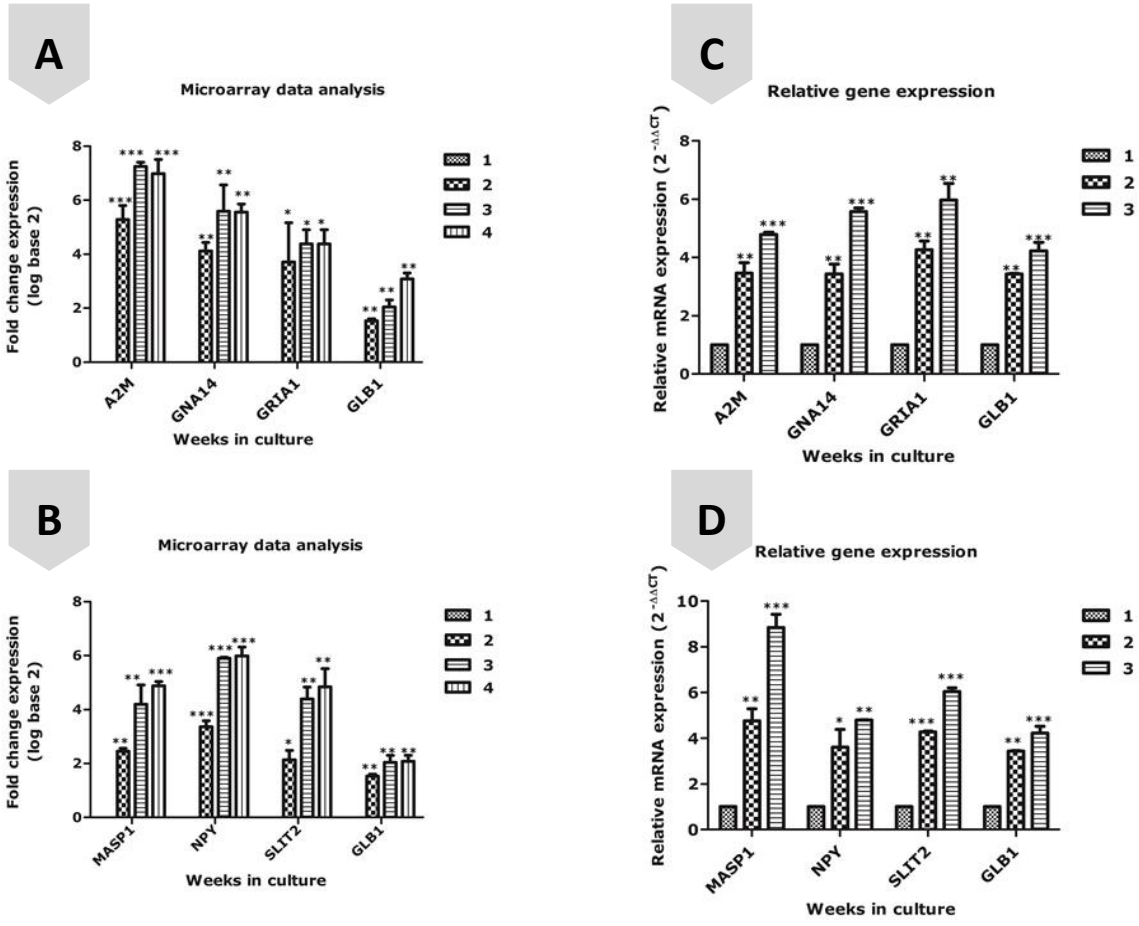

Figure 24: Validation of differential gene expression by qPCR

Panels A and B show fold change expression by Microarray analysis. **Panels C and D** depict validation by q- RT PCR of genes – A2M, GNA14, GRIA1, MASP1, NPY, SLIT2 and GLB1. q-RT PCR analysis reveals significant increase in relative expression of all genes through the weeks as per statistical analysis, One Way ANOVA (*Tukey post hoc* test) (*P< 0.05, **P< 0.01, ***P< 0.001). 1W healthy CGNs were taken as control. Values are represented as mean ± SD and n = 6. Comparitive C_T method was employed to evaluate the gene transcript pattern in ageing cultures.

Figure 25

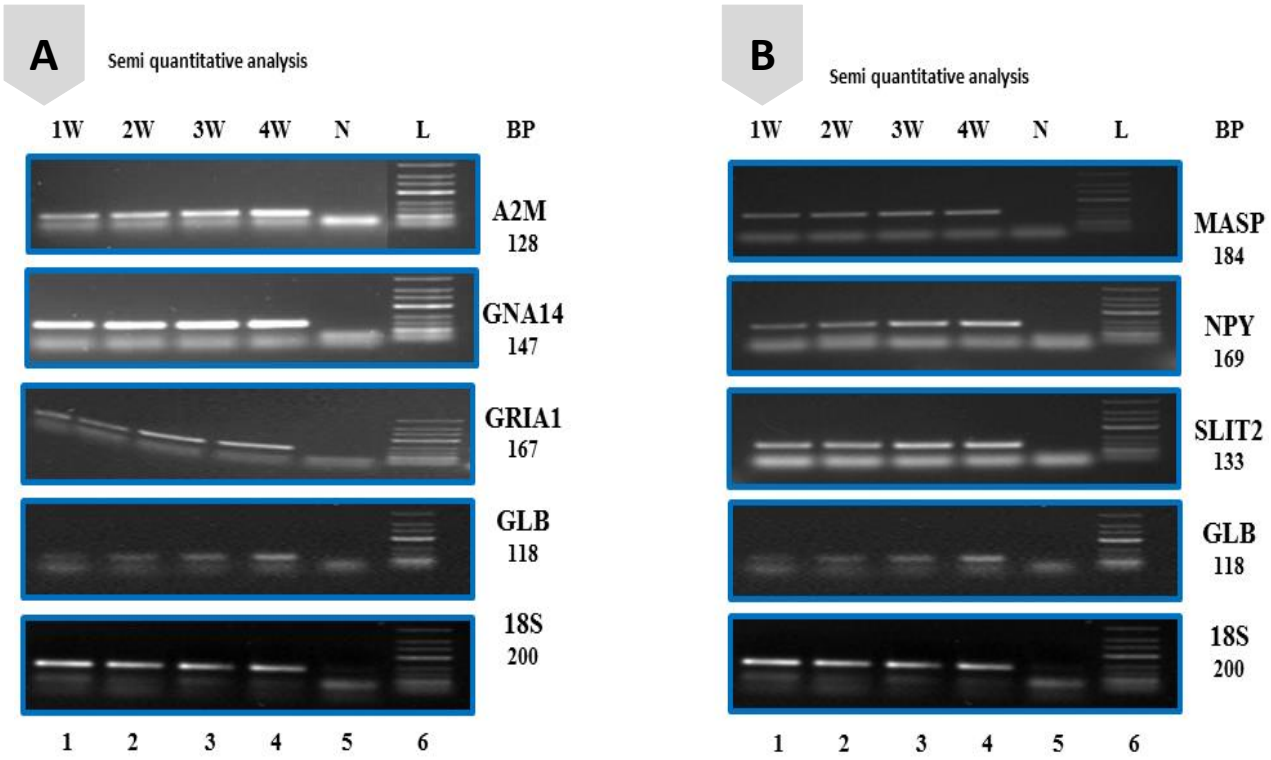

Figure 25: Semi quantitative PCR analysis

Panels A and B show semi-quantitative gene expression of A2M, GNA14 , GRIA1, MASP1, NPY, SLIT2 and GLB1. All the genes showed significant increased expression in 2W, 3W and 4W over 1W. Lanes 1-4 correspond to 1W to 4W transcript expression, lane 5 is no template control (NTC) and lane 6 is 50 bp ladder. Semi quantitative analysis was done to ensure single product amplification.

Discussion

CGNs are the smallest neurons and also constitute the largest homogenous population in human brain. CGNs have proven invaluable in uncovering the signaling pathways governing neuronal migration, differentiation and survival (Contestabile, 2002). Upon receiving signals from multiple mossy fibers, CGNs respond. The combination of multiple inputs results in cerebellum being able to make precise distinction between the input patterns (Marr, 1969). Studies of neuronal apoptosis have frequently relied on cultures of granule neurons, exploiting their responses to activity and growth factor deprivation as well as oxidative stress. These studies have led to the identification of key neuroprotective molecules including insulin-like growth factor 1, myocyte enhancer factor 2 and many others (D'Mello et al., 1993; Li et al., 2001). Loss of CGNs is associated with punctate deposits of prion proteins in Creutzfeldt-Jacob disease (Faucheux et al., 2009). Mutant prion proteins (PrP) suppress glutaminergic neurotransmission by reducing the number of functional channels in CGNs (Senatore et al., 2012). Hence, owing to the varied roles of CGNs, it appears that detailed gene expression profiling of ageing CGNs might provide an important clue to understand and delay senescence.

Ageing brain in neurodegenerative diseases like Alzheimer's disease (AD) condition is a morpho molecular senescence of cortical circuits (Hof and Morrison, 2004). AD is accompanied by dramatic neuron death and destruction of cortical circuits which are very much essential for cognitive functions; senescence in the absence of AD leaves these circuits intact but susceptible to

synaptic compromise (Hof and Morrison, 2004). Also seen was altered neuronal gene expression in brain regions differentially affected by AD (Liang et al., 2008). Just as identifying differences in gene profiling between healthy elderly persons and AD diagnosed people may throw light in understanding molecular pathogenesis that drives AD, similarly a comparison between gene profile of healthy CGNs and aged CGNs may throw light on the molecular mechanisms of senescence.

About 20-40% of cortical, hippocampal and peripheral neurons and 40-80% of Purkinje neurons in the myenteric plexus from six C57B1 old mice showed severe DNA damage, high ROS, oxidative damage, IL6 production, heterochromatinization and SA-β-Gal activity (Jurk et al., 2012). Frequency of these senescence like neurons increased with age in CGNs cultured in *in vitro* conditions (Gupta and Kondapi, unpublished work). Further, in this study we have found that aberrant expression of genes in categories– Tumor suppressor, anti-apoptotic, apoptotic, topoisomerases, BER pathway and polymerases (**Figure 23**) might be responsible for senescence. Senescent CGNs act as a potential causal factor for ageing in mammals (Baker et al., 2008; Herbig et al., 2006). Despite long established evidence for significant DNA damage in postmitotic neurons (Gupta and Kondapi, unpublished work), the possibility of postmitotic cells developing senescence like phenotype has not been evaluated before.

A2M, also known as alpha 2 macroglobulin is a serum pan-protease inhibitor and is involved in acute phase response. The protein exhibits enzyme-growth factor binding (Rat Genome Database- RGD). Its role in clearance and degradation of A-

beta, the major component of beta amyloid deposits has been implicated. Inheritance of deletion of A2M confers increased risk for AD suggesting that it plays a role in a common neuropathogenic pathway leading to AD (Blacker et al., 1998). A2M exposure at 50 μM reduces calcium responses to N-methyl-D-aspartate (NMDA) via low density lipoprotein receptor-related protein in cultured hippocampal neurons suggesting that A2M can alter the neuronal responses to excitatory neurotransmitters and its pre-treatment can selectively downregulate NMDA receptors (Qiu et al., 2002). Results in **Figure 24** depict significant increase in the gene expression of A2M suggesting that, it may confer neuroprotection against possible risk of AD and hence, may prove to be a potential marker for senescence in ageing CGNs. Mannan binding lectin serine peptidase 1 denoted by Masp1 is a serine protease that plays a role in the mannan-binding lectin complement pathway (RGD). The gene encodes a protein that exhibits calcium ion binding, involved in complement activation. Methionine deficiency co-treated with choline deficiency and folic acid deficiency resulted in lowered expression MASP mRNA (Tryndyak et al., 2011). In this study, we identified statistically significant upregulated expression of G proteins, GRIA1 and GNA14 as well as of NPY and SLIT2 (**Figure 24 and 25**). Guanine nucleotide binding protein, alpha 14 abbreviated as GNA 14, exhibits GTPase activity involved in signal transduction and protein amino acid ADP ribosylation (RGD). It participates in G protein mediated signaling pathway and belongs to the q-family. Blalock et al., (1999) reported lowered G protein mediated regulation and shift in calcium channel types with ageing hippocampal cultures. Moreover forebrain specific inactivation of Gq/ G11 family G proteins results in age

dependent epilepsy and impaired endocannabinoid formation (Wettschureck et al., 2006) implicating that Gq family negatively regulates neuronal excitability. This suggests that GNA14 can emerge as a marker with neuroprotective role. Glutamate receptor ionotropic AMPA 1 abbreviated as GRIA1 encodes a protein exhibiting ionotropic glutamate receptor activity and G protein α subunit binding, and is known to be associated with the CNS. A marked increase in the GRIA1 subunit mRNA expression in adult hippocampal neurons during CNS inflammation was reported (Galic et al., 2009). Further, in cortical neurons during intrauterine growth retardation, suppressed expression of glutamate receptors such as GRIA1 and GluN2A was also reported (Ninomiya et al., 2010) which implicates its role in schizophrenia like behavior. Borbely et al., (2009) have shown increased expression and modification of GRIA1 mediated signal transmission in the rat hippocampus following repeated brief seizures. Slit homolog 2 (Drosophila) encodes a protein that exhibits heparin sulphate proteoglycan binding, GTPase inhibitor activity and has been reported to be involved in brain development. Since glypican-1 ligands are synthesized by hippocampal-pyramidal cells and CGNs, SLIT 2 family proteins being functional ligands of glypican-1 in nervous tissue suggests that their interaction may be critical for certain stages of CNS histogenesis (Liang et al., 1999). Slit 2 homologue showed altered expression in this study. Neuropeptide Y abbreviated as Npy1 encodes a protein which exhibits neuropeptide Y receptor binding with G protein coupled receptor binding (RGD) and is known to be associated with cerebral hemorrhage and may be involved in its pathogenesis. (Donner et al., 2012; Xu et al., 2004) have reported involvement of NPY in determining

predisposition to anxiety disorders. Decreased cerebrospinal fluid NPY in patients with depression implicates that impaired NPY signaling could be involved in the pathophysiology of anxiety and depression (Heilig et al., 2004). So, may be explored further as a marker for senescence.

Conclusion

In this study, we present an expression profile detailing levels of steady-state expression of all rodent genes and transcripts in ageing CGN brains. Along with , we propose that the genes A2M, MASP1, GRIA1, GNA14, NPY and SLIT2 could be potential markers for senescence. G proteins form the central dogma of most signaling cascade, so are bound to play a vital role in ageing and could serve as potential markers for senescence. A2M being a pan protease inhibitor too can make a marker of interest in the context of neuronal senescence. Postmitotic neurons develop senescence like phenotype driven by DNA damage response. While downstream functional studies like gene knock down will be needed in future to elucidate the roles of these factors, this total genome expression profile will serve as an important resource for future research aimed at early detection and therapeutics of ageing and related neurodegenerative diseases.

CONCLUSIONS

Role of TopoIIβ in Base excision repair in CGNs

- TopoIIβ deficient neurons do not support BER enzyme activities like that of UDG and Ligase.
- BER, UDG and Ligase activities were unaffected when TopoIIβ was catalytically inhibited using ICRF-193 at 0.5, 10 μM.
- However, BER, UDG and Ligase activities were affected at 50 μM ICRF-193, the TopoIIβ downregulated condition. These results are supported by siRNA mediated downregulation suggesting the possible role of TopoIIβ protein in regulating BER activities.
- TopoIIβ is essential for promoting the repair of ENU-mediated DNA damage via BER pathway.

Modeling Senescence-associated stress responses and repair in *in vitro* cultured CGNs

- Gradual increase in SSB, DSB and alkali labile sites corroborates with increased ROS, lowered thiols and altered gene expression of antioxidant genes.
- Cells seemed to be healthy until 2nd week and exhibited a gradual decline in mitochondrial membrane potential with age due to increased ROS.
- Overall BER repair capacity significantly decreased from 2W and was in line with lowered gene expression of key players of BER pathway- POL β, LIG1, LIG3, APEX and TOP2B.

Analysis of gene expression elevation during ageing of CGNs in culture

- Microarray data analysis showed aberrant gene expression along with decrease in gene expression of TopoIIβ.
- The gene patterns of A2M, GRIA1, GNA14, MASP, NPY and SLIT2 have been validated by q-RT PCR and showed significant increased gene expression with age. Thus, making them markers of potential interest.

Schematic representation of neuronal senescence based on observed results

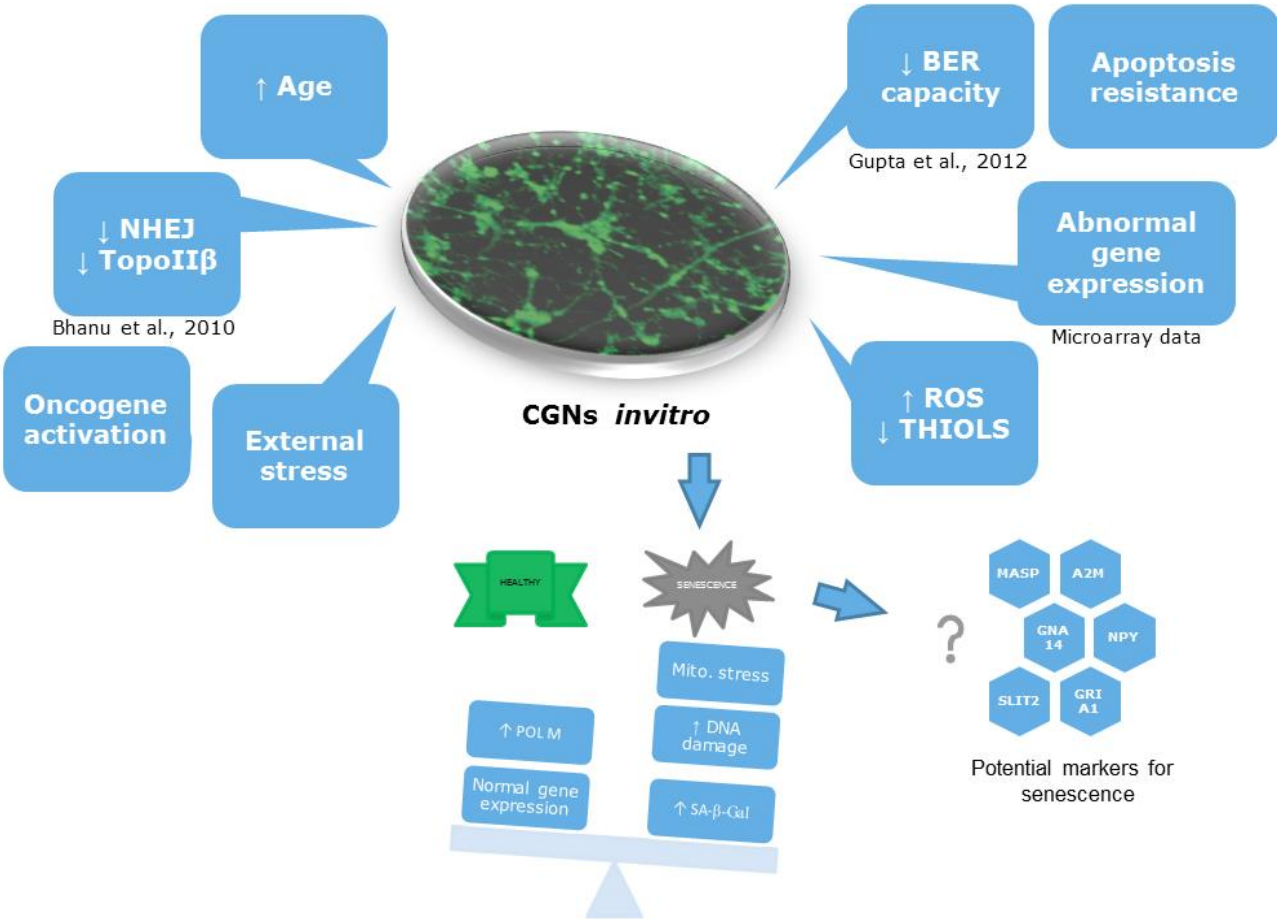

The siRNA mediated knock down of TopoIIβ clearly points out that BER activity, especially UDG and LIG requires the presence of TopoIIβ in neurons for protection against the possible encounter of insults from alkylating agents. TopoIIβ catalytic activity *per se* is not involved in BER activity but might be playing a role in regulating the same. A composite study characterizing BER associated senescence in primary neurons was carried out. Increased mitochondrial stress, ROS coupled with decline in both in Base excision repair capacity and free thiols and aberrant gene expression led to neuronal senescence.

PUBLICATIONS FROM THESIS

1. **Topoisomerase IIβ regulates base excision repair capacity of neurons**

   K. Preeti Gupta, Umakanta Swain, Kalluri Subba Rao, Anand K. Kondapi. Mechanism of Ageing and Development 133 (2012) 203-213.

2. **Characterizing senescence in *in vitro* cultured cerebellar granule neurons**

   K. Preeti Gupta, Anand. K. Kondapi –MANUSCRIPT COMMUNICATED

3. **Aberrant gene expression in *in vitro* ageing CGNs**

   K. Preeti Gupta, Pankaz Singh, Anand. K. Kondapi –MANUSCRIPT UNDER PREPARATION

4. **Presented a poster at 'DNA damage, mutation and Cancer'**

   GORDON RESEARCH CONFERENCE, LA, USA held in March 21st to 24th, 2010 (sponsored by CSIR)

   Role of TopoIIβ in Base Excision Repair in Cerebellar Granule Neurons

   K. Preeti Gupta, Umakanta Swain, Anand K. Kondapi.

REFERENCES

- Acosta, J.C., O'Loghlen, A., Banito, A., Raguz, S., and Gil, J. (2008). Control of senescence by CXCR2 and its ligands. Cell Cycle *7*, 2956-2959.
- Alexander, P. (1967). The role of DNA lesions in the processes leading to aging in mice. Symp Soc Exp Biol *21*, 29-50.
- Ames, B.N. (1983). Dietary carcinogens and anticarcinogens. Oxygen radicals and degenerative diseases. Science *221*, 1256-1264.
- Aravind, L., and Koonin, E.V. (1999). DNA polymerase beta-like nucleotidyltransferase superfamily: identification of three new families, classification and evolutionary history. Nucleic Acids Res *27*, 1609-1618.
- Augustin-Voss, H.G., Voss, A.K., and Pauli, B.U. (1993). Senescence of aortic endothelial cells in culture: effects of basic fibroblast growth factor expression on cell phenotype, migration, and proliferation. J Cell Physiol *157*, 279-288.
- Baker, D.J., Perez-Terzic, C., Jin, F., Pitel, K.S., Niederlander, N.J., Jeganathan, K., Yamada, S., Reyes, S., Rowe, L., Hiddinga, H.J., *et al.* (2008). Opposing roles for p16Ink4a and p19Arf in senescence and ageing caused by BubR1 insufficiency. Nat Cell Biol *10*, 825-836.
- Barrows, L.R., and Magee, P.N. (1982). Nonenzymatic methylation of DNA by S-adenosylmethionine in vitro. Carcinogenesis *3*, 349-351.
- Beard, W.A., Prasad, R., and Wilson, S.H. (2006). Activities and mechanism of DNA polymerase beta. Methods Enzymol *408*, 91-107.
- Beausejour, C.M., Krtolica, A., Galimi, F., Narita, M., Lowe, S.W., Yaswen, P., and Campisi, J. (2003). Reversal of human cellular senescence: roles of the p53 and p16 pathways. EMBO J *22*, 4212-4222.
- Beckman, K.B., and Ames, B.N. (1998). The free radical theory of aging matures. Physiol Rev *78*, 547-581.
- Beranek, D.T. (1990). Distribution of methyl and ethyl adducts following alkylation with monofunctional alkylating agents. Mutat Res *231*, 11-30.
- Beranek, D.T., Heflich, R.H., Kodell, R.L., Morris, S.M., and Casciano, D.A. (1983). Correlation between specific DNA-methylation products and mutation induction at the HGPRT locus in Chinese hamster ovary cells. Mutat Res *110*, 171-180.
- Berger, J.M., Gamblin, S.J., Harrison, S.C., and Wang, J.C. (1996). Structure and mechanism of DNA topoisomerase II. Nature *379*, 225-232.
- Bernstein, C. and Bernstein, H. (1991) Aging, sex, and DNA repair. Academic Press, San Diego ; London.
- Bhanu, M.U., Mandraju, R.K., Bhaskar, C., and Kondapi, A.K. (2010). Cultured cerebellar granule neurons as an in vitro aging model: topoisomerase IIbeta as an additional biomarker in DNA repair and aging. Toxicol In Vitro *24*, 1935-1945.
- Bigioni, M., Zunino, F., Tinelli, S., Austin, C.A., Willmore, E., and Capranico, G. (1996). Position-specific effects of base mismatch on mammalian topoisomerase II DNA cleaving activity. Biochemistry *35*, 153-159.
- Blacker, D., Wilcox, M.A., Laird, N.M., Rodes, L., Horvath, S.M., Go, R.C., Perry, R., Watson, B., Jr., Bassett, S.S., McInnis, M.G., *et al.* (1998). Alpha-2 macroglobulin is genetically associated with Alzheimer disease. Nat Genet *19*, 357-360.
- Blalock, E.M., Porter, N.M., and Landfield, P.W. (1999). Decreased G-protein-mediated regulation and shift in calcium channel types with age in hippocampal cultures. J Neurosci *19*, 8674-8684.
- Bohr, V., Anson, R.M., Mazur, S., and Dianov, G. (1998). Oxidative DNA damage processing and changes with aging. Toxicol Lett *102-103*, 47-52.
- Boiteux, S., and Guillet, M. (2004). Abasic sites in DNA: repair and biological consequences in Saccharomyces cerevisiae. DNA Repair (Amst) *3*, 1-12.
- Bokov, A., Chaudhuri, A., and Richardson, A. (2004). The role of oxidative damage and stress in aging. Mech Ageing Dev *125*, 811-826.
- Borbely, S., Dobo, E., Czege, D., Molnar, E., Bakos, M., Szucs, B., Vincze, A., Vilagi, I., and Mihaly, A. (2009). Modification of ionotropic glutamate receptor-mediated processes in the rat hippocampus following repeated, brief seizures. Neuroscience *159*, 358-368.
- Bradford, M.M. (1976). A rapid and sensitive method for the quantitation of microgram quantities of protein utilizing the principle of protein-dye binding. Anal Biochem *72*, 248-254.
- Braig, M., and Schmitt, C.A. (2006). Oncogene-induced senescence: putting the brakes on tumor development. Cancer Res *66*, 2881-2884.
- Cabelof, D.C., Raffoul, J.J., Yanamadala, S., Ganir, C., Guo, Z., and Heydari, A.R. (2002). Attenuation of DNA polymerase beta-dependent base excision repair and increased DMS-induced mutagenicity in aged mice. Mutat Res *500*, 135-145.
- Caldecott, K.W. (2004). DNA single-strand breaks and neurodegeneration. DNA Repair (Amst) *3*, 875-882.
- Campisi, J. (2001). Cellular senescence as a tumor-suppressor mechanism. Trends Cell Biol *11*, S27-31.
- Campisi, J., and d'Adda di Fagagna, F. (2007). Cellular senescence: when bad things happen to good cells. Nat Rev Mol Cell Biol *8*, 729-740.
- Capranico, G., Tinelli, S., Austin, C.A., Fisher, M.L., and Zunino, F. (1992). Different patterns of gene expression of topoisomerase II isoforms in differentiated tissues during murine development. Biochim Biophys Acta *1132*, 43-48.
- Carrel, A. (1912). On the Permanent Life of Tissues Outside of the Organism. J Exp Med *15*, 516-528.
- Chakravarti, D., Ibeanu, G.C., Tano, K., and Mitra, S. (1991). Cloning and expression in Escherichia coli of a human cDNA encoding the DNA repair protein N-methylpurine-DNA glycosylase. J Biol Chem *266*, 15710-15715.
- Chang, B.D., Swift, M.E., Shen, M., Fang, J., Broude, E.V., and Roninson, I.B. (2002). Molecular determinants of terminal growth arrest induced in tumor cells by a chemotherapeutic agent. Proc Natl Acad Sci U S A *99*, 389-394.
- Chen, Q.M., Liu, J., and Merrett, J.B. (2000). Apoptosis or senescence-like growth arrest: influence of cell-cycle position, p53, p21 and bax in H2O2 response of normal human fibroblasts. Biochem J *347*, 543-551.
- Christen, Y. (2000). Oxidative stress and Alzheimer disease. Am J Clin Nutr *71*, 621S-629S.
- Chu, G. (1997). Double strand break repair. J Biol Chem *272*, 24097-24100.
- Chung, H.Y., Cesari, M., Anton, S., Marzetti, E., Giovannini, S., Seo, A.Y., Carter, C., Yu, B.P., and Leeuwenburgh, C. (2009). Molecular inflammation: underpinnings of aging and age-related diseases. Ageing Res Rev *8*, 18-30.

- Collado, M., and Serrano, M. (2006). The power and the promise of oncogene-induced senescence markers. Nat Rev Cancer *6*, 472-476.
- Contestabile, A. (2002). Cerebellar granule cells as a model to study mechanisms of neuronal apoptosis or survival in vivo and in vitro. Cerebellum *1*, 41-55.
- Cooke, M.S., Evans, M.D., Dizdaroglu, M., and Lunec, J. (2003). Oxidative DNA damage: mechanisms, mutation, and disease. FASEB J *17*, 1195-1214.
- Coppe, J.P., Patil, C.K., Rodier, F., Sun, Y., Munoz, D.P., Goldstein, J., Nelson, P.S., Desprez, P.Y., and Campisi, J. (2008). Senescence-associated secretory phenotypes reveal cell-nonautonomous functions of oncogenic RAS and the p53 tumor suppressor. PLoS Biol *6*, 2853-2868.
- Cortopassi, G.A., and Wong, A. (1999). Mitochondria in organismal aging and degeneration. Biochim Biophys Acta *1410*, 183-193.
- Cristofalo, V.J. (1996). Ten years later: what have we learned about human aging from studies of cell cultures? Gerontologist *36*, 737-741.
- D'Mello, S.R., Galli, C., Ciotti, T., and Calissano, P. (1993). Induction of apoptosis in cerebellar granule neurons by low potassium: inhibition of death by insulin-like growth factor I and cAMP. Proc Natl Acad Sci U S A *90*, 10989-10993.
- Davalos, A.R., Coppe, J.P., Campisi, J., and Desprez, P.Y. (2010). Senescent cells as a source of inflammatory factors for tumor progression. Cancer Metastasis Rev *29*, 273-283.
- Day, R.S. (1975). Xeroderma pigmentosum variants have decreased repair of ultraviolet-damaged DNA. Nature *253*, 748-749.
- de Laat, W.L., Jaspers, N.G., and Hoeijmakers, J.H. (1999). Molecular mechanism of nucleotide excision repair. Genes Dev *13*, 768-785.
- de Wind, N., Dekker, M., Berns, A., Radman, M., and te Riele, H. (1995). Inactivation of the mouse Msh2 gene results in mismatch repair deficiency, methylation tolerance, hyperrecombination, and predisposition to cancer. Cell *82*, 321-330.
- Demple, B., Herman, T., and Chen, D.S. (1991). Cloning and expression of APE, the cDNA encoding the major human apurinic endonuclease: definition of a family of DNA repair enzymes. Proc Natl Acad Sci U S A *88*, 11450-11454.
- Di Leonardo, A., Linke, S.P., Clarkin, K., and Wahl, G.M. (1994). DNA damage triggers a prolonged p53-dependent G1 arrest and long-term induction of Cip1 in normal human fibroblasts. Genes Dev *8*, 2540-2551.
- Di Lisa, F., and Bernardi, P. (2005). Mitochondrial function and myocardial aging. A critical analysis of the role of permeability transition. Cardiovasc Res *66*, 222-232.
- Di Micco, R., Cicalese, A., Fumagalli, M., Dobreva, M., Verrecchia, A., Pelicci, P.G., and di Fagagna, F. (2008). DNA damage response activation in mouse embryonic fibroblasts undergoing replicative senescence and following spontaneous immortalization. Cell Cycle *7*, 3601-3606.
- Dimri, G.P., Lee, X., Basile, G., Acosta, M., Scott, G., Roskelley, C., Medrano, E.E., Linskens, M., Rubelj, I., Pereira-Smith, O.*, et al.* (1995). A biomarker that identifies senescent human cells in culture and in aging skin in vivo. Proc Natl Acad Sci U S A *92*, 9363-9367.
- Donner, J., Sipila, T., Ripatti, S., Kananen, L., Chen, X., Kendler, K.S., Lonnqvist, J., Pirkola, S., Hettema, J.M., and Hovatta, I. (2012). Support for involvement of glutamate decarboxylase 1 and neuropeptide Y in anxiety susceptibility. Am J Med Genet B Neuropsychiatr Genet *159B*, 316-327.
- Donze, O., and Picard, D. (2002). RNA interference in mammalian cells using siRNAs synthesized with T7 RNA polymerase. Nucleic Acids Res *30*, e46.
- Drake, F.H., Zimmerman, J.P., McCabe, F.L., Bartus, H.F., Per, S.R., Sullivan, D.M., Ross, W.E., Mattern, M.R., Johnson, R.K., Crooke, S.T.*, et al.* (1987). Purification of topoisomerase II from amsacrine-resistant P388 leukemia cells. Evidence for two forms of the enzyme. J Biol Chem *262*, 16739-16747.
- Dringen, R., and Hirrlinger, J. (2003). Glutathione pathways in the brain. Biol Chem *384*, 505-516.
- Earnshaw, W.C., Halligan, B., Cooke, C.A., Heck, M.M., and Liu, L.F. (1985). Topoisomerase II is a structural component of mitotic chromosome scaffolds. J Cell Biol *100*, 1706-1715.
- Eisen, J.A., and Hanawalt, P.C. (1999). A phylogenomic study of DNA repair genes, proteins, and processes. Mutat Res *435*, 171-213.
- El-Khamisy, S.F., Saifi, G.M., Weinfeld, M., Johansson, F., Helleday, T., Lupski, J.R., and Caldecott, K.W. (2005). Defective DNA single-strand break repair in spinocerebellar ataxia with axonal neuropathy-1. Nature *434*, 108-113.
- Emmons, M., Boulware, D., Sullivan, D.M., and Hazlehurst, L.A. (2006). Topoisomerase II beta levels are a determinant of melphalan-induced DNA crosslinks and sensitivity to cell death. Biochem Pharmacol *72*, 11-18.
- Epstein, J., Williams, J.R., and Little, J.B. (1974). Rate of DNA repair in progeric and normal human fibroblasts. Biochem Biophys Res Commun *59*, 850-857.
- Epstein, J.H., Fukuyama, K., Reed, W.B., and Epstein, W.L. (1970). Defect in DNA synthesis in skin of patients with xeroderma pigmentosum demonstrated in vivo. Science *168*, 1477-1478.
- Eveno, E., Bourre, F., Quilliet, X., Chevallier-Lagente, O., Roza, L., Eker, A.P., Kleijer, W.J., Nikaido, O., Stefanini, M., Hoeijmakers, J.H.*, et al.* (1995). Different removal of ultraviolet photoproducts in genetically related xeroderma pigmentosum and trichothiodystrophy diseases. Cancer Res *55*, 4325-4332.
- Fan, J., and Wilson, D.M., 3rd (2005). Protein-protein interactions and posttranslational modifications in mammalian base excision repair. Free Radic Biol Med *38*, 1121-1138.
- Faucheux, B.A., Privat, N., Brandel, J.P., Sazdovitch, V., Laplanche, J.L., Maurage, C.A., Hauw, J.J., and Haik, S. (2009). Loss of cerebellar granule neurons is associated with punctate but not with large focal deposits of prion protein in Creutzfeldt-Jakob disease. J Neuropathol Exp Neurol *68*, 892-901.
- Filkov, V. (2005) Handbook of Computational Molecular Biology. Chapter 27, Chapman&Hall/CRC Press.
- Fishel, M.L., Vasko, M.R., and Kelley, M.R. (2007). DNA repair in neurons: so if they don't divide what's to repair? Mutat Res *614*, 24-36.
- Fishel, R., Lescoe, M.K., Rao, M.R., Copeland, N.G., Jenkins, N.A., Garber, J., Kane, M., and Kolodner, R. (1993). The human mutator gene homolog MSH2 and its association with hereditary nonpolyposis colon cancer. Cell *75*, 1027-1038.
- Focher, F., Mazzarello, P., Verri, A., Hubscher, U., and Spadari, S. (1990). Activity profiles of enzymes that control the uracil incorporation into DNA during neuronal development. Mutat Res *237*, 65-73.

- Fortini, P., Pascucci, B., Parlanti, E., D'Errico, M., Simonelli, V., and Dogliotti, E. (2003). The base excision repair: mechanisms and its relevance for cancer susceptibility. Biochimie *85*, 1053-1071.
- Fortini, P., Pascucci, B., Parlanti, E., Sobol, R.W., Wilson, S.H., and Dogliotti, E. (1998). Different DNA polymerases are involved in the short- and long-patch base excision repair in mammalian cells. Biochemistry *37*, 3575-3580.
- Franceschi, C., Bonafe, M., Valensin, S., Olivieri, F., De Luca, M., Ottaviani, E., and De Benedictis, G. (2000). Inflamm-aging. An evolutionary perspective on immunosenescence. Ann N Y Acad Sci *908*, 244-254.
- Friedberg, E. C., Walker, G. C. and Siede, W. (1995) DNA repair and mutagenesis. ASM Press, Washington.
- Fukae, J., Takanashi, M., Kubo, S., Nishioka, K., Nakabeppu, Y., Mori, H., Mizuno, Y., and Hattori, N. (2005). Expression of 8-oxoguanine DNA glycosylase (OGG1) in Parkinson's disease and related neurodegenerative disorders. Acta Neuropathol *109*, 256-262.
- Fulop, T., Larbi, A., Kotb, R., de Angelis, F., and Pawelec, G. (2011). Aging, immunity, and cancer. Discov Med *11*, 537-550.
- Funayama, R., and Ishikawa, F. (2007). Cellular senescence and chromatin structure. Chromosoma *116*, 431-440.
- Galic, M.A., Riazi, K., Henderson, A.K., Tsutsui, S., and Pittman, Q.J. (2009). Viral-like brain inflammation during development causes increased seizure susceptibility in adult rats. Neurobiol Dis *36*, 343-351.
- Garg, L.C., DiAngelo, S., and Jacob, S.T. (1987). Role of DNA topoisomerase I in the transcription of supercoiled rRNA gene. Proc Natl Acad Sci U S A *84*, 3185-3188.
- Gates, K.S., Nooner, T., and Dutta, S. (2004). Biologically relevant chemical reactions of N7-alkylguanine residues in DNA. Chem Res Toxicol *17*, 839-856.
- Gilmour, D.S., Pflugfelder, G., Wang, J.C., and Lis, J.T. (1986). Topoisomerase I interacts with transcribed regions in Drosophila cells. Cell *44*, 401-407.
- Gorbunova, V., Seluanov, A., Mao, Z., and Hine, C. (2007). Changes in DNA repair during aging. Nucleic Acids Res *35*, 7466-7474.
- Goto, T., and Wang, J.C. (1985). Cloning of yeast TOP1, the gene encoding DNA topoisomerase I, and construction of mutants defective in both DNA topoisomerase I and DNA topoisomerase II. Proc Natl Acad Sci U S A *82*, 7178-7182.
- Gupta, K.P., Swain, U., Rao, K.S., and Kondapi, A.K. (2012). Topoisomerase IIbeta regulates base excision repair capacity of neurons. Mech Ageing Dev *133*, 203-213.
- Hagen, T.M., Yowe, D.L., Bartholomew, J.C., Wehr, C.M., Do, K.L., Park, J.Y., and Ames, B.N. (1997). Mitochondrial decay in hepatocytes from old rats: membrane potential declines, heterogeneity and oxidants increase. Proc Natl Acad Sci U S A *94*, 3064-3069.
- Halliwell, B., Gutteridge, J. M. C (1999) Free Radicals in Biology, Medicine, 3rd ed., Oxford University Press, Oxford
- Hamilton, M.L., Van Remmen, H., Drake, J.A., Yang, H., Guo, Z.M., Kewitt, K., Walter, C.A., and Richardson, A. (2001). Does oxidative damage to DNA increase with age? Proc Natl Acad Sci U S A *98*, 10469-10474.
- Hang, B., Singer, B., Margison, G.P., and Elder, R.H. (1997). Targeted deletion of alkylpurine-DNA-N-glycosylase in mice eliminates repair of 1,N6-ethenoadenine and hypoxanthine but not of 3,N4-ethenocytosine or 8-oxoguanine. Proc Natl Acad Sci U S A *94*, 12869-12874.
- Harman, D. (1972). Free radical theory of aging: dietary implications. Am J Clin Nutr *25*, 839-843.
- Hayflick, L. (1965). The Limited in Vitro Lifetime of Human Diploid Cell Strains. Exp Cell Res *37*, 614-636.
- Hayflick, L. (1985a). The cell biology of aging. Clin Geriatr Med *1*, 15-27.
- Hayflick, L. (1985b). Theories of biological aging. Exp Gerontol *20*, 145-159.
- Heck, M.M., Hittelman, W.N., and Earnshaw, W.C. (1988). Differential expression of DNA topoisomerases I and II during the eukaryotic cell cycle. Proc Natl Acad Sci U S A *85*, 1086-1090.
- Heflich, R.H., Beranek, D.T., Kodell, R.L., and Morris, S.M. (1982). Induction of mutations and sister-chromatid exchanges in Chinese hamster ovary cells by ethylating agents. Mutat Res *106*, 147-161.
- Heilig, M., Zachrisson, O., Thorsell, A., Ehnvall, A., Mottagui-Tabar, S., Sjogren, M., Asberg, M., Ekman, R., Wahlestedt, C., and Agren, H. (2004). Decreased cerebrospinal fluid neuropeptide Y (NPY) in patients with treatment refractory unipolar major depression: preliminary evidence for association with preproNPY gene polymorphism. J Psychiatr Res *38*, 113-121.
- Hemminki, A., Peltomaki, P., Mecklin, J.P., Jarvinen, H., Salovaara, R., Nystrom-Lahti, M., de la Chapelle, A., and Aaltonen, L.A. (1994). Loss of the wild type MLH1 gene is a feature of hereditary nonpolyposis colorectal cancer. Nat Genet *8*, 405-410.
- Herbig, U., Ferreira, M., Condel, L., Carey, D., and Sedivy, J.M. (2006). Cellular senescence in aging primates. Science *311*, 1257.
- Herbig, U., Jobling, W.A., Chen, B.P., Chen, D.J., and Sedivy, J.M. (2004). Telomere shortening triggers senescence of human cells through a pathway involving ATM, p53, and p21(CIP1), but not p16(INK4a). Mol Cell *14*, 501-513.
- Hilbert, T.P., Chaung, W., Boorstein, R.J., Cunningham, R.P., and Teebor, G.W. (1997). Cloning and expression of the cDNA encoding the human homologue of the DNA repair enzyme, Escherichia coli endonuclease III. J Biol Chem *272*, 6733-6740.
- Hof, P.R., and Morrison, J.H. (2004). The aging brain: morphomolecular senescence of cortical circuits. Trends Neurosci *27*, 607-613.
- Holm, C., Goto, T., Wang, J.C., and Botstein, D. (1985). DNA topoisomerase II is required at the time of mitosis in yeast. Cell *41*, 553-563.
- Horton, J.K., Baker, A., Berg, B.J., Sobol, R.W., and Wilson, S.H. (2002). Involvement of DNA polymerase beta in protection against the cytotoxicity of oxidative DNA damage. DNA Repair (Amst) *1*, 317-333.
- Hsiang, Y.H., Wu, H.Y., and Liu, L.F. (1988). Proliferation-dependent regulation of DNA topoisomerase II in cultured human cells. Cancer Res *48*, 3230-3235.
- Hung, C.W., Chen, Y.C., Hsieh, W.L., Chiou, S.H., and Kao, C.L. (2010). Ageing and neurodegenerative diseases. Ageing Res Rev *9 Suppl 1*, S36-46.
- Hutchinson, F. (1985). Chemical changes induced in DNA by ionizing radiation. Prog Nucleic Acid Res Mol Biol *32*, 115-154.
- Intano, G.W., Cho, E.J., McMahan, C.A., and Walter, C.A. (2003). Age-related base excision repair activity in mouse brain and liver nuclear extracts. J Gerontol A Biol Sci Med Sci *58*, 205-211.

- Ishitani, R., Sunaga, K., Hirano, A., Saunders, P., Katsube, N., and Chuang, D.M. (1996). Evidence that glyceraldehyde-3-phosphate dehydrogenase is involved in age-induced apoptosis in mature cerebellar neurons in culture. J Neurochem *66*, 928-935.
- Jahangir, A., Ozcan, C., Holmuhamedov, E.L., and Terzic, A. (2001). Increased calcium vulnerability of senescent cardiac mitochondria: protective role for a mitochondrial potassium channel opener. Mech Ageing Dev *122*, 1073-1086.
- Jeyapalan, J.C., and Sedivy, J.M. (2008). Cellular senescence and organismal aging. Mech Ageing Dev *129*, 467-474.
- Johnson, F.B., Sinclair, D.A., and Guarente, L. (1999). Molecular biology of aging. Cell *96*, 291-302.
- Ju, B.G., Lunyak, V.V., Perissi, V., Garcia-Bassets, I., Rose, D.W., Glass, C.K., and Rosenfeld, M.G. (2006). A topoisomerase IIbeta-mediated dsDNA break required for regulated transcription. Science *312*, 1798-1802.
- Jurk, D., Wang, C., Miwa, S., Maddick, M., Korolchuk, V., Tsolou, A., Gonos, E.S., Thrasivoulou, C., Saffrey, M.J., Cameron, K.*, et al.* (2012). Postmitotic neurons develop a p21-dependent senescence-like phenotype driven by a DNA damage response. Aging Cell *11*, 996-1004.
- Justice, M.J., Noveroske, J.K., Weber, J.S., Zheng, B., and Bradley, A. (1999). Mouse ENU mutagenesis. Hum Mol Genet *8*, 1955-1963.
- Kass, E.M., and Jasin, M. (2010). Collaboration and competition between DNA double-strand break repair pathways. FEBS Lett *584*, 3703-3708.
- Kaur, P., Schulz, K., Heggland, I., Aschner, M., and Syversen, T. (2008). The use of fluorescence for detecting MeHg-induced ROS in cell cultures. Toxicol In Vitro *22*, 1392-1398.
- Khachaturian, Z.S. (1994). Calcium hypothesis of Alzheimer's disease and brain aging. Ann N Y Acad Sci *747*, 1-11.
- Kingma, P.S., Corbett, A.H., Burcham, P.C., Marnett, L.J., and Osheroff, N. (1995). Abasic sites stimulate double-stranded DNA cleavage mediated by topoisomerase II. DNA lesions as endogenous topoisomerase II poisons. J Biol Chem *270*, 21441-21444.
- Kingma, P.S., Greider, C.A., and Osheroff, N. (1997). Spontaneous DNA lesions poison human topoisomerase IIalpha and stimulate cleavage proximal to leukemic 11q23 chromosomal breakpoints. Biochemistry *36*, 5934-5939.
- Kingma, P.S., and Osheroff, N. (1997). Apurinic sites are position-specific topoisomerase II poisons. J Biol Chem *272*, 1148-1155.
- Klungland, A., and Lindahl, T. (1997). Second pathway for completion of human DNA base excision-repair: reconstitution with purified proteins and requirement for DNase IV (FEN1). EMBO J *16*, 3341-3348.
- Kondapi, A.K., Mulpuri, N., Mandraju, R.K., Sasikaran, B., and Subba Rao, K. (2004). Analysis of age dependent changes of Topoisomerase II alpha and beta in rat brain. Int J Dev Neurosci *22*, 19-30.
- Kraemer, K.H., Lee, M.M., and Scotto, J. (1987). Xeroderma pigmentosum. Cutaneous, ocular, and neurologic abnormalities in 830 published cases. Arch Dermatol *123*, 241-250.
- Kraemer, K.H., Levy, D.D., Parris, C.N., Gozukara, E.M., Moriwaki, S., Adelberg, S., and Seidman, M.M. (1994). Xeroderma pigmentosum and related disorders: examining the linkage between defective DNA repair and cancer. J Invest Dermatol *103*, 96S-101S.
- Krishna, T.H., Mahipal, S., Sudhakar, A., Sugimoto, H., Kalluri, R., and Rao, K.S. (2005). Reduced DNA gap repair in aging rat neuronal extracts and its restoration by DNA polymerase beta and DNA-ligase. J Neurochem *92*, 818-823.
- Krokan, H., Haugen, A., Myrnes, B., and Guddal, P.H. (1983). Repair of premutagenic DNA lesions in human fetal tissues: evidence for low levels of O6-methylguanine-DNA methyltransferase and uracil-DNA glycosylase activity in some tissues. Carcinogenesis *4*, 1559-1564.
- Kulkarni, A., and Wilson, D.M., 3rd (2008). The involvement of DNA-damage and -repair defects in neurological dysfunction. Am J Hum Genet *82*, 539-566.
- Kwong, L.K., and Sohal, R.S. (2000). Age-related changes in activities of mitochondrial electron transport complexes in various tissues of the mouse. Arch Biochem Biophys *373*, 16-22.
- Lai, L.W., Ducore, J.M., and Rosenstein, B.S. (1987). DNA-protein crosslinking in normal human skin fibroblasts exposed to solar ultraviolet wavelengths. Photochem Photobiol *46*, 143-146.
- Lanigan, F., Geraghty, J.G., and Bracken, A.P. (2011). Transcriptional regulation of cellular senescence. Oncogene *30*, 2901-2911.
- Lau, A.Y., Scharer, O.D., Samson, L., Verdine, G.L., and Ellenberger, T. (1998). Crystal structure of a human alkylbase-DNA repair enzyme complexed to DNA: mechanisms for nucleotide flipping and base excision. Cell *95*, 249-258.
- Lawless, C., Wang, C., Jurk, D., Merz, A., Zglinicki, T., and Passos, J.F. (2010). Quantitative assessment of markers for cell senescence. Exp Gerontol *45*, 772-778.
- LeBel, C.P., and Bondy, S.C. (1992). Oxidative damage and cerebral aging. Prog Neurobiol *38*, 601-609.
- Lee, C.Y., Delaney, J.C., Kartalou, M., Lingaraju, G.M., Maor-Shoshani, A., Essigmann, J.M., and Samson, L.D. (2009). Recognition and processing of a new repertoire of DNA substrates by human 3-methyladenine DNA glycosylase (AAG). Biochemistry *48*, 1850-1861.
- Lenaz, G. (1998). Role of mitochondria in oxidative stress and ageing. Biochim Biophys Acta *1366*, 53-67.
- Lesuisse, C., and Martin, L.J. (2002). Immature and mature cortical neurons engage different apoptotic mechanisms involving caspase-3 and the mitogen-activated protein kinase pathway. J Cereb Blood Flow Metab *22*, 935-950.
- Li, M., Linseman, D.A., Allen, M.P., Meintzer, M.K., Wang, X., Laessig, T., Wierman, M.E., and Heidenreich, K.A. (2001). Myocyte enhancer factor 2A and 2D undergo phosphorylation and caspase-mediated degradation during apoptosis of rat cerebellar granule neurons. J Neurosci *21*, 6544-6552.
- Liang, W.S., Dunckley, T., Beach, T.G., Grover, A., Mastroeni, D., Ramsey, K., Caselli, R.J., Kukull, W.A., McKeel, D., Morris, J.C.*, et al.* (2008). Altered neuronal gene expression in brain regions differentially affected by Alzheimer's disease: a reference data set. Physiol Genomics *33*, 240-256.
- Liang, Y., Annan, R.S., Carr, S.A., Popp, S., Mevissen, M., Margolis, R.K., and Margolis, R.U. (1999). Mammalian homologues of the Drosophila slit protein are ligands of the heparan sulfate proteoglycan glypican-1 in brain. J Biol Chem *274*, 17885-17892.
- Lin, A.W., Barradas, M., Stone, J.C., van Aelst, L., Serrano, M., and Lowe, S.W. (1998). Premature senescence involving p53 and p16 is activated in response to constitutive MEK/MAPK mitogenic signaling. Genes Dev *12*, 3008-3019.
- Lin, H.K., Chen, Z., Wang, G., Nardella, C., Lee, S.W., Chan, C.H., Yang, W.L., Wang, J., Egia, A., Nakayama, K.I.*, et al.* (2010). Skp2 targeting suppresses tumorigenesis by Arf-p53-independent cellular senescence. Nature *464*, 374-379.

- Lin, M.T., and Beal, M.F. (2006). Mitochondrial dysfunction and oxidative stress in neurodegenerative diseases. Nature *443*, 787-795.
- Lindahl, T., and Nyberg, B. (1972). Rate of depurination of native deoxyribonucleic acid. Biochemistry *11*, 3610-3618.
- Lindahl, T., and Nyberg, B. (1974). Heat-induced deamination of cytosine residues in deoxyribonucleic acid. Biochemistry *13*, 3405-3410.
- Little, J.B., Epstein, J., and Williams, J.R. (1975). Repair of DNA strand breaks in progeric fibroblasts and aging human diploid cells. Basic Life Sci *5B*, 793-800.
- Liu, B., Wang, Z., Ghosh, S., and Zhou, Z. (2012). Defective ATM-Kap-1-mediated chromatin remodeling impairs DNA repair and accelerates senescence in progeria mouse model. Aging Cell.
- Liu, R.M. (2002). Down-regulation of gamma-glutamylcysteine synthetase regulatory subunit gene expression in rat brain tissue during aging. J Neurosci Res *68*, 344-351.
- Livak, K.J., and Schmittgen, T.D. (2001). Analysis of relative gene expression data using real-time quantitative PCR and the 2(-Delta Delta C(T)) Method. Methods *25*, 402-408.
- Loeb, L.A. (1985). Apurinic sites as mutagenic intermediates. Cell *40*, 483-484.
- Loeb, L.A. (1989). Endogenous carcinogenesis: molecular oncology into the twenty-first century--presidential address. Cancer Res *49*, 5489-5496.
- Loeb, L.A. (1994). Microsatellite instability: marker of a mutator phenotype in cancer. Cancer Res *54*, 5059-5063.
- Lovell, M.A., and Markesbery, W.R. (2007). Oxidative DNA damage in mild cognitive impairment and late-stage Alzheimer's disease. Nucleic Acids Res *35*, 7497-7504.
- Lovell, M.A., Xie, C., and Markesbery, W.R. (2000). Decreased base excision repair and increased helicase activity in Alzheimer's disease brain. Brain Res *855*, 116-123.
- Lu, S.C. (1999). Regulation of hepatic glutathione synthesis: current concepts and controversies. FASEB J *13*, 1169-1183.
- Maher, P. (2005). The effects of stress and aging on glutathione metabolism. Ageing Res Rev *4*, 288-314.
- Mandraju, R., Chekuri, A., Bhaskar, C., Duning, K., Kremerskothen, J., and Kondapi, A.K. (2011). Topoisomerase IIbeta associates with Ku70 and PARP-1 during double strand break repair of DNA in neurons. Arch Biochem Biophys.
- Mandraju, R.K., Kannapiran, P., and Kondapi, A.K. (2008). Distinct roles of Topoisomerase II isoforms: DNA damage accelerating alpha, double strand break repair promoting beta. Arch Biochem Biophys *470*, 27-34.
- Mantelingu, K., Reddy, B.A., Swaminathan, V., Kishore, A.H., Siddappa, N.B., Kumar, G.V., Nagashankar, G., Natesh, N., Roy, S., Sadhale, P.P*., et al.* (2007). Specific inhibition of p300-HAT alters global gene expression and represses HIV replication. Chem Biol *14*, 645-657.
- Markesbery, W.R., and Lovell, M.A. (2006). DNA oxidation in Alzheimer's disease. Antioxid Redox Signal *8*, 2039-2045.
- Marr, D. (1969). A theory of cerebellar cortex. J Physiol *202*, 437-470.
- Matalon, S., Hardiman, K.M., Jain, L., Eaton, D.C., Kotlikoff, M., Eu, J.P., Sun, J., Meissner, G., and Stamler, J.S. (2003). Regulation of ion channel structure and function by reactive oxygen-nitrogen species. Am J Physiol Lung Cell Mol Physiol *285*, L1184-1189.
- Mather, M.W., and Rottenberg, H. (2002). The inhibition of calcium signaling in T lymphocytes from old mice results from enhanced activation of the mitochondrial permeability transition pore. Mech Ageing Dev *123*, 707-724.
- Mattson, M.P. (1992). Calcium as sculptor and destroyer of neural circuitry. Exp Gerontol *27*, 29-49.
- Maynard, S., Schurman, S.H., Harboe, C., de Souza-Pinto, N.C., and Bohr, V.A. (2009). Base excision repair of oxidative DNA damage and association with cancer and aging. Carcinogenesis *30*, 2-10.
- Mazzarello, P., Focher, F., Verri, A., and Spadari, S. (1990). Misincorporation of uracil into DNA as possible contributor to neuronal aging and abiotrophy. Int J Neurosci *50*, 169-174.
- Milligan, J.F., and Uhlenbeck, O.C. (1989). Synthesis of small RNAs using T7 RNA polymerase. Methods Enzymol *180*, 51-62.
- Minamino, T., and Komuro, I. (2007). Vascular cell senescence: contribution to atherosclerosis. Circ Res *100*, 15-26.
- Mitra, S., and Kaina, B. (1993). Regulation of repair of alkylation damage in mammalian genomes. Prog Nucleic Acid Res Mol Biol *44*, 109-142.
- Mosmann, T. (1983). Rapid colorimetric assay for cellular growth and survival: application to proliferation and cytotoxicity assays. J Immunol Methods *65*, 55-63.
- Munro, J., Barr, N.I., Ireland, H., Morrison, V., and Parkinson, E.K. (2004). Histone deacetylase inhibitors induce a senescence-like state in human cells by a p16-dependent mechanism that is independent of a mitotic clock. Exp Cell Res *295*, 525-538.
- Nakamura, A.J., Chiang, Y.J., Hathcock, K.S., Horikawa, I., Sedelnikova, O.A., Hodes, R.J., and Bonner, W.M. (2008). Both telomeric and non-telomeric DNA damage are determinants of mammalian cellular senescence. Epigenetics Chromatin *1*, 6.
- Nealon, K., Nicholl, I.D., and Kenny, M.K. (1996). Characterization of the DNA polymerase requirement of human base excision repair. Nucleic Acids Res *24*, 3763-3770.
- Negri, C., Chiesa, R., Cerino, A., Bestagno, M., Sala, C., Zini, N., Maraldi, N.M., and Astaldi Ricotti, G.C. (1992). Monoclonal antibodies to human DNA topoisomerase I and the two isoforms of DNA topoisomerase II: 170- and 180-kDa isozymes. Exp Cell Res *200*, 452-459.
- Nicholls, D.G. (2004). Mitochondrial membrane potential and aging. Aging Cell *3*, 35-40.
- Nicholls, D.G., and Budd, S.L. (2000). Mitochondria and neuronal survival. Physiol Rev *80*, 315-360.
- Ninomiya, M., Numakawa, T., Adachi, N., Furuta, M., Chiba, S., Richards, M., Shibata, S., and Kunugi, H. (2010). Cortical neurons from intrauterine growth retardation rats exhibit lower response to neurotrophin BDNF. Neurosci Lett *476*, 104-109.
- O'Neill, J.P. (1982). Induction and expression of mutations in mammalian cells in the absence of DNA synthesis and cell division. Mutat Res *106*, 113-122.
- O'Neill, J.P. (2000). DNA damage, DNA repair, cell proliferation, and DNA replication: how do gene mutations result? Proc Natl Acad Sci U S A *97*, 11137-11139.

- Olive, P.L., and Banath, J.P. (2006). The comet assay: a method to measure DNA damage in individual cells. Nat Protoc *1*, 23-29.
- Osheroff, N. (1989). Effect of antineoplastic agents on the DNA cleavage/religation reaction of eukaryotic topoisomerase II: inhibition of DNA religation by etoposide. Biochemistry *28*, 6157-6160.
- Osheroff, N., Zechiedrich, E.L., and Gale, K.C. (1991). Catalytic function of DNA topoisomerase II. Bioessays *13*, 269-273.
- Ostling, O., and Johanson, K.J. (1984). Microelectrophoretic study of radiation-induced DNA damages in individual mammalian cells. Biochem Biophys Res Commun *123*, 291-298.
- Pawelec, G., Rehbein, A., Haehnel, K., Merl, A., and Adibzadeh, M. (1997). Human T-cell clones in long-term culture as a model of immunosenescence. Immunol Rev *160*, 31-42.
- Peak, M.J., Peak, J.G., and Jones, C.A. (1985). Different (direct and indirect) mechanisms for the induction of DNA-protein crosslinks in human cells by far- and near-ultraviolet radiations (290 and 405 nm). Photochem Photobiol *42*, 141-146.
- Peterson, C.A. (1995). Cell culture systems as tools for studying age-related changes in skeletal muscle. J Gerontol A Biol Sci Med Sci *50 Spec No*, 142-144.
- Pfeiffer, P., and Vielmetter, W. (1988). Joining of nonhomologous DNA double strand breaks in vitro. Nucleic Acids Res *16*, 907-924.
- Powell, C.L., Swenberg, J.A., and Rusyn, I. (2005). Expression of base excision DNA repair genes as a biomarker of oxidative DNA damage. Cancer Lett *229*, 1-11.
- Qiu, Z., Strickland, D.K., Hyman, B.T., and Rebeck, G.W. (2002). alpha 2-Macroglobulin exposure reduces calcium responses to N-methyl-D-aspartate via low density lipoprotein receptor-related protein in cultured hippocampal neurons. J Biol Chem *277*, 14458-14466.
- Radicella, J.P., Dherin, C., Desmaze, C., Fox, M.S., and Boiteux, S. (1997). Cloning and characterization of hOGG1, a human homolog of the OGG1 gene of Saccharomyces cerevisiae. Proc Natl Acad Sci U S A *94*, 8010-8015.
- Rana, P., Nadanaciva, S., and Will, Y. (2011). Mitochondrial membrane potential measurement of H9c2 cells grown in high-glucose and galactose-containing media does not provide additional predictivity towards mitochondrial assessment. Toxicol In Vitro *25*, 580-587.
- Rao, K.S. (2002). Base excision repair (BER) and the brain. J Biochem Mol Biol Biophys *6*, 71-83.
- Rao, K. S. (2003b) DNA-Repair and Brain Aging: The importance of base excision repair and DNA-polymerase beta. . Proc. Indian. National Sciences Academy-B, 69, 141-156.
- Rao, K.S. (2007). DNA repair in aging rat neurons. Neuroscience *145*, 1330-1340.
- Ressler, S., Bartkova, J., Niederegger, H., Bartek, J., Scharffetter-Kochanek, K., Jansen-Durr, P., and Wlaschek, M. (2006). p16INK4A is a robust in vivo biomarker of cellular aging in human skin. Aging Cell *5*, 379-389.
- Rinchik, E.M., Carpenter, D.A., and Johnson, D.K. (2002). Functional annotation of mammalian genomic DNA sequence by chemical mutagenesis: a fine-structure genetic mutation map of a 1- to 2-cM segment of mouse chromosome 7 corresponding to human chromosome 11p14-p15. Proc Natl Acad Sci U S A *99*, 844-849.
- Robbins, J.H., Otsuka, F., Tarone, R.E., Polinsky, R.J., Brumback, R.A., Moshell, A.N., Nee, L.E., Ganges, M.B., and Cayeux, S.J. (1983). Radiosensitivity in alzheimer disease and Parkinson disease. Lancet *1*, 468-469.
- Robson, C.N., Hochhauser, D., Craig, R., Rack, K., Buckle, V.J., and Hickson, I.D. (1992). Structure of the human DNA repair gene HAP1 and its localisation to chromosome 14q 11.2-12. Nucleic Acids Res *20*, 4417-4421.
- Roca, J. (1995). The mechanisms of DNA topoisomerases. Trends Biochem Sci *20*, 156-160.
- Rodier, F., Campisi, J., and Bhaumik, D. (2007). Two faces of p53: aging and tumor suppression. Nucleic Acids Res *35*, 7475-7484.
- Rosenquist, T.A., Zharkov, D.O., and Grollman, A.P. (1997). Cloning and characterization of a mammalian 8-oxoguanine DNA glycosylase. Proc Natl Acad Sci U S A *94*, 7429-7434.
- Rubin, H. (1997). Cell aging in vivo and in vitro. Mech Ageing Dev *98*, 1-35.
- Rutten, B.P., Steinbusch, H.W., Korr, H., and Schmitz, C. (2002). Antioxidants and Alzheimer's disease: from bench to bedside (and back again). Curr Opin Clin Nutr Metab Care *5*, 645-651.
- Rydberg, B., and Lindahl, T. (1982). Nonenzymatic methylation of DNA by the intracellular methyl group donor S-adenosyl-L-methionine is a potentially mutagenic reaction. EMBO J *1*, 211-216.
- Sabourin, M., and Osheroff, N. (2000). Sensitivity of human type II topoisomerases to DNA damage: stimulation of enzyme-mediated DNA cleavage by abasic, oxidized and alkylated lesions. Nucleic Acids Res *28*, 1947-1954.
- Samson, L., Derfler, B., Boosalis, M., and Call, K. (1991). Cloning and characterization of a 3-methyladenine DNA glycosylase cDNA from human cells whose gene maps to chromosome 16. Proc Natl Acad Sci U S A *88*, 9127-9131.
- Saul, R. L., Ames B.N (1985) Mechanisms of DNA damage and repair. Plenum Press, New York.
- Scharer, O.D., and Jiricny, J. (2001). Recent progress in the biology, chemistry and structural biology of DNA glycosylases. Bioessays *23*, 270-281.
- Scholes, G. (1983). Radiation effects on DNA. The Silvanus Thompson Memorial Lecture, April 1982. Br J Radiol *56*, 221-231.
- Schulz, J.B., Lindenau, J., Seyfried, J., and Dichgans, J. (2000). Glutathione, oxidative stress and neurodegeneration. Eur J Biochem *267*, 4904-4911.
- Schumacher, B., Garinis, G.A., and Hoeijmakers, J.H. (2008). Age to survive: DNA damage and aging. Trends Genet *24*, 77-85.
- Seki, S., Hatsushika, M., Watanabe, S., Akiyama, K., Nagao, K., and Tsutsui, K. (1992). cDNA cloning, sequencing, expression and possible domain structure of human APEX nuclease homologous to Escherichia coli exonuclease III. Biochim Biophys Acta *1131*, 287-299.
- Senatore, A., Colleoni, S., Verderio, C., Restelli, E., Morini, R., Condliffe, S.B., Bertani, I., Mantovani, S., Canovi, M., Micotti, E., *et al.* (2012). Mutant PrP suppresses glutamatergic neurotransmission in cerebellar granule neurons by impairing membrane delivery of VGCC alpha(2)delta-1 Subunit. Neuron *74*, 300-313.
- Serrano, M., Lin, A.W., McCurrach, M.E., Beach, D., and Lowe, S.W. (1997). Oncogenic ras provokes premature cell senescence associated with accumulation of p53 and p16INK4a. Cell *88*, 593-602.
- Setlow, R.B. (1982). DNA repair, aging, and cancer. Natl Cancer Inst Monogr *60*, 249-255.

- Shiloh, Y. (1997). Ataxia-telangiectasia and the Nijmegen breakage syndrome: related disorders but genes apart. Annu Rev Genet *31*, 635-662.
- Sikora, E., Arendt, T., Bennett, M., and Narita, M. (2011). Impact of cellular senescence signature on ageing research. Ageing Res Rev *10*, 146-152.
- Singh, N.P., McCoy, M.T., Tice, R.R., and Schneider, E.L. (1988). A simple technique for quantitation of low levels of DNA damage in individual cells. Exp Cell Res *175*, 184-191.
- Smith, M.A., Rottkamp, C.A., Nunomura, A., Raina, A.K., and Perry, G. (2000). Oxidative stress in Alzheimer's disease. Biochim Biophys Acta *1502*, 139-144.
- Snapka, R.M., Powelson, M.A., and Strayer, J.M. (1988). Swiveling and decatenation of replicating simian virus 40 genomes in vivo. Mol Cell Biol *8*, 515-521.
- Soffer, D., Grotsky, H.W., Rapin, I., and Suzuki, K. (1979). Cockayne syndrome: unusual neuropathological findings and review of the literature. Ann Neurol *6*, 340-348.
- Srivastava, D.K., Berg, B.J., Prasad, R., Molina, J.T., Beard, W.A., Tomkinson, A.E., and Wilson, S.H. (1998). Mammalian abasic site base excision repair. Identification of the reaction sequence and rate-determining steps. J Biol Chem *273*, 21203-21209.
- Swain, U., and Rao, K.S. (2012). Age-dependent decline of DNA base excision repair activity in rat cortical neurons. Mech Ageing Dev *133*, 186-194.
- Swain, U., Sindhu, K.K., Boda, U., Pothani, S., Giridharan, N.V., Raghunath, M., and Rao, K.S. (2011). Studies on the molecular correlates of genomic stability in rat brain cells following Amalakirasayana therapy. Mech Ageing Dev.
- Swain, U., and Subba Rao, K. (2011). Study of DNA damage via the comet assay and base excision repair activities in rat brain neurons and astrocytes during aging. Mech Ageing Dev *132*, 374-381.
- Tanabe, K., Ikegami, Y., Ishida, R., and Andoh, T. (1991). Inhibition of topoisomerase II by antitumor agents bis(2,6-dioxopiperazine) derivatives. Cancer Res *51*, 4903-4908.
- Tanaka, K., and Wood, R.D. (1994). Xeroderma pigmentosum and nucleotide excision repair of DNA. Trends Biochem Sci *19*, 83-86.
- Tchekneva, E.E., Rinchik, E.M., Polosukhina, D., Davis, L.S., Kadkina, V., Mohamed, Y., Dunn, S.R., Sharma, K., Qi, Z., Fogo, A.B., *et al.* (2007). A sensitized screen of N-ethyl-N-nitrosourea-mutagenized mice identifies dominant mutants predisposed to diabetic nephropathy. J Am Soc Nephrol *18*, 103-112.
- Tchkonia, T., Morbeck, D.E., Von Zglinicki, T., Van Deursen, J., Lustgarten, J., Scrable, H., Khosla, S., Jensen, M.D., and Kirkland, J.L. (2010). Fat tissue, aging, and cellular senescence. Aging Cell *9*, 667-684.
- Tepper, C.G., Seldin, M.F., and Mudryj, M. (2000). Fas-mediated apoptosis of proliferating, transiently growth-arrested, and senescent normal human fibroblasts. Exp Cell Res *260*, 9-19.
- Thibault, O., Hadley, R., and Landfield, P.W. (2001). Elevated postsynaptic [Ca2+]i and L-type calcium channel activity in aged hippocampal neurons: relationship to impaired synaptic plasticity. J Neurosci *21*, 9744-9756.
- Thompson, L.H., and Schild, D. (1999). The contribution of homologous recombination in preserving genome integrity in mammalian cells. Biochimie *81*, 87-105.
- Toescu, E.C., and Verkhratsky, A. (2000a). Assessment of mitochondrial polarization status in living cells based on analysis of the spatial heterogeneity of rhodamine 123 fluorescence staining. Pflugers Arch *440*, 941-947.
- Toescu, E.C., and Verkhratsky, A. (2000b). Neuronal ageing in long-term cultures: alterations of Ca2+ homeostasis. Neuroreport *11*, 3725-3729.
- Tosal, L., Comendador, M.A., and Sierra, L.M. (2001). In vivo repair of ENU-induced oxygen alkylation damage by the nucleotide excision repair mechanism in Drosophila melanogaster. Mol Genet Genomics *265*, 327-335.
- Towbin, H., Staehelin, T., and Gordon, J. (1979). Electrophoretic transfer of proteins from polyacrylamide gels to nitrocellulose sheets: procedure and some applications. Proc Natl Acad Sci U S A *76*, 4350-4354.
- Troen, B.R. (2003). The biology of aging. Mt Sinai J Med *70*, 3-22.
- Tryndyak, V.P., Han, T., Muskhelishvili, L., Fuscoe, J.C., Ross, S.A., Beland, F.A., and Pogribny, I.P. (2011). Coupling global methylation and gene expression profiles reveal key pathophysiological events in liver injury induced by a methyl-deficient diet. Mol Nutr Food Res *55*, 411-418.
- Tsai-Pflugfelder, M., Liu, L.F., Liu, A.A., Tewey, K.M., Whang-Peng, J., Knutsen, T., Huebner, K., Croce, C.M., and Wang, J.C. (1988). Cloning and sequencing of cDNA encoding human DNA topoisomerase II and localization of the gene to chromosome region 17q21-22. Proc Natl Acad Sci U S A *85*, 7177-7181.
- Tsutsui, K., Sano, K., Kikuchi, A., and Tokunaga, A. (2001). Involvement of DNA topoisomerase IIbeta in neuronal differentiation. J Biol Chem *276*, 5769-5778.
- Uemura, T., and Tanagida, M. (1986). Mitotic spindle pulls but fails to separate chromosomes in type II DNA topoisomerase mutants: uncoordinated mitosis. EMBO J *5*, 1003-1010.
- Uemura, T., and Yanagida, M. (1984). Isolation of type I and II DNA topoisomerase mutants from fission yeast: single and double mutants show different phenotypes in cell growth and chromatin organization. EMBO J *3*, 1737-1744.
- Vermeulen, W., Scott, R.J., Rodgers, S., Muller, H.J., Cole, J., Arlett, C.F., Kleijer, W.J., Bootsma, D., Hoeijmakers, J.H., and Weeda, G. (1994). Clinical heterogeneity within xeroderma pigmentosum associated with mutations in the DNA repair and transcription gene ERCC3. Am J Hum Genet *54*, 191-200.
- Vijg, J., and Uitterlinden, A.G. (1987). A search for DNA alterations in the aging mammalian genome: an experimental strategy. Mech Ageing Dev *41*, 47-63.
- Villeponteau, B. (1997). The heterochromatin loss model of aging. Exp Gerontol *32*, 383-394.
- Wada, T., Joza, N., Cheng, H.Y., Sasaki, T., Kozieradzki, I., Bachmaier, K., Katada, T., Schreiber, M., Wagner, E.F., Nishina, H., *et al.* (2004). MKK7 couples stress signalling to G2/M cell-cycle progression and cellular senescence. Nat Cell Biol *6*, 215-226.
- Wang, A.M., Elion, G.B., Friedman, H.S., Bodell, W.J., Bigner, D.D., and Schold, S.C., Jr. (1991). Positive therapeutic interaction between thiopurines and alkylating drugs in human glioma xenografts. Cancer Chemother Pharmacol *27*, 278-284.
- Wang, C., Jurk, D., Maddick, M., Nelson, G., Martin-Ruiz, C., and von Zglinicki, T. (2009). DNA damage response and cellular senescence in tissues of aging mice. Aging Cell *8*, 311-323.
- Wang, J.C. (1985). DNA topoisomerases. Annu Rev Biochem *54*, 665-697.
- Wang, J.C. (1996). DNA topoisomerases. Annu Rev Biochem *65*, 635-692.

- Warren, W., Clark, J.P., Gardner, E., Harris, G., Cooper, C.S., and Lawley, P.D. (1990). Chemical induction of thymomas in AKR mice: interaction of chemical carcinogens and endogenous murine leukemia viruses. Comparison of N-methyl-N-nitrosourea and methyl methanesulphonate. Mol Carcinog *3*, 126-133.
- Weissman, L., Jo, D.G., Sorensen, M.M., de Souza-Pinto, N.C., Markesbery, W.R., Mattson, M.P., and Bohr, V.A. (2007). Defective DNA base excision repair in brain from individuals with Alzheimer's disease and amnestic mild cognitive impairment. Nucleic Acids Res *35*, 5545-5555.
- Wettschureck, N., van der Stelt, M., Tsubokawa, H., Krestel, H., Moers, A., Petrosino, S., Schutz, G., Di Marzo, V., and Offermanns, S. (2006). Forebrain-specific inactivation of Gq/G11 family G proteins results in age-dependent epilepsy and impaired endocannabinoid formation. Mol Cell Biol *26*, 5888-5894.
- Wilkin, G.P. (1995) Neural cell culture: a practical approach. Oxford University Press, USA.
- Wilson, D.M., 3rd, and Bohr, V.A. (2007). The mechanics of base excision repair, and its relationship to aging and disease. DNA Repair (Amst) *6*, 544-559.
- Wilson, D.M., 3rd, and McNeill, D.R. (2007). Base excision repair and the central nervous system. Neuroscience *145*, 1187-1200.
- Wilstermann, A.M., and Osheroff, N. (2001). Base excision repair intermediates as topoisomerase II poisons. J Biol Chem *276*, 46290-46296.
- Wistrom, C., and Villeponteau, B. (1990). Long-term growth of diploid human fibroblasts in low serum media. Exp Gerontol *25*, 97-105.
- Woessner, R.D., Mattern, M.R., Mirabelli, C.K., Johnson, R.K., and Drake, F.H. (1991). Proliferation- and cell cycle-dependent differences in expression of the 170 kilodalton and 180 kilodalton forms of topoisomerase II in NIH-3T3 cells. Cell Growth Differ *2*, 209-214.
- Wood, R.D., Mitchell, M., and Lindahl, T. (2005). Human DNA repair genes, 2005. Mutat Res *577*, 275-283.
- Wu, X., Li, J., Li, X., Hsieh, C.L., Burgers, P.M., and Lieber, M.R. (1996). Processing of branched DNA intermediates by a complex of human FEN-1 and PCNA. Nucleic Acids Res *24*, 2036-2043.
- Xiao, H., Mao, Y., Desai, S.D., Zhou, N., Ting, C.Y., Hwang, J., and Liu, L.F. (2003). The topoisomerase IIbeta circular clamp arrests transcription and signals a 26S proteasome pathway. Proc Natl Acad Sci U S A *100*, 3239-3244.
- Xiong, J., Camello, P.J., Verkhratsky, A., and Toescu, E.C. (2004). Mitochondrial polarisation status and [Ca2+]i signalling in rat cerebellar granule neurones aged in vitro. Neurobiol Aging *25*, 349-359.
- Xu, G., Herzig, M., Rotrekl, V., and Walter, C.A. (2008). Base excision repair, aging and health span. Mech Ageing Dev *129*, 366-382.
- Xu, Z.Q., Chen, M.E., Jiang, X.J., and Wang, J.Z. (2004). [Changes of neuropeptide Y activity in plasma and brain tissue during intracerebral hemorrhage in rats]. Zhongguo Wei Zhong Bing Ji Jiu Yi Xue *16*, 218-220.
- Yan, L., Bulgar, A., Miao, Y., Mahajan, V., Donze, J.R., Gerson, S.L., and Liu, L. (2007). Combined treatment with temozolomide and methoxyamine: blocking apurininc/pyrimidinic site repair coupled with targeting topoisomerase IIalpha. Clin Cancer Res *13*, 1532-1539.
- Yang, D.G., Liu, L., and Zheng, X.Y. (2008). Cyclin-dependent kinase inhibitor p16(INK4a) and telomerase may co-modulate endothelial progenitor cells senescence. Ageing Res Rev *7*, 137-146.
- Yoon, I.K., Kim, H.K., Kim, Y.K., Song, I.H., Kim, W., Kim, S., Baek, S.H., Kim, J.H., and Kim, J.R. (2004). Exploration of replicative senescence-associated genes in human dermal fibroblasts by cDNA microarray technology. Exp Gerontol *39*, 1369-1378.
- Young, I.S., and Woodside, J.V. (2001). Antioxidants in health and disease. J Clin Pathol *54*, 176-186.
- Zhang, H., Pan, K.H., and Cohen, S.N. (2003). Senescence-specific gene expression fingerprints reveal cell-type-dependent physical clustering of up-regulated chromosomal loci. Proc Natl Acad Sci U S A *100*, 3251-3256.
- Zhao, S., Weng, Y.C., Yuan, S.S., Lin, Y.T., Hsu, H.C., Lin, S.C., Gerbino, E., Song, M.H., Zdzienicka, M.Z., Gatti, R.A., *et al.* (2000). Functional link between ataxia-telangiectasia and Nijmegen breakage syndrome gene products. Nature *405*, 473-477.
- Zhu, J., Woods, D., McMahon, M., and Bishop, J.M. (1998). Senescence of human fibroblasts induced by oncogenic Raf. Genes Dev *12*, 2997-3007.

Mechanisms of Ageing and Development 133 (2012) 203–213

Contents lists available at SciVerse ScienceDirect

Mechanisms of Ageing and Development

journal homepage: www.elsevier.com/locate/mechagedev

Topoisomerase IIβ regulates base excision repair capacity of neurons

K. Preeti Gupta [b], Umakanta Swain [b], Kalluri Subba Rao [b], Anand K. Kondapi [a,b,*]

[a] Department of Biotechnology, School of Life Sciences, University of Hyderabad, Hyderabad 500046, Andhra Pradesh, India
[b] Department of Biochemistry, School of Life Sciences, University of Hyderabad, Hyderabad 500046, Andhra Pradesh, India

ARTICLE INFO

Article history:
Available online 17 March 2012

Keywords:
Topoisomerase IIβ
Base excision repair
Ageing
Cerebellar granule neurons

ABSTRACT

Topoisomerase IIβ (TopoIIβ), an enzyme involved in DNA rearrangements, is predominantly present in brain and its levels are shown to decrease with age. This study characterizes the function of TopoIIβ in regulating BER (base excision repair) activity. TopoIIβ deficient granule neurons (CGNT$^-$) show greater sensitivity to N-ethyl N-nitroso urea (ENU)-mediated DNA damage. The cell-free extracts of TopoIIβ knockdown cells (ECGNT$^-$) show a significant decrease in G-U BER activity during ENU-treatment as well as during recovery, suggesting that TopoIIβ promotes G-U BER activity. Since G-U BER activity is not affected in the presence of ICRF-193, catalytic inhibitor of TopoIIβ, the activity of enzyme *per se* may not be participating in BER activity. Further characterization of the activities of BER enzymes present in ECGNT$^-$ shows that uracil DNA-glycosylase (UDG) and ligase (LIG) activities decrease significantly in both ENU treatment and recovery. Supplementation of TopoIIβ to ECGNT$^-$ does not restore ligation activity and ICRF-193 does not influence the LIG activity. These results suggest a role, at least an indirect one, of TopoIIβ in the repair of ENU-mediated strand breaks *via* BER pathway including the activities of UDG and LIG.

1. Introduction

DNA repair, being a fundamental evolutionary process for maintaining the genomic integrity, assumes vital importance in postmitotic, yet highly active tissues like the brain (Wilson and Bohr, 2007a; Kass and Jasin, 2010), and is very important to restore cellular and biological functioning. DNA is under constant attack by DNA damaging agents which may be either endogenous like peroxide or environmental like nitrosoamines. The repair processes are activated by stimulating the production of various proteins participating in the reorganization of chromosome, leading to the repair of damaged DNA through various events namely activation of expression of repair genes (Ju et al., 2006), formation of multimeric repair complexes (Fan and Wilson, 2005), stabilization of damaged regions (Pfeiffer and Vielmetter, 1988), rearrangement and re-sealing of broken ends of the DNA through correction, processing, synthesis and ligation. During this process, torsional stress will be embedded in the upstream and downstream of the damaged site. The maintenance of torsional integrity is promoted by a class of enzymes known as topoisomerases. These topoisomerases play vital roles in a number of fundamental nuclear processes, including DNA replication, transcription, recombination as well as chromosome organization and segregation (Osheroff et al., 1991; Wang, 1996).

Topoisomerase II is present in two isoforms: 170 kDa alpha (Topoisomerase IIα) and 180 kDa beta (Topoisomerase IIβ) (Drake et al., 1987; Tsai-Pflugfelder et al., 1988). A significant activity of Topoisomerase IIβ (TopoIIβ) in nuclei isolated from postmitotic neuronal cells was reported before (Tsutsui et al., 2001). TopoIIβ is also shown to be expressed in other nonproliferating and fully differentiated tissues (Capranico et al., 1992). Of the two isoforms, beta isoform is predominant in the brain (Tsutsui et al., 2001). The level of TopoIIβ in the brain decreases during ageing (Kondapi et al., 2004) and TopoIIβ deficient SK-N-SH, neuroblastoma cells and granule neurons show sensitivity to peroxide mediated DNA damage in a non-homologous end-joining pathway (Mandraju et al., 2008, 2011), thus implicating the role of TopoIIβ in DNA repair pathways. Further, the catalytic activity of TopoII is known to be stimulated by abasic, oxidized and monoalkylated DNA (Sabourin and Osheroff, 2000). Since these studies covered only plasmids containing abasic sites, it is difficult to extrapolate the significance of these findings to highly structured cellular DNA. TopoIIβ has been reported to participate in the repair of melphalan induced DNA crosslinks in myelogenous leukemia, wherein

Abbreviations: APE1, apurinic endonuclease 1; BER, base excision repair; CGNs, cerebellar granule neurons; CGNT$^-$, cerebellar granule neurons downregulated for TopoIIβ; ECGNT$^-$, extracts of TopoIIβ knockdown cells; ENU, N-ethyl N-nitroso urea; LIG, ligase; POLβ, DNA polymerase β; siRNA, small interfering RNA; SSBs, single-strand breaks; TopoIIβ, topoisomerase IIβ; UDG, uracil DNA-glycosylase.

* Corresponding author at: Department of Biotechnology, University of Hyderabad, Hyderabad 500046, Andhra Pradesh, India. Tel.: +91 40 23134571; fax: +91 40 23010145.
E-mail addresses: akksl@uohyd.ernet.in, akondapi@yahoo.com (A.K. Kondapi).

0047-6374/$ – see front matter © 2012 Elsevier Ireland Ltd. All rights reserved.
doi:10.1016/j.mad.2012.03.010

TopoIIβ levels are determinant of the magnitude of DNA crosslinks and cell survival, following treatment with melphalan (Emmons et al., 2006).

N-Ethyl N-nitrosourea (ENU) is a point mutagen and carcinogen (Warren et al., 1990). It is an SN1 monofunctional alkylating agent and transfers its ethyl group to oxygen and nitrogen radicals in DNA, which results in mispairing and base-pair substitutions (Beranek, 1990; Justice et al., 1999). The popular forms of DNA adducts include N^7-ethyl guanine (N^7-G), O^6-ethyl guanine (O^6-G), O^2-ethyl thymine (O^2-T), N^3-ethyl adenine (N^3-A),O^2-ethyl cytosine (O^2-C) and O^4-ethyl thymine (O^4-T) (Heflich et al., 1982; Beranek et al., 1983). Such a base modification is identified by the repair machinery or is subjected to replication. However, upon replication, a distinct increase in the frequency of transitions GC → AT and AT → GC and AT → TA transversions is seen (O'Neill, 1982; Rinchik et al., 2002; Tchekneva et al., 2007). ENU treated cells upon replication show 50% mutated cells where as if base excision repair (BER) or nucleotide excision repair (NER) were to occur, then either 100% or 0% of the population would be mutated (O'Neill, 1982). NER players recognize the DNA adducts caused due to the nitrosourea compounds, probably by the distortion of the base-pairing stability (Tosal et al., 2001). An O^6 or O^4 alkyl residue is repaired by alkyl DNA alkyl transferase (AGT) (O'Neill, 2000). N^7eG adducts are not harmful yet their downstream processing like deprotonation, depurination, decomposition and C^8G adduct formation can lead to DNA strand breaks (Gates et al., 2004). N^7eG is recognized and exclusively repaired by N-methyl purine DNA-glycosylase (MPG) (Hang et al., 1997; Lee et al., 2009), an initiator glycosylase of the BER pathway (Lau et al., 1998). This generates an abasic site and initiates the BER pathway (Srivastava et al., 1998).

The present study is a special focus on the BER pathway initiated during ENU mediated DNA damage and the role of TopoIIβ in promoting BER activity. BER pathway is known to repair single-base lesions like alkylated and oxidized base forms in DNA. Excision of a methylated base or of uracil (U) calls for a replacement of only the modified nucleotide and is termed single-nucleotide BER or short-patch BER. A monofunctional glycosylase (*e.g.*, N-methylpurine- or UDG) initiates the reaction, followed by strand cleavage at 5′ to the apurinic/apyrimidinic (AP) site by apurinic endonuclease 1 (APE1) which generates a 5′-deoxyribose phosphate (dRP) moiety. This is followed by DNA synthesis and removal of dRP by polymerase β (POLβ) and finally ligation of the nick by a DNA ligase (Horton et al., 2002; Rao, 2007; Wilson and Bohr, 2007a; Wilson and McNeill, 2007b). The long-patch BER may remove the dRP residue along with several downtream nucleotides by flap-endonuclease I (FEN1) that along with DNA ligase I interacts with proliferating cellular nuclear antigen (PCNA) to complete repair synthesis (Fortini et al., 2003). The most rate limiting factors of BER in ageing neurons are POLβ and ligase (Krishna et al., 2005).

The principal objective of our study is to characterize the function of TopoII isoforms in DNA damage and repair in primary neurons, without the interference of the replicative functions. This is because the exact role of the TopoIIβ in irreversibly differentiated cells like neurons is not yet understood. In the present investigation, using ENU mediated DNA damage as a model; we studied the damaged base repair efficiency of CGNs in the presence as well as in the absence of TopoIIβ *via* the BER pathway. Investigations were carried out by downregulating TopoIIβ using siRNA mediated knockdown in CGNs. We also assayed the activities of the various enzymes in the BER pathway. Similarly, parallel studies were carried out on *in vitro* ageing model CGNs (Bhanu et al., 2010). The study has essentially shown that BER capacity of CGNs is impaired during ageing as well as in the TopoIIβ downregulated condition leading to the conclusion that TopoIIβ is essential for normal BER activity in CGNs, especially the cellular LIG activity, and therefore may play a role in the decreased BER capacity of ageing CGNs.

2. Materials and methods

2.1. Chemicals

The following antibodies were used in the present study at the indicated dilutions: mouse and human TopoIIβ monoclonal at 1:500 (BD Biosciences, NJ, USA); mouse and human β actin monoclonal at 1:1000 (Sigma chemical Co., MO, USA); goat anti-mouse HRP IgG at 1:5000 (Upstate, MA, USA). Reagents used were: poly-D-lysine, ENU, Bradford reagent, creatine phosphate, creatine phospho kinase, NAD, ATP, Sephadex G 50, acrylamide, bis-acrylamide, DAPI (Sigma Chemical Co., MO, USA); Earle's balanced salt solution (EBSS), minimal essential medium (MEM), penicillin streptomycin, fetal bovine serum (FBS), Trypsin, Glutamax (GIBCO, NY, USA); dNTPs (Fermentas, MD, USA); pure enzymes T_4 DNA ligase (Invitrogen, NY, USA); APE1 (Trevigen, MD, USA); UDG and T_4 polynucleotide kinase (Bangalore Genei, India); recombinant human DNA polymerase β was kindly gifted by Dr. Rajendra Prasad and Dr. Samuel Wilson, (Laboratory of Structural Biology, National Institute of Environmental Health Sciences, Research Triangle Park, NC, USA); [γ-^{32}P]ATP and [α-^{32}P]dCTP were purchased from BRIT (Mumbai, India); Super signal west pico chemiluminescent substrate (Pierce, IL, USA). All the other chemicals and reagents were of biochemical grade.

2.2. Animals

Wistar rats were maintained in accordance with the animal ethics committee approval, University of Hyderabad. The rats were maintained in a pathogen-free environment with a 12 h light and darkness cycle. Food and water were provided *ad libitum*.

2.3. Cell culture and treatment

Primary CGNs were prepared from the cerebella of postnatal 6–8-day-old Wistar pups by cervical dislocation and the tissue was stored in ice-cold EBSS. The tissue was minced in 0.1% trypsin as previously described (Wilkin, 1995). The CGN cultures were prepared by triturating and diluting the cell pellet with the plating medium (MEM supplemented with 10% FBS, 33 mM glucose, 24.5 mM KCl, 1× Glutamax, 5 mg/mL and 5000 U/mL of penicillin streptomycin (500 μL for 100 mL medium). Cells were plated at 2.5×10^6 cells/60 mm dish and were grown at 37 °C in 5% humidified CO_2 atmosphere. After 24 h of plating, the entire medium was changed and 10 μM of cytosine arabinoside, a mitotic inhibitor was added to inhibit the growth of astrocytes and glial cells. Neuronal cell cultures were fed weekly once by replacing with fresh culture medium. Day of neuronal isolation was considered as day 1 and CGNs were aged for 5 weeks. Cells were pelleted week-wise (at an interval of 7 days) starting from day 3.1 W to 5 W refers to the 1st week to the 5th week. The cells were maintained for 7 days after which they were treated with 1 and 2 mM, ENU for 12 h. The treated cells were also recultured for 48 h in fresh medium for recovery and induction of repair activity. At the end of 12 h and 48 h of recovery, the cells were pelleted and extracts prepared as described in Section 2.7.

2.4. Immunofluorescence

Adherent CGN cultures grown on poly-D-lysine coated cover slips were washed with phosphate buffered saline (PBS). The cultures were fixed and permeabilized in 4% paraformaldehyde prepared in PBS with 0.05% Tween-20 for 5 min at room temperature. The cells were gently washed thrice with 1× PBS and blocked with 10% FBS in PBS for 1 h at room temperature. The fixed cultures were incubated overnight with primary antibody at 4 °C. Next day, they were washed thrice with 1× PBS each time for 5 min. To this, secondary antibody was added with a DNA dye, DAPI (1 μg/mL) and incubated for 1 h at room temperature. This was followed by three washes and the cover slips were mounted onto glass slides with 50% glycerol. Finally, the slides were viewed under confocal microscope and images captured.

2.5. siRNA synthesis

TopoIIβ downregulation was brought about using siRNA that was synthesized as described later. Double stranded siRNA oligos were synthesized *in vitro* (Donze and Picard, 2002). In brief, desalted DNA oligonucleotides (Table 1) were procured from (Sigma Chemical Co., MO, USA). The oligonucleotide-directed production of small RNA transcripts with T7 RNA polymerase has been described (Milligan and Uhlenbeck, 1989). For each transcription reaction, 1 nM of each oligonucleotide was annealed in 50 μL of TE buffer (10 mM Tris–HCl, pH 8.0, and 1 mM EDTA) by heating at 95 °C; after 2 min, the heating block was switched off and allowed to cool slowly to obtain double-strand DNA. Transcription was performed in 50 μL of transcription mix: 1× T7 transcription buffer (40 mM Tris–HCl, pH 7.9, 6 mM $MgCl_2$, 10 mM DTT, 10 mM NaCl and 2 mM spermidine), 1 mM dNTPs, 0.1 U yeast pyrophosphatase (Sigma Chemical Co., MO, USA), 40 U RnaseOUT (Ambion, NY, USA) and 100 U T7 RNA polymerase (Invitrogen, NY, USA) containing 200 pmol of the double-strand DNA as template. After incubation at 37 °C for 2 h, 1 U RNase-free DNase

Table 1
Oligonucleotide sequences for *in vitro* transcription of TopoIIβ siRNA.

Name	siRNA sense template sequence	siRNA antisense template sequence
TopoIIβ siRNA	5′-AAA GCT TAA CAA TCA AGC CCG CTA TAG TGA GTC GTA TTA-3′	5′-AAC GGG CTT GAT TGT TAA GCT CTA TAG TGA GTC GTA TTA-3′
TopoIIβ scrambled siRNA	5′-ACA CTC GAT CAA TCC AAG GAA CTA TAG TGA GTC GTA TTA-3′	5′-CAC TGG ATT GAT CGA GAT GTT CTA TAG TGA GTC GTA TTA-3′
T7 promoter	5′-TAA TAC GAC TCA CTA TAG-3′	

(Ambion, NY, USA) was added at 37 °C for 15 min. Sense and antisense 21-nt RNAs generated in separate reactions were annealed by mixing both crude transcription reactions, heating at 95 °C for 5 min followed by 1 h at 37 °C to obtain 'T7 RNA polymerase synthesized small interfering double-strand RNA' (T7 siRNA). The mixture (100 μL) was then adjusted with 0.2 M sodium acetate, pH 5.2, and precipitated with 2.5 volumes of ethanol. After centrifugation, the pellet was washed once with 70% ethanol, dried and resuspended in 50 μL of water.

2.6. siRNA transfection

CGNs (1×10^6 million) were transfected using Lipofectamine 2000 (Invitrogen, NY, USA) with 0.5 μm of non-silencing and silencing TopoIIβ siRNA. Western blot analysis was carried out with time lapse of 36 h after treatment with siRNA.

2.7. Western blotting

Protein extracts were prepared as described (Bhanu et al., 2010). Briefly, 5×10^6 cells were harvested by scraping in ice-cold phosphate buffered saline and pelleted by centrifuging at 1500 × *g* for 5 min. The cell pellet was suspended in 100 μL of extraction buffer (20 mM Tris–HCl, pH 7.5, 0.1 mM β-mercaptoethanol, 1 mM $MgCl_2$, 0.1 mM EDTA, 5% glycerol, 0.1% Triton X-100, 0.5 mM KCl, 0.5 mM PMSF and 1 μg/mL pepstatin and leupeptin). The homogenate was kept at 4 °C for 1 h, followed by sonication for 15–20 s and centrifuged at 100,000 × *g* for an hour in an ultracentrifuge. The supernatant containing the cytosolic and nuclear proteins was used for all the activity assays. The protein concentration in cell lysates was measured using the Bradford reagent (Bradford, 1976). Forty micrograms of protein was separated by 7.5% sodium dodecyl sulfate polyacrylamide gel electrophoresis (SDS-PAGE) followed by transferring the gel to nitrocellulose membrane (Towbin et al., 1979). The membrane was blocked with 5% non-fat dry milk in TBS containing 0.05% Tween-20 for 1 h and then incubated overnight at 4 °C with corresponding protein specific antibody. After washing and incubating for 1 h at 22 °C with a secondary antibody conjugated with horseradish peroxidase, the membranes were washed and immunoreactive bands were visualized by chemiluminescence. To evaluate relative levels of protein, the integrated optical density of signal was determined by densitometry of scanned images using the ImageJ 1.43u software, NIH, USA.

2.8. Alkaline comet assay

DNA damage was evaluated using alkaline (pH > 13) single-cell gel electrophoresis or comet assay (Singh et al., 1988; Kent et al., 1995). Alkaline comet assay detects single-strand breaks (SSBs), double-strand breaks (DSBs) and alkali labile

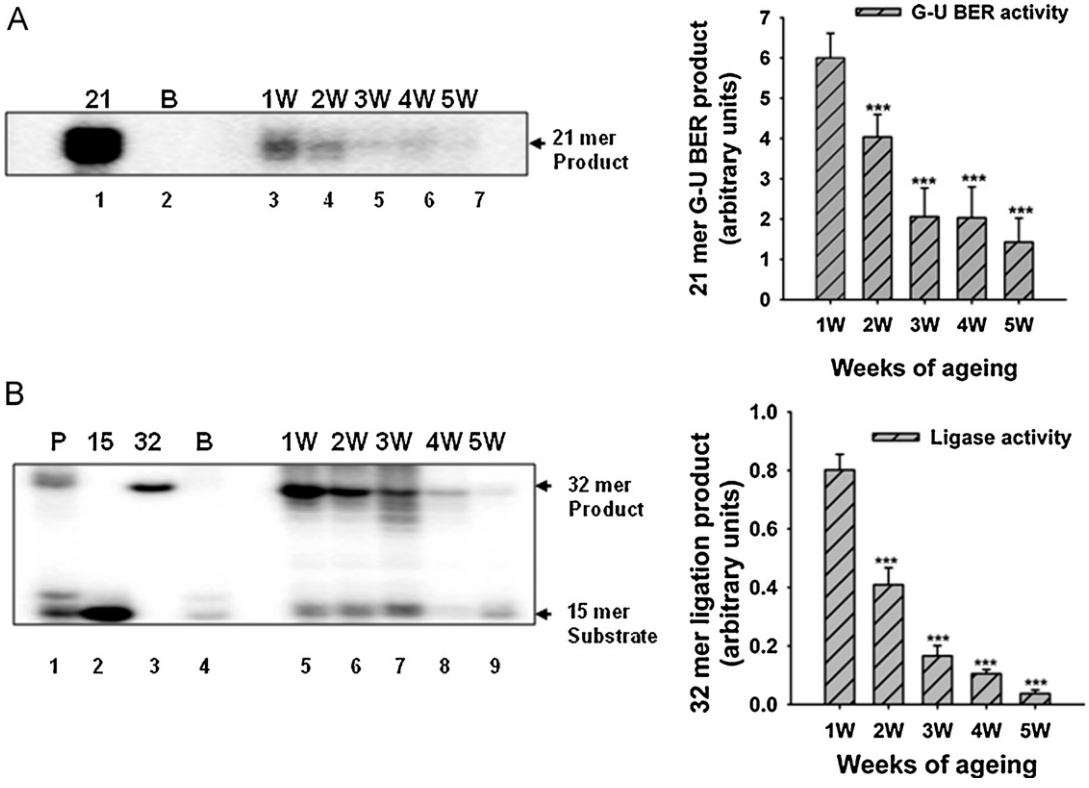

Fig. 1. Effect of *in vitro* ageing on G-U BER and ligase activity in CGNs. Cultured CGNs were pelleted at the end of every week for 5 weeks and cell extracts prepared. Panel A depicts a representative autoradiogram showing G-U BER activity in ageing CGN extracts. The substrate for G-U BER assay is a 3 pmol of 21 mer double stranded uracil (U) containing oligonucleotide. The BER activity of the extracts involves base hydrolysis of U, cleaving the phosphodiester backbone followed by the polymerase gap filling and ligation. Lane 1 is a 21 mer; lane 2 shows activity in blank (B), *i.e.* only 3 pmol of substrate DNA; lanes 3–7 depict G-U BER activity in CGN extracts aged 1 (1 W) to 5 weeks (5 W), respectively. Seen is a gradual decline in the activity of the ageing extracts in terms of 21 mer product formed in arbitrary units. Activity in 1 W old CGN extract was taken as control with which the activity in 2–5 W CGN extracts was compared using One Way ANOVA (Holm-Sidak method). The difference in the activities was found to be statistically significant (***$P < 0.001$). Panel B illustrates the effect of *in vitro* ageing on ligase (LIG) activity in CGNs. Substrate is a 400 fmol of 5′-[γ-^{32}P]ATP end labeled 32 mer double stranded oligonucleotide containing a nick. The LIG activity of the extracts involves sealing the nick in the phosphodiester backbone that results in a 32 mer product formation. Lanes 1–4 correspond to LIG activity by 10 U of pure enzyme, T_4 DNA ligase (P), 15 mer (15), 32 mer (32), blank (B), *i.e.* 400 fmol of substrate DNA; lanes 5–9 depict LIG activity in CGN extracts aged 1 (1 W) to 5 weeks (5 W), respectively. Representative autoradiogram shows gradual decline in the activity of the ageing extracts in terms of 32 mer product formed in arbitrary units. Activity in 1 W old CGN extract was taken as control. Using One Way ANOVA (Holm-Sidak method), the difference in the activities was found to be statistically significant (***$P < 0.001$). Bar charts depict mean ± SD.

Table 2
Oligonucleotide sequences for *in vitro* activity assays.

	Assay	Sequence
G-U BER	5' U 3'	Oligo 1: 5′-GCC ATT G**U**G CTA CCG ATC GCG-3′ (21 mer) Oligo 2: 3′-CGG TAA C**G**C GAT GGC TAG CGC-5′ (21 mer)
UDG	3' G 5' *5' U 3'	Oligo 1: *5′-GCC ATT G**U**G CTA CCG ATC GCG-3′ (21 mer) Oligo 2: 3′-CGG TAA C**G**C GAT GGC TAG CGC-5′ (21 mer)
AP	3' G 5' *5' F 3'	Oligo 3: *5′-CGC GAT CGG TAG C**F**C AAT GGC-3′ (21 mer) Oligo 4: 3′-GCG CTA GCC ATC GCG TTA CCG-5′ (21 mer)
LIGASE	3' 5' *5' 3' 3' 5'	Oligo 5: *5′-CGA GCC ATG GCC GCC-3′ (15 mer) Oligo 6: 5′-AGA TTT TTT GCG GTG CC-3′ (17 mer) Oligo 7: 5′-GGC ACC GCA AAA AAT CTG GCG GCC ATG GCT CG-3′ (32 mer)

[γ-^{32}P]ATP end labeling has been indicated by *.

sites. The cells were subjected to treatment as mentioned before, were washed in ice-cold PBS and the cell pellet suspended in 500 μL of cold PBS and 1.5 mL of 1% agarose was added to each sample. The agarose-cell suspension was gently layered on a frosted end-glass microscopic slide that was pre-coated with 0.75% agarose and was allowed to solidify for 5 min, and placed immediately in ice-cold lysis buffer (2.5 M NaCl, 100 mM EDTA, 10 mM Tris (pH 10.0) and 1% Triton X-100) overnight at 4 °C. After lysis, slides were incubated for 1 h in electrophoresis buffer (300 mM NaOH and 1 mM EDTA, pH 13). After electrophoresis (1 h, 25 V, 300 mA), slides were neutralized with 0.4 M Tris, pH 7.5, for 30 min, placed in 100% ethanol for 5 min and then air-dried. The DNA was then stained with 20 μg/mL of ethidium bromide (Sigma chemical Co., MO, USA) for 20 min and slides were washed twice, each time for 5 min in 1× TBE. To ensure random sampling, 50 images/slide were captured. The images were captured on a confocal microscope (Lieca, IL, USA) and quantified by using Comet-IV software (Perceptive Instruments, Suffolk, UK).

2.9. Oligonucleotides

For end labeling, equimolar concentrations of oligos (Table 2) and [γ-^{32}P]ATP (specific activity – 3000 Ci/mmol) were added to the reaction mixture containing T_4 polynucleotide kinase (2.5 U/pmol of substrate) and T_4 PNK buffer (70 mM

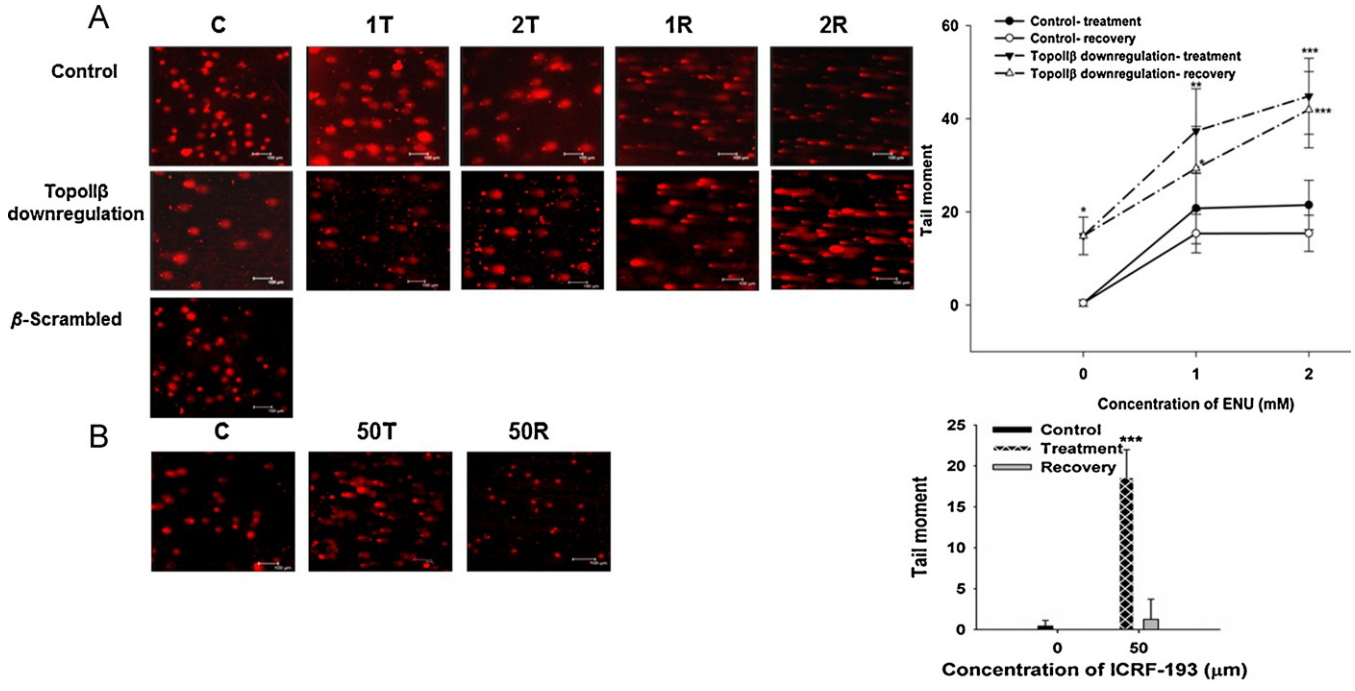

Fig. 2. TopoIIβ downregulation affects repair of ENU mediated SSBs in CGNs. The induction of DNA damage by ENU was investigated using alkaline comet assay which provides a measure of SSBs, DSBs and alkali labile sites. Cultured CGNs were treated with ENU at 1, 2 mM concentrations for 12 h (1T and 2T), subjected to fresh media change and allowed to recover for 48 h (1R and 2R) from DNA damage. After 12 h of treatment and 48 h of recovery, cells were pelleted and processed for alkaline comet assay. Panel A shows comets on treatment in control batch, $CGNT^-$ batch and TopoIIβ scrambled siRNA treated batch. Panel B shows comets due to DNA damage after 12 h and recovery after 48 h upon treatment with 50 μM ICRF-193. Corresponding bar charts depict mean ± SD. Average of 50 cells was chosen for every experiment (n = 3). DNA damage was measured in terms of tail moment. There was a concentration dependent production of DNA damage in control batch. ICRF-193 showed DNA damage activity. DNA damage was quantified using Comet-IV software (Perceptive Instruments, Suffolk UK). Scale bar = 100 μm. Tail moment was found to be statistically higher in $CGNT^-$ batch, compared with the control batch among similar treatments using One Way ANOVA (Holm-Sidak method) (*$P < 0.05$, **$P < 0.01$, ***$P < 0.001$).

Tris–HCl, pH 7.6, 10 mM $MgCl_2$ and 5 mM DTT). The reaction was carried out at 37 °C for 40 min and terminated by adding 5 μL of 0.5 M EDTA. For annealing, equimolar concentrations of oligos as indicated in Table 2 were hybridized in a reaction mixture containing 50 mM NaCl and 5 mM $MgCl_2$ at 70 °C and allowed to gradually cool to room temperature. The annealed product was purified through a Sephadex G50 column (Sigma Chemical Co., MO, USA) and stored at −20 °C until use.

2.9.1. In vitro G-U base excision repair assay (G-U BER)

In vitro G-U BER assay was performed as described previously (Beard et al., 2006). U containing DNA oligo duplex was prepared by annealing oligo 1 to oligo 2 (Table 2). The BER activity of the neuronal extracts was assayed using the above mentioned substrate. The reaction mixture in a final volume of 50 μL contained 3 pmol of substrate, 4 mM ATP, 5 mM creatine phosphate, 100 μg/mL CPK, 0.5 mM NAD, 10 mM $MgCl_2$, 10 μCi [α-^{32}P]dCTP and BER buffer containing 50 mM HEPES, pH 7.5, 20 mM KCl, 2 mM DTT, 1 mM EDTA, pH 8. The reaction was initiated by adding 15 μg of neuronal extract and was incubated at 37 °C for 20 min. Incorporation of [α-^{32}P]dCTP by CGN extracts was used as a measure of G-U BER. The reaction was stopped by the addition of 5 μL 0.5 M EDTA. The reaction mixture was purified by extraction with phenol:chloroform:isoamyl alcohol (25:24:1). The repaired oligo duplex was recovered after 2 h by ethanol precipitation at −80 °C in the presence of glycogen at 1 μg/μL of original reaction mixture volume. The supernatant was discarded and tubes containing oligos were allowed to dry overnight, 6 μL of 6× loading dye (0.002% bromophenol blue and xylene cyanol in formamide) was added to each of the tubes and oligo duplexes were denatured at 90 °C for 5 min and snap-cooled. The reaction products along with markers were separated by electrophoresis in a 20% polyacrylamide sequencing gel electrophoresis (PAGE) with 7 M urea in 90 mM Tris-borate EDTA buffer, pH 8.3 at 2300 V for 3 h. The repaired products (21 mer) were analyzed by autoradiography followed by densitometric scan.

2.9.2. Uracil DNA-glycosylase assay

The assay was carried out as described (Swain and Subba Rao, 2011). U containing DNA oligoduplex was prepared by annealing a previously 5′-[γ-^{32}P]ATP labeledoligo 1 to unlabeled oligo 2 (Table 2). UDG activity of the neuronal extracts was assayed using the above mentioned substrate. The reaction mixture in a final volume of 20 μL containing 200 fmol of U containing oligo duplex, 10 μg of neuronal cell extract and 1× UDG buffer (50 mM Tris–HCl, pH 7.4, 1 mM EDTA, 1 mM DTT, 25 μg/mL bovine serum albumin) was incubated at 37 °C for 20 min. The reaction was terminated by the addition of 3× alkali loading dye (300 mM NaOH and 97% formamide). The reaction products were analyzed by 20% PAGE with 7 M urea and autoradiography as described in Section 2.9.1. The percentage of product formed was determined using the formula [product/(product + substrate) × 100].

2.9.3. AP endonuclease assay

The assay was performed as described (Swain and Subba Rao, 2011). Oligo duplex substrate for AP endonuclease assay was prepared by annealing a previously 5′-[γ-^{32}P]ATP labeled F containing oligo 3 to unlabeled oligo 4 (Table 2). F is tetrahydrofuran, synthetic analog of AP site. AP endonuclease activity of the neuronal extracts was assayed using the above mentioned substrate. The reaction mixture in a final volume of 20 μL containing 200 fmol of oligo duplex, 1× APE1 buffer (10 mM HEPES-KOH, pH 7.4, 100 mM KCl, 10 mM $MgCl_2$) and 0.5 μg of neuronal extract was incubated at 37 °C for 10 min. The reaction was terminated by 0.5 M EDTA. The reaction products were analyzed by 20% PAGE with 7 M and autoradiography as described in Section 2.9.1. The percentage of product formed was determined using the formula [product/(product + substrate) × 100].

2.9.4. Ligase assay

We designed a nicked substratum for LIG assay. An oligo duplex having a nick in one of the strands was prepared by annealing a previously 5′-[γ-^{32}P]ATP labeled oligo 5 and an ATP labeled oligo 6 to unlabeled oligo 8 as shown in Table 2. Repair *via* DNA ligation by protein equivalent of 10 μg of the neuronal extract was assayed using 400 fmol of nicked substrate in the BER reaction buffer. The reaction mixture was incubated for 15 min at 37 °C and the reaction was terminated by heating the mixture at 70 °C for 10 min. The repaired oligo duplex was recovered after 2 h by ethanol precipitation at −80 °C in the presence of glycogen at 1 μg/μL of original

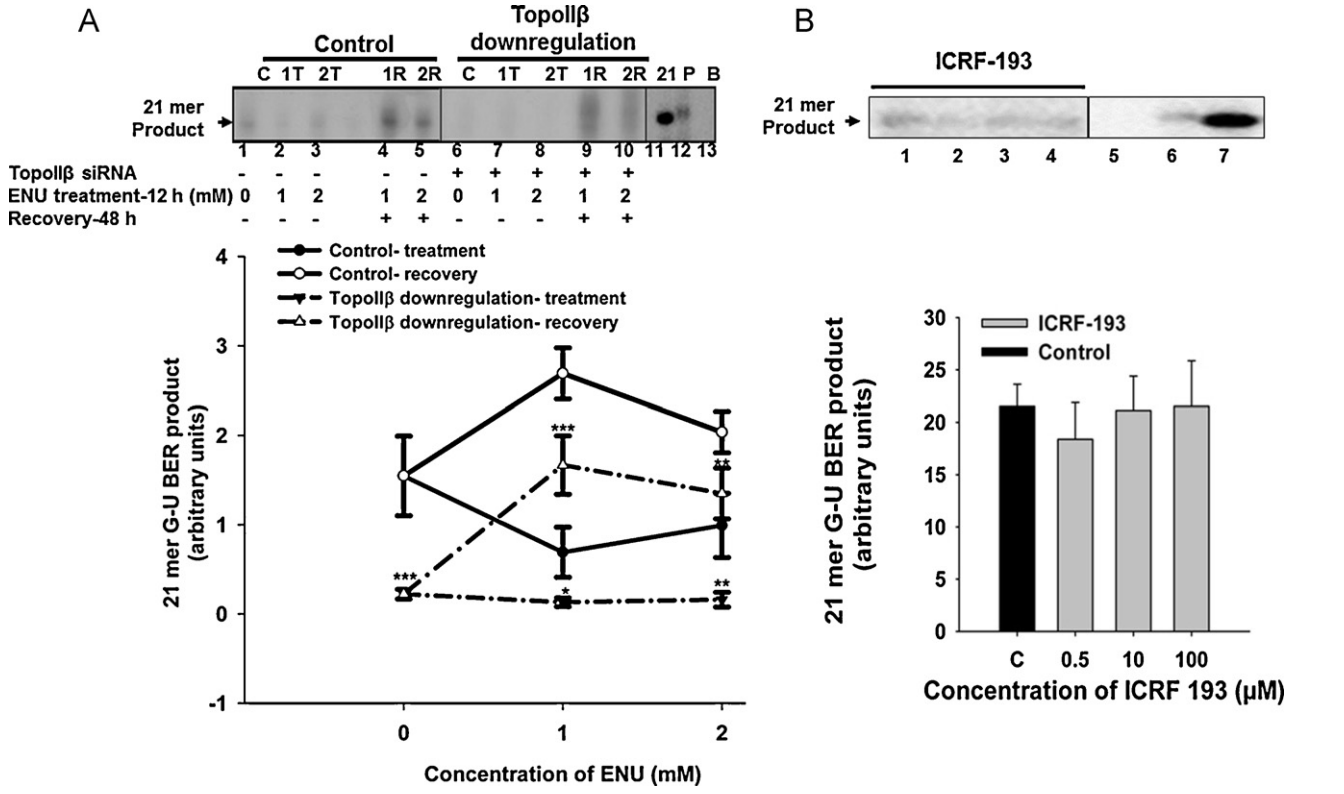

Fig. 3. TopoIIβ knockdown neurons are deficient in G-U BER activity. Panel A depicts a representative autoradiogram showing G-U BER activity in CGNs upon ENU treatment and TopoIIβ downregulation. CGNs and CGNT$^-$ were incubated in the presence of indicated concentrations of ENU for 12 h (treatment) followed by 48 h of recovery by washing the cells in a fresh medium and then recultured in complete medium. Cell-free extracts prepared and checked for G-U BER activity. Lane 1 is G-U BER activity in control untreated cells (C); lanes 2 and 3 show activity of protein extracts in terms of 21 mer G-U BER product formation from CGNs treated for 1 and 2 mM ENU for 12 h (1T and 2T); lanes 4 and 5 show the same for treatment followed by 48 h of recovery (1R and 2R), respectively; lane 6 shows activity from untreated ECGNT$^-$ (C); lanes 7 and 8 show the same in ECGNT$^-$, 12 h ENU treatment (1T and 2T) and lanes 9 and 10 for treatment followed by 48 h recovery (1R and 2R). Lane 11 depicts 21 mer; lane 12 is pure enzyme control (P); lane 13 depicts blank (B), *i.e.* 3 pmol of G-U BER substrate. Panel B depicts the effect of ICRF-193 on G-U BER activity. TopoIIβ inhibitor ICRF-193 was used to demonstrate the direct participation of TopoIIβ catalytic activity in the repair of G-U mismatch. 0.5, 10, 100 μM ICRF-193 (corresponding to lanes 2, 3 and 4) was directly added to *in vitro* G-U BER reaction. Lanes 5, 6 and 7 correspond to blank (B), pure enzyme control (P) and 21 mer (21). The amount of 21 mer G-U BER product formed was densitometrically measured using ImageJ 1.43u software, NIH, USA and the values represented as bar graphs. The difference in the activities of control and CGNT$^-$ extracts among similar treatments was found to be highly significant using One Way ANOVA (Holm-Sidak method), ($^*P < 0.05$, $^{**}P < 0.01$, $^{***}P < 0.001$). Bar charts depict mean ± SD.

reaction mixture volume. The supernatant was discarded and tubes containing oligos were allowed to dry overnight. 6 μL of loading dye (0.002% bromophenol blue and xylene cyanol in formamide) was added to each of the tubes and oligo duplexes were denatured at 90 °C for 5 min and snap-cooled. The reaction products were analyzed 20% PAGE with 7 M and autoradiography as described in Section 2.9.1. The end product, 32 mer was densitometrically quantified using ImageJ 1.43u software, NIH, USA.

2.10. Immunoprecipitation

Young (2–4 day) rat brain tissue extract was prepared in extraction buffer mentioned in Section 2.7. Approximately 1 mg protein was precleared with mice pre immune IgG and 100 μL of protein A agarose. The precleared protein was incubated overnight at 4 °C with 0.5 μg of TopoIIβ antibody. 100 μL of protein A agarose slurry was added and rocked for another 30 min at room temperature. Protein A agarose mix was washed with IP buffer of increasing concentrations of 150, 300, 500 and 750 mM NaCl, twice at each concentration by centrifuging at 1500 × *g* for 3 min. Supernatant or wash through was collected. Protein A agarose beads along with immunoprecipitated TopoIIβ was taken for the reaction.

2.11. Statistical analysis

Experiments were performed in triplicate and repeated independently thrice. Data was averaged and presented as mean ± SD. Statistical comparisons were made using Sigma Plot 11.0, One Way ANOVA with Holm-Sidak *post hoc* test. *P*-value < 0.05 was considered to be statistically significant. The test was used to compare control with TopoIIβ downregulated condition at a particular treatment level.

3. Results

3.1. Isolation of pure CGN cultures

Cultured CGNs were isolated to homogeneity from rat cerebellum (Bhanu et al., 2010). TopoIIβ isoform was down-regulated in CGNs by siRNA specific to TopoIIβ (CGNT$^-$) as explained earlier (Fig. S1 and S2).

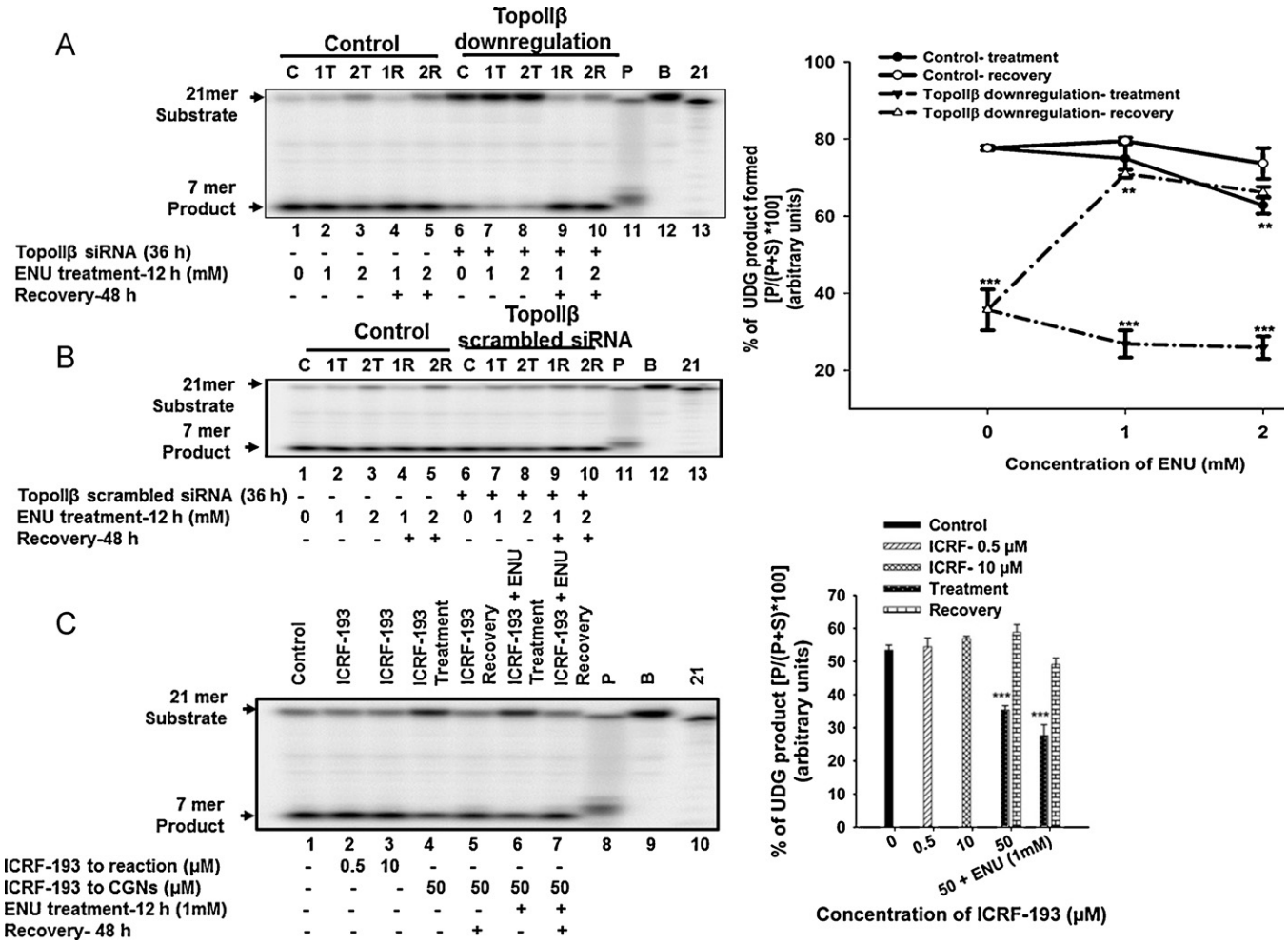

Fig. 4. UDG activity is not enhanced in TopoIIβ deficient condition during ENU treatment. The substrate is 200 fmol of 5′-[γ-^{32}P]ATP end labeled 21 mer double stranded U containing oligonucleotide. UDG activity involves base hydrolysis of U, resulting in a 7 mer product. Panel A is a representative autoradiogram showing UDG activity upon ENU treatment and TopoIIβ downregulation. Lane 1 illustrates UDG activity in control untreated cells (C); lanes 2 and 3 show activity of protein extracts in terms of 7 mer product formation from CGNs treated with 1 and 2 mM ENU for 12 h (1T and 2T); lanes 4 and 5 show the same for treatment followed by 48 h of recovery (1R and 2R) respectively; lane 6 shows activity from untreated ECGNT$^-$ (C); lanes 7 and 8 show the same in ECGNT$^-$, 12 h treatment (1T and 2T) and lanes 9 and 10 for treatment followed by 48 h recovery (1R and 2R). Lane 11, activity by 0.5 U of pure enzyme, UDG (P); lane 12, activity in blank (B), *i.e.* 200 fmol of substrate; lane 13 depicts 21 mer (21). Treatments given as indicated in the figure. Panel B shows representative autoradiogram showing UDG activity in CGN extracts treated with TopoIIβ scrambled siRNA to rule out any direct effect of siRNA on UDG activity. The experimental procedure and product quantification were done as described in Section 2.9.1. Panel C shows the effect of ICRF-193 on UDG activity, in culture and *in vitro*. Lane 1 shows UDG activity in healthy CGNs; lanes 2 and 3, UDG activity upon direct addition of 0.5 and 10 μM ICRF-193; lanes 4 and 5, activity upon 12 h treatment and 48 h recovery from 50 μM ICRF-193; lanes 6 and 7, activity upon treatment with ICRF-193 (12 h) followed by 1 mM ENU (12 h) and recovery (48 h) as indicated in Fig. 4C. Lanes 8, 9 and 10, activity by 0.5 U pure enzyme, UDG (P), blank (B) and 21 mer (21). Percentage of glycosylated product was measured in arbitrary units. Densitometric analysis carried out using ImageJ 1.43u software, NIH, USA. Mean ± SD values represented in bar graphs. The difference in the UDG activities of control and CGNT$^-$ extracts among similar treatments, control and ICRF-193 treated CGN extracts was found to be highly significant using One Way ANOVA (Holm-Sidak method) ($^{**}P < 0.01$, $^{***}P < 0.001$).

3.2. BER activity of CGNs decreased during ageing

Analysis of G-U BER activity (Fig. 1A) in ageing CGNs showed that the G-U BER activity decreases significantly from the second week, with very low activity from fourth week of ageing CGNs. The LIG activity (Fig. 1B) in extracts of ageing neurons showed a significant decrease from second week onwards reaching very low levels by the fifth week in culture. Further, these results viewed together with the earlier observation that TopoIIβ levels decrease in ageing neurons (Bhanu et al., 2010) clearly point out the requirement for characterizing the sensitivity of CGNT$^-$ to BER activating compound ENU.

3.3. TopoIIβ downregulated neurons (CGNT$^-$) showed increased DNA damage

CGNT$^-$ were treated with 1 and 2 mM ENU for 12 h followed by recovery for 48 h and the neurons analyzed for the formation of SSBs, DSBs and alkali labile sites in genomic DNA using alkaline comet assay. The results showed that downregulation of TopoIIβ in comparison to healthy CGNs (Fig. 2A) induced higher strand breaks during both treatment and recovery and were inefficient to repair during recovery. This suggests that CGNT$^-$ have decreased BER capacity, thus becoming more sensitive to DNA damage by ENU. This was further confirmed by increased DNA damage in CGNs when cultured in the presence of 50 μM ICRF-193 (treatment), which was restored during recovery due to the reversibility of the ICRF-193 mediated action after 48 h of drug removal (Fig. 2B).

3.4. TopoIIβ downregulated neurons (CGNT$^-$) showed decreased BER capacity

Since CGNT$^-$ showed higher DNA damage upon treatment with ENU, we have analyzed the BER activity of the cell-free extracts prepared from ENU treated, recovered and TopoIIβ downregulated granule neurons (ECGNT$^-$). The BER activity was analyzed using U containing synthetic radio labeled oligonucleotides. The results showed that G-U BER activity was almost absent during treatment, while it was partially restored during recovery (Fig. 3A). TopoIIβ inhibitor, ICRF-193 was used to demonstrate the direct participation of catalytic activity of TopoIIβ in the repair of G-U mismatch. But the TopoII catalytic inhibitor was found ineffective against the G-U BER activity, when added *in vitro* to the reaction at concentrations of 0.5, 10, 100 μM (Fig. 3B) suggesting TopoIIβ catalytic activity *per se* may not be involved in promoting BER activity.

3.5. Action of TopoIIβ on the activities of enzymes in BER pathway

BER pathway involves base hydrolysis of the mismatched base, U by UDG, followed by depurination by APE1. The base substitution is promoted by POLβ followed by sealing of the repaired ends by LIG. The activities of UDG, AP endonuclease and LIG were analyzed in CGNT$^-$ during treatment and recovery from ENU-mediated DNA damage. The results showed that the UDG activity significantly decreased in extracts prepared from ENU-treated CGNT$^-$ (Fig. 4A), while addition of ICRF-193 *in vitro*, at 0.5 and 10 μM concentration had no effect on UDG activity (Fig. 4C). ICRF-193 mediated downregulation of TopoIIβ at 50 μM reduced UDG activity during treatment. Change in AP endonuclease activity amongst control and CGNT$^-$ was not significant (Fig. 5A). LIG activity was significantly affected in extracts prepared from both ENU-treated and recovered CGNT$^-$ (Fig. 6A). Also, ICRF-193 did not alter LIG activity (Fig. 6B). Furthermore, 50 μM ICRF-193 treatment resulted in decreased LIG activity in ENU-treated ECGNT$^-$ (Fig. 6C). Fig. 7 depicts significant decrease in ligated product formation in the absence of TopoIIβ as well as in TopoIIβ supplemented condition, indicating that TopoIIβ is not directly involved in the ligation step.

To elucidate direct participation of TopoIIβ in BER pathway, ICRF-193 was directly added to the reaction. We found no significant change in the activities of the extracts in terms of product formation in all the three assays – G-U BER, UDG, and LIG

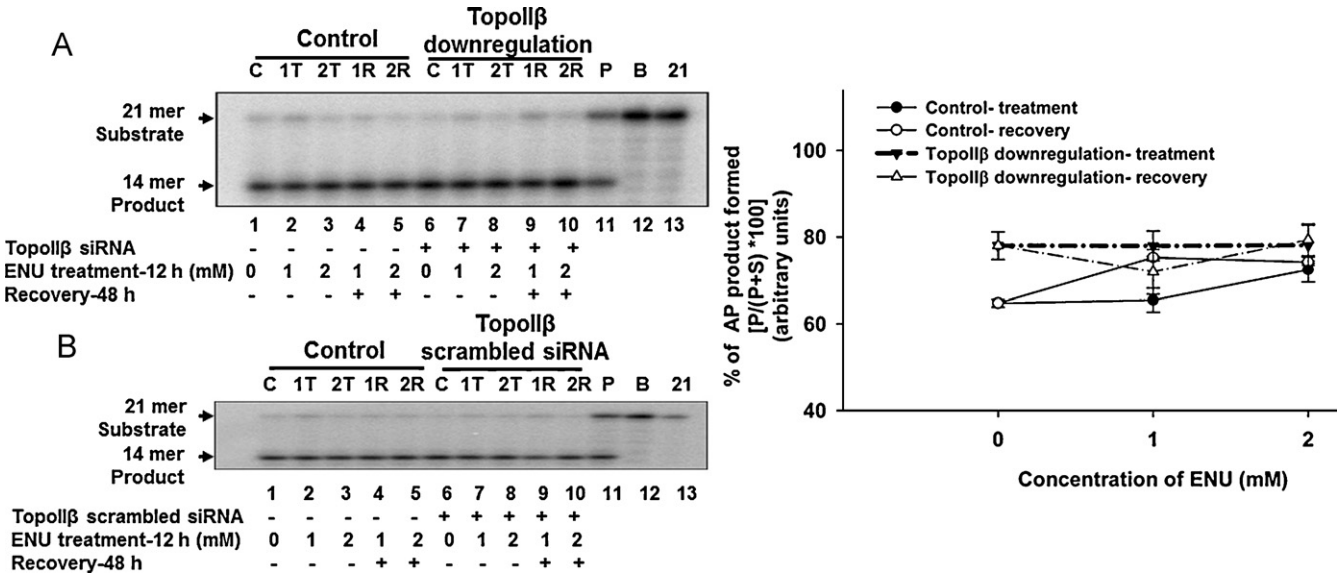

Fig. 5. AP endonuclease activity slightly increased by TopoIIβ downregulation. Panel A is a representative autoradiogram showing AP endonuclease (APE) activity. The substrate is 200 fmol of 5′-[γ-^{32}P]ATP end labeled 21 mer double stranded oligonucleotide containing F, tetrahydrofuran (AP site analog). The APE activity involves the cleavage of phosphodiester backbone on the 3′ side of F. Lane 1 illustrates activity in control untreated cells (C); lanes 2 and 3 show activity of protein extracts in terms of 14 mer AP product formation from CGNs treated for 1 and 2 mM ENU for 12 h (IT and 2T); lanes 4 and 5 show the same for treatment followed by 48 h of recovery (1R and 2R) respectively; lane 6 shows activity from untreated ECGNT$^-$ (C); lanes 7 and 8 show the same in ECGNT$^-$, 12 h treatment (1T and 2T) and lanes 9 and 10 for treatment followed by 48 h recovery (1R and 2R). Lane 11, activity by 1 U of pure enzyme, human APE1 (P); lane 12, activity in blank (B), *i.e.* 200 fmol of substrate; lane 13 depicts 21 mer (21). Panel B shows APE activity in CGN extracts treated with TopoIIβ scrambled siRNA to rule out any direct effect of siRNA on APE activity. Percentage of 14 mer product was measured in terms of arbitrary units. Experimental procedure and densitometric quantification were carried out as described in Section 2.9.1. Bar graph depicts mean ± SD.

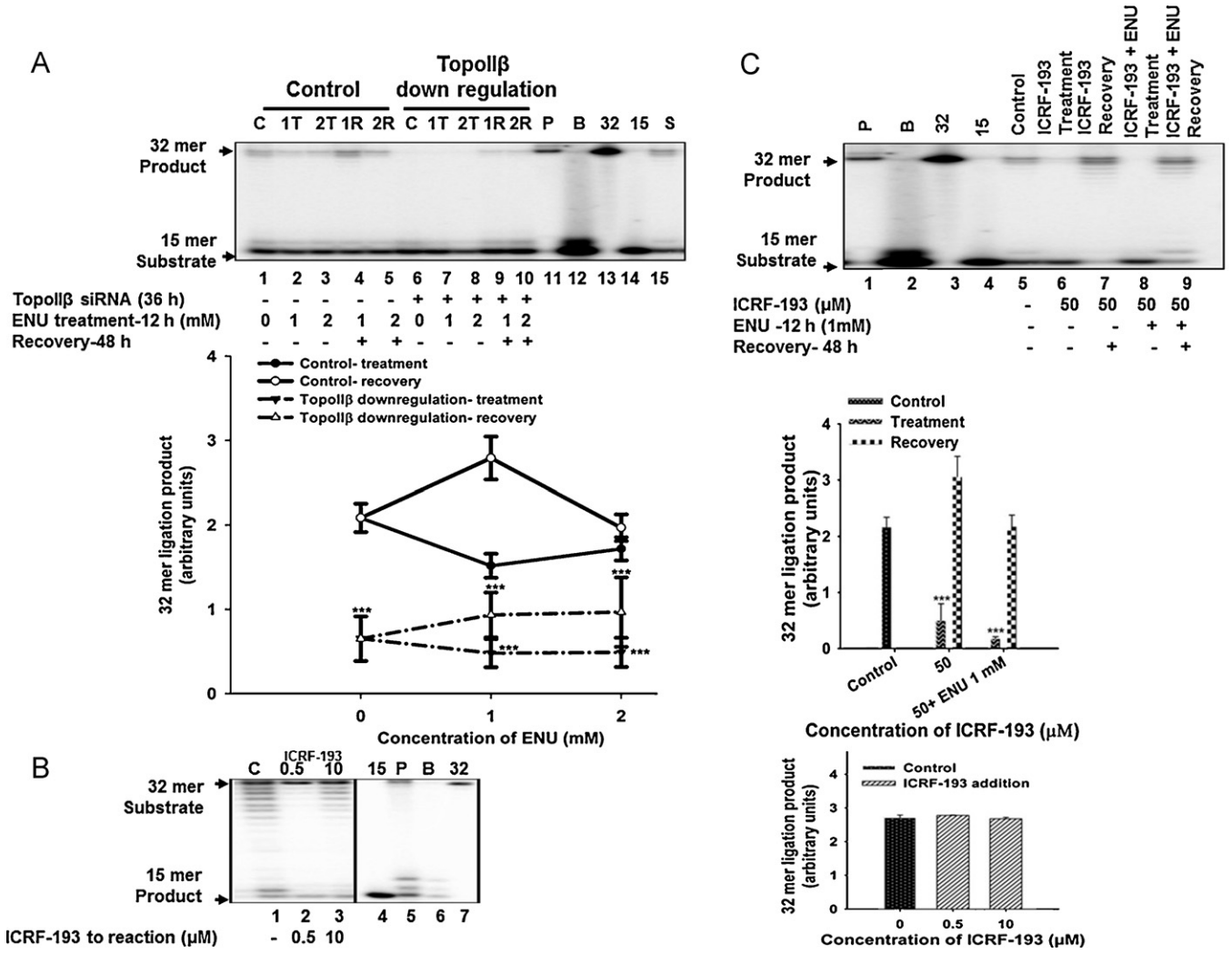

Fig. 6. LIG activity is affected in the ECGNT$^-$ cells during recovery from ENU mediated strand breaks. Panel A is a representative autoradiogram depicting LIG activity. CGNs and CGNT$^-$ were incubated in the presence of indicated concentrations of ENU for 12 h (treatment) followed by 48 h of recovery by washing the cells in fresh medium and then recultured in complete medium. Lane 1 corresponds to LIG activity in control untreated cells (C); lanes 2 and 3 show LIG activity of protein extracts in terms of ligated product formation from 1 and 2 mM ENU treated CGNs for 12 h (1T and 2T); lanes 4 and 5 show the same for treatment followed by 48 h of recovery (1R and 2R);lane 6 shows activity from untreated ECGNT$^-$ (C); lanes 7 and 8 show the same in ECGNT$^-$ subjected to 12 h ENU treatment (1T and 2T); lanes 9 and 10 for treatment followed by 48 h recovery (1R and 2R); lane 11 corresponds to LIG activity by 10 U of pure enzyme, T_4 DNA ligase (P); lane 12 corresponds to blank (B), *i.e.* 400 fmol of substrate DNA; lanes 13 and 14–32 mer and 15 mer marker, respectively and lane 15 to LIG activity due to scrambled TopoIIβ siRNA (S). The activity in control CGN extract was found to be significantly higher than ECGNT$^-$, compared between similar treatments. Panel B illustrates the effect of TopoIIβ inhibitor, ICRF-193 on LIG activity. Experimental procedure as described in Section 2.9.1. Lanes 1, 2 and 3 correspond to activity in control (C), 0.5 and 10 μm ICRF-193 additions to *in vitro* LIG reaction. Lanes 4–7 correspond to 15 mer (15), pure enzyme (P), blank (B) and 32 mer (32), respectively. Panel C illustrates the effect of ICRF-193 treatment on LIG activity in cultured CGNs. Lanes 1–4 correspond to LIG activity in pure enzyme (P), blank (B), 32 mer (32) and 15 mer (15), respectively. Lane 5 shows LIG activity in control (C); lanes 6 and 7 correspond to activity in ICRF-193 treated and recovered culture; lanes 8 and 9 correspond to activity in ICRF-193 (12 h) and ENU (12 h) treated and recovered cultures at indicated concentrations. The amount of 32 mer ligated product formed was densitometrically measured using ImageJ 1.43u software, NIH, USA. Mean ± SD values represented as bar graph. The difference in the activities of control and ICRF-193 treated CGNs was found to be highly significant using One Way ANOVA (Holm-Sidak method) (**$P < 0.01$, ***$P < 0.001$).

(Figs. 3B, 4C and 6B). These results together point out that TopoIIβ catalytic activity does not participate in the BER activity. The observed significant decrease of G-U BER activity as well as the activities of UDG and LIG in TopoIIβ downregulated neurons unequivocally establishes that TopoIIβ plays a crucial role and its knock down would significantly affect the BER activity, especially in regulating UDG and LIG activities.

4. Discussion

Abasic sites are the most commonly formed DNA lesions in the cell and are produced by numerous endogenous and environmental insults. Most abasic sites in cells exist as processed BER intermediates that contain DNA strand breaks proximal to the damaged residue (Krokan et al., 1983). Abasic sites, usually developed at the initial stage of BER (Wilson, 1998), when present in a TopoII DNA cleavage site, they create suicidal substrates, namely BER intermediates containing 5′- or 3′-nicked abasic sites or dRP flaps that are not re-ligated readily by the enzyme and can generate permanent DNA cleavage (Wilstermann and Osheroff, 2001). Thus, they act as TopoII poisons and dramatically stimulate enzyme-mediated DNA cleavage leading to DSBs (Wilstermann and Osheroff, 2001). This is evident from the higher sensitivity of CGNs to ICRF-193 (Fig. 2B). Of the lesions examined to date, AP sites seem to be the most active (Kingma et al., 1995; Bigioni et al., 1996; Kingma et al., 1997; Kingma and Osheroff, 1997; Sabourin and Osheroff, 2000; Powell et al., 2005). When AP sites are located within TopoII cleavage sites, they significantly stimulate TopoII

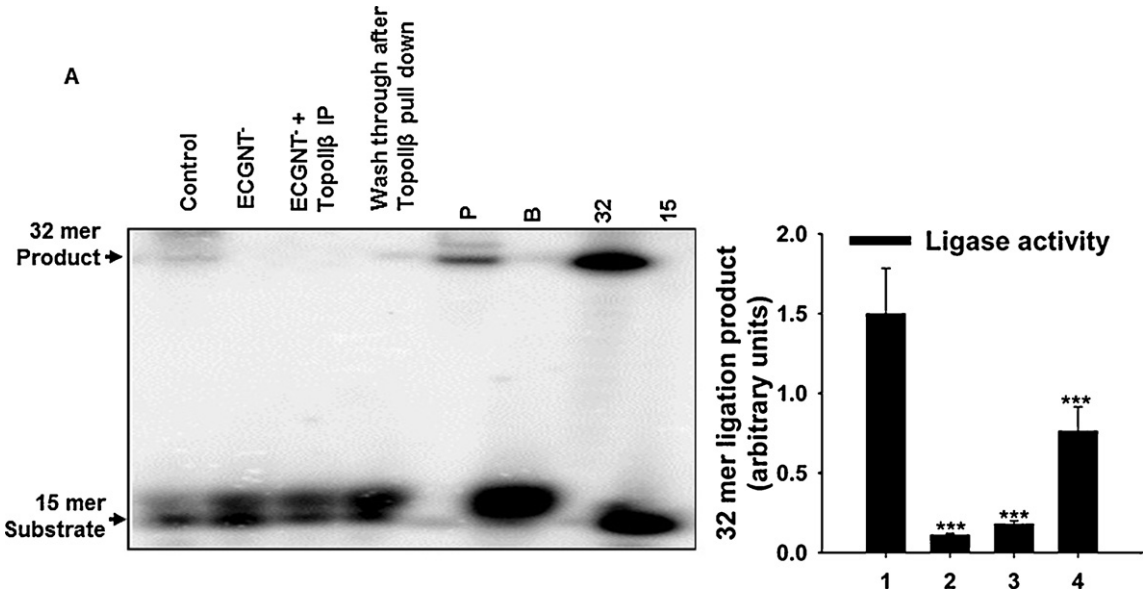

Fig. 7. TopoIIβ activity *per se* not required for LIG activity. Representative autoradiogram depicts TopoIIβ is not directly involved in the ligation step. Lanes 1–4 correspond to LIG activity in control, ECGNT$^-$, ECGNT + TopoIIβ immunoprecipitated (IP) and wash through after TopoIIβ pull down. Lanes 5–8 correspond to pure enzyme control (P), blank (B), 32 mer (32) and 15 mer (15). Using One Way ANOVA (Holm-Sidak method), statistically significant lowered LIG activity was seen in ECGNT$^-$, ECGNT$^-$ + TopoIIβ immunoprecipitated condition (***$P < 0.001$). Mean ± SD values depicted in bar graphs.

mediated DNA cleavage (Kingma et al., 1995; Sabourin and Osheroff, 2000). These results show that AP sites are potentially lethal. Methoxyamine-bound apurinic/apyrimidinic (MX-AP) site in TopoII cleavage sites in DNA act as dual lethal targets, not only for functionally disrupting the BER pathway but also for potentially poisoning TopoII. MX-AP sites are refractory to the catalytic activity of AP endonuclease, indicating their ability to block BER. MX-AP sites are indeed cleaved by purified TopoII, thus suggesting that these sites stimulate TopoII mediated DNA cleavages (Yan et al., 2007). The presence of TopoII cleavage sites in the vicinity of AP sites and methoxyamine related toxicity provides a possible overlap of the TopoII binding and cleavage sites in the vicinity of BER processing region thus implicating TopoIIβ activity in the regulation of BER intermediates in the pathway. The repair of AP sites is the primary defense system, which proceeds more rapidly compared to the repair of a single base such as a U or an 8-oxoguanine base (Boiteux and Guillet, 2004). If the BER pathway is interrupted, nonrepaired AP sites exhibit toxicity (Loeb, 1985). This suggests the importance of understanding the role of intact BER mechanism in recovering cells in relation to protection from the incidence of modifications of the base as well as AP sites. This will be more prominent in primary neurons, whose recovery is essential for restoration of neuronal functions. Although most of the above studies of TopoII activities against AP DNA were invoking TopoIIα and like enzymes, it is not clear if similar activities also take place in case of TopoIIβ, which is the only TopoII isoform expressed in primary neurons. Neurons are prone to high frequency of DNA damage due to increased reactive oxygen species and various other reasons. The present study is an effort to understand the DNA repair function of TopoIIβ in primary neurons.

The results of the present study using the siRNA mediated knock down of TopoIIβ clearly point out that BER activity, especially UDG and LIG requires the presence of TopoIIβ in neurons for protection against the possible encounter of insults from alkylating agents. The diminishing activity of TopoIIβ with age both in ageing rat brain (Kondapi et al., 2004) and in CGNs (Bhanu et al., 2010) points to the importance of restoration of TopoIIβ in ageing brain, specifically neurons for protection from physiological insults. The significant decrease of G-U BER and LIG activities observed in ageing CGNs with concomitant decrease in the level of TopoIIβ (Bhanu et al., 2010) clearly implicates the role of TopoIIβ in the maintenance of BER capacity of neurons against their degeneration during ageing. The present study indicates the regulatory role of TopoIIβ rather than the catalytic role in the maintenance of BER activity.

TopoIIβ, unlike TopoIIα is present in all cell types and specifically present in terminally differentiated cells like neurons. The presence of TopoIIβ in these neurons implicate its role in various neuronal activities like neuronal development, maintenance and gene regulation, Some of the reports of probable interaction of TopoIIβ in repair initiation complexes (Ju et al., 2006) and non-homologous end joining (NHEJ) proteins (Mandraju et al., 2011) supports the possible interaction of TopoIIβ to various repair initiation complexes in promoting the repair process. The molecular activities provided could be through direct interaction of TopoIIβ with repair protein(s), stabilizing the repair complex or/and the presence of TopoIIβ in the repair complex may confer torsional integrity to the DNA during the repair and associated unwinding and re-winding of the DNA without torsional strain.

ICRF-193, bis (2,6-dioxopiperazine) is a strong catalytic inhibitor of Topoisomerase II at lower concentrations (Tanabe et al., 1991) and downregulates TopoIIβ protein expression at higher concentrations (Xiao et al., 2003). Hence, we used both conditions to check the association of TopoIIβ catalytic activity and the protein itself in BER pathway. ICRF-193 traps TopoII into circular clamps on chromatin which impedes the movement of elongating RNA polymerases (Xiao et al., 2003). The suppression of the transcriptional induction of amphiphysin and synaptophysin, nerve terminal stabilizing proteins in CGNs upon ICRF treatment, suggests that TopoII may be involved in the transcriptional regulation (Tsutsui et al., 2001). TopoIIβ *per se* is not involved in BER activity but an active form of TopoIIβ is required for regulating the same. It is possible that TopoIIβ may be interacting with various cellular machineries in restoration of BER activity. This could also be *via* interacting with various partners involved in transcription (Ju et al., 2006).

The present study thus implicates an indirect but significant role of TopoIIβ in modulating or regulating the BER capacity, thus

becoming an important and basic constituent factor for promoting the repair of DNA breaks through BER pathway. Further studies are required to elucidate the obvious regulatory functions of TopoIIβ in neurons.

5. Conclusions

TopoIIβ is essential for promoting the repair of ENU-mediated strand breaks *via* BER pathway. Our overall results suggest a role atleast an indirect one of TopoIIβ in the repair of ENU induced BER pathway including the activities of UDG and LIG.

Acknowledgments

This research work was supported by the Department of Science and Technology (DST) Government of India, through a research project under Health Sciences. We thank the Indian Council of Medical Research, Council for Scientific and Industrial Research, Government of India, for providing Doctoral fellowships to Ms. K. Preeti Gupta and Dr. Umakanta Swain. We thank Prof. C.R. Rao for statistical analysis, Ms. Nalini for technical assistance in confocal microscopy and Mr. P.M. Rao for proof reading the manuscript. The infrastructure developed under various programs including UGC-UPE, XI plan, Centre for Advanced Studies, University of Hyderabad, Department of Biotechnology, Department of Biochemistry, Centre for Research and Education in Biology and Biotechnology, DST-FIST were used to carry out this work.

Appendix A. Supplementary data

Supplementary data associated with this article can be found, in the online version, at doi:10.1016/j.mad.2012.03.010.

References

Beard, W.A., Prasad, R., Wilson, S.H., 2006. Activities and mechanism of DNA polymerase beta. Methods Enzymol. 408, 91–107.
Beranek, D.T., 1990. Distribution of methyl and ethyl adducts following alkylation with monofunctional alkylating agents. Mutat. Res. 231, 11–30.
Beranek, D.T., Heflich, R.H., Kodell, R.L., Morris, S.M., Casciano, D.A., 1983. Correlation between specific DNA-methylation products and mutation induction at the HGPRT locus in Chinese hamster ovary cells. Mutat. Res. 110, 171–180.
Bhanu, M.U., Mandraju, R.K., Bhaskar, C., Kondapi, A.K., 2010. Cultured cerebellar granule neurons as an in vitro aging model: topoisomerase IIbeta as an additional biomarker in DNA repair and aging. Toxicol In Vitro 24, 1935–1945.
Bigioni, M., Zunino, F., Tinelli, S., Austin, C.A., Willmore, E., Capranico, G., 1996. Position-specific effects of base mismatch on mammalian topoisomerase II DNA cleaving activity. Biochemistry 35, 153–159.
Boiteux, S., Guillet, M., 2004. Abasic sites in DNA: repair and biological consequences in Saccharomyces cerevisiae. DNA Repair (Amst.) 3, 1–12.
Bradford, M.M., 1976. A rapid and sensitive method for the quantitation of microgram quantities of protein utilizing the principle of protein-dye binding. Anal. Biochem. 72, 248–254.
Capranico, G., Tinelli, S., Austin, C.A., Fisher, M.L., Zunino, F., 1992. Different patterns of gene expression of topoisomerase II isoforms in differentiated tissues during murine development. Biochim. Biophys. Acta 1132, 43–48.
Donze, O., Picard, D., 2002. RNA interference in mammalian cells using siRNAs synthesized with T7 RNA polymerase. Nucleic Acids Res. 30, e46.
Drake, F.H., Zimmerman, J.P., McCabe, F.L., Bartus, H.F., Per, S.R., Sullivan, D.M., Ross, W.E., Mattern, M.R., Johnson, R.K., Crooke, S.T., et al., 1987. Purification of topoisomerase II from amsacrine-resistant P388 leukemia cells. Evidence for two forms of the enzyme. J. Biol. Chem. 262, 16739–16747.
Emmons, M., Boulware, D., Sullivan, D.M., Hazlehurst, L.A., 2006. Topoisomerase II beta levels are a determinant of melphalan-induced DNA crosslinks and sensitivity to cell death. Biochem. Pharmacol. 72, 11–18.
Fan 3rd, J., Wilson, D.M., 2005. Protein–protein interactions and posttranslational modifications in mammalian base excision repair. Free Radic. Biol. Med. 38, 1121–1138.
Fortini, P., Pascucci, B., Parlanti, E., D'Errico, M., Simonelli, V., Dogliotti, E., 2003. The base excision repair: mechanisms and its relevance for cancer susceptibility. Biochimie 85, 1053–1071.
Gates, K.S., Nooner, T., Dutta, S., 2004. Biologically relevant chemical reactions of N7-alkylguanine residues in DNA. Chem. Res. Toxicol. 17, 839–856.
Hang, B., Singer, B., Margison, G.P., Elder, R.H., 1997. Targeted deletion of alkylpurine-DNA-N-glycosylase in mice eliminates repair of 1,N6-ethenoadenine and hypoxanthine but not of 3,N4-ethenocytosine or 8-oxoguanine. Proc. Natl. Acad. Sci. U.S.A. 94, 12869–12874.
Heflich, R.H., Beranek, D.T., Kodell, R.L., Morris, S.M., 1982. Induction of mutations and sister-chromatid exchanges in Chinese hamster ovary cells by ethylating agents. Mutat. Res. 106, 147–161.
Horton, J.K., Baker, A., Berg, B.J., Sobol, R.W., Wilson, S.H., 2002. Involvement of DNA polymerase beta in protection against the cytotoxicity of oxidative DNA damage. DNA Repair (Amst.) 1, 317–333.
Ju, B.G., Lunyak, V.V., Perissi, V., Garcia-Bassets, I., Rose, D.W., Glass, C.K., Rosenfeld, M.G., 2006. A topoisomerase IIbeta-mediated dsDNA break required for regulated transcription. Science 312, 1798–1802.
Justice, M.J., Noveroske, J.K., Weber, J.S., Zheng, B., Bradley, A., 1999. Mouse ENU mutagenesis. Hum. Mol. Genet. 8, 1955–1963.
Kass, E.M., Jasin, M., 2010. Collaboration and competition between DNA double-strand break repair pathways. FEBS Lett. 584, 3703–3708.
Kent, C.R., Eady, J.J., Ross, G.M., Steel, G.G., 1995. The comet moment as a measure of DNA damage in the comet assay. Int. J. Radiat. Biol. 67, 655–660.
Kingma, P.S., Corbett, A.H., Burcham, P.C., Marnett, L.J., Osheroff, N., 1995. Abasic sites stimulate double-stranded DNA cleavage mediated by topoisomerase II. DNA lesions as endogenous topoisomerase II poisons. J. Biol. Chem. 270, 21441–21444.
Kingma, P.S., Greider, C.A., Osheroff, N., 1997. Spontaneous DNA lesions poison human topoisomerase IIalpha and stimulate cleavage proximal to leukemic 11q23 chromosomal breakpoints. Biochemistry 36, 5934–5939.
Kingma, P.S., Osheroff, N., 1997. Apurinic sites are position-specific topoisomerase II poisons. J. Biol. Chem. 272, 1148–1155.
Kondapi, A.K., Mulpuri, N., Mandraju, R.K., Sasikaran, B., Subba Rao, K., 2004. Analysis of age dependent changes of Topoisomerase II alpha and beta in rat brain. Int. J. Dev. Neurosci. 22, 19–30.
Krishna, T.H., Mahipal, S., Sudhakar, A., Sugimoto, H., Kalluri, R., Rao, K.S., 2005. Reduced DNA gap repair in aging rat neuronal extracts and its restoration by DNA polymerase beta and DNA-ligase. J. Neurochem. 92, 818–823.
Krokan, H., Haugen, A., Myrnes, B., Guddal, P.H., 1983. Repair of premutagenic DNA lesions in human fetal tissues: evidence for low levels of O6-methylguanine-DNA methyltransferase and uracil-DNA glycosylase activity in some tissues. Carcinogenesis 4, 1559–1564.
Lau, A.Y., Scharer, O.D., Samson, L., Verdine, G.L., Ellenberger, T., 1998. Crystal structure of a human alkylbase-DNA repair enzyme complexed to DNA: mechanisms for nucleotide flipping and base excision. Cell 95, 249–258.
Lee, C.Y., Delaney, J.C., Kartalou, M., Lingaraju, G.M., Maor-Shoshani, A., Essigmann, J.M., Samson, L.D., 2009. Recognition and processing of a new repertoire of DNA substrates by human 3-methyladenine DNA glycosylase (AAG). Biochemistry 48, 1850–1861.
Loeb, L.A., 1985. Apurinic sites as mutagenic intermediates. Cell 40, 483–484.
Mandraju, R., Chekuri, A., Bhaskar, C., Duning, K., Kremerskothen, J., Kondapi, A.K., 2011. Topoisomerase IIbeta associates with Ku70 and PARP-1 during double strand break repair of DNA in neurons. Arch. Biochem. Biophys. 71 (September (6)), 1022–1029.
Mandraju, R.K., Kannapiran, P., Kondapi, A.K., 2008. Distinct roles of Topoisomerase II isoforms: DNA damage accelerating alpha, double strand break repair promoting beta. Arch. Biochem. Biophys. 470, 27–34.
Milligan, J.F., Uhlenbeck, O.C., 1989. Synthesis of small RNAs using T7 RNA polymerase. Methods Enzymol. 180, 51–62.
O'Neill, J.P., 1982. Induction and expression of mutations in mammalian cells in the absence of DNA synthesis and cell division. Mutat. Res. 106, 113–122.
O'Neill, J.P., 2000. DNA damage, DNA repair, cell proliferation, and DNA replication: how do gene mutations result? Proc. Natl. Acad. Sci. U.S.A. 97, 11137–11139.
Osheroff, N., Zechiedrich, E.L., Gale, K.C., 1991. Catalytic function of DNA topoisomerase II. BioEssays 13, 269–273.
Pfeiffer, P., Vielmetter, W., 1988. Joining of nonhomologous DNA double strand breaks in vitro. Nucleic Acids Res. 16, 907–924.
Powell, C.L., Swenberg, J.A., Rusyn, I., 2005. Expression of base excision DNA repair genes as a biomarker of oxidative DNA damage. Cancer Lett. 229, 1–11.
Rao, K.S., 2007. DNA repair in aging rat neurons. Neuroscience 145, 1330–1340.
Rinchik, E.M., Carpenter, D.A., Johnson, D.K., 2002. Functional annotation of mammalian genomic DNA sequence by chemical mutagenesis: a fine-structure genetic mutation map of a 1- to 2-cM segment of mouse chromosome 7 corresponding to human chromosome 11p14-p15. Proc. Natl. Acad. Sci. U.S.A. 99, 844–849.
Sabourin, M., Osheroff, N., 2000. Sensitivity of human type II topoisomerases to DNA damage: stimulation of enzyme-mediated DNA cleavage by abasic, oxidized and alkylated lesions. Nucleic Acids Res. 28, 1947–1954.
Singh, N.P., McCoy, M.T., Tice, R.R., Schneider, E.L., 1988. A simple technique for quantitation of low levels of DNA damage in individual cells. Exp. Cell Res. 175, 184–191.
Srivastava, D.K., Berg, B.J., Prasad, R., Molina, J.T., Beard, W.A., Tomkinson, A.E., Wilson, S.H., 1998. Mammalian abasic site base excision repair. Identification of the reaction sequence and rate-determining steps. J. Biol. Chem. 273, 21203–21209.
Swain, U., Subba Rao, K., 2011. Study of DNA damage via the comet assay and base excision repair activities in rat brain neurons and astrocytes during aging. Mech. Ageing Dev. 132, 374–381.

Tanabe, K., Ikegami, Y., Ishida, R., Andoh, T., 1991. Inhibition of topoisomerase II by antitumor agents bis(2,6-dioxopiperazine) derivatives. Cancer Res. 51, 4903–4908.

Tchekneva, E.E., Rinchik, E.M., Polosukhina, D., Davis, L.S., Kadkina, V., Mohamed, Y., Dunn, S.R., Sharma, K., Qi, Z., Fogo, A.B., Breyer, M.D., 2007. A sensitized screen of N-ethyl-N-nitrosourea-mutagenized mice identifies dominant mutants predisposed to diabetic nephropathy. J. Am. Soc. Nephrol. 18, 103–112.

Tosal, L., Comendador, M.A., Sierra, L.M., 2001. In vivo repair of ENU-induced oxygen alkylation damage by the nucleotide excision repair mechanism in Drosophila melanogaster. Mol. Genet. Genomics 265, 327–335.

Towbin, H., Staehelin, T., Gordon, J., 1979. Electrophoretic transfer of proteins from polyacrylamide gels to nitrocellulose sheets: procedure and some applications. Proc. Natl. Acad. Sci. U.S.A. 76, 4350–4354.

Tsai-Pflugfelder, M., Liu, L.F., Liu, A.A., Tewey, K.M., Whang-Peng, J., Knutsen, T., Huebner, K., Croce, C.M., Wang, J.C., 1988. Cloning and sequencing of cDNA encoding human DNA topoisomerase II and localization of the gene to chromosome region 17q21-22. Proc. Natl. Acad. Sci. U.S.A. 85, 7177–7181.

Tsutsui, K., Sano, K., Kikuchi, A., Tokunaga, A., 2001. Involvement of DNA topoisomerase IIbeta in neuronal differentiation. J. Biol. Chem. 276, 5769–5778.

Wang, J.C., 1996. DNA topoisomerases. Annu. Rev. Biochem. 65, 635–692.

Warren, W., Clark, J.P., Gardner, E., Harris, G., Cooper, C.S., Lawley, P.D., 1990. Chemical induction of thymomas in AKR mice: interaction of chemical carcinogens and endogenous murine leukemia viruses. Comparison of N-methyl-N-nitrosourea and methyl methanesulphonate. Mol. Carcinog. 3, 126–133.

Wilkin, G.P., 1995. Neural Cell Culture: A Practical Approach. Oxford University Press, USA.

Wilson 3rd, D.M., Bohr, V.A., 2007a. The mechanics of base excision repair, and its relationship to aging and disease. DNA Repair (Amst.) 6, 544–559.

Wilson 3rd, D.M., McNeill, D.R., 2007b. Base excision repair and the central nervous system. Neuroscience 145, 1187–1200.

Wilson, S.H., 1998. Mammalian base excision repair and DNA polymerase beta. Mutat. Res. 407, 203–215.

Wilstermann, A.M., Osheroff, N., 2001. Base excision repair intermediates as topoisomerase II poisons. J. Biol. Chem. 276, 46290–46296.

Xiao, H., Mao, Y., Desai, S.D., Zhou, N., Ting, C.Y., Hwang, J., Liu, L.F., 2003. The topoisomerase IIbeta circular clamp arrests transcription and signals a 26S proteasome pathway. Proc. Natl. Acad. Sci. U.S.A. 100, 3239–3244.

Yan, L., Bulgar, A., Miao, Y., Mahajan, V., Donze, J.R., Gerson, S.L., Liu, L., 2007. Combined treatment with temozolomide and methoxyamine: blocking apurininc/pyrimidinic site repair coupled with targeting topoisomerase IIalpha. Clin. Cancer Res. 13, 1532–1539.